THE DEVELOPMENT OF A NOVEL, SELECTIVE DESULFURIZATION PROCESS

PROEFSCHRIFT

ter verkrijging van
de graad van doctor aan de Universiteit Twente,
op gezag van de rector magnificus,
prof.dr. W.H.M. Zijm,
volgens besluit van het College voor Promoties
in het openbaar te verdedigen
op woensdag 13 september 2006 om 13.15 uur

door

Hendrik ter Maat
Geboren op 8 juni 1968
te Rijssen, Nederland

Dit proefschrift is goedgekeurd door de promotor

prof.dr.ir. G.F. Versteeg

en door de assistent promotor

Dr..ir. J.A. Hogendoorn

Maat, H. ter

The development of a novel, selective desulfurization process.
Thesis University of Twente, The Netherlands.

10 digit ISBN 90-9021050-4
13 digit ISBN 978-90-9021050-4

Printed by Wöhrmann Print service, Zutphen, The Netherlands

Summary

The removal of hydrogen sulfide from natural, industrial of bio gas is an operation that is frequently encountered in process industry. Driven by tight sulfur specifications and the everlasting need for cost reduction a considerable research effort is made in this field, sprouting numerous new developments in desulfurization technology.

The procede desulfurization process is a regenerative process that is capable of removing H_2S from a gas stream without the uptake of CO_2. The removal of H_2S is selective since the absorption process is based on the precipitation reaction of H_2S with metal ions present in an aqueous solution under the formation of metal sulfide.

The desulfurization of gas streams using aqueous iron(II)sulfate ($Fe(II)SO_4$), zinc sulfate ($ZnSO_4$) and copper sulfate ($CuSO_4$) solutions as washing liquor is studied theoretically and experimentally **(Chapter 2**. A thermodynamic study has been used to determine a theoretical operating window, with respect to the pH of the scrubbing solution, in which the metal sulfate solution can react with hydrogen sulfide (H_2S), but not with carbon dioxide (CO_2) from the gas or hydroxide ions from the scrubbing solution. When the absorption is carried out in this window the proposed process should be capable of removing H_2S from the gas stream without uptake of CO_2 or the formation of metal hydroxides. The pH operating window increases in the order of iron, zinc to copper.

Experimental verification showed that the proposed process indeed efficiently removes H_2S when an aqueous $Fe(II)SO_4$, $ZnSO_4$ or $CuSO_4$ solution is used as absorbent. However, for an efficient desulfurization the lower pH of the experimental pH operating window using the $Fe(II)SO_4$ or $ZnSO_4$ solution was higher than indicated by thermodynamics. The reason for this must probably be attributed to a reduced precipitation rate at decreasing pH. When a $CuSO_4$ solution is used as washing liquor the solution can efficiently remove H_2S over the entire pH range studied (as low as pH = 1.4). In this case only the upper pH boundary of the operating window (that indicates the possible formation of copper hydroxide or copper carbonates) seems to be a relevant limit in practice.

The laboratory experiments indicate that the absorption of H_2S in a $CuSO_4$ solution, at the experimental conditions tested, is a gas phase mass transfer limited process. This allows a high degree of H_2S removal in a relatively compact contactor. In addition to the lab scale experiments the potential of the new desulfurization process has also been successfully demonstrated for an industrial biogas using a pilot scale packed bed reactor operated with a fresh and regenerated $CuSO_4$ solution.

Summary

The desulfurization of gas streams using aqueous copper sulfate ($CuSO_4$) solutions as washing liquor is subject of a more detailed investigation **(Chapter 3)**. Absorption experiments of H_2S in aqueous $CuSO_4$ solutions were carried out in a Mechanically Agitated Gas Liquid Reactor. The experiments were conducted at a temperature of 293 K and $CuSO_4$ concentrations between 0.01 and 0.1 M. These experiments showed that the process efficiently removes H_2S. The experiments indicate that the absorption of H_2S in a $CuSO_4$ solution may typically be considered a mass transfer limited process at, for this type of industrial process, relevant conditions.

The extended model developed by Al-Tarazi et al. has been used to predict the rate of H_2S absorption. This model describes the absorption and accompanying precipitation process in terms of, among others, elementary reaction steps, particle nucleation and growth. The results from this extended model were compared to results obtained with a much simpler model, regarding the absorption of H_2S in $CuSO_4$ containing aqueous solutions as absorption of a gas accompanied by an instantaneous irreversible reaction. From this comparison it appeared that the absorption rate of H_2S in a $CuSO_4$ solution can, under certain conditions, be considered as a mass transfer rate controlled process. Under a much wider range of conditions the error that is made by assuming that the absorption process is a mass transfer controlled process, is still within engineering accuracy. This simplification allows for a considerable reduction of the theoretical effort needed for the design of a G/L contacting device, thereby still assuring that the desired gas specification can be met under a wide range of operating conditions.

The oxidation of copper(II)sulfide to copper(II) oxide, required for the regeneration of copper sulfide is studied **(Chapter 4).** The possibilities for a selective and efficient method to convert copper(II)sulfide (CuS) into copper(II)oxide (CuO)of CuS are investigated. The reaction routes of the oxidation of copper sulfide as a function of reaction temperature and gas composition are established. The oxidation of copper sulfide is studied experimentally using a Thermo Gravimetric Analyzer (TGA) at temperatures ranging from 450ºC to 750 ºC and oxygen concentrations of 5 and 10 V%. It appeared that the products formed upon the oxidation of copper sulfide depend on the reaction temperature. However, in all cases the conversion time using the powdered samples was much shorter than expected based on literature results (typically 3 minutes versus 1-3 hours as mentioned in literature). The first reaction step in the oxidation of copper sulfide always was the fast decomposition of CuS into Cu_2S and gaseous sulfur, which immediately is oxidized further to SO_2. Subsequently, Cu_2S is then oxidized, the route depending on the reaction conditions. Oxidation experiments carried out at various temperatures showed that Cu_2S is oxidized selectively to CuO at temperatures above 650 ºC, while at temperatures below 650 ºC (basic) copper sulfate was also formed. The oxidation

from Cu_2S to CuO appeared to be the result of two consecutive reactions. Cu_2S is first converted into Cu_2O, which is subsequently oxidized to CuO. The experimental results allowed for the determination a rate expression and (Arrhenius) relation for the reaction rate constant of the conversion of Cu_2S to Cu_2O between 650 and 750 ºC and oxygen concentrations between 5 and 10 V%.

The process design and economic potential of the procede desulfurization process were studied **(Chapter 5)**. The high selectivity towards H_2S of this process, along with the relatively high value of the obtained final products are key advantages. The economic performance of this process was studied using a Discounted Cash Flow analysis (DCF). The economic performance of the procede desulfurization process in comparison to its main, large scale, competitor: the amine based gas sweetening process was established.

It was found that although both processes (logically) cost money when the product revenues were neglected, the economic performance of the novel process was substantially better than the economic performance of a conventional, amine based desulfurization unit. Owing to the relatively low operating costs, retrofitting an existing amine based desulfurization unit can be a very attractive option. It was also established that the competitive edge of the procede desulfurization process improved at higher CO_2 or lower H_2S concentrations in the feed gas, but decreases when copper losses during regeneration occur.

Furthermore the economic advantage of the copper sulfate based process over the amine based process increased further when the product revenues were taken into account.

Samenvatting

De verwijdering van zwavelwaterstof uit aard- industrieel of biogas is een processtap die regelmatig wordt toegepast in de procesindustrie. Aangedreven door strakke zwavelspecificaties en de voortdurende drang naar kostenreductie worden aanzienlijke onderzoeksinspanningen gepleegd naar beteren ontzwavelingsmogelijkheden. Dit resulteert in vele ontwikkelingen binnen de ontzwavelingstechnologie. Het procede ontzwavelingsproces is zo'n ontwikkeling.

Het procede ontzwavelingsproces is een proces dat in staat is om selectief zwavelwaterstof te verwijderen uit een gasstroom. De verwijdering van zwavelwaterstof is selectief omdat het absorptieproces gebaseerd is op de precipitatiereactie die optreedt als metaalionen aanwezig in een waterige oplossing in contact worden gebracht met zwavelwaterstof.

De ontzwaveling van gasstromen met behulp van waterige ijzer(II)sulfaat ($Fe(II)SO_4$), zinksulfaat ($ZnSO_4$) en kopersulfaat ($CuSO_4$) oplossingen als zijn experimenteel theoretisch en bestudeerd **(Hoofdstuk 2)**. Een thermodynamische studie is gebruikt om een zgn. 'pH operating window', te bepalen, waarin de oplossing van het metaalsulfaat met waterstofsulfide (H_2S), maar niet met kooldioxide (CO_2) uit de gasstroom of met hydroxylionen van de het wasoplossing kan reageren. Wanneer het absorptieproces in deze 'pH operating window' wordt uitgevoerd zou het voorgestelde proces in staat moeten zijn om H_2S uit de gasstroom zonder co-absorptie van CO_2 of de vorming van metaalhydroxyde. Het 'operating window' wordt groter in de volgorde ijzer, zink koper.

Experimentele verificatie toonde aan dat het voorgestelde proces inderdaad efficiënt H_2S verwijdert wanneer een waterige oplossing $Fe(II)SO_4$, $ZnSO_4$ of $CuSO_4$ wordt gebruikt. Nochtans, voor een efficiënte ontzwaveling bleek dat de onderste pH-grens van het 'operating window' voor het gebruik van $Fe(II)SO_4$ of $ZnSO_4$ oplossing oplossingen hoger was dan vastgesteld middels thermodynamica. De reden voor dit moet waarschijnlijk aan een verlaagde precipitatiesnelheid bij lage pH worden toegeschreven. Wanneer een $CuSO_4$ oplossing wordt gebruikt als wasvloeistof bleek de het mogelijk om H_2S efficiënt te verwijderen bij alle onderzochte pH waarden (tot pH = 1.4). In dit geval lijkt de bovenste pH grens van het 'operating window' (bepaald door de mogelijke vorming van koperhydroxide of kopercarbonaten) een relevante grens te zijn.

De laboratoriumexperimenten wijzen erop dat de absorptie van H_2S in een $CuSO_4$ oplossing, bij de experimentele geteste condities, een gasfase stoftransport gelimiteerd proces is. Dit staat een hoge graad van H_2S verwijdering in een vrij compacte reactor toe. Naast de experimenten op de laboratoriumschaal is het potentieel van het nieuwe

ontzwavelingsprocédé ook met succes aangetoond voor een industrieel biogas op pilot plant schaal. Hiervoor is zowel verse als geregenereerde $CuSO_4$ oplossing gebruikt..
De ontzwaveling van gasstromen met behulp van waterige kopersulfaat ($CuSO_4$) oplossing als wasvloeistof is onderworpen van een meer gedetailleerd onderzoek **(Hoofdstuk 3)**. Absorptie experimenten werden uitgevoerd in een a Mechanically Agitated Gas Liquid Reactor. De experimenten werden uitgevoerd bij een temperatuur van 293K en $CuSO_4$ concentraties tussen 0,01 en 0,1 M. Deze experimenten toonden aan dat het proces efficiënt H2S verwijdert. De experimenten wijzen erop dat de absorptie van H2S in een $CuSO_4$ oplossing kan worden beschouwd als een stoftransport gelimiteerd proces onder voor dit type proces, industrieel relevante condities.

Het uitgebreide model dat door Al-Tarazi *et al.* is ontwikkeld is gebruikt om de H_2S absorptiesnelheid te voorspellen. Dit model beschrijft de absorptie en precipitatie van H_2S in elementaire reactiestappen, deeltjes-nucleatie en groei. De resultaten van dit uitgebreide model werden vergeleken bij resultaten die met een veel eenvoudiger model, dat de absorptie van H_2S in $CuSO_4$ oplossing beschouwt als absorptie van een gas in een vloeistof, gevolgd door een instantane onomkeerbare reactie. Uit deze vergelijking bleek het dat het absorptiesnelheid van H_2S in een $CuSO_4$ oplossing, onder bepaalde omstandigheden, als een massaoverdracht gelimiteerd proces kan worden beschouwd. De fout die wordt gemaakt door te veronderstellen dat het absorptieproces een massaoverdracht gelimiteerd proces blijft binnen 'engineering accuracy' onder een veel bredere range aan condities. Deze vereenvoudiging staat een aanzienlijke vermindering van de inspanning nodig voor het ontwerp van de gas/vloeistof contactor toe, terwijl nog steeds gegarandeerd kan worden dat de gewenste gasspecificatie gehaald wordt onder een onder een brede range aan procesomstandigheden. van werkende voorwaarden kan worden ontmoet.

De oxidatie van koper(II)sulfide tot koper(II)oxide, nodig voor de regeneratie van kopersulfide is aan een onderzoek onderworpen **(Hoofdstuk 4).** De mogelijkheden voor een selectieve en efficiënte methode om koper(II)sulfide (CuS) in koper(II)oxide (CuO) om te zetten zijn onderzocht. De reactieroutes betreffende de oxidatie van kopersulfide zijn vastgesteld als functie van reactietemperatuur en gaassamenstelling.

De oxidatie van kopersulfide is experimenteel bestudeerd experimenteel in een Thermo Gravimetrische Analysator (TGA) bij temperaturen die variërend van 450ºC tot 750 ºC en zuurstofconcentraties van 5 en 10 V%. Het bleek dat de producten die op de oxidatie van kopersulfide worden gevormd een functie zijn van de reactietemperatuur. Nochtans, in alle gevallen was de omzettingstijd van het gebruikte kopersulfide poeder veel korter dan verwacht op basis van literatuurresultaten (typisch 3 minuten tegenover 1-3 uren vermeld in

literatuur). De eerste reactiestap in de oxidatie van kopersulfide altijd was de snelle decompositie van CuS in Cu_2S en gasvormig zwavel, dat onmiddellijk tot SO_2 verder geoxideerd werld. Het gevormde Cu_2S wordt dan verder geoxideerd, de reactieroute is afhankelijk van de reactieomstandigheden.
Oxidatie-experimenten bij diverse temperaturen uitgevoerd toonden aan dat Cu_2S boven 650 ºC selectief oxideert tot CuO, terwijl bij temperaturen onder 650 ºC ook (basisch) koper sulfaat werd gevormd. De oxidatie van Cu_2S tot CuO bleek het resultaat van twee opeenvolgende reacties te zijn. Cu_2S wordt eerst omgezet in Cu_2O, die later verder oxideert tot CuO. De experimentele resultaten lieten tot dat voor de oxidatie van Cu_2S tot Cu_2O bij een temperatuur tussen 650 en 750 ºC en zuurstofconcentraties tussen toe 5 en 10 V% en reactiesnelheidsvergelijking en een (Arrhenius) relatie werden opgesteld.

Het procesontwerp en het economische potentieel van het procede ontzwavelingsproces werden bestudeerd **(Hoofdstuk 5)**. De hoge H_2S verwijderingsselectiviteit van dit proces, samen met de relatief hoge waarde van de verkregen producten zijn zeer belangrijke voordelen. De economische potentie van dit proces werden bestudeerd door een discounted cash flow (DCF) analyse. De economische prestaties van het procede ontzwavelingsproces in vergelijking met zijn belangrijkste concurrent voor ontzwaveling op grote schaal,: de amine gebaseerde gasontzwavelingprocessen zijn vastgesteld. .

Het bleek dat, hoewel beide processen geld kosten als de productopbrengsten niet meegenomen werden, de economische prestaties van het nieuwe proces wezenlijk beter waren dan de economische prestaties van het conventionele, op amine gebaseerde ontzwavelingsproces. Ook het retrofitten van bestaande op amine gebaseerde ontzwavelingsunits kan zeer aantrekkelijk zijn ten gevolge van de vrij lage bedrijfskosten

Ook is vastgesteld dat de aantrekkelijkheid van het procede gasontzwavelingsproces toeneemt hogere CO_2 of lagere H_2S concentraties in het het te reinigen gas. De aantrekkelijkheid staat onder druk wanneer de koperverliezen tijdens regeneratie optreden. Verder bleek dat het economische voordeel van het op kopersulfaat gebaseerde proces boven het op amine gebaseerde proces verder toeneemt als de productopbrengsten in de berekening mee werden genomen.

Contents

Chapter 1: Introduction.

1 Procede desulfurization process description.

The procede desulfurization process is a regenerative process that is capable of removing H_2S from a gas stream without the uptake of CO_2. Therefore it will have a competitive advantage over various existing processes where the co-absorption of CO_2 increases the cost of operation. The desulfurization takes place in a reactor, in which the gas stream that has to be desulfurized is brought in contact with a copper sulfate containing washing liquid. The removal of H_2S is selective since the absorption process is based on the precipitation reaction of H_2S with copper ions present in an aqueous solution *(Eq. 1)*.

$$Cu^{2+} + H_2S + 2H_2O \leftrightarrow CuS\downarrow + 2H_3O^+ \qquad (1)$$

It is possible to remove H_2S without co-absorption of CO_2, since copper carbonate will not be formed under the process conditions. The precipitated copper sulfide is separated from the washing liquid, which is then replenished and subsequently reticulated to the contactor.

The replenishment of the washing liquid takes place by dissolving copper oxide in the circulation liquid. When (basic) copper oxide is brought into contact with the (acidic) washing liquor, the oxide will react with the hydronium ions under the formation of water and metal ions *(Eq. 2)*.

$$CuO + 2\,H_3O^+ + SO_4^{2-} \rightarrow Cu^{2+} + 3\,H_2O + SO_4^{2-} \qquad (2)$$

The copper sulfide, which is formed during the absorption, is separated from the washing liquid, and oxidized to copper oxide *(Eq. 3)*.

$$CuS + 1\,1/2\,O_2 \rightarrow CuO + SO_2 \qquad (3)$$

The sulfur dioxide in the gases released during the oxidation of the metal sulfide can be converted into marketable products like sulfuric acid or gypsum. Using this configuration of process "building blocks" a complete regenerative process is obtained. A possible flowscheme for this process is shown in Figure 1.

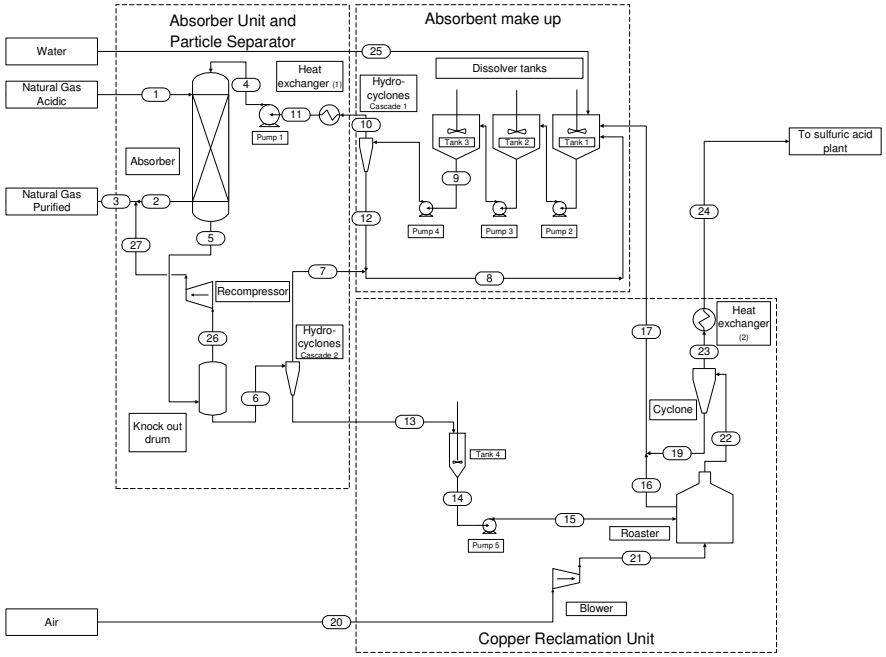

Figure 1: Process Flowsheet

The product of the overall process (see also Table 1) is a cleaned gas stream and a gas stream contained a concentration of sulfur dioxide, suitable for further processing. In Table 1 also the range of possible process conditions is given. The procede process can be used to clean all kinds of hydrogen sulfide containing gas streams, but will be most attractive when the selective removal of H_2S is required, as will be the case in most gases containing a high level of CO_2. Examples of such gasses are biogas, a product of anaerobic digestion of organic waste, and sour gas, the principle product of gas well exploitation.

Table 1: Overall reactions of the 3 processing steps and process conditions

Processing step	*Reaction*	*Process conditions*		
		P	T	pH
Absorption of H_2S in $CuSO_4$ solution (Eq. 1)	$Cu^{2+} + H_2S + 2\,H_2O + SO_4^{2-} \rightarrow CuS\downarrow + 2\,H_3O^+ + SO_4^{2-}$	atmospheric to high pressure	20 – 50 ºC Higher temp. possible	<7
Dissolution reaction (Eq. 2)	$CuO + 2\,H_3O^+ + SO_4^{2-} \rightarrow Cu^{2+} + 3\,H_2O + SO_4^{2-}$	atmospheric	20-80 ºC	<2
Oxidation of CuS (Eq. 3)	$CuS + 1\,{}^1\!/\!_2\,O_2 \rightarrow CuO + SO_2$	atmospheric	800 ºC	-
Overall reaction (Eq. 4)	$H_2S + 1\,{}^1\!/\!_2\,O_2 \rightarrow H_2O + SO_2$			

A variant of the proposed process may be composed of a number of small-scale independently working and decentralized absorption units in combination with a central, larger regeneration unit. The absorption units will generate metal sulfide, which has to be collected and converted into a metal oxide in the centralized regeneration unit. By centrally regenerating the spent absorbent the operation costs, which are mainly determined by the cost of the absorbent in the case of a singe-use process, are lowered and a competitive edge can be gained over the current chemical consuming processes. Another variant of the proposed process may be consisting of a single large-scale absorption unit in combination with a regeneration unit, on a different geographic location. A schematical representation of both process variants is given in Figure 2.

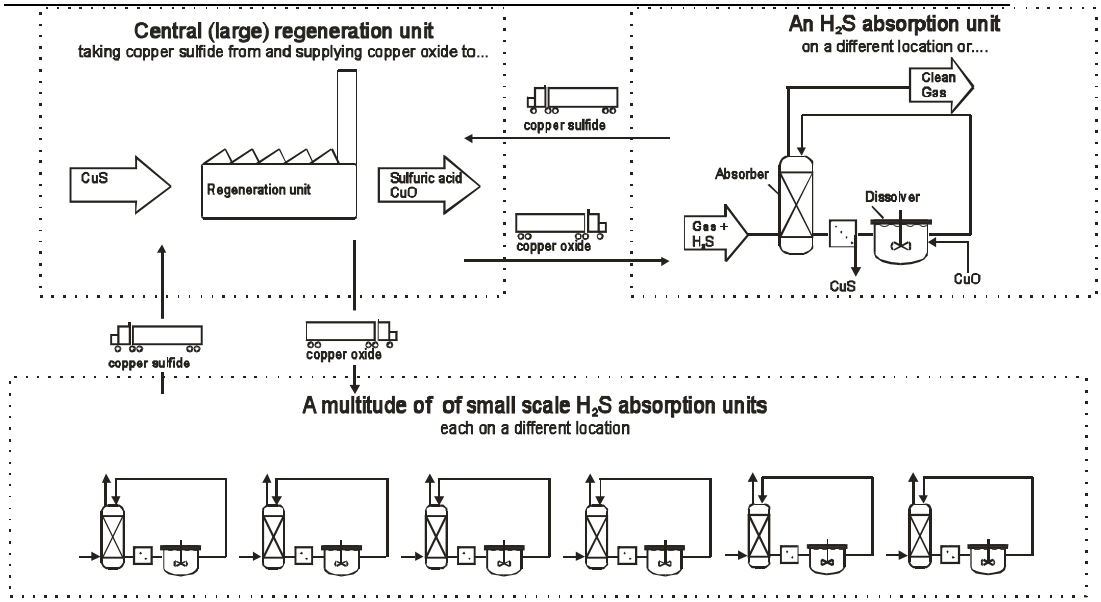

Figure 2: Process variants

2 Outline of this thesis

Chapter 2

In chapter 2 the applicability of a number of aqueous metal sulfate solutions for the desulfurization of gas streams has been investigated theoretically and experimentally. The possibilities for selective removal were established and it was verified on laboratory scale that the proposed process indeed efficiently removes H_2S when an aqueous $Fe(II)SO_4$, $ZnSO_4$ or $CuSO_4$ solution is used as absorbent. In addition to the laboratory scale experiments the procede desulfurization was also successfully demonstrated for an industrial biogas using a pilot scale packed bed reactor operated with a fresh and regenerated $CuSO_4$ solution.

Chapter 3

In chapter 3 the desulfurization of gas streams using aqueous copper sulfate ($CuSO_4$) solutions as washing liquor is studied. Absorption experiments of H_2S in aqueous $CuSO_4$ solutions carried out in a Mechanically Agitated Gas Liquid Reactor are described in this Chapter. The applicability of the model developed by Al-Tarazi et al. (2004) and a much simpler model, regarding the absorption of H_2S in $CuSO_4$ containing aqueous solutions as absorption of a gas accompanied by an instantaneous irreversible reaction to predict the rate of H_2S absorption is described.

Chapter 4

Chapter 4 focusses on the regeneration section. In this Chapter the possibilities for a selective and efficient method to convert copper(II)sulfide (CuS) into copper(II)oxide (CuO)of CuS are investigated. The reaction routes of the oxidation of copper sulfide as a function of reaction temperature and gas composition are given in this chapter. Reaction kinetics for the oxidation of Cu_2S to Cu_2O are also given.

Chapter 5

In Chapter 5 the technical and economical viability of the procede desulfurization process is studied. A process design was made and analyzed. The high selectivity towards H_2S of this process, along with the relatively high value of the obtained final products were found to be key advantages over existing alternative desulfurization processes.

Chapter 6

Due to the innovating nature of the novel desulfurization process it was possible to patent it. The text of this patent is given in Chapter 6.

Chapter 2: The absorption of hydrogen sulfide in metal sulfate solutions.

Abstract

The desulfurization of gas streams using aqueous iron(II)sulfate ($Fe(II)SO_4$), zinc sulfate ($ZnSO_4$) and copper sulfate ($CuSO_4$) solutions as washing liquor is studied theoretically and experimentally. The desulfurization is accomplished by a precipitation reaction that occurs when sulfide ions and metal ions are brought into contact with each other.

A thermodynamic study has been used to determine a theoretical operating window, with respect to the pH of the scrubbing solution, in which the metal sulfate solution can react with hydrogen sulfide (H_2S), but not with carbon dioxide (CO_2) from the gas or hydroxide ions from the scrubbing solution. When the absorption is carried out in this window the proposed process should be capable of removing H_2S from the gas stream without uptake of CO_2 or the formation of metal hydroxides. The pH operating window increases in the order of iron, zinc to copper.

Experimental verification showed that the proposed process indeed efficiently removes H_2S when an aqueous $Fe(II)SO_4$, $ZnSO_4$ or $CuSO_4$ solution is used as absorbent. However, for an efficient desulfurization the lower pH of the experimental pH operating window using the $Fe(II)SO_4$ or $ZnSO_4$ solution was higher than indicated by thermodynamics. The reason for this must probably be attributed to a reduced precipitation rate at decreasing pH. When a $CuSO_4$ solution is used as washing liquor the solution can efficiently remove H_2S over the entire pH range studied (as low as pH = 1.4). In this case only the upper pH boundary of the operating window (that indicates the possible formation of copper hydroxide or copper carbonates) seems to be a relevant limit in practice.

The laboratory experiments indicate that the absorption of H_2S in a $CuSO_4$ solution, at the experimental conditions tested, is a gas phase mass transfer limited process. This allows a high degree of H_2S removal in a relatively compact contactor. In addition to the lab scale experiments the potential of the new desulfurization process has also been successfully demonstrated for an industrial biogas using a pilot scale packed bed reactor operated with a fresh and regenerated $CuSO_4$ solution.

This study indicates that the precipitation reaction of metal sulfates with H_2S can be used successfully in a (selective) desulfurization process, and that it can be an attractive alternative to the desulfurization methods currently used.

Key words: desulfurization, metal sulfide, precipitation reactions.

1 Introduction

Many natural and industrial gases contain H_2S. The presence of H_2S usually prohibits the direct use of these gases because of its toxic properties, the formation of SO_2 upon combustion (acid rain), and the problems it (usually) gives in downstream processing (e.g. catalyst poisoning and corrosion of pipelines and process equipment). This means that it is often necessary to remove H_2S from the gas stream prior to use. If any CO_2 is present in the gas, simultaneous removal of CO_2 from the gas stream can occur. This phenomenon usually increases the amount of chemicals required during the removal step, and is therefore usually not desired. Many, more or less efficient, processes have been developed to remove H_2S from gas streams. In case of regenerative processes the reagent used to capture H_2S can be recovered. Two of the better-known regenerative gas-liquid processes are the amine based processes and the iron chelate based processes that are typically applied only for relatively large gas streams.

The amine based process consist of an H_2S absorption step in which the H_2S is removed from a process stream using an absorbent, a H_2S desorption step in which the absorbent is regenerated and a concentrated H_2S stream is liberated, and a process step in which the concentrated H_2S stream is processed further. The amine-based processes use the reversible absorption of H_2S (a weak acid) in aqueous alkanolamine (a weak base) solutions to remove H_2S from a gas stream. For e.g. a secondary amine this reaction will be

$$R_1R_2NH + H_2S(l) \leftrightarrow R_1R_2NH_2^+ + HS^- \qquad (1)$$

In the desorption step the process conditions are chosen such that the reverse reaction occurs. This is realized by applying a relative high temperature and low pressure, resulting in a regenerated aqueous amine stream and a gaseous stream with a high concentration of H_2S. In a consecutive third process step this concentrated H_2S stream can be processed into elemental sulfur via a Claus process. The main advantage of the amine-based process is the low operating cost of the plant since basically no chemicals are consumed. A disadvantage is the co-absorption of CO_2 (also a weak acid) from the gas stream into the amine. This lowers the capacity of the desulfurization plant and can cause problems in the Claus reactor.

Furthermore, due to the complex configuration, the capital cost of the amine-based plant is high in comparison with other process alternatives.

Another type of regenerative desulfurization process oxidizes H_2S directly to elemental sulfur using oxidants like e.g. iron chelates. The iron chelate based processes (e.g. the SULFEROX process) use chemicals (iron chelates) capable of direct conversion of H_2S into elemental sulfur according to:

$$H_2S + 2Fe^{3+}L^{n-} \Rightarrow S + 2Fe^{2+}L^{n-} + 2H^+ \qquad (2)$$

In a separate process step the iron chelate is regenerated using oxygen from air.

$$O_2 + 4Fe^{2+}L^{n-} + 2H_2O \Rightarrow 4Fe^{3+}L^{n-} + 4OH^- \qquad (3)$$

Main advantage of this process compared to the amine based processes is that no co-absorption of CO_2 takes place. One disadvantage of iron chelate based processes is the degradation of the ligand L that takes place during regeneration. Therefore a make up stream of iron chelate must be added. This causes the operating cost of the plant to be higher than the operating cost of an amine based plant. The capital cost of the iron chelate-based plant is lower than the capital cost of an amine-based plant since it is a less complicated process, however the produced sulfur is of lower quality than the sulfur produced in the Claus process (the sulfur produced is even frequently classified as chemical waste).

In addition to the abovementioned processes, a large number of chemical consuming processes is available for H_2S abatement. These processes make use of e.g. activated carbon, metal oxides or caustic soda. The main characteristic of this type of processes is that the chemical or adsorbent involved in the H_2S removal is used only a limited number of times and has to be disposed after use. It will be clear that these processes have relatively high operating costs, mainly caused by the replacement of the ab- or adsorbent. The capital costs associated with the chemical consuming processes are relatively low, since the desulfurization unit is usually of a relatively simple design. For a more extended overview of H_2S removal methods the reader is referred to Nagl (1997), or Kohl and Nielsen (1997).

As stated before the operating cost and the capital cost of the different desulfurization methods vary widely for the different methods mentioned (amine, chelate and chemical consuming), and therefore each of the process classes has its own “niche” in the desulfurization market (Nagl, 1997). In Table 1 a general overview of the processes is given.

Table 1: Overview of the desulfurization processes.

	Capacity range [ton S/day]	Typical capacity [ton S/day]	Capital cost For typical cap. [US$]	Operating cost [US$/ton S]
Amine-Claus processes	Over 50	50	4.500.000	70
Iron chelate processes	0.05-50	10	1.000.000	250
Chemical consuming	Up to 0.05	0.025	140.000	5000

It will be clear that a regenerative process that is capable of removing H_2S from a gas stream without the uptake of CO_2 will have a competitive advantage over various existing processes where the co-absorption of CO_2 increases the cost of operation.

A selective regenerative H_2S removal process can also be accomplished by using a process based on the precipitation reaction of H_2S with metal ions present in an aqueous solution and a subsequent regeneration of the solid metal sulfide formed. For the reaction of e.g. a bivalent metal ion and the sulfide ion the following overall precipitation reaction can take place:

$$Me^{2+} + H_2S + 2H_2O \leftrightarrow MeS\downarrow + 2H_3O^+ \qquad (4)$$

It is possible, with the proper choice of metal ion and process circumstances, to remove H_2S without co-absorption of CO_2. To obtain a regenerative process it will be clear that the hydronium ions have to be neutralized using a base produced in the closed loop process. A cost effective method to recover the metal ions and neutralize the hydronium ions formed is the oxidation of the precipitated metal sulfide to metal oxide. When the obtained metal oxide is brought into contact with the (acidic) washing liquor, the oxide will react with the hydronium ions under the formation of water and metal ions. The sulfur dioxide in the gases released during the oxidation of the metal sulfide can be converted into marketable products like sulfuric acid or gypsum. In this way a complete regenerative process can be obtained.

A variant of the proposed process may be composed of a number of small-scale independently working and decentralized absorption units in combination with a central, larger regeneration unit. The absorption units will generate metal sulfide, which has to be collected and converted into a metal oxide in the centralized regeneration unit. By centrally regenerating the spent absorbent the operation costs, which are mainly determined by the cost of the absorbent in the case of a singe-use process, are lowered and a competitive edge can be gained over the current chemical consuming processes. The proposed process will be most attractive when the selective removal of H_2S is required, as will be the case in most

gases containing a high level of CO_2. An example of such a gas is biogas, a product of anaerobic digestion of organic waste. A typical composition of such a biogas is given in Table 2 (Pauss, 1987). Normally the H_2S specification for the product gas will vary between 4 and 500 ppmV H_2S, depending upon further use.

Table 2:Typical Biogas composition

Component	Composition [V%]
CH_4	52 - 95
CO_2	9 - 45
H_2S	0.001 - 2
H_2	0.01 - 2
N_2	0.1 - 4
O_2	0.02 - 6.5
Ar	0.001
CO	0.001 - 2
NH_3	trace
Organics	trace

In the past a number of processes have been developed to utilize the precipitation reaction of metal ions with sulfide. So far, the main utilization of this reaction is found in the removal of heavy metal ions from e.g. electroplating waste streams. In these cases the primary interest was the efficient removal of metal ions from the waste stream. In contrast, only a few processes are dedicated to the removal of H_2S from a gas stream using metal ions. An example is the chemsweet process, (Manning, 1979), a non-regenerative process that utilizes zinc ions to remove H_2S from sour gases. In this semi-batch process solid zinc salts are dissolved to replenish the washing liquor. To account for the acid formed during the precipitation reaction the zinc compounds have to be of a basic nature, e.g. ZnO or $ZnCO_3$. Regenerative processes for the removal of H_2S from geothermal steam have been described by Brown (1980), and in the patents of Spevack (1980) and Harvey (1980). These processes utilize copper solutions to remove H_2S from geothermal steam. Ammonia, also present in the geothermal steam, is used to neutralize the acid formed during the precipitation reaction. In the regeneration step copper sulfide is oxidized to CuSO4 in the presence of ammonium ions in a pressure vessel at a temperature of approximately 100 - 200 °C, and an oxygen partial pressure of 1.5 Bara. The product of this type of process is, apart from a cleaned up steam flow, a concentrated stream of ammonium sulfate. The application of this process is rather limited because the process cannot operate in a closed loop manner if understoichiometric amounts of ammonia are present in the gas stream to be cleaned.

For other processes mentioned in literature the recovery of the metal ions from the metal sulfide formed is rather cumbersome in the absence of ammonia. Ehnert *et al.* (1973) describe the use of a cupric halogenide to remove H_2S from a gas. Copper was recovered by means of oxidation of the copper sulfide at elevated temperatures. The products were a regenerated copper solution and elemental sulfur. However the obtained sulfur still contained large quantities of copper; amounts from 1.5% to well over 30 % copper in sulfur were found. Broekhuis (1992) used an acidic $Fe(III)_2(SO_4)_3$ solution as oxidizing agent at elevated temperatures to oxidize the metal sulfide (in his case copper- and zinc sulfide) to metal sulfate and elemental sulfur, but a complete conversion of the metal sulfide was not achieved.

In the process presently under development the regeneration of the absorbent will be done by means of oxidation of the precipitated metal sulfide to metal oxide (Ter Maat *et al.*, 2003a, Ter Maat *et al.*, 2003b). In order to prevent the contamination of the off gases of the oxidation step with components other than sulfur dioxide and water, metal sulfate salts will preferably be used as absorbent. Presented in this contribution are the results of the experiments conducted to investigate the absorption of H_2S in some selected metal sulfates.

2 Theory

2.1 General theory

Sulfides of most bivalent metal ions, e.g. zinc, copper, silver, lead, magnesia, nickel and tin are highly insoluble. Therefore aqueous solutions containing these metal ions can be used as washing liquid in a desulfurization process. The overall reaction between H_2S and a bivalent metal ion is given in Eq. 4. The absorption of H_2S in, and the subsequent reaction with a metal sulfate solution will take place in several elementary steps. First H_2S will be transported from the gas phase and dissolve physically in the liquid phase.

$$H_2S_G \Leftrightarrow H_2S_L \qquad (5)$$

The concentrations in the gas phase and the liquid phase at the gas liquid interface are not equal. However, in most practical cases equilibrium exists at the interface, and the ratio of gas and liquid concentrations can be expressed as a distribution coefficient m (Westerterp, 1984). The distribution coefficient is a function of liquid composition and temperature only when the gas phase behaves ideally.

$$m_{H_2S} = \frac{[H_2S_L]_i}{[H_2S_G]_i} = \left(\frac{[H_2S]_L}{[H_2S]_G} \right)_{Equilibrium} \qquad (6)$$

After this, the dissolved H_2S molecule can act as a diprotic acid. It can dissociate in two steps according to the equilibrium reactions given in Eq. 7 and 8[1]. The first dissociation step takes place according to :

$$H_2S_L + H_2O \Leftrightarrow HS^- + H_3O^+ \qquad K_{a1_{H_2S}} = \frac{\left[HS^-\right]\left[H_3O^+\right]}{\left[H_2S_L\right]} \qquad (7)$$

In the second dissociation step the sulfur atom looses its second and last proton according to:

$$HS^- + H_2O \Leftrightarrow S^{2-} + H_3O^+ \qquad K_{a2_{H_2S}} = \frac{\left[S^{2-}\right]\left[H_3O^+\right]}{\left[HS^-\right]} \qquad (8)$$

If the solubility product of the metal sulfide is exceeded then solid metal sulfide can form. The precipitation reaction is given by Eq. 9.

$$S^{2-} + Me^{2+} \Leftrightarrow MeS\downarrow \qquad K_{sp} = \left[S^{2-}\right]\left[Me^{2+}\right] \qquad (9)$$

Another reaction that can possibly occur when CO_2 is also present is the reaction between CO_2 and the metal ion in the washing liquor. This unwanted side reaction takes place according to a scheme similar to the reaction scheme of the precipitation reaction between H_2S and the metal ion. CO_2 is first physically dissolved in water:

$$CO_{2,G} \Leftrightarrow CO_{2,L} \qquad m_{CO_2} = \frac{\left[CO_{2,L}\right]_i}{\left[CO_{2,G}\right]_i} = \left(\frac{\left[CO_{2,L}\right]}{\left[CO_{2,G}\right]}\right)_{Equilibrium} \qquad (10)$$

Dissolved CO_2 then dissociates stepwise into bicarbonate and carbonate.

$$CO_{2,L} + H_2O \Leftrightarrow HCO_3^- + H_3O^+ \qquad K_{a1_{CO_2}} = \frac{\left[HCO_3^-\right]\left[H_3O^+\right]}{\left[CO_{2,L}\right]} \qquad (11)$$

$$HCO_3^- + H_2O \Leftrightarrow CO_3^{2-} + H_3O^+ \qquad K_{a2_{CO_2}} = \frac{\left[CO_3^{2-}\right]\left[H_3O^+\right]}{\left[HCO_3^-\right]} \qquad (12)$$

[1] No allowance has been made for non-ideality in the equilibrium model.

The metal carbonate can then be formed according to the reaction given in Eq. 13. Whether this precipitation indeed occurs depends on the solubility product

$$CO_3^{2-} + Me^{2+} \Leftrightarrow MeCO_3 \downarrow \qquad K_{sp} = \left[CO_3^{2-}\right]\left[Me^{2+}\right] \qquad (13)$$

The numerical value of the equilibrium constant of the bisulfide/sulfide equilibrium, as well as the equilibrium constant for the solubility products for the metal sulfides can be found in the work of Licht (1988), who evaluated these constants critically. The numerical values for the other equilibrium constants can be found in literature (e.g. Perrin, 1982). An overview of the numerical value of the various equilibrium constants at a temperature of 298 K is given in Tables 3 and 4.

Table 3: The solubility products of the carbonate, hydroxide and sulfide salts of the metal ions used in this study at a temperature of 298K (Lide, 1995, Licht, 1988).

Me^{n+}	X^{m-}		
	CO_3^{2-}	OH^-	S^{2-}
Fe^{2+}	$3.1*10^{-11}$ $FeCO_3$	$4.9*10^{-17}$ $Fe(OH)_2$	$1.0*10^{-21}$ FeS
Zn^{2+}	$1.2*10^{-10}$ $ZnCO_3$	$4.1*10^{-17}$ $Zn(OH)_2$	$3.2*10^{-26}$ ZnS
Cu^{2+}	$6.0*10^{-6}$ $CuCO_3$	$2.4*10^{-13}$ $Cu(OH)_2$	$5.0*10^{-41}$ CuS

Table 4: First and second dissociation constants of CO_2 and H_2S at a temperature of 298 K (Perrin, 1982, Licht, 1988).

Equilibrium	pK_a
H_2S/HS^-	7.05
HS^-/S^{2-}	17.3
CO_2/HCO_3^-	6.35
HCO_3^-/CO_3^{2-}	10.33

2.2 Application of the equilibrium model for the determination of an operating window assuring selective desulfurization for a 1 molar metal sulfate solution.

For a given concentration of metal ions in solution the maximum concentrations of sulfide, carbonate and hydroxyl ions that can be present in the washing solution without the formation of a precipitate can be calculated using the equilibrium constants given in Table 4. The corresponding concentrations of undissociated H_2S and CO_2 in the liquid can then be determined from the chemical equilibria stated in Equations 7, 8, 11 and 12. The corresponding equilibrium concentrations of H_2S and CO_2 in the gas phase can then be determined using the distribution coefficients m. Since the concentrations of H_2S and CO_2

present in the gas leaving the desulfurization unit are determined by the product specification, the relations given above can also be used to determine if a scrubbing solution is a suitable reactant for a selective desulfurization process.

In Figures 1, 2 and 3 the equilibrium vapor pressure of H_2S and CO_2 is plotted against the pH for a 1 molar metal sulfate solution. When the specification of the product gas is known, these Figures can be used to determine a possible operating window for a selective H_2S removal. This window defines a pH region in which metal sulfide precipitation can, but metal carbonate or metal hydroxide precipitation cannot occur. Normally the H_2S specification for the product gas will vary between 4 and 500 ppmV H_2S, depending upon further use. As an example a possible specification can be 10 ppmV H_2S and 30 V% CO_2, which is typical for a biogas. This specification will be used in the following examples.

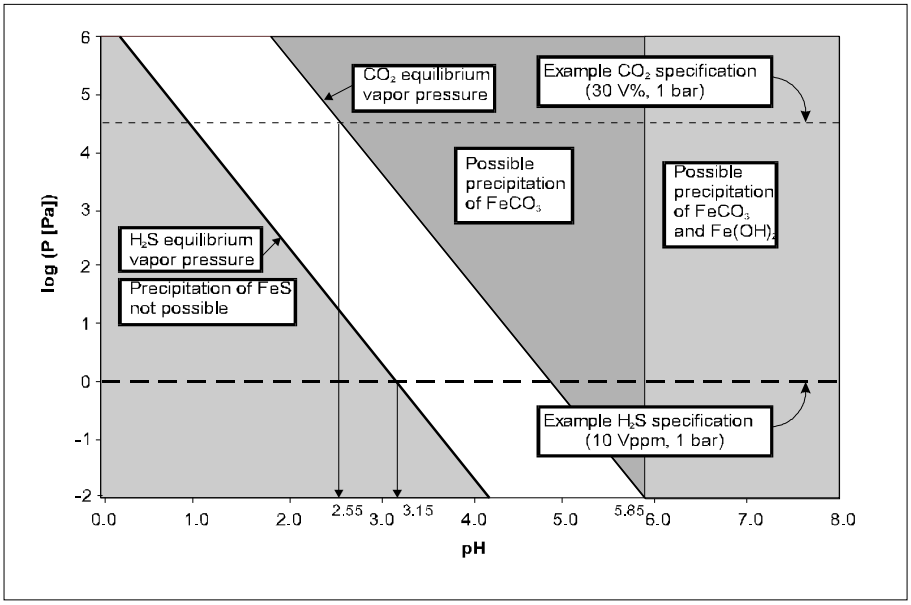

Figure 1: Equilibrium vapor pressures of CO_2 and H_2S as a function of pH for a 1 M $FeSO_4$ solution at a temperature of 293 K. The dotted lines are the H_2S outlet specification (10 ppmV at 1 bara) and the CO_2 vapor pressure in the inlet gas (30V% at 1 bara).

In Figure 1 the theoretical equilibrium vapor pressures of H_2S and CO_2 are plotted as a function of the pH in case of a 1 molar $Fe(II)SO_4$ solution. The lines of the equilibrium pressure and gas phase specification intersect at the pH where precipitation can just take place when a 1 molar $Fe(II)SO_4$ solution is used. At a lower pH no precipitation will take place.

Also, if the actual partial pressure is lower than the equilibrium vapor pressure then no precipitation will occur. From Figure 1 it can be seen that a pH of 3.15 is minimally needed to allow precipitation of iron sulfide when H_2S has to be removed from the gas phase below 10 ppmV (293K, 1 bara). To prevent the precipitation of iron hydroxide the pH must not be higher than 5.85. From Figure 1 it can also be seen that the precipitation of iron carbonate can take place when a 1M molar $Fe(II)SO_4$ solution at a pH of 2.55 and higher is brought in contact with a gas phase at 1 bara, containing 30 V% CO_2. This means that these theoretical calculations predict that it is not possible to remove H_2S down to 10 ppmV without removing CO_2 if that component is present in a concentration of 30 V% at a total pressure of 1 bara.

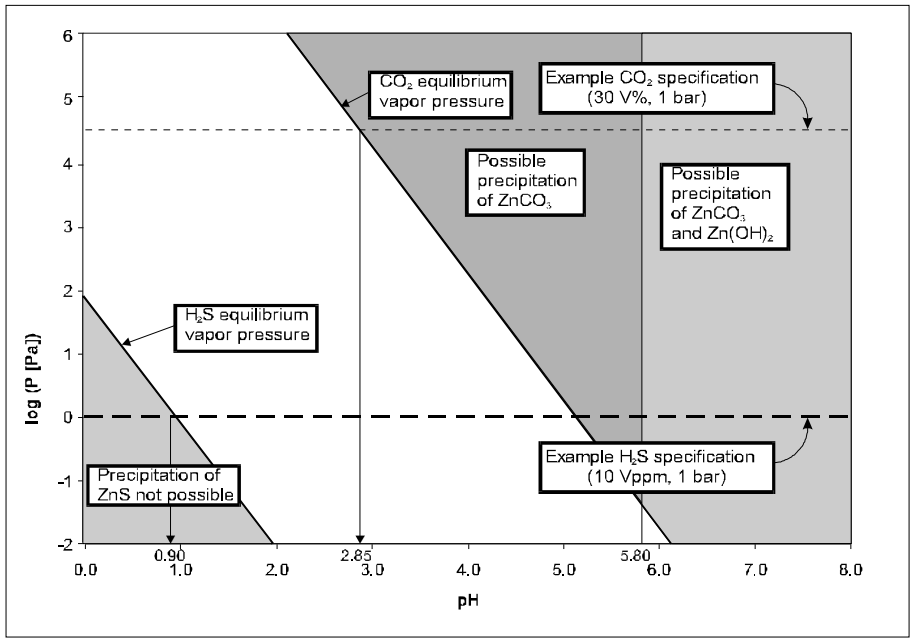

Figure 2: Equilibrium vapor pressures of CO_2 and H_2S as a function of pH for a 1 M $ZnSO_4$ solution at a temperature of 293 K. The dotted lines are the H_2S outlet specification (10 ppmV at 1 bara) and the CO_2 vapor pressure in the inlet gas (30V% at 1 bara).

Figure 2 shows the theoretically calculated equilibrium and the arbitrarily specified vapor pressures of H_2S and CO_2 as a function of the pH for a 1 molar $ZnSO_4$ solution. From Figure 2 it can be seen that a pH of at least 0.90 is required to allow precipitation of zinc sulfide when the gas phase concentration of H_2S is just at the desired specification of 10 ppmV at 1 bara. To prevent the precipitation of zinc hydroxide the pH must not be higher than 5.80. Figure 2 shows that in case sufficient CO_2 is also present, precipitation of zinc carbonate may take

place. In this example, with 30V% CO_2 at a pressure of 1 bara, the precipitation of zinc carbonate can take place at a pH of 2.85 and higher. Thus, theoretical calculations show that for a selective desulfurization down to 10 ppmV H_2S without the co-precipitation of zinc carbonate the pH of the solution must be regulated between 0.90 and 2.85.

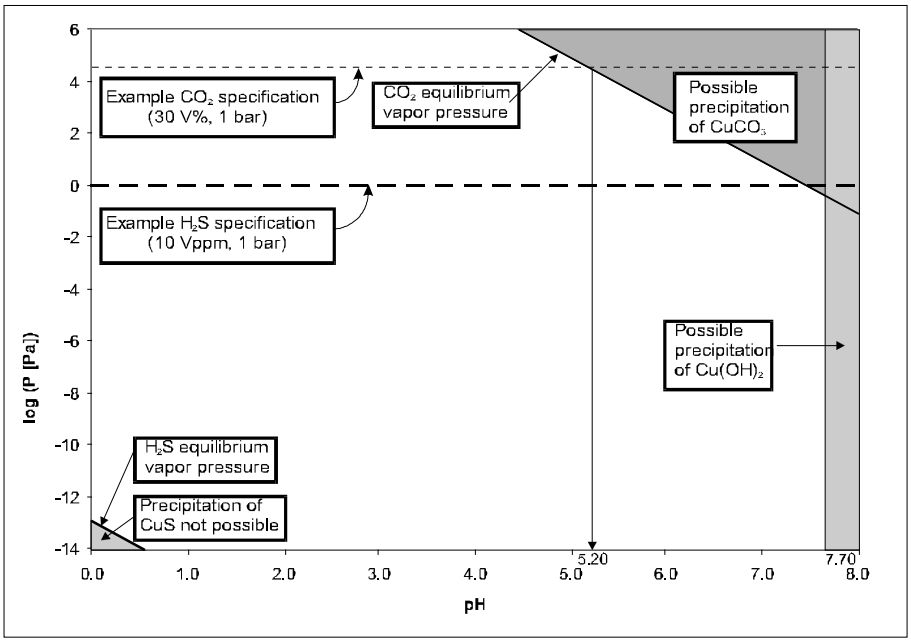

Figure 3: Equilibrium vapor pressures of CO_2 and H_2S as a function of pH for a 1 M $CuSO_4$ solution at a temperature of 293 K. The dotted lines are the H_2S outlet specification (10 ppmV at 1 bara) and the CO_2 vapor pressure in the inlet gas (30V% at 1 bara).

In Figure 3 the theoretical equilibrium vapor pressures and the specified vapor pressures are plotted as a function of the pH for the case of a 1 molar $CuSO_4$ solution. From Figure 3 it can be concluded that precipitation of copper sulfide can always occur if the pH is higher than 0 and the H_2S vapor pressure is higher than 10^{-12} Pa. To prevent the precipitation of copper hydroxide the pH must not be higher than 7.70. From Figure 3 it can also be seen that, with a gas phase composition of 30 V% CO_2 at a pressure of 1 bara, the precipitation of copper carbonate can take place at a pH of 5.20 and higher. This means that when using a $CuSO_4$ solution a very large operating window is obtained. For this theoretical example it is shown that as long as the pH is lower than 5.20 a selective removal of H_2S is possible.

These examples, which are given for 1 M metal sulfate solutions, show that for a selective H_2S removal process in the presence of CO_2 the operating range increases in the order from Fe, Zn to Cu.[2]

3 Experimental

Absorption experiments have been carried out in a laboratory scale set-up schematically shown in Figure 4. The set-up consists of three sections; a gas mixing section to prepare the desired gas mixture, a reactor section, and an analysis section.

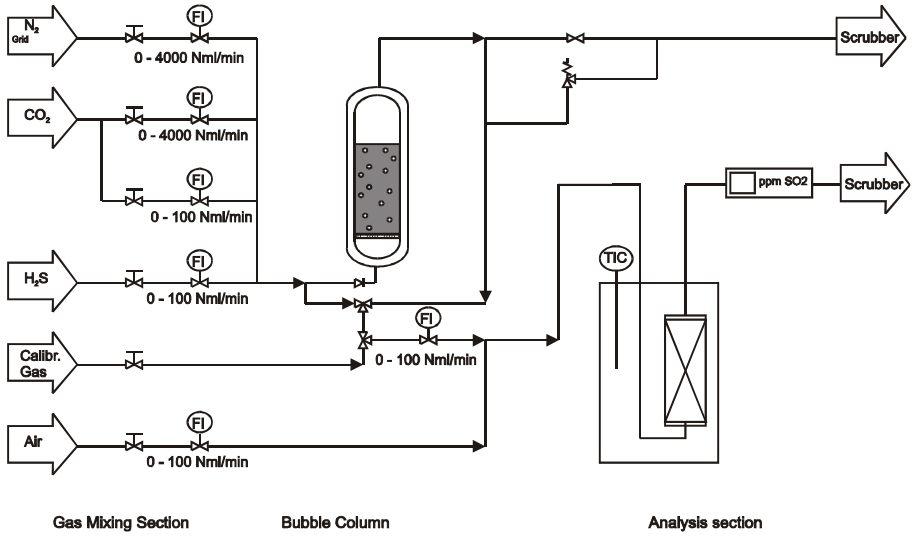

Figure 4: Schematic representation of the experimental set-up

A more detailed drawing of the bubble column reactor, with a height of 62 cm and an inner diameter of 3 cm, is given in Figure 5. During an experiment the bubble column was operated batch wise with respect to the liquid phase, and continuously with respect to the gas phase. The flow rate and composition of the gases were controlled using Brooks 5150 thermal mass flow controllers. A glass frit was used as bottom plate to create an even distribution of the bubbles in the reactor. To ensure isothermal operation of the bubble column a thermostatic bath (Tamson T 1000) was used to pump water with constant temperature through the

[2] It should be noted that for differently concentrated metal sulfate solutions, the same method can be applied to determine an operating window. However, for all concentrations the width of the operating window will increase in the same (Fe, Zn to Cu) order as found for a 1M solutions.

annular space of the double walled reactor. The pH of the solution in the reactor was monitored by means of a Schott pH electrode. The pressure in the reactor was measured using a pressure gauge. The void fraction of the solution in the reactor could be determined by means of a gauge glass. Via small side openings the addition of e.g. anti-foaming agent or NaOH solution was possible if desired.

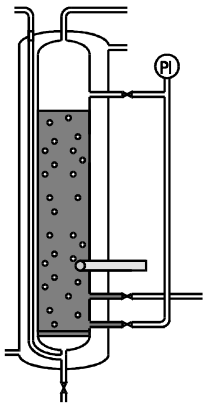

Figure 5: Schematic representation of the reactor.

The following experimental procedure was applied. The bubble column was filled with the desired metal sulfate solution and a small amount of NaOH solution (containing 10 mmol NaOH) was added to set the initial pH of the solution to the desired value and to generate a small amount of metal hydroxide. During the course of an experiment the pH will gradually decrease since hydronium ions are generated in the reaction; the metal hydroxide will act as a buffer and prevent a swift drop in pH immediately after the start of an experiment. When the metal sulfate solution in the reactor reached a constant temperature of 293 K, a gas with the desired composition was bubbled through the reactor at a superficial gas velocity of 0.02 m/s. The pressure in the reactor was kept at 1.1 bara. A continuous gas sample flow was drawn from the reactor effluent stream. The H_2S content of this stream was determined by mixing the sample stream with air and converting the H_2S present in the sample stream to sulfur dioxide over stainless steel wool at 350 ºC to sulfur dioxide (Neomagus, 1998). A MAIHAK UNOR 610 IR sulfur dioxide analyzer was used to determine the concentration of sulfur dioxide and therefore, indirectly the concentration of H_2S. During the experiments the concentration of SO_2 that left the reactor and the pH of the solution were recorded

The $Fe(II)SO_4$, $ZnSO_4$ and $CuSO_4$ used were of analytical grade and were obtained from Across Chimica. N_2 and CO_2 were obtained from Hoek Loos, and had a purity of at least 99.9 %. H_2S was obtained from Hoek Loos and had a purity of 99.0%. The calibration gas was

prepared by Scott Specialty Gasses, and had a composition of 1.0V% H_2S ± 0.05%. The air used for oxidation of the gas stream used for analysis was synthetic air and was obtained from Hoek Loos (21 V% O_2).

The method of analysis was checked using a mixture of the H_2S calibration gas and air in a known ratio. The H_2S in this mixture is then converted to sulfur dioxide over a catalyst at 350 ºC. The resulting mixture was then sent to the IR analyzer. The deviation between the measured concentration and the expected concentration was typically smaller than 2.5%

4 Results and Discussion

4.1 Characterization of the bubble column with an aqueous NaOH solution

To characterize the bubble column some experiments were performed using the absorption of H_2S in an aqueous 0.1 molar NaOH solution. That system was chosen because the reaction of H_2S and an NaOH solution is instantaneous with respect to mass transfer and the absorption of H_2S is therefore gas phase mass transfer limited if the concentration of the NaOH concentration is sufficiently high (Danckwerts, 1970). At the start of an experiment with NaOH the pH of the solution was 13, and dropped gradually during operation. At a pH of approximately 9 the H_2S uptake of the solution dropped significantly and a small amount of concentrated NaOH was added to the solution to bring the pH back to its original value. Then a gas stream with a different concentration of H_2S was brought in contact with the solution. Using this procedure the concentration of H_2S in the gas entering the reactor was varied between 1 and 4 V%. The experimental data are presented in Figure 6. From Figure 6 it can be seen that the conversion of H_2S was more than 99.5 % at a pH of 10 or above. When the pH dropped below 9.5 the removal efficiency decreased significantly.

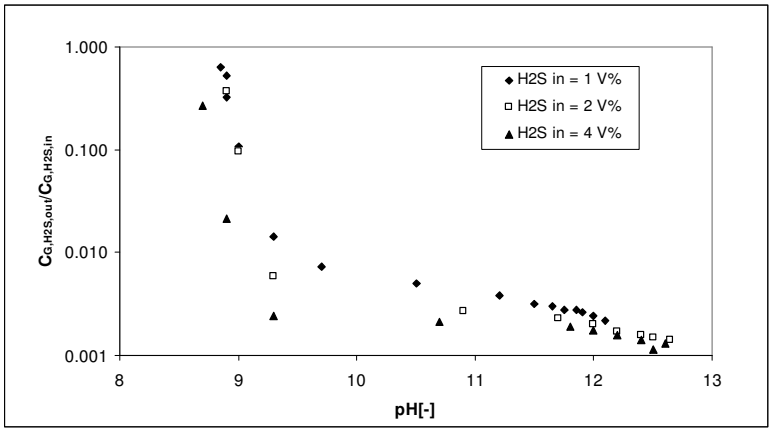

Figure 6: The absorption of H_2S in a NaOH solution at superficial gas velocity of 0.02 m/s and a liquid column height of 0.265 m at a temperature of 293 K, and a pressure of 1.1 bara.

Figure 6 shows that at a pH higher than 11 the degree of H_2S removal appears to be more or less independent of the pH and the initial concentration of H_2S in the gas[3]. This indicates that the mass transfer resistance in the gas phase determines the absorption rate. The gas phase mass transfer coefficient ($k_G a$) can then be determined with Eq 14. (Westerterp, 1984 p 367):

$$k_G a = -\ln\left[\frac{C_{out}}{C_{in}}\right] * \frac{v_{\sup G}}{h} \qquad (14)$$

For the NaOH/H_2S system, $k_G a$ was determined to be approximately 0.5 s^{-1} in the present set-up. It should be mentioned that this value could not be determined accurately since the concentration of H_2S in the gas leaving the reactor is very low (approximately 20 – 80 ppmV) and therefore the concentration of SO_2 in the gas entering the analyzer was near the lower limit of the operating range of the analyzer. Therefore a small deviation in the measured concentration of H_2S in the gas leaving the reactor value causes a large deviation in the determined value for $k_G a$.

4.2 The absorption of H_2S in an aqueous solution of Fe(II)SO_4

The absorption of H_2S in aqueous 1 molar Fe(II)SO_4 solutions has been studied as a function of the pH of the solution and the concentration of H_2S in the gas entering the reactor. At the start of an experiment the pH was brought to a value of approximately 7 by adding some NaOH. During the experiment the pH gradually decreased since hydronium ions are generated by the dissociation of H_2S towards S^{2-} and H_3O^+. At a pH of approximately 4 the H_2S uptake of the solution decreased significantly and a small amount of NaOH was added to bring the pH of the solution back to its original value. Then a gas stream with a different concentration of H_2S was brought in contact with the solution and the experiment was repeated. Using this procedure the concentration of H_2S in the gas entering the reactor was varied between 1 and 4 V%. During the entire experiment the conversion with respect to the metal ions was less than 8%, and thus the assumption that the concentration of metal ions did not change significantly during the experiment is justified. The experimental data are presented in Figure 7.

[3] It is likely that the relatively small increase in removal efficiency with increasing pH (that can be observed in Figure 6 at a pH above approximately 11.5) is caused by a change in column characteristics as e.g. a change in specific surface area, in turn caused by the altering composition of the washing liquid.

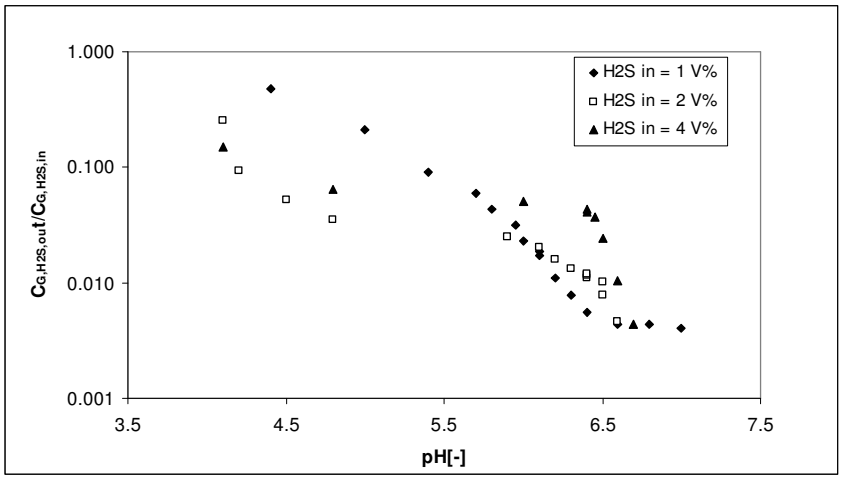

Figure 7: The absorption of H_2S in a 1.0 M Fe(II)SO_4 solution at a superficial gas velocity of 0.02 m/s and a column height of 0.495 m at a temperature of 293 K, and a pressure of 1.1 bara.

From the experimental results obtained with an Fe(II)SO_4 solution it can be concluded that it is possible to remove more than 99% of the H_2S from a gas stream that initially contains in between 1 and 4 V% H_2S when the pH of the solution is higher than 6.7. With the pH above 6.7 the conversion of H_2S appeared to be somewhat lower than the conversion of H_2S when using NaOH with a pH above 11 (maximally 99.8% H_2S removal when using a NaOH solution as compared to maximally 99.6% removal when using a Fe(II)SO_4 solution), however in this case a much longer liquid column was needed to attain this conversion. This might be caused by a change in specific contact area in the reactor in case the process is still gas phase mass transfer controlled. However, another cause of the lower conversion (than the one expected for a gas phase limited process) may be that the absorption of H_2S was not (completely) gas phase mass transfer limited, but also partly influenced by precipitation kinetics and/or liquid phase mass transfer. At a pH lower than 5 the experimentally determined conversion of H_2S drops considerably. The results of the equilibrium calculations, given in Table 5, however, show that a virtually complete desulfurization should be possible at pH values as low as 3. Since the bulk concentration of Fe^{2+} ions has not dropped significantly due to the precipitation reaction, the most probable cause for this discrepancy[4] is that the speed of the precipitation reaction drops significantly long before the reacting system approaches equilibrium, an effect also reported by Nielsen (1964) and Söhnel (1992).

[4] Assuming that the thermodynamic model gives a reliable prediction of equilibrium.

Table 5: Comparison of the experimental results and the results of the theoretical calculations regarding the absorption of H_2S in an aqueous 1 M solution of $FeSO_4$ for a $C_{G\ H2S\ in}$ of 1 V%. The lower detection limit of the equipment does not allow measurements below a value of 20 ppmV H_2S, thus the lowest possible experimentally determined value for $C_{G\ H2S\ out}/C_{G\ H2S\ in}$ was 0.002.

pH	$C_{G\ H2S\ out}/C_{G\ H2S\ in}$		
	experimental results (Fig. 7)	theoretical prediction	
		Gas phase mass transport limited absorption *	Equilibrium calculations
6.7	0.004	$4.2 * 10^{-6}$	$7.9 * 10^{-11}$
6	0.023	$4.2 * 10^{-6}$	$2.0 * 10^{-9}$
5	0.21	$4.2 * 10^{-6}$	$2.0 * 10^{-7}$
4	0.5	$4.2 * 10^{-6}$	$2.0 * 10^{-5}$
3	--	$4.2 * 10^{-6}$	$2.0 * 10^{-3}$
2	--	$4.2 * 10^{-6}$	$2.0 * 10^{-1}$
1	--	$4.2 * 10^{-6}$	--

* *Based on experimental conditions as specified in section 4.2 and a k_Ga value of 0.5 s^{-1},*

From the present results for $FeSO_4$ solutions, it is clear that in order to remove H_2S efficiently in this bubble column the pH should be 6.7 or higher. However, thermodynamic equilibrium calculations show that at these pH values one cannot exclude the formation of solid iron(II) hydroxide or iron(II) carbonate (see Figure 1). Even at lower pH values, where the scrubbing solution would be less efficient (and consequently a longer contact time would be required), the possible formation of iron carbonate cannot be excluded when CO_2 is present in the gas. From the experiments it can be concluded that the operational width for a proper operation seems to be smaller than indicated by thermodynamics. Aqueous Fe(II)SO_4 solutions therefore do not seem very suited when a selective desulfurization process is required.

4.3 The absorption of H_2S in an aqueous solution of $ZnSO_4$

For an aqueous $ZnSO_4$ solution the H_2S conversion was also measured for various ingoing H_2S concentrations and as a function of the pH of the solution. The experimental procedure was identical to the procedure in the experiments with $FeSO_4$ solutions. The pH of the solution immediately after the addition of the NaOH was 5.8 (the precipitation of zinc hydroxide at that pH prohibits a higher pH value).

During an experiment the concentration of H_2S that left the reactor and the pH of the solution were recorded. At a pH of approximately 2.5 the H_2S conversion became lower than 75% and the experiment was stopped. A number of experiments was performed with superficial gas

velocities varying between 0.02 and 0.04 m/s and with H_2S concentrations in the gas entering the reactor varying between 1 and 4 V%. The experimental data are presented in Figure 8.

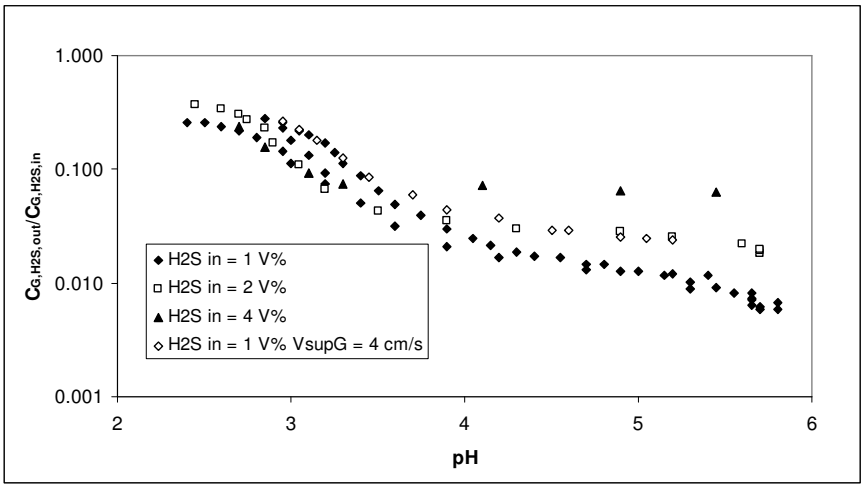

Figure 8: The absorption of H_2S in a 1.0 M $ZnSO_4$ solution at a superficial gas velocity of 0.02 and 0.04 m/s and a liquid height of 0.495 m

When the experimental results are compared, it can be seen that aqueous $ZnSO_4$ and $Fe(II)SO_4$ solutions behave similarly with respect to the absorption of H_2S. Again the experimental maximum conversion of H_2S was slightly lower than the conversion observed when using a NaOH solution with a pH above 11, (maximally 99.8% H_2S removal when using a NaOH solution as compared to maximally 99.4% removal when using a $ZnSO_4$ solution), although a longer liquid column was used. When the absorption of H_2S in a $ZnSO_4$ solution is compared to the absorption of H_2S in an $Fe(II)SO_4$ solution, a noticeable difference is that when using a $ZnSO_4$ solution a high conversion of H_2S can also be achieved at pH values below 6. It appeared for example to be possible to remove more than 99% of H_2S from a gas stream that initially contained 1 V% H_2S at a pH value of 5. To see a substantial decrease in H_2S conversion, the pH had to drop below a value of 4. Equilibrium calculations however, show that for the conditions applied a near complete removal of H_2S should be possible at pH values as low as 0.90 (See also Figure 2 and Table 6). A possible explanation for the difference between the experimentally determined conversion and the maximum theoretical conversion (being the lowest of either the value predicted by the equilibrium calculations or the value predicted by the relation for a gas phase mass transfer limited process) could be the aforementioned decrease in the rate of the precipitation reaction.

Table 6: Comparison of the experimental results and the results of the theoretical calculations regarding the absorption of H_2S in an aqueous 1 M solution of $ZnSO_4$ for a $C_{G\ H2S\ in}$ of 1 V%. The lower detection limit of the equipment does not allow measurements below a value of 20 ppmV H_2S, thus the lowest possible experimentally determined value for $C_{G\ H2S\ out}/C_{G\ H2S\ in}$ was 0.002.

pH	$C_{G\ H2S\ out}/C_{G\ H2S\ in}$		
	experimental results (Fig 8)	theoretical prediction	
		Gas phase mass transport limited absorption*	Equilibrium calculations
7	--	$4.2 * 10^{-6}$	$6.3 * 10^{-16}$
5.7	0.006	$4.2 * 10^{-6}$	$2.5 * 10^{-13}$
5	0.01	$4.2 * 10^{-6}$	$6.3 * 10^{-13}$
4	0.02	$4.2 * 10^{-6}$	$6.3 * 10^{-10}$
3	0.18	$4.2 * 10^{-6}$	$6.3 * 10^{-8}$
2	--	$4.2 * 10^{-6}$	$6.3 * 10^{-6}$
1	--	$4.2 * 10^{-6}$	$6.3 * 10^{-4}$
0	--	$4.2 * 10^{-6}$	$6.3 * 10^{-2}$

* *Based on experimental conditions as specified in section 4.3 and a k_Ga value of 0.5 s^{-1},*

The experimental results in Figure 8 show that, in order to maintain a high H_2S conversion when using a $ZnSO_4$ solution in the experimental set-up, the pH of the washing liquor must be kept at a value of 5 or higher. From Figure 2 it can be seen that at a pH of 5 the formation of solid zinc carbonate is already possible at CO_2 vapor pressures as low as 1.6 Pa. Therefore the precipitation of $ZnCO_3$ that can occur when CO_2 is present in the gas stream that has to be desulfurized can only be excluded when the column is operated at lower pH values, where a high H_2S conversion might only be possible at the cost of a much longer contact time, and thus much larger equipment size. The equilibrium diagram given in Figure 2 therefore only seems suitable to establish an operating window to assure a selective desulfurization using a $ZnSO_4$ solution, but does not tell everything about the width of the operating window for an *efficient* H_2S removal process.

4.4 The absorption of H_2S in an aqueous solution of $CuSO_4$

Since copper sulfide has an extremely low solubility product, it is expected that a $CuSO_4$ solution will have the best desulfurization performance of the three metal sulfate solutions studied. A H_2S absorption experiment using a 1 molar $CuSO_4$ solution was carried out to verify this. Since H_2S conversions of more than 99% could be achieved during the entire experiment, no NaOH was added to the solution during the entire experiment. The initial pH of

the $CuSO_4$ solution was 3.2. During the experiment the amount of H_2S in the gas entering the reactor was varied between 1 and 4 V%. The experimental results are presented in Figure 9.

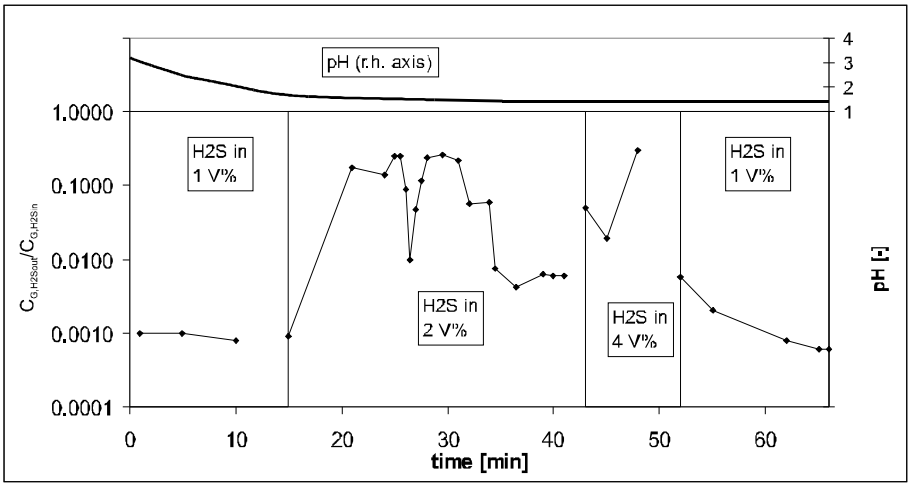

Figure 9: The absorption of H_2S in a 1.0 M $CuSO_4$ solution at a superficial gas velocity of 0.02 m/s and a liquid height in the column of 0.265 m

4.4.1 Absorption of H_2S from a gas containing 1 V% H_2S in a $CuSO_4$ solution.

During two periods of the experiment (from the start of the experiment until t = 15 min, and from t = 52 min to t = 66 min) the concentration of H_2S in the inlet gas was 1V %. From Figure 9 it can be seen that a conversion of H_2S of more than 99.5 % could be reached during these periods. The pH of the solution decreased from 3.2 to 2.1 during the first period, and remained constant at a value of 1.4 during the 2nd period.

During the experiment the solid copper sulfide formed appeared to induce foaming in the bubble column. An anti-foaming agent (a silicon oil/water emulsion) was added to the solution to reduce the extent of foaming and to improve the column performance. Small amounts of anti-foaming agent were added to the $CuSO_4$ solution during the initial 15 minutes of the experiment.

When precautions taken to prevent foaming are effective, like e.g. during the first 10 minutes of the experiment of which the results are shown in Figure 9, the observed conversion appeared to be similar to the conversion of H_2S when using a 0.1 M NaOH solution. In both cases ultimately approximately 99.9% of the H_2S present in a gas stream containing 1 V% H_2S when fed to the column was removed.

During the second period of the experiment in which the concentration of H_2S in the inlet gas was 1V % (from t = 52 min to t = 66 min), the conversion of H_2S increased gradually from 99.5 % to 99.9 %. This H_2S concentration in the outlet gas however is too close to the lower detection limit of the set-up to allow for a conclusion with respect to the observed variation in H_2S concentration.

4.4.2 Absorption of H_2S from a gas containing 2 V% H_2S in a $CuSO_4$ solution

When a gas containing 2 V% H_2S was fed to the reactor the extent of foaming increased, therefore, larger amounts of antifoaming agent were added to the solution; 1 ml of anti-foaming agent was added after 15, 21, 25 and 31 minutes while 4 ml of anti-foaming agent was added after 32 minutes. The results presented in Figure 9 show that the H_2S conversion varies between approximately 75% and 90% when the foaming phenomena is insufficiently suppressed (in the time frame from 15 to 32 minutes), however more than 99% conversion of H_2S can be achieved if sufficient anti-foaming agent is added to the washing solution (from t = 32 min to t = 41 min). The maximum observed conversion of H_2S is somewhat lower than the conversion when 1 V% of H_2S was present in the gas entering the bubble column, but this effect can probably be ascribed to a change in the specific contact area in the reactor, or a slightly different gas flow pattern.

4.4.3 Absorption of H_2S from a gas containing 4 V% H_2S in a $CuSO_4$ solution

Due to foaming of the solution in the bubble column it was not possible to realize stable operation at a H_2S concentration of 4 Vol% (from t = 43 min to t = 52 min). In this situation the observed conversion of H_2S dropped significantly, but this most probably has to be attributed to precipitation related foaming phenomena.

4.4.4 General conclusions regarding the absorption of H_2S from a gas stream in an aqueous solution of $CuSO_4$

The results of the experiments carried out in a bubble column using a 1M $CuSO_4$ solution show that the H_2S conversion can be similar to the conversion of H_2S when using a 0.1 M NaOH solution at similar column lenghts. In both the $CuSO_4$ and the NaOH case approximately 99.8% of the H_2S present in a gas stream containing 1 V% H_2S could be removed. No restrictions were found with respect to a lower limit of the pH during the experiment (the pH value of the solution varied between 3.2 and 1.4 during the experiment).

It also appeared that the H_2S removal efficiency of the bubble column decreased significantly with increasing H_2S concentration in the inlet gas. It is likely that the cause for this must be found in foaming related changes in the hydrodynamic behavior of the column.

From the results of the thermodynamical equilibrium calculations shown in Figure 3, and the experimental results it can be concluded that a relatively large operating window to assure a selective desulfurization using a $CuSO_4$ solution can be defined: to avoid the precipitation of $CuCO_3$ at a CO_2 vapor pressure of 0.3 bara (30V% at 1 bara) the pH of the solution must be kept below 5.20, while experiments show that the scrubbing solution still works effectively at pH values as low as 1.4.

4.5 Carbonate precipitation

The possible formation of solid carbonates has been experimentally studied by filling the reactor with a 1M metal sulfate solution, and allowing a stream of pure CO_2 to bubble through the reactor (1.1bara, 293K). Visually no solid carbonate formation in the solutions was observed. The pH of the $Fe(II)SO_4$, the $ZnSO_4$ and the $CuSO_4$ solution saturated with CO_2 was 3.40, 3.90 and 3.92 respectively and did not change in time, indicating that no reaction other than the hydrolysis of CO_2 in water was taking place. However, thermodynamic equilibrium calculations show that the formation of solid carbonates from the solutions of $Fe(II)SO_4$ and $ZnSO_4$ is very well possible. The apparent absence of the formation of solid carbonates during the time of the experiment must probably be attributed to the relatively low driving force for the precipitation reaction in combination with a low concentration of nuclei on which these solids can deposit (Nielsen (1964), Söhnel (1992)).

5 Pilot-Plant scale experiments : the absorption of H_2S from a biogas stream.

5.1 Introduction

To demonstrate the absorption of H_2S from an industrial gas in a $CuSO_4$ solution on a larger scale a pilot plant was constructed. In this pilot plant a biogas containing H_2S was brought in contact with a $CuSO_4$ solution. The feasibility of the re-use of a regenerated copper sulfate solution was also investigated.

5.2 Experimental Set-up and procedure

The pilot plant (see Figure 10) can be subdivided in the reactor section and the liquid circulation circuit.

5.2.1 Reactor section and gas circuit

From a biogas holder, in which biogas is stored at a pressure of 0.008 barg and at ambient temperature, a gas stream was withdrawn. The bio-gas stream consisted of a mixture of CO_2 (approximately 35 V %) and CH_4 (approximately 65 V %) with a H_2S content varying from 350 ppmV to 2000 ppmV. The biogas was led through the reactor (K1), which was operated in co-current down flow mode. The inner diameter of the reactor was 0.15 meter. In the reactor a random packing, consisting of polypropylene Pall rings with a diameter of 16 mm was dumped. The height of the packing was 0.8 m. A liquid distributor was used to ensure a good division of the $CuSO_4$ solution over the packing. The co-current down flow packed bed contactor was chosen because it is suited for a fast reaction, has a low pressure drop, and allows for a high gas phase reactant conversion (Trambouze, 1988).

In the reactor the $CuSO_4$ solution reacts with H_2S present in the biogas to form insoluble copper sulfide and sulfuric acid. The desulfurized gas that leaves the absorber was led through vessel V2 and a gas flow meter (Fl1). To prevent the possible carry-over of foam that might have formed in the biogas scrubber a gas-liquid separator (V2) was installed in the gas outlet

5.2.2 Liquid circulation circuit

The $CuSO_4$ solution was stored in vessel V1. The centrifugal pump P1 was used to transport the $CuSO_4$ solution from vessel V1 via flow meter Fl2 to the packed bed reactor (K1). After the slurry leaves the reactor, it flows into a vessel under the reactor, designed to separate the solid particles from the solution. An overflow on the separator vessel allows the washing liquor to flow back to vessel V1. The settled particles can, together with a certain amount of washing liquid, be removed from the set-up through valve T1.

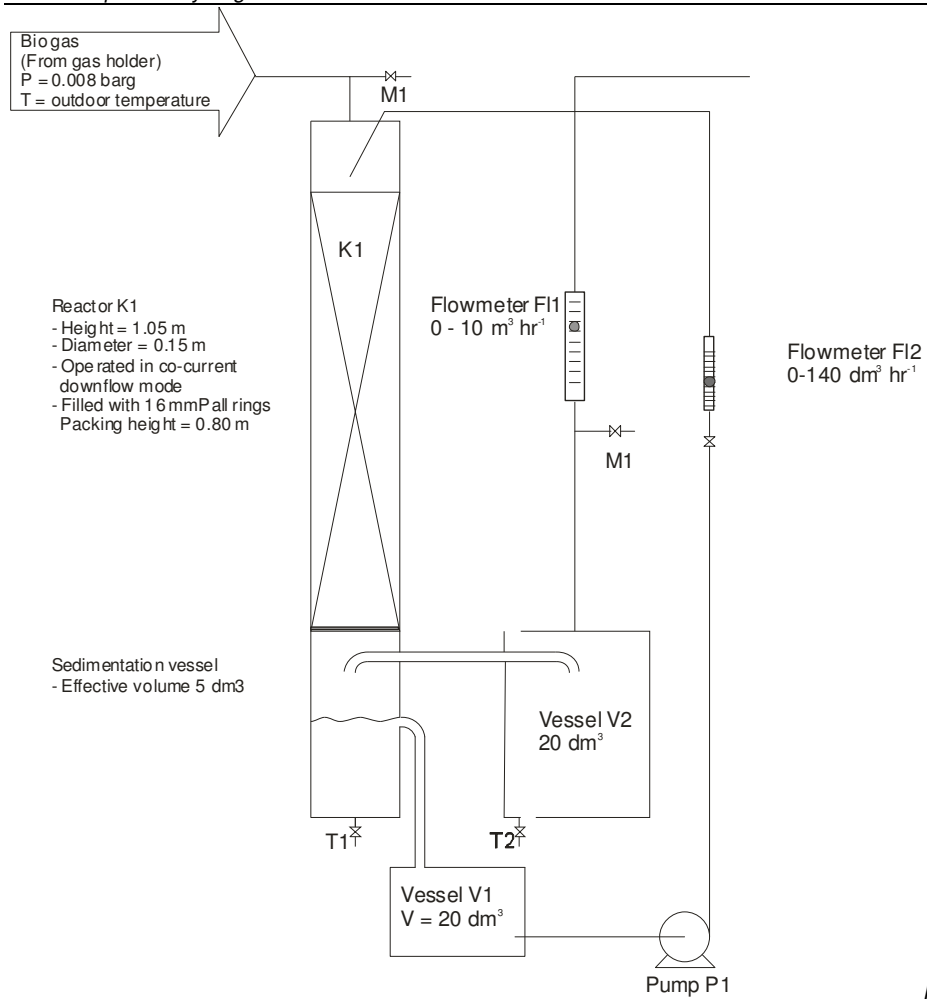

Figure 10 Schematical representation of the experimental set-up.

5.2.3 Experimental procedure

To ensure adequate supervision, the pilot plant was operated during day shift hours only. During the weekend the biogas producing facility was not operated, and hence the pilot plant was also not operated. The following experimental procedure was applied. Vessel V1 was filled with 20 liters of a $CuSO_4$ solution. When the ambient temperature was below the freezing point some anti-freeze (Ethylene glycol) was added to the washing liquid. The washing liquid was pumped through the liquid circulation circuit at a fixed flow rate. Once the liquid circulation was operational the biogas was fed to the pilot plant. During operation the concentration of H_2S of the gas entering and leaving the reactor was monitored daily. The experiment was terminated when the degree of H_2S removal decreased considerably.

5.3 Results

To demonstrate experimentally that H_2S can be removed efficiently from a biogas stream 2 long-term experiments have been carried out with the pilot plant set-up. First goal was to show that the proposed desulfurization process is suitable to realize a high degree of H_2S removal (See section 5.3.1). Secondly, the effect of the re-use of the copper on the absorption characteristics was investigated (See section 5.3.2).

5.3.1 Experimental series 1 in the Pilot Plant.

A total of 20 dm^3 of an aqueous 0.5 M $CuSO_4$ solution was brought in vessel V1. Since the ambient temperature varied between -5 and 9 ºC, 5 liters of anti-freeze (Ethylene glycol) were added to the washing liquid, resulting in a mixture of 25 dm^3 0.37 M $CuSO_4$. The gas stream through the column was set at approximately 3 $m^3\ hr^{-1}$ and the flow of the washing liquid was approximately 0.14 $m^3\ hr^{-1}$.

During operation the concentration of H_2S of the gas entering and leaving the reactor was monitored daily (See Figure 11). From this Figure it can be seen that when the $CuSO_4$ concentration in the washing liquid is sufficiently high, the scrubber is capable of decreasing the H_2S concentration in the gas with approximately 85%. The average concentration of H_2S in the gas stream leaving the absorber was approximately 170 ppm. This removal efficiency may seem somewhat lower than might be expected based on the removal efficiency of the lab scale bubble column experiments, but the relatively small wetted fraction of the packing explains for this observation as will be demonstrated via calculations of which the results are shown in Table 7. The $CuSO_4$ concentration is also plotted in Figure 11 as a function of time[5]. When the $CuSO_4$ concentration decreased to approximately 0.17 mole dm^{-3} (at a pH value of approximately 0.60), the degree of removal dropped substantially. It is not likely that the lower copper ion concentration is responsible for this effect. However, since a steadily increasing concentration of (hydrophobic) CuS particles is present in the circulating liquid (as was visually observed) the foaming phenomenon (also observed during the lab scale bubble column experiments) might be held responsible for the decrease in H_2S removal efficiency.

[5] The course of the copper sulfate concentration in time has been estimated from the total absorbed amount of H_2S. The initial and final copper concentration of the washing liquid have been determined analytically however. The difference between the two approaches appeared to be less than 20%, which seems quite acceptable taking into consideration that e.g. the H_2S concentration in the biogas varies during the day and was not monitored continuously.

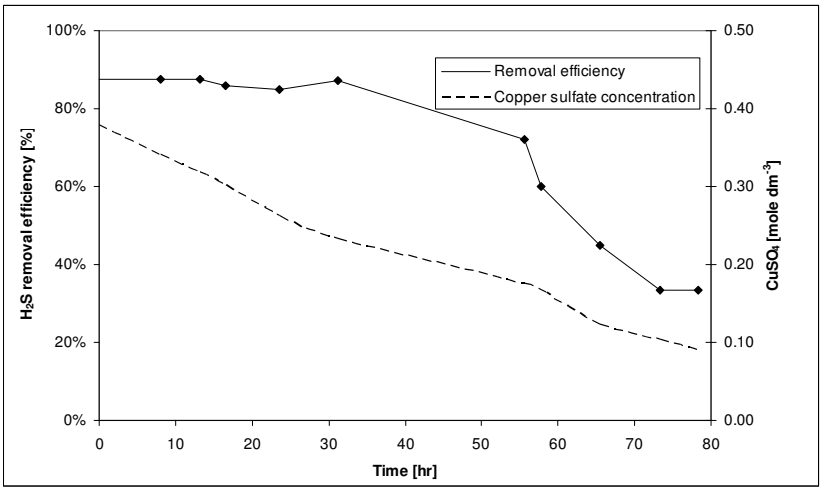

Figure 11: H_2S conversion as a function of time during experiment 1, T = -5 – 9 ºC, P = 1 atm, $[CuSO_4]_{initial}$= 0.37 M, $[H_2S]_{in}$ = 500-2000 ppm.

In Table 7 the characteristics of the absorption column are listed together with the mass transfer parameters of that column calculated using the well known relations given by Onda *et al.* (1968). It appears that the experimentally obtained degree of H_2S removal (85% removal) agrees quite well with the theoretical degree of H_2S removal expected in case of a totally gas phase mass transfer limited H_2S absorption (79% removal).

Table 7: Absorption column characteristics and calculated performance based on a gas phase mass transfer limited process

Parameter	*unit*	*Experiment 1*	*Experiment 2*
	Column		
Diameter	m	0.15	0.15
Height packing	m	0.8	0.8
Temperature	°C	-5 – 9 ºC	5 – 12 ºC
Pressure	Pa	10^5	10^5
	Packing		
Type		Pall rings	Pall rings
Diameter	m	$16 * 10^{-3}$	$16 * 10^{-3}$
Specific surface area	$m^2\ m^{-3}$	340	340
	Absorbent Flow		
Mass flow liquid	$kg\ s^{-1}$	0.039	0.28
Copper concentration	$mole\ m^{-3}$	170-370	90-370
Liquid loading	$kg\ m^{-2}\ s^{-1}$	2.2	15.8
Hydrodynamic regime		Trickling flow	Trickling flow
	Gas Flow		
Gas volume flow	$m^3\ s^{-1}$	$8.3 * 10^{-4}$	$11.5 * 10^{-4}$
Gas loading	$kg\ m^{-2}\ s^{-1}$	0.031	0.042
Gas residence time	s	22	16
	Mass transfer parameters		
k_L (Onda, 1968)	$m\ s^{-1}$	$1.1 * 10^{-4}$	$2.6 * 10^{-4}$
a_w (Onda, 1968)	$m^2\ m^{-3}$	46	93
k_G (Onda, 1968)	$m\ s^{-1}$	$2.0 * 10^{-3}$	$2.4 * 10^{-3}$
k_La	s^{-1}	$5.3 * 10^{-3}$	$2.5 * 10^{-2}$
k_Ga	s^{-1}	$9.0 * 10^{-2}$	$2.3 * 10^{-1}$
	Fraction of H_2S removed		
Theoretical conversion in case of gas phase mass transfer limitation *(Eq 14)*	--	**0.79**	**0.96**
Experimental value	--	**0.85**	**0.985**

5.3.3 Experimental series 2 in the Pilot Plant.

The objective of this experiment was to demonstrate that H_2S can be efficiently removed from a biogas stream, on a pilot plant scale, using a regenerated $CuSO_4$ solution. The spent solution from the previous experiment (Experimental series 1 in the Pilot Plant) was regenerated and used in the subsequent experimental series. The following procedure was used to regenerate the solution. First the copper sulfide particles were separated from the spent solution and then the copper sulfide was oxidized to copper oxide (For the regeneration procedure see Ter Maat *et al.*, (2003a)). Finally the $CuSO_4$ solution was regenerated by dissolving the obtained copper oxide in the original (acidic) spent solution.

A total amount of 20 liters of an aqueous $CuSO_4$ solution (0.37 M) was brought in vessel V1. The temperature of the set-up was equal to the outdoor temperature. During this experiment the gas stream through the column was approximately 4 $m^3\ hr^{-1}$, and to maximize the wetted fraction of the packing (as a learning experience of the results from the previous experiment) the flow of the washing liquid was increased to approximately 1.0 $m^3\ hr^{-1}$.

During operation the concentration of H_2S of the gas entering and leaving the reactor was monitored daily. When the $CuSO_4$ concentration in the washing liquid was above approximately 0.15 mole dm^{-3}, the scrubber was capable of decreasing the H_2S concentration in the gas with approximately 98.5%. This is quite close to the theoretically predicted conversion of 96% given in Table 7 for a gas transfer limited process. When the $CuSO_4$ concentration of the circulating liquid decreased until approximately 0.15 mole dm^{-3} (at a pH value of approximately 0.60), as in the previous experiment), the degree of removal dropped considerably. The exact reason for this behavior is unknown, but it can probably be ascribed to the appearance of foaming in the column caused by the increasing concentration of CuS particles in the circulating liquid.[6].

[6]After the experiment was terminated a relatively large amount (7 dm^3) of liquid was found in the overflow vessel. The copper concentration of that liquid was found to be 0.20 mole dm^{-3}. The copper concentration demonstrates that that at least a significant fraction of that liquid must have entered the overflow vessel in the time frame before the decrease in removal efficiency occurred (See Figure 2). The most likely mechanism that causes the carry-over of the washing liquid to the overflow vessel is foaming. This indicates that prior to the sudden decrease in removal efficiency, at least some degree of foaming took place.

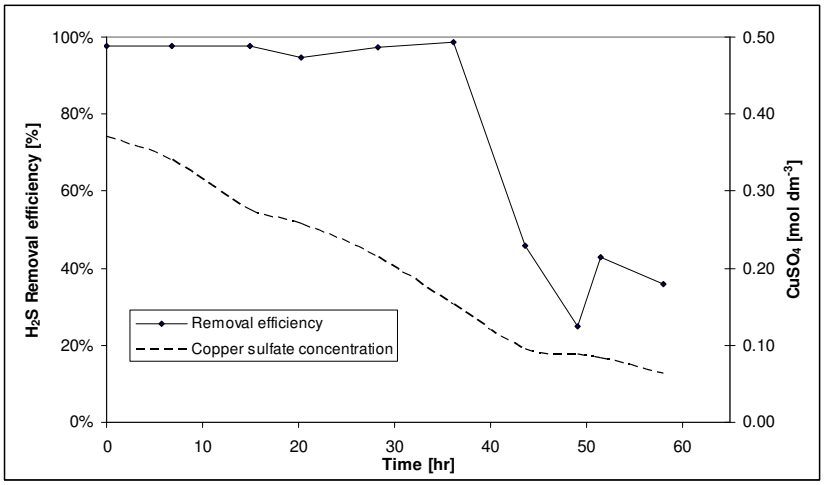

Figure 12: H_2S conversion as a function of time during experiment 2. P = 1 atm, $[CuSO_4]_{initial}$ = 0.375 M, $[H_2S]_{in}$ = 350-1000 ppm.

As a consequence of the high liquid circulation rate the solid particles did not settle completely in vessel V1 (this was observed visually). However, the solids in the slurry (at the end of the experiment the slurry contained approximately 3 wt% of solids) did not cause any notable problems with respect to plugging of the packed bed.

The experimental results show that the removal of H_2S on a pilot plant scale can take place very efficiently. The concentration of H_2S in the biogas that leaves the scrubber is comparable to the concentration of H_2S in the biogas leaving the reactor in case of a gas phase mass transfer limited absorption process (See Table 7). Furthermore, it is shown that the regeneration of the $CuSO_4$ solution did not cause any efficiency loss.

6 Conclusions

The desulfurization of gas streams using aqueous $Fe(II)SO_4$, $ZnSO_4$ and $CuSO_4$ solutions as washing liquor has been studied theoretically and experimentally. A thermodynamic study has been used to determine a theoretical operating window, with respect to the pH of the scrubbing solution, in which the metal sulfate solution can react with H_2S, but not with CO_2 in the gas or hydroxide from the solution. When the absorption is carried out in this window the proposed process should be capable of removing H_2S from the gas stream without uptake of CO_2 or the formation of metal hydroxides. The theoretical operating window increases in the order of iron, zinc to copper.

Experimental verification in a lab scale bubble column showed that when a 1 molar Fe(II)SO_4 solution was used as washing liquor the degree of acidity in the bubble column appeared to have a pronounced influence on the desulfurization performance. Only above a pH value of 6.7 a high H_2S conversion could be reached in the experimental set-up. This experimentally determined pH value is clearly above the lower pH limit calculated from the equilibrium model (~3.15). Equilibrium calculations show that at the experimentally required pH the precipitation of iron carbonates is hard to prevent when CO_2 is also present in the gas that has to be desulfurized. Furthermore, as the initial pH of an unbuffered $FeSO_4$ solution is approximately 3.0 only a small theoretical loading capacity exists. The small loading capacity and the possible loss of selectivity by the formation of solid iron carbonate makes it unlikely that an aqueous Fe(II)SO_4 solution is an efficient absorbent when a selective desulfurization process is required.

The experimental results show that, although the operating window becomes larger, an aqueous $ZnSO_4$ solution behaves similarly with respect to the absorption of H_2S as an $FeSO_4$ solution. At a pH of 5.0 or higher a high (99% or more) conversion of H_2S could be obtained with the experimental set-up. At lower pH values the conversion of H_2S decreased significantly although theoretical predictions indicate that a pH of ~ 2 should still result in a high degree of H_2S removal. The most likely explanation for the reduction of the experimental operating window as compared to the theoretical predictions is a decrease in the rate of the precipitation reaction with decreasing pH. In that case, with decreasing pH the absorption increasingly becomes a reaction rate or liquid side mass transfer rate limited process instead of the desired gas phase mass transfer limited process. This would mean that operating a scrubber using a $ZnSO_4$ solution at a pH below 5 but above 2 could still yield the desired degree of H_2S removal, provided that the residence time of the gas phase is sufficiently long. Equilibrium calculations show that at these lower pH values the formation of solid zinc carbonate can be avoided for a typical biogas composition. Therefore an aqueous $ZnSO_4$ solution shows some promise for a selective desulfurization process as long as the pH of the solution is regulated within certain boundaries ($2 < pH < 2.85$ for a typical biogas composition.).

A high H_2S conversion could be obtained down to a pH of 1.4 (lowest pH tested) when a 1M $CuSO_4$ solution was used as absorbent. The experimentally observed H_2S conversion when using a concentration of 1V% H_2S in the inlet stream appeared to be similar to the conversion of H_2S when using a 0.1 M NaOH solution, indicating that in this case the absorption was gas phase mass transfer controlled. Unfortunately during the experiments the copper sulfide precipitate caused foaming problems in the column; the extent of foaming increased with an increasing percentage H_2S in the gas stream entering the column. Addition of an anti-foaming

agent reduced these problems to a certain extent. Since thermodynamic calculations show that the formation of solid copper hydroxide is only possible at a pH above 7.70, an acidic or unbuffered $CuSO_4$ solution is a suitable solvent for the proposed desulfurization process. Selective desulfurization is only possible when the co-precipitation of copper carbonate is avoided. The exact value of the pH at which this precipitation occurs depends on the partial pressure of CO_2 in the contaminated gas stream: at a pH value of 5.2 the theoretical maximum allowable CO_2 partial pressure using a 1M $CuSO_4$ solution is 30000 Pa (30% at 1 bar).

To demonstrate the potential of the desulfurization process additional desulfurization experiments have been carried out on a pilot plant scale using an industrial biogas stream. The pilot plant was a co-current operated packed bed reactor in which fresh and regenerated $CuSO_4$ solutions were used. The experimental results show that the removal of H_2S from biogas takes place very efficiently and is probably dictated by gas phase mass transfer limitations. No problems with respect to plugging of the random packing by the precipitate were encountered. However, it is likely that for long operation times foaming in the packed column did occur.

From these pilot plant results, and the results obtained from the laboratory scale absorber, it can be concluded that when using a $CuSO_4$ solution this new desulfurization process is able to remove H_2S from gas streams selectively with respect to CO_2. The observed high conversion of H_2S over a wide operating window makes the further development of a selective desulfurization process based on the use of aqueous $CuSO_4$, and possibly $ZnSO_4$ solutions very attractive.

7 Nomenclature

Symbols

a	Specific surface area in the bubble column	[m^2 m^{-3}]
h	Height of the liquid in the bubble column	[m]
k	Mass transfer coefficient	[m s^{-1}]
m	distribution coefficient	[-]
v	Velocity	[m s^{-1}]
C	Concentration	[mole m^{-3}]
K	Equilibrium constant	[mole m^{-3}]
		[$mole^2$ m^{-6}]
P	Pressure	[Pa]
T	Temperature	[K]

Subscripts

a	Acid
i	interface
in	Referring to the gas entering the bubble column
out	Referring to the gas leaving the bubble column
sp	Solubility Product
sup	Superficial
G	Referring to the gas phase
L	Referring to the liquid phase

8 References

Broekhuis, R.R., Koch, D.J., Lynn, S., 1992, A medium temperature process for removal of hydrogen sulfide from sour gas streams with aqueous metal sulfate solutions, *Ind. Eng. CHem. Res.*, **31**, 2635-42

Brown, F.C., Dyer, W.H., Status of the EIC process for hydrogen sulfide abatement, *Geothermal Resources council Transactions*, **4**, 667-9

Danckwerts, P.V., 1970, Gas-Liquid Reactions, McGraw-Hill Book Company.

Ehnert H.H., *et al.*, 1973, Verfahren zum entfernen von Schwefelwasserstoff aus diesen enthaltenden Gasen, *German Patent 2304497*

Harvey, W.W., 1980, Process for removing hydrogen sulfide and ammonia from gaseous streams, *US Patent 4,191,854*.

Kohl, A.L., Nielsen, R.B., 1997, Gas Purification 5th ed., Gulf Publishing Co. Houston.

Licht. S, 1988, Aqueous Solubilities, Solubility Products and Standard Oxidation-Reduction Potentials of the Metal Sulfides, *J. Electrochem. Soc.*, **135**, 2971-5

Lide D.R. 1995, Handbook of Chemistry and Physics, 76th ed., CRC Press, New York

Maat, H. ter., Hogendoorn, J.A., Versteeg, G.F., 2003, The oxidation of copper sulfide – an experimental study. Chapter 4 of this thesis

Maat, H. ter., Hogendoorn, J.A., Versteeg, G.F., 2003, Selective desulfurization using copper sulfate solutions – Process design and economic evaluation. Chapter 5 of this thesis

Manning, W.P., 1979, Chemsweet, a new process for sweetening low value sour gas, *Oil and Gas Journal*, **77**, 42-p122-4

Nagl, G., 1997, Controlling H_2S Emissions, *Chem. Engng.* **3**, 125-131.

Neomagus, H.W.J.P., Swaaij, W.P.M van, Versteeg, G.F., 1998, The catalytic oxidation of H_2S in a Stainless Steel membrane Reactor with separate Feed of Reactants, *J. Membr. Sci.*, **148**, 147-60

Nielsen, A.E., 1964, Kinetics of Precipitation, Pergamon Press

Onda, K, Takeuchi, H. Okumoto, Y., 1968, Mass transfer coefficients between gas and liquid phases in packed columns, *J. Chem. Eng. Japan*, **1**, 56

Pauss, A., Naveau, H., Nyns, E.-J., 1987, Biomass : Regenerable Energy, Chichester 273 - 291.

Perrin, D.B., 1982, Ionization constants of Inorganic Acids and Bases in Aqueous Solution, 2nd edition, Pergamon, Oxford

Söhnel, O, Garside, J., 1992, Precipitation, basic principles and Industrial Applications. Butterwoth Heinemann Ltd.

Spevack, J.S., 1980, Process for controlling environmental pollution from steam containing hydrogen sulfide, *US Patent 4,202,864*,

Westerterp, K.R., Swaaij, W.P.M. van, Beenackers, A.A.C.M., 1984, Chemical Reactor Design and Operation, John Wiley & Sons,

Chapter 3: Theoretical and experimental study of the absorption rate of H_2S in $CuSO_4$ solutions: The effect of enhancement of mass transfer by a precipitation reaction

Abstract

In the current study the desulfurization of gas streams using aqueous copper sulfate ($CuSO_4$) solutions as washing liquor is studied theoretically and experimentally. The desulfurization is accomplished by a precipitation reaction that occurs when sulfide ions and metal ions are brought into contact with each other.

Absorption experiments of H_2S in aqueous $CuSO_4$ solutions were carried out in a Mechanically Agitated Gas Liquid Reactor. The experiments were conducted at a temperature of 293 K and $CuSO_4$ concentrations between 0.01 and 0.1 M. These experiments showed that the process efficiently removes H_2S. Furthermore the experiments indicate that the absorption of H_2S in a $CuSO_4$ solution may typically be considered a mass transfer limited process at, for this type of industrial process, relevant conditions.

The extended model developed by Al-Tarazi et al. (2004) has been used to predict the rate of H_2S absorption. This model describes the absorption and accompanying precipitation process in terms of, among others, elementary reaction steps, particle nucleation and growth. The results from this extended model were compared to results obtained with a much simpler model, regarding the absorption of H_2S in $CuSO_4$ containing aqueous solutions as absorption of a gas accompanied by an instantaneous irreversible reaction. From this comparison it appeared that the absorption rate of H_2S in a $CuSO_4$ solution can, under certain conditions, be considered as a mass transfer rate controlled process. Under a much wider range of conditions the error that is made by assuming that the absorption process is a mass transfer controlled process, is still within engineering accuracy. This simplification allows for a considerable reduction of the theoretical effort needed for the design of a G/L contacting device, thereby still assuring that the desired gas specification can be met under a wide range of operating conditions.

A comparison of the experimental results and the simulated results showed that the extended model gives an under prediction of the H_2S absorption rate for the experimental conditions applied.

1 Introduction

Gas-liquid processes are commonly employed in the chemical industry, for example when reacting gaseous and liquid reactants. In the case of removal of H_2S from a gas stream, the scrubbing solution may contain dissolved basic reagents (e.g. alkanolamines or NaOH), oxidizing chemicals (e.g. Fe^{3+} ligands) or components forming solids upon the reaction with S^{2-} (like most Me^{2+} ions). For a more complete overview of the existing technologies we would like to refer to the textbook by Kohl and Nielsen (1997). When the absorbed gaseous component reacts in the liquid, it is possible that the rate of absorption of the gaseous component is enhanced by the chemical reaction. Understanding how the reaction (rate) influences the gas absorption rate is therefore a vital prerequisite for a reliable design of a contactor.

For simple irreversible reactions this effect can readily be estimated using analytical or approximate solutions of various mass transfer models. These analytical solutions can for example be found in the textbook of Westerterp *et al.* (1984). For other cases (e.g. complex or equilibrium reactions) the effect of the reaction on the gas absorption rate cannot be determined analytically, making a numerical approach necessary. For the case of H_2S absorption in, and reaction with, a metal sulfate containing solution, the rate at which H_2S absorbs in the solution is the result of a number of process steps involving absorption and reaction. All process steps (see Figure 1) need to be taken into account to yield an accurate description of the H_2S absorption process.

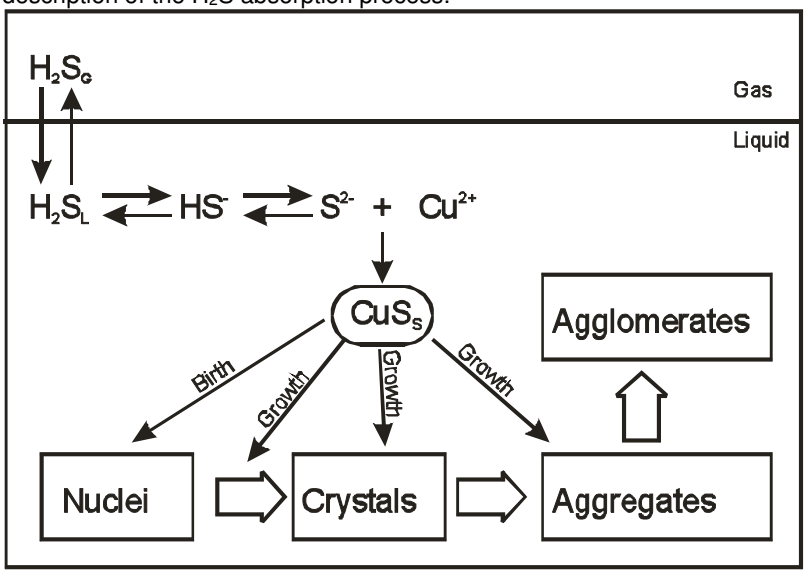

Figure 1 : Schetmatic overview of the process steps during H2S absorption in an aqueous solution containing coppersulfate.

Unfortunately, not much is known about the exact reaction rate of S^{2-} with the metal ions, although some precipitation models are available in literature The reaction rate at which S^{2-} and metal ions react to form solid metal sulfide is determined by two processes: firstly, the formation of new metal sulfide nuclei and, secondly, the growth of existing precipitates. These precipitation models state that the rate of formation of new precipitate particles is a highly non–linear function of the concentration of the reacting components (Nielsen (1964), Söhnel and Garside (1992)). Furthermore, the rate of growth of existing particles seems to be the result of a number of process steps (like diffusion of reacting components to the precipitate surface and the rate at which the ions are incorporated in the crystal), all of which can be rate-limiting.

Clearly an accurate model incorporating all absorption and reaction steps is required to describe the rate of absorption of H_2S in a metal salt solution. Such a model has been developed by Al-Tarazi *et al.* (2004). This extensive model was developed as a tool for the design of contactors for the removal of heavy metal salts from a liquid stream using H_2S, but can theoretically also be used as a tool for the design of contactors for the removal of H_2S from a gas stream using metal salt solutions. Parallel to this extensive model, experimental results (e.g. ter Maat (2005)) seem to indicate that, for many operating conditions, the absorption of H_2S into a $CuSO_4$ solution can also be described with a simple model that considers the absorption of H_2S in a $CuSO_4$ solution to be a process of mass transfer accompanied by an instantaneous irreversible reaction, or even as gas phase mass transfer limited absorption process. This simplified model can be regarded as an asymptotic case of the extensive model of Al Tarazi *et al.* In this contribution the theoretical results of this simplified approach will be compared with the theoretical results of the rigorous model of Al-Tarazi *et al.* (2004), and the applicability of this simplified approach will be discussed. Apart from this, an extensive experimental study on the absorption of H_2S in various copper sulfate solutions has been performed, and these results will be discussed and also compared to the results of the theoretical predictions.

2 Literature

The use of H_2S for the (selective) precipitation of valuable metal compounds from leaching solutions has been known to the ore refining industry for a long time (for a review see Kroschwitz and Howe-Grant, 1991). Thus far, only limited fundamental research on the phenomenon of absorption of H_2S in a solution, accompanied by a precipitation reaction of a highly insoluble metal sulfide, has been performed. The work of Mishra and Kapoor (1978) can be regarded as a pioneering attempt to couple the mass transfer theory of absorption of a gas in a reactive liquid and the theory of precipitation dynamics. They investigated the

precipitation of cadmium(II) sulfide from a cadmium(II) chloride solution in a bubble column reactor. The absorption of pure H_2S in a diluted cadmium chloride solution could, according to their own conclusions, be described by assuming that the absorption of H_2S into the solution was accompanied by an instantaneous irreversible reaction between H_2S and the metal ion. The mass transfer model used in their study was based on the Higbie penetration model (Higbie, 1935). It must be noted however that the cadmium chloride concentration applied was so low, that the influence of the reaction of the absorption rate was rather small, and therefore that the reliability of their conclusions might be debatable.

The absorption of H_2S into a diluted copper sulfate solution was investigated by Oktaybas *et al.* (1994), who used an experimental setup identical to the one used by Mishra and Kapoor (1978). Oktaybas *et al.* also used the Higbie penetration model and the assumption of an irreversible instantaneous reaction between H_2S and Cu^{2+} to explain the results. Although the agreement between theory and experiment was good for pH values larger than 2, their model did not explain the observed dependency of the absorption rate on the pH, observed at pH values below 2. Oktaybas *et al.*(1994) ascribed the decrease of the absorption rate with decreasing pH to the shift in the $H_2S/HS^-/S^{2-}$ equilibria and the resulting lower S^{2-} concentration.

Broekhuis *et al.* (1992) investigated the removal of dilute H_2S from a gas stream using copper and zinc sulfate solutions in a stirred cell reactor. Here, the rate of absorption of H_2S in a copper sulfate solution was found to be gas phase mass transfer limited, while the absorption rate of H_2S into a zinc sulfate solution was found to be a function of the amount of unconverted zinc sulfate. They did not attempt to present a fundamental description of the simultaneous absorption and precipitation of H_2S in metal sulfate solutions. Ter Maat *et al.* (2005) investigated the removal of dilute H_2S from a gas stream using copper, zinc and iron sulfate solutions in a bubble column reactor. The $CuSO_4$ solution was shown to be the most suitable solution for H_2S removal. The laboratory experiments indicated that the absorption of H_2S in a $CuSO_4$ solution, at the experimental conditions tested, is a gas phase mass transfer limited process. In the same study the applicability of a $CuSO_4$ solution for the removal of H_2S from a biogas stream was successfully demonstrated on a pilot plant scale.
Additionally, the use of metal salt solutions for desulfurization has been mentioned in open literature in articles by Manning (1979) and Brown (1980), and in the patents of Spevack (1980) and Harvey (1980), but no model description of the absorption of H_2S into a metal salt solution, accompanied by a precipitation reaction, was presented. Such a more fundamental model, describing the absorption of H_2S into an aqueous solution of (a mixture of) metal salts, accompanied by a precipitation reaction, was developed by Al-Tarazi *et al.* (2004). This mass transfer model, which will also be used in this study, also takes specific precipitation related

phenomena, such as the nucleation of new particles and particle growth, into account and can be used as a tool for the design of contactors.

3 Theory

3.1 Reaction scheme

Upon the absorption of H_2S into an aqueous bivalent metal sulfate solution the following reactions will occur. After H_2S is dissolved in water (Eq. 1) it dissociates in two steps according to Eq. 2 and 3:

$$H_2S(G) \longleftrightarrow H_2S(L) \quad (1)$$

$$H_2S + H_2O \underset{k_{1,2}}{\overset{k_{1,1}}{\longleftrightarrow}} HS^- + H_3O^+ \quad (2)$$

$$HS^- + H_2O \underset{k_{2,2}}{\overset{k_{2,1}}{\longleftrightarrow}} S^{2-} + H_3O^+ \quad (3)$$

When sufficient thermodynamic driving force (i.e. at a supersaturation ratio larger than 1) is present the subsequent precipitation reaction between the sulfide ion formed during the second dissociation step, and the metal ions can occur:

$$Me^{2+} + S^{2-} \xrightarrow{k_3} MeS\downarrow \quad (4)$$

The supersaturation ratio is defined as[7]:

$$S = \frac{[Me^{2+}][S^{2-}]}{K_{SP}} \quad (5)$$

Other reactions that occur are the water equilibrium (Eq. 6), and the dissociation reaction of the bisulfate ion (Eq. 7):

$$H_3O^+ + OH^- \underset{k_{5,2}}{\overset{k_{5,1}}{\longleftrightarrow}} 2\,H_2O \quad (6)$$

$$HSO_4^- + H_2O \underset{k_{6,2}}{\overset{k_{6,1}}{\longleftrightarrow}} H_3O^+ + SO_4^{2-} \quad (7)$$

The equilibrium constants of Eq. 2 to 7 are presented in Table 1.

[7] Note that no allowance has been made for non-ideality in the equilibrium model

Table 1 Equilibrium constants

Reaction	*Equilibrium constant*	*Numerical value pK*	*Source*
2	$K_{a1,H_2S} = \frac{[HS^-][H_3O^+]}{[H_2S]}$	6.97	Horvath, 1985
3	$K_{a2,H_2S} = \frac{[S^{2-}][H_3O^+]}{[HS^-]}$	12.9	Horvath, 1985
4	$K_{SP} = [Me^{2+}][S^{2-}]$	23.7 for ZnS 39.2 for CuS	Dean,1992
6	$K_w = [H_3O^+][OH^-]$	14	Horvath, 1985
7	$K_{a2,H_2SO_4} = \frac{[H_3O^+][SO_4^{2-}]}{[HSO_4^-]}$	2.0	Horvath, 1985

The absorption process consists of several steps, shown in Figure 2 (Note: for this graphical representation in Figure 2 the concentration profiles according to the film model are assumed. [1])

- First, component A diffuses from the bulk of the gas to the G/L interface. The driving force is the concentration difference between the bulk and the G/L interface.
- At the G/L interface component A is transferred from the gas to the liquid. In most practical cases local equilibrium exists at the interface, and the ratio of gas and liquid concentrations can be expressed as a distribution coefficient m (Westerterp, 1984). The distribution coefficient is only a function of the liquid composition and temperature when the gas phase behaves ideally.
- Component A diffuses from the G/L interface to the bulk of the liquid. The driving force for this process is the concentration gradient of A. In case of mass transfer without reaction and application of the film model, the concentration profile will be linear. For the case of absorption followed by a gas-liquid reaction, it is inevitable that some degree of reaction occurs in the mass transfer layer. In that case the consumption of A in the liquid film may affect the concentration profile to a certain extent. If this happens the rate of absorption is enhanced by the chemical reaction. The effect of an increasing reaction rate on the concentration profile is also shown in Figure 2.

[1] Note that species as HS^- and S^{2-} are not shown in this graph. Equilibrium between H_2S, HS^- and S^{2-} is reached instantaneously w.r.t. mass transport.

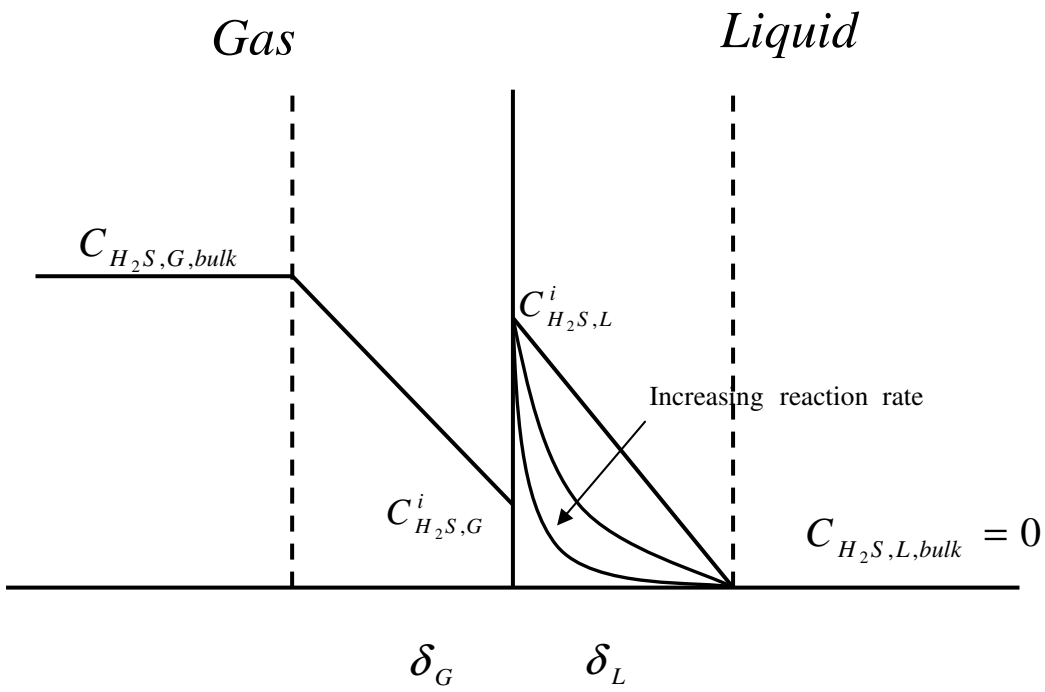

Figure 2: Concentration profile near G/L interface when H_2S absorbs in reactive liquid.

When the chemical kinetics are accurately known the effect of a homogeneous reaction on the absorption rate can be calculated using dedicated mass transfer models. However, a precipitation reaction is heterogeneous and moreover, the kinetics of most precipitation reactions are poorly known and complex. For example, the apparent reaction order for the formation of new particles is a strong function of the thermodynamic driving force for precipitation. A measure for this thermodynamic driving force is the supersaturation ratio S (Eq.5). This is illustrated by Figure 3, taken from Söhnel (1992), in which the rate of the formation of new precipitate particles is plotted against the degree of supersaturation for different values of the surface tension of the precipitates. At a supersaturation ratio larger than one, but below a certain critical value, a meta-stable situation exists. New precipitate particles are not formed at a significant rate. At values of S above the critical value new nuclei are formed and the precipitation reaction will take place at a notable speed (homogeneous nucleation). The transition from a (meta-stable) situation where the formation of new precipitates is very slow to a situation where new precipitates are formed very fast takes place with only a small change in the supersaturation ratio (Söhnel 1992, Nielsen, 1964) (e.g. for particles with a surface tension of 100 mJm^{-2} a change in log S from 1.5 to 1.75 results in a 10^7 fold increase in the rate at which new nuclei are formed). With the currently available

models, these phenomena cannot be described and therefore this hampers an accurate overall description of precipitation enhanced absorption processes as is shown in the model of Al-Tarazi et al. (2004).

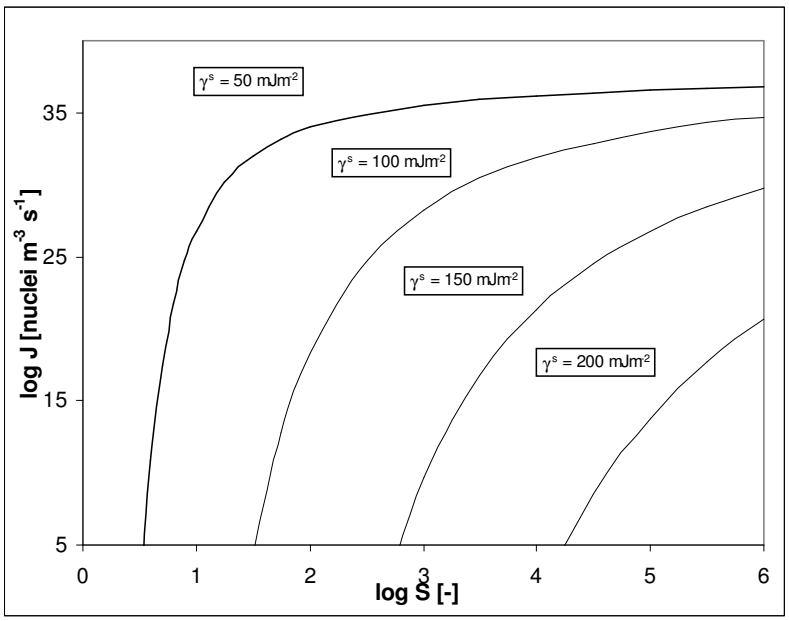

Figure 3: The rate of homogeneous nucleation from a solution as a function of the supersaturation ratio for different values of the solid interfacial energy of the precipitating substance (Söhnel 1992)

However, it is likely that for a process in which highly insoluble precipitates (as is the case for copper sulfide) are formed, the precipitation (nucleation) rate may be considered to be fast or even instantaneous with respect to the mass transfer rate. In that case, it is possible to derive a simple set of equations that describe the rate of H_2S absorption.

In this contribution the results of both the fundamental model developed by Al-Tarazi *et al.* (2004) and the simplified model will be evaluated and compared to experimental results.

4 Mass transfer models

4.1 Extended model description

Al Tarazi *et al.* (2004) have developed a model that describes mass transfer accompanied by a precipitation reaction (see Figure 3 for a schematic overview of the steps incorporated in the model). The model was specifically developed for the case of the precipitation of metal sulfides in an aqueous solution containing heavy metal ions (more specifically Cu^{2+} and Zn^{2+}) that is continuously contacted with a H_2S containing gas. This model aims to predict the effect

of operation, process conditions and reactor layout on the rate of H_2S absorption, precipitation and particle size distribution. First, the model of Al Tarazi, which has been adopted here in unchanged form, will shortly be discussed.

In Al-Tarazi's model, mass transport in the gas phase is modeled using the film model, and at the G-L interface local equilibrium is assumed. The physical equilibrium solubility of the gas in the solvent can be estimated from literature data (Horvath, 1985). The mass transfer zone is modelled according to Higbie's penetration model (Higbie, 1935), and mass balances for all species have been set up incorporating Eq 2 – 7. As a driving force not only the concentration gradient has been used, but the electrostatic potential gradient has also been taken into account. The concentration profile of the individual species in the mass transfer layer can be calculated as a function of contact time using:

$$\frac{\partial C_i}{\partial t} = D_i \frac{\partial^2 C_i}{\partial x^2} - z_i D_i \frac{F}{RT} \frac{\partial (\phi C_i)}{\partial x} - r_i \qquad (8)$$

With the exception of the rate of precipitation, all reaction rate equations are (the summation of) first order reactions. A separate mass balance for CuS has to be used since the rate of crystal growth and nucleation are separate functions of the supersaturation ratio and for these population balances have been used (for details see Al Tarazi *et al.* (2004)).

The electrostatic potential needed in Eq. 8 can be calculated by use of the Nernst-Einstein equation (Newman, 1973) (for this type of systems typically resulting in dynamic electroneutrality).

$$\phi(x,t) = \frac{RT}{F} \frac{\sum_{i=1}^{NC} z_i D_i \frac{\partial C_i}{\partial x}}{\sum_{i=1}^{NC} z_i^2 D_i C_i} \qquad (9)$$

The linear growth rate of particles is described by (Al Tarazi *et al.* 2004):

$$G = k_g \left[\frac{\sqrt{C_{Cu^{2+}} C_{S^{2-}}}}{\sqrt{K_{SP}}} - 1 \right]^g \qquad (10)$$

the molar growth rate of particles is given by (Al Tarazi *et al.* 2004):

$$G' = \sum_{i=1}^{\infty} \left\{ \beta \rho n(z, L_i^2) G L_i^2 (L_i - L_{i-1}) \right\} \qquad (11)$$

and the molar rate of birth of new particles B' is expressed by (Al Tarazi *et al.* 2004):

$$B' = \alpha \rho L_0^3 * k_n \left[\frac{\sqrt{C_{Cu^{2+}} C_{S^{2-}}}}{\sqrt{K_{SP}}} - 1 \right]^n \qquad (12)$$

The particle size distribution of the formed metal sulfide particles has been calculated using the population balance as proposed by Randolph (1988). Further details of the model description, the applied boundary conditions and relations used to describe the population balances can be found in Al-Tarazi *et al.* (2004). For the relation between the various chemical reactions the reader is referred to Figure 1.

The nucleation and precipitation growth parameters as needed in Eq. 10-12; (α.L_o. k_g, g, k_n and n) have been determined by Al Tarazi et al. (2004) by doing laminar jet experiments of gaseous H_2S in $CuSO_4$ solutions (Al Tarazi *et al.*, 2004). Using these data, the model can now be used for the prediction of the H_2S absorption rate under various process conditions.

4.2 Simplified model description

When it is assumed that the overall precipitation reaction is infinitely fast and irreversible, the mathematical description of the absorption of H_2S in a metal salt solution is dramatically simplified. Two cases can be distinguished: 1) a gas and liquid phase mass transfer limited regime and 2) as an asymptotic case of case 1), a gas phase mass transfer limited regime.

4.2.1 Case 1: gas and liquid phase mass transfer limited regime

In case of an instantaneous irreversible reaction, components A (H_2S) and B (Cu^{2+}) cannot exist simultaneously at the same location. The concentration profile (film model) in these cases is shown in Figure 4 and 5.

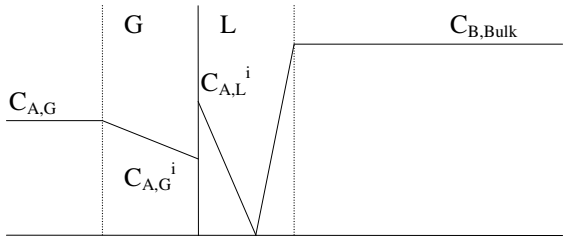

Figure 4: Instantaneous irreversible reaction in the liquid film

For the film model, the mass transfer enhancement factor for the gas and liquid phase mass transfer limited regime can be described with the infinite enhancement-factor (Westerterp, 1995):

$$E_{H_2S,\infty} = \left(1 + \frac{D_{Cu} C_{Cu,L}}{D_{H_2S} m C_{H_2S,Gi}}\right) \tag{13}$$

The H_2S absorption rate (film model) can then be described by :

$$J_{H_2S} = k_L E_{H_2S,\infty} \left(C_{H_2S,Li} - 0\right) = k_L \left(mC_{H_2S,Gi} + \frac{D_{Cu} C_{Cu,L}}{D_{H_2S}}\right) \tag{14}$$

If the interfacial H_2S concentration is eliminated from Eq. 14, the overall mass transfer (volumetric transfer rate) can be described by:

$$J_{H_2S} a = \frac{C_{H_2S,G} E^*_{H_2S}}{\frac{1}{m k_{L,H_2S} a} + \frac{1}{k_{G,H_2S} a}} \tag{15}$$

with the enhancement factor of the instantaneous irreversible reaction (for the overall mass transfer) $E_{H2S,\infty}^{*}$ defined as

$$E^*_{H_2S,\infty} = \left(1 + \frac{D_{Cu} C_{Cu,L}}{D_{H_2S} m C_{H_2S,G}}\right) \tag{16}$$

4.2.2 Case 2: gas phase mass transfer limited regime

If the absorption is carried out with a large excess of copper ions and/or low H_2S gas phase concentrations, the enhancement is typically high enough to result in a totally gas film controlled mass transfer process. The resulting concentration profile is shown in Figure 5.

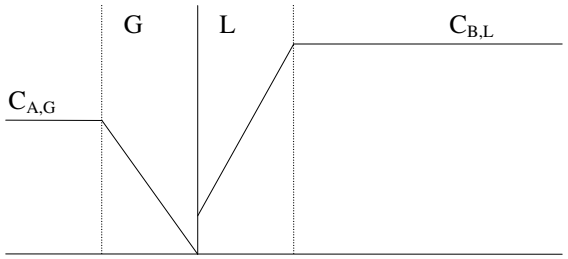

Figure 5: Instantaneous reaction at the interface

If the mass transfer rate of Cu^{2+}-ions from the liquid bulk to the interface is high compared to the mass transfer rate of H_2S from the gas bulk to the interface, only the gas side mass transfer resistance determines the overall rate of absorption. The gas side limited mass transfer of H_2S is then expressed by:

$$J_{H_2S}a = k_{g\,H_2S}aC_{H_2S} \qquad (17)$$

In case the simplification is allowed the minimum of these two cases (case 1 by Eq. 15 and, as upper limit, case 2 by Eq. 17) defines the overall mass transfer rate of the absorption process. In this study it will be investigated to which degree, and under which conditions, this simplification is allowed. For this comparison of the absorption rate as experimentally determined, and predicted with both the simplified model and the extended model of Al-Tarazi et al. (2004) will be made.

5 Experimental setup

The experiments were performed in a Mechanically Agitated Gas-Liquid Reactor (MAGLR) (See Figure 6). The experimental setup consisted of a gas mixing section, in which the desired gas flow could be composed, a reactor section, and a gas analysis section. The MAGLR was operated batch wise with respect to the liquid phase and continuously with respect to the gas phase.

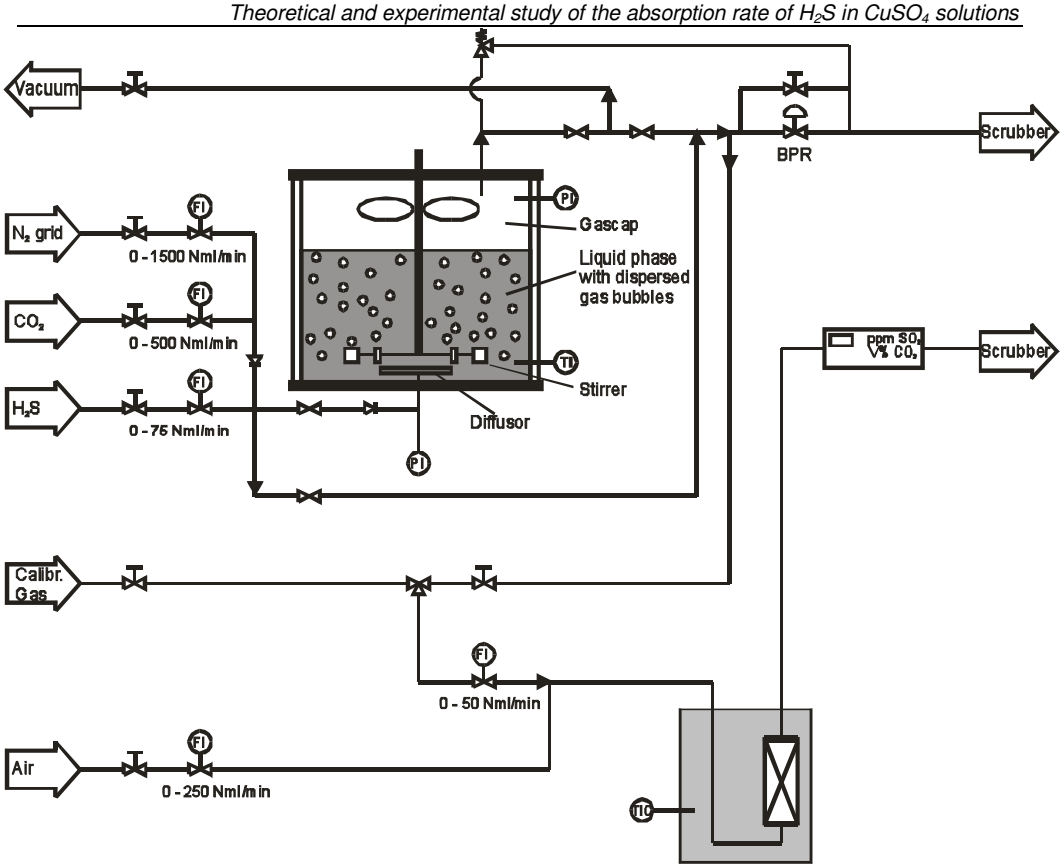

Figure 6: Schematic representation of the experimental set-up

The glass double walled reactor, internal diameter 8.25 cm, volume 1065 cm^3, was operated batchwise with respect to the liquid phase and continuously with respect to the gas phase.

The liquid could be intensely stirred with a six bladed rushton turbine, diameter 45 mm, height 11 mm, located 42 mm from the bottom of the reactor. The gas phase was mixed with a 2-bladed stirrer with a diameter of 72 mm. Both stirrers were mounted on a single axis with a diameter of 10 mm. The speed of the stirrer could be varied between 0 and 2000 rpm. The reactor was equipped with 4 baffles with a height of 104 mm and a width of 8 mm. Gas was sparged into the liquid with a diffusor placed about halfway the turbine stirrer and the bottom of the reactor. The diameter of the diffusor was 25 mm. The diffusor had 5 holes in a rectangular pitch with a diameter of 1 mm.

Isothermal operation was ensured by pumping water with a constant temperature from a thermostatic bath (Tamson T 1000) through the annular space of the double walled reactor.

The temperature of the reactor contents was measured using a K-type thermocouple. The pressure in the reactor was determined with a Druck PDCR 910 pressure transducer.

In the gas mixing section a feed gas mixture with the desired flow rate and composition was prepared from pure gases using Brooks 5150 thermal mass flow controllers. The gas leaving the reactor was led through a caustic scrubber, before discharge to the atmosphere. A Tescom series 1700 back pressure regulator was used to regulate the reactor operating pressure.

For H_2S absorption experiments the gas-liquid reactor was filled with the desired solution (metal sulfate or sodium hydroxide). To avoid interference from gasses that might have absorbed from the atmosphere (e.g. N_2 or CO_2), the reactor content was subsequently degassed by evacuation. The temperature of the metal sulfate solution in the reactor was maintained at 293 K, after which, at t = 0, a gas stream with the desired composition was fed into the reactor at a flowrate of 5.0 Nml/s[2]. The pressure in the reactor was kept at 120 kPa. A small gas sample stream from the reactor effluent was diluted with air, and the H_2S in that stream was converted to SO_2 at 350 ºC over stainless steel wool as catalyst. The resulting SO_2 concentration in the sample stream was determined using a MAIHAK MULTOR 610 multicomponent IR analyser, which simultaneously was able to determine the CO_2 concentration if any CO_2 was present in the gas (For details see also Ter Maat, 2005).

The volumetric mass transfer coefficient of the MAGLR was determined from CO_2 absorption experiments in pure water or metal sulfate solutions. These experiments were performed either by adding CO_2 to a stream of pure N_2 (to determine the physical characteristics of the setup), or to a mixture of N_2 and H_2S (to determine the $k_{OV}a$ during an actual H_2S absorption experiment (See Appendix A for a more detailed description of the interpretation of the experimental data)).

$CuSO_4$ and NaOH (analytical grade) were obtained from Across Chimica, N_2 and CO_2 (purity of at least 99.9 %) and H_2S (purity of 99.0%) were obtained from Hoek Loos. The calibration gas was prepared by Scott Specialty Gasses, and had a composition of 1.0 V% H_2S ± 0.05%. The air used for analysis was synthetic air obtained from Hoek Loos (21 V% O_2).

[2] At a temperature of 273 K and a pressure of 1.013 bar.

6 Experimental results and discussion

During introductory (batch) experiments using a stirred cell with an undisturbed, flat G/L interface, the formed copper sulfide particles floated on the liquid surface, probably due to their hydrophobic nature. This hampered the interpretation of the experimental results. Therefore, the mechanically agitated gas-liquid reactor (in which the G/L interface is less static) was subsequently chosen as a model reactor. An extra advantage of the MAGLR is that the G/L behavior of a MAGLR more closely resembles that of an industrial absorber than that of a flat interface model reactor. A drawback of this reactor type appeared to be that the Residence Time Distribution (RTD) of the gas phase could not be described by plug flow nor by CISTR like behaviour. A review article by Joshi *et al.* (1981) concludes that the gas phase RTD in MAGLR's is equivalent to a single CISTR or two CISTR's in series or in between the two. Hanhart *et al.* (1963) found that the RTD of the gas phase can be described adequately by a single CISTR at stirring speeds above the critical stirring speed[3] (900 rpm for the setup used). At lower stirring speeds, as mostly applied during this study, the RTD of the gas phase can be described by 2 CISTR's in series. Thus, the concentration of the gas leaving the reactor is not representative for the concentration of the gas phase in the reactor. This is especially important when the H_2S conversion is high, and H_2S concentrations in the gas phase may vary considerably from bubble to bubble. The method of interpretation of the experiments is described in Appendix A.

6.1 Determination of the volumetric overall mass transfer coefficient (k_La)

First a series of experiments was performed to characterize the Mechanically Agitated Gas-Liquid Reactor (MAGLR) and to determine the volumetric overall mass transfer coefficient (k_La) as a function of the stirrer speed. These experiments were performed using the absorption of CO_2 in water. At the start of an experiment a gas flow of 5 Nml s^{-1}, containing 10 V% of CO_2 was led through the experimental setup. First, the reactor was bypassed. At t = 0 s the gas stream was led through the reactor, and the CO_2 content of the gasses leaving the reactor was monitored. A typical result of an experiment is shown in Figure 7. The method described in Appendix A was used to interpret the results and determine the k_La. The results are also shown in Figure 7. It can be seen that the fit gives a good description of the experimental data. The accuracy of the k_La determined with this method is approximately 15-20%, and decreases with increasing k_La (See Fig. 6). The assumed RTD of the gas only has a relatively small influence on the k_La obtained[4].

[3] The critical stirring speed is defined as the stirrer speed at which the k_La is notably influenced by the stirrer speed.

[4] Assuming 3 CISTR's in series results in a k_La that deviates less than 10% between duplicate experiments at stirrer speeds <300 rpm. The deviation increases to 20-30% at higher stirrer speeds.

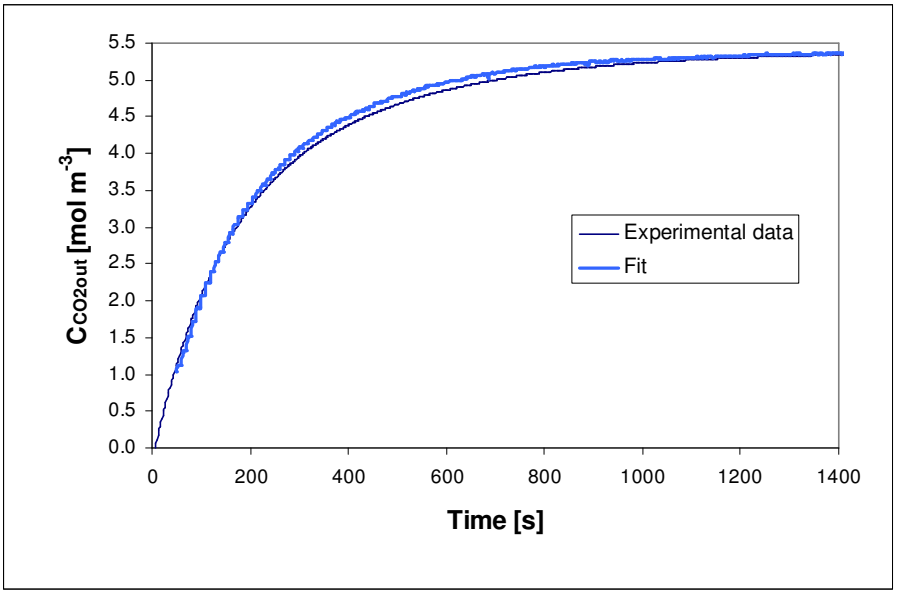

Figure 7: The result of a typical physical absorption experiment, T = 293 K, P = 120000 Pa, V = 700 ml, N = 200 rmp, CO_2 = 10 V%. k_La fitted = 3.3 * 10^{-3} s^{-1}.

The volumetric mass transfer coefficient obtained via the method described above is plotted as a function of the stirrer speed in Figure 8. In Figure 8 also the k_La calculated with various relations mentioned in literature is shown (Reith, 1968 and Yagi and Yoshida, 1975). As reference the k_La value for non-stirred bubble column reactors (Akita and Yoshida, 1973 and 1974) is also shown in this graph. The relation given by Reith (1968) [5] gives k_La as a function of the power input per unit volume. The power may stem from either a mechanical stirrer or from rising gas bubbles. In this plot the sum of both is taken as the specific power input. The relation of Reith (1968) can also be used to estimate the k_La in the absence of a stirrer (Trambouze, 1988), i.e. at N =0. The relation given by Yagi and Yoshida (1975) relates the k_La to the stirrer speed, and is only valid above the critical stirrer speed N_{RM}.

[5] Reith (1968) and Yoshide (1973) correlate the specific surface area, a, to the power input. Both recommend the relation of Calderbank (1958) to estimate k_L.

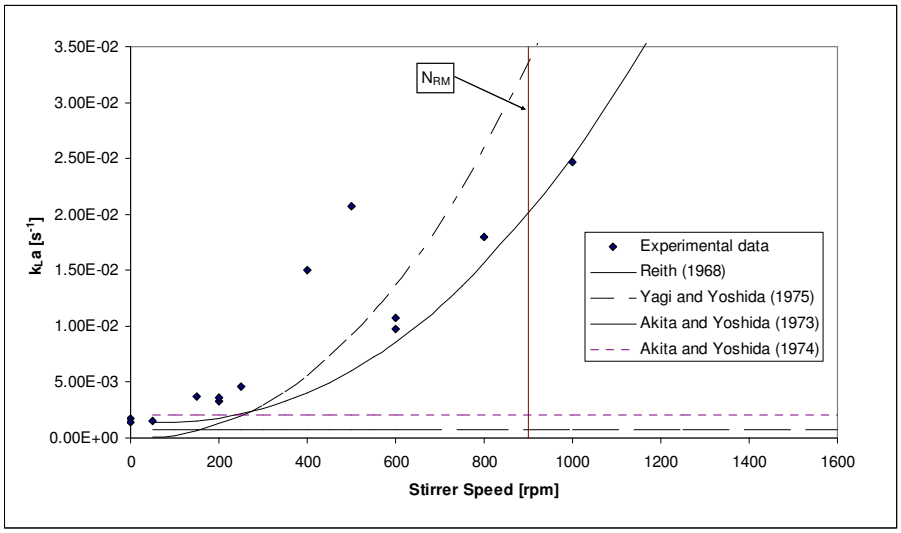

Figure 8: k_La as a function of stirrer speed. T = 293 K, P = 120000 Pa, V = 700 ml, CO_2 = 10 V%.

The results show that k_La is strongly influenced by the stirrer speed above 200 rpm., whereas at lower stirrer speeds, the influence of the stirrer speed is relatively small. For this reason further H_2S absorption experiments were carried out at a stirrer speed of 200 rpm. A discontinuity in the experimental results can be seen at a stirrer speed of approximately 600 rpm. Above this speed, a foam layer started to build. Furthermore, Figure 8 shows that in the absence of a stirring action, the relations given by Reith (1968), and Akita and Yoshida (1974) yield a k_La that corresponds well with the experimental value. Figure 8 also shows that above and around N_{RM} the relation given by Reith (1968) gives a good description of the k_La. The relation given by Yagi and Yoshida (1975) gives an overestimation. In the area between 150 and 400 rpm none of the correlations found in literature is capable of giving a correct estimate for the experimental k_La value. This is not surprising, since these relations were developed to correlate the data obtained above the critical stirrer speed N_{RM}. This underlines the importance of experimental determination of the k_La value during H_2S absorption experiments to be able to interpret the experiments correctly.

6.2 Absorption of H_2S in NaOH solutions

To further characterize the experimental setup an H_2S absorption experiment using an aqueous 0.0198 molar NaOH solution was performed. This experiment was continued up to the point where the NaOH solution was fully depleted. The reaction between H_2S and NaOH is known to be instantaneous with respect to mass transfer (Danckwerts, 1970). The H_2S absorption in a NaOH solution is therefore usually gas phase mass transfer limited, provided the gas does not consist of pure H_2S and the concentration of NaOH is sufficiently high.

Therefore this experiment was suitable to determine the H_2S concentration in the gas leaving the reactor in the case of a gas phase limited mass transport process. At the start of the experiment 600 ml of a NaOH solution was added to the reactor. After the desired reaction temperature was reached a gas stream containing 2 V% H_2S was fed to the reactor. In steady state (up to t = 2000 s) the concentration of H_2S in the gas leaving the reactor varied around 30 ppmV. The result of this experiment is shown in Figure 9: The NaOH concentration in the reactor was estimated by integration over the H_2S mass balance in time.

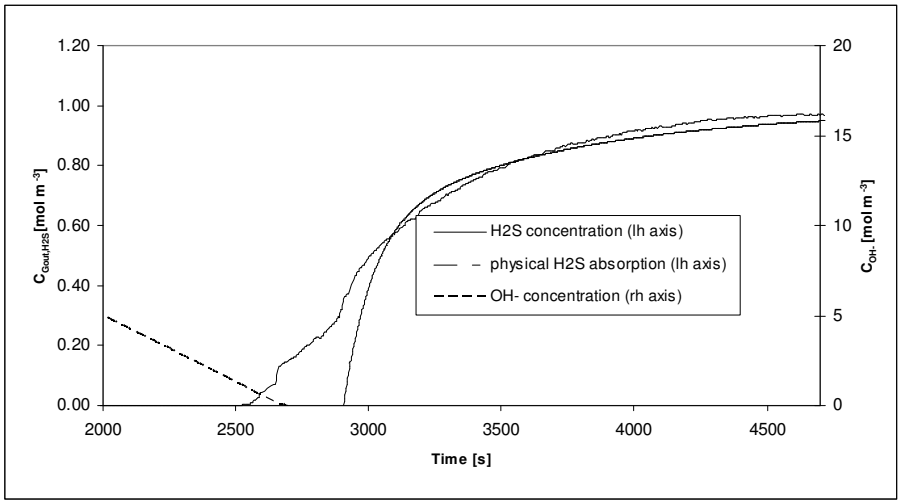

Figure 9 : The concentration of H_2S in the gas stream leaving the reactor and the concentration of NaOH as a function of time. T = 293 K, P = 120000 Pa, V_L = 600 ml, Φ_G = 5 Nml s^{-1}, N = 200 rmp,H_2S = 2 V%, $NaOH_{init}$ = 0.0198 M

It appeared that the H_2S concentration of the gas leaving the reactor was not a function of the NaOH concentration of the solution until the NaOH solution was nearly depleted. Thus, up to this point H_2S absorption apparently takes place in the gas phase mass transfer limited regime as was also expected (See also Eq. 17). When the solution is depleted the H_2S concentration in the reactor effluent increases rapidly. As reference the theoretical H_2S concentration that would occur at the outlet in the case of physical absorption in a non-reactive liquid is also shown. The time at which the theoretical curve for the physical H_2S absorption starts was chosen arbitrarily but, of course, after the experimental time at which H_2S breakthrough occurred (~2500 s). As can be seen in Figure 9, there is a remarkable resemblance between the two curves, especially from $\frac{C_{H_2S,G,out}}{C_{H_2S,G,in}} > 0.4$.

6.3 Absorption of H_2S in $CuSO_4$ solutions

With the physical characteristics of the reactor known, the absorption of H_2S in a copper sulfate solution was studied using a 0.5 M $CuSO_4$ solution. For H_2S concentrations of 4% or more foaming occurred (This effect was also mentioned in Ter Maat *et al.*, 2005). Therefore, the H_2S concentration in the feed gas was kept at 2%. It appeared that before break through of H_2S (< 12000 s) very high H_2S conversions could be obtained for a H_2S percentage in the feed gas of 2 V% or lower; concentrations of H_2S in the reactor effluent varied between 20 and 40 ppmV, which is comparable to the H_2S concentration when using a NaOH solution as absorbent.

Next, an experiment was carried out with 0.1 M $CuSO_4$ solution up to the point where the $CuSO_4$ solution was fully depleted. As with the NaOH absorption experiment the concentration of H_2S in the gas leaving the reactor in "steady state" (up to t ~ 13000 s) again varied around 30 ppmV. The $CuSO_4$ concentration had no influence on the H_2S conversion until the $CuSO_4$ concentration dropped below a very low 4 - 10 mol m^{-3} (the copper concentration in the liquid was estimated from the integration of the H_2S mass balance, the accuracy of this mass balance was approximately 5 – 10 %). Only after the $CuSO_4$ concentration dropped below 4 - 10 mol m^{-3}, indicating a Cu^{2+} conversion of more than 90%, the H_2S concentration in the reactor effluent started to increase. Taken together with the results from the NaOH experiments this demonstrates that the H_2S absorption in a copper sulfate solution most probably takes place in the gas phase mass transfer limited absorption regime if the copper concentration is sufficiently high. Because of this, a reliable performance of copper sulfate based industrial gas desulfurization units can be assured as long as there is a low concentration of copper ions in the solution. When the solution is completely depleted of Cu^{2+}, the H_2S concentration in the reactor effluent increases rapidly. As reference the increase in H_2S concentration that would occur in the case of physical absorption only is also shown in Figure 10. Just as in the case with NaOH, the experimental breakthrough curve has a close resemblance to the theoretically calculated physical breakthrough curve.

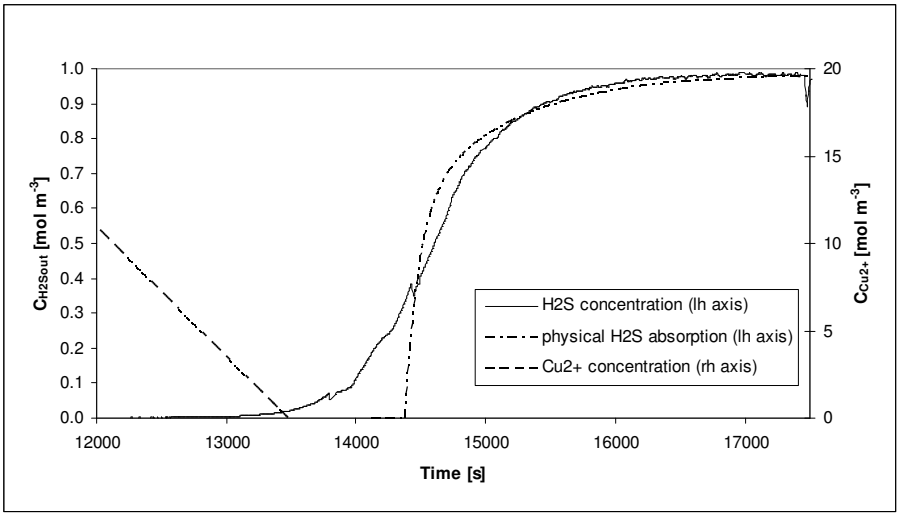

Figure 10 : The concentration of Cu^{2+} in the liquid and the concentration of H_2S in the gas stream leaving the reactor as a function of time. T = 293 K, P = 120000 Pa, V_L = 700 ml, Φ_G = 5 Nml s^{-1}, N = 200 rmp, H_2S = 2 V%, $CuSO_{4,init}$ = 0.1 M.

In a series of experiments the influence of the stirrer speed on the H_2S concentration in the reactor effluent was investigated using a 0.1 M $CuSO_4$ solution as absorbent (See Table 2). Within the experimental accuracy, the concentration of H_2S in the reactor effluent did not depend on stirrer speed. This can be explained since the relatively small increase in the overall gas phase mass transfer coefficient that occurs with increasing stirrer speed may be offset by the increasing fraction of gas bubbles with a relatively short residence time (the gas phase will show a more CISTR-like behavior with increasing stirrer speed).

Table 2: The concentration of H_2S in the gas stream leaving the reactor as a function of stirrer speed. T = 293 K, P = 120000 Pa, V = 700 ml, N = 200 rmp H_2S = 2 V%, $CuSO_4$ = 0.1 M.

N [rpm]	***H_2S [ppmV]***
50	39.0
100	45.3
150	35.1
200	33.2
250	42.2

7 Discussion

Comparison simplified and extended model results

As already pointed out in the section "Mass transfer models", if the precipitation reaction is sufficiently fast, the absorption of H_2S in the Me^{2+}-ions containing solution may be regarded as absorption of a gaseous component into a solution, accompanied by a very fast irreversible reaction. This can occur when the driving force for the precipitation reaction is sufficiently high (as is usually the case for the formation of highly insoluble metal sulfides). In this case the absorption rate can be described with equation 15 or, in the case of gas phase mass transfer limitation equation 17, which can be regarded as limiting cases of the extended model given by Al-Tarazi *et al.* (2005). This simplification allows for a considerable reduction in modelling effort and the (computation) time needed for the design of a G/L contacting device. Of course, this simplified approach will not allow for the calculation of the particle size distribution of the precipitate.

The ratio of the absorption rate as obtained with the extended model by Al-Tarazi to the flux predicted by the simplified model (Eq's 15 and 17) is shown in Figures 11 through 13. Each plot shows the ratio at a different pH. *The ratio varies from 0.3 to 0.4 (lighter grey area) to 1.0 (black).*

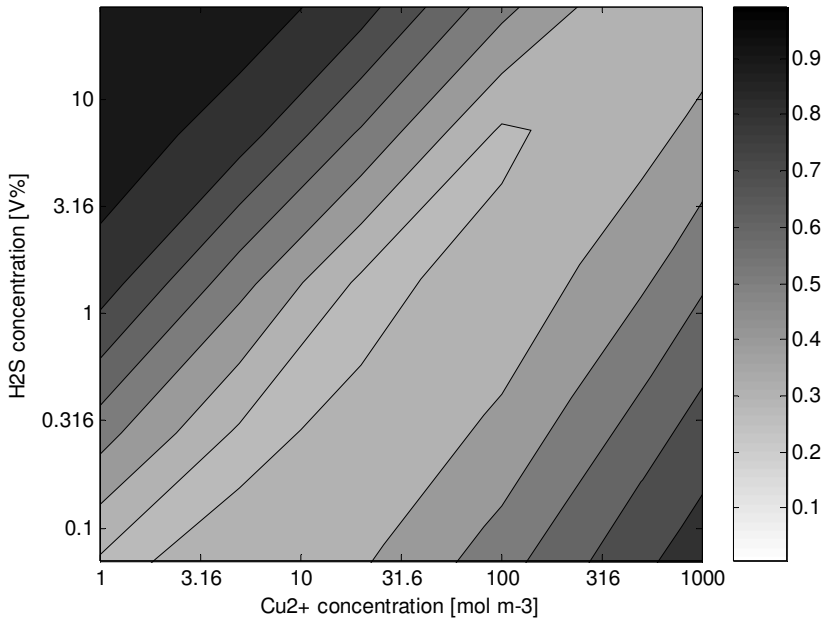

Figure 11: Absorption of H_2S in a $CuSO_4$ solution: ratio of simulated absorption rate according to the extended model and the absorption rate according to the simplified model at pH = 5.5 $k_L = 1.1*10^{-5}$ m s^{-1}, $k_G = 1.1*10^{-4}$ m s^{-1}

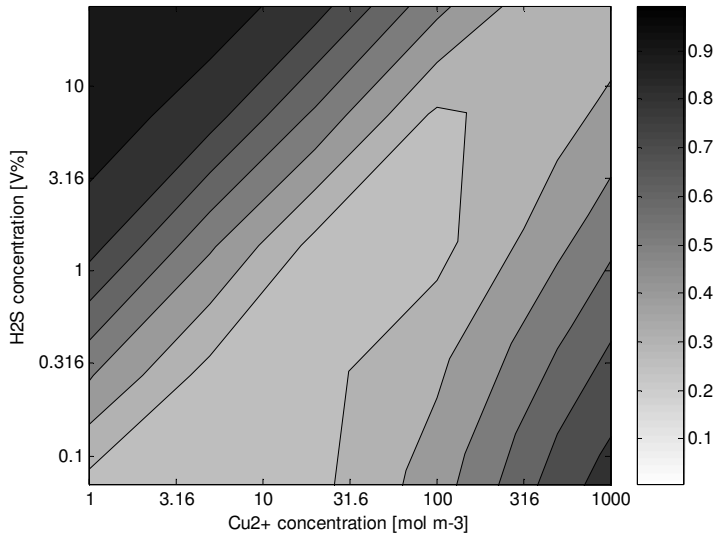

Figure 12: Absorption of H_2S in a $CuSO_4$ solution: ratio of simulated absorption rate according to the extended model and the absorption rate according to the simplified model at pH = 3.5 $k_L = 1.1*10^{-5}$ m s^{-1}, $k_G = 1.1*10^{-4}$ m s^{-}

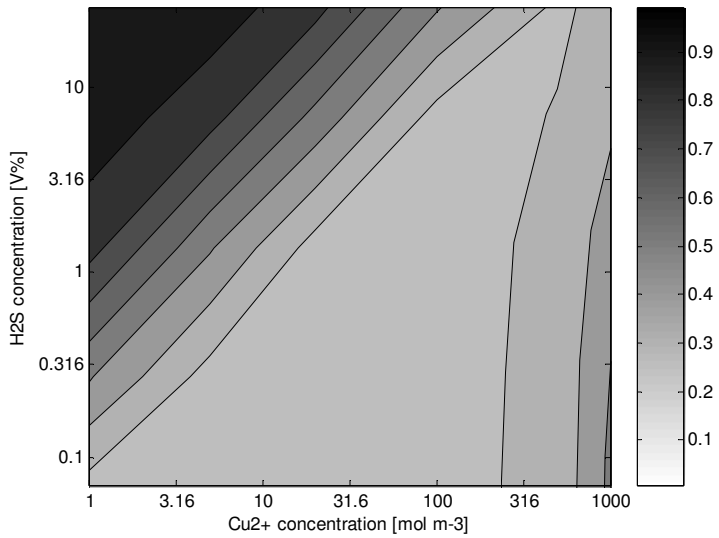

Figure 13: Absorption of H_2S in a $CuSO_4$ solution: ratio of simulated absorption rate according to the extended model and the absorption rate according to the simplified model at pH = 2.0 $k_L = 1.1*10^{-5}$ m s^{-1}, $k_G = 1.1*10^{-4}$ m s^{-}

From these Figures it can be seen that the differences between the flux as predicted by the simplified model and the predicted flux according to the extended model decreases with increasing pH. This is a consequence of the fact that the reaction rate between H_2S and Cu^{2+} predicted by the extended model decreases with decreasing pH.

Furthermore, it can be seen that the differences between the maximal possible flux as predicted by the simpified model and the predicted flux according to the extended model are relatively small (<30%) for large areas of the investigated combinations of Cu^{2+} and H_2S concentrations. At high concentrations of H_2S and low concentrations of Cu^{2+} the differences are negligible. Under process conditions that could realistically occur in a biogas desulfurization unit (<2% H_2S, high copper concentration, pH 3.5 or higher), the simplification can also be applied, however loss of accuracy (differences 30-45%) will occur.

At the remaining, more extreme, combinations Cu^{2+} and H_2S concentrations the simplified model will give a significantly different result than the extended model (the lighter areas in Figures 11 through 13, indicating differences up to 60%).

7.1 Comparison model and experimental results

H_2S absorption experiments were carried out using an H_2S concentration of 2V% and a copper concentration that varied between 0.01 and 0.1 mole dm^{-3}. The removal of H_2S took place very efficiently. The experimental results show that the concentration of H_2S in the gas leaving the reactor is comparable to the concentration of H_2S in the gas leaving the reactor in case of a gas phase mass transfer limited absorption process.

As can be seen in Figures 11 through 13, results from the models show that, for a H_2S concentration of 2V% and a copper concentration of approximately 0.1 mole dm^{-3} (the conditions at which the experiments where carried out) a significant difference between the H_2S absorption rate predicted by the extended model (incorporating mass transfer and crystal growth kinetics) and the simplified model (assuming a mass transfer limited process) exists. The results of the simplified model are in accordance with the observations that can be made from the experiments, while the results from the extended model deviate from these observations.

Hence in can be concluded that the experiments have shown that the applicability of the simplified model description is better than the extended model for the experimental conditions applied and that the extended model gives, for the experimental conditions applied, an under prediction of the H_2S absorption rate. This can be explained since, for the extended model, the kinetic parameters (particle birth and growth) are fitted from the particle size distribution of

the produced CuS, and not fitted taking the H_2S absorption rate into account. Hence the extended model will be more aimed at giving a correct prediction of the particle size distribution of the produced CuS, than at giving a correct prediction of the H_2S absorption rate.

Also bear in mind that, biogas contains (usually) less than 2 V% H_2S, while the preferred concentration of $CuSO_4$ in a $CuSO_4$ based desulfurization unit will be more than 200 mol m^{-3} (Ter Maat et al., 2005). Hence the conditions under which an actual desulfurization unit will operate are such that the removal of H_2S from biogas can be efficient and will therefore probably take place in the gas phase mass transfer limited regime.

8 Conclusions

In this study the desulfurization of gas streams using aqueous copper sulfate ($CuSO_4$) solutions as washing liquor has been studied theoretically and experimentally.

Absorption experiments were carried out in a Mechanically Agitated Gas Liquid Reactor. This reactor was characterized using the absorption of CO_2 in water. The results matched reasonably well with relations found in literature (in the area that those relations are valid). H_2S absorption experiments were conducted at a temperature of 293 K and $CuSO_4$ concentrations between 0.01 and 0.1 M. These experiments showed that the copper sulfate solution efficiently removes H_2S even at very low copper concentrations. The experimental results indicate that for industrially relevant process conditions the absorption of H_2S in a $CuSO_4$ solution may be considered a gas phase mass transfer limited process. This will result in a reliable performance of copper sulfate based industrial gas desulfurization units.

An extended model developed by Al-Tarazi *et al* (2004) has been used to predict the rate of H_2S absorption and results of it were compared to the results obtained with a simplified mass transfer model model that assumes an instantaneous irreversible reaction. This comparison showed that for many industrially relevant conditions the simplified model is able to predict the absorption rate of H_2S in a $CuSO_4$ solution within 30% of the exact result of the extended model. Under a much wider range of conditions the error the results of the simplified model are still within engineering accuracy of the theoretical result of the extended model.

Furthermore it was shown that the results from the simplified model correspond with the experimental results, while a difference between the H_2S absorption rate predicted by the extended model and the experimental results exists. For the experimental conditions applied the extended model gives a prediction for the H_2S absorption rate that is lower than the absorption rate indicated by the experiments. This deviation may be caused by that the fact that extended model was set up as a description of the precipitation process, rather than being set up to give an accurate description of the absorption rate.

9 Nomenclature

Symbols

a	Specific surface area	[m^{-1}]
g	Exponent in growth rate expression	[-]
k	Reaction constant	[s^{-1}], [m^3 $mole^{-1}$ s^{-1}]
k	Mass transfer coefficient	[m s^{-1}]
m	Gas distribution coefficient	[-]
n	Number of CISTR's in series	[-]
n	Exponent in nucleation rate expression	[-]
r	reaction rate	[mole m^{-3} s^{-1}]
t	Time variable	[s]
x	Place variable	[m]
z	Ion valency	[-]
A	Area	[m^2]
B	Particle nucleation rate	[mole m^{-3} s^{-1}]
C	Concentration	[mole m^{-3}]
D	Diffusion coefficient	[m^2 s^{-1}]
E	Residence time distribution	[-]
E	Chemical enhancement factor	[-]
F	Faraday constant	[C $mole^{-1}$]
G	Particle growh rate	[m s^{-1}] or [mole m^{-3} s^{-1}]
J	Gas absorption rate	[mole m^{-2} s^{-1}]
K	Equilibrium constant	[mole m^{-3}]
L	Particle diameter	[m]
N	Stirrer speed	[rmp]
R	Universal gas constant	[mole J^{-1} K^{-1}]
S	Degree of supersaturation	[-]
T	Temperature	[K]
V	Volume	[m^3]

Greek

α	Particle volume to length factor	[m^2]
β	Particle surface to length factor	[m]
δ	Film thickness	[m]
ε	Void fraction	[-]
ϕ	Electrostatic potential gradient	[V m^{-1}]
γ^s	Surface tension	[J m^2]
ρ	Density	[kg m^{-3}]
Δ	Denoting a difference	[-]
Φ	Volumetric flow rate	[m^3 s^{-1}]
τ	Residence time	[s]
θ'	Dimensionless time	[-]

Superscripts

i	referring to interface

Subscripts

a	Referring to acidity
bulk	Referring to the liquid bulk
g	Referring to particle growth
i	Referring to component i
n	Referring to particle nucleation
w	Referring to water
G	Referring to gas
L	Referring to liquid
OV	Overall
SP	Referring to the solubility product
SUP	Referring to superficial
0	Referring to critical nucleus
∞	Infinite

10 References

Al-Tarazi M., Heesink A.B.M., Versteeg G.F., 2004, The precipitation of water dissolved heavy metals using gaseous hydrogen sulfide: mathematical modeling. *Chem. Eng. Sci.*, **3**, 567-79.3

Akita K., Yoshida F., 1973, *Ind. Eng. Chem. Proc. Des. Dev.* **12** (1), 76

Akita K., Yoshida F., 1973, *Ind. Eng. Chem. Proc. Des. Dev.* **13** (1), 84

Broekhuis R.R., Koch D.J., Lynn S., 1992, A medium temperature process for removal of hydrogen sulfide from sour gas streams with aqueous metal sulfate solutions, *Ind. Eng. Chem. Res.*, **31**, 2635-42.

Brown F.C., Dyer W.H., Status of the EIC process for hydrogen sulfide abatement, *Geothermal Resources Council Transactions*, **4**, 667-9.

Calderbank P.H., 1958, *Transact. Int. Chem. Eng*, **36,** 443

Danckwerts P.V., 1970, Gas-Liquid Reactions, McGraw-Hill Book Company, New York.

Dean J. A., 1992, Lange's Handbook of Chemistry, Fourteenth edition, McGraw-Hill, New York.

Fair J.R., Steinmeyer D.E., Penney W.R., Crocker B.B., 1984, Gas Liquid systems, *Perry's Chemical Engineers' Handbook 6rh Ed,* McGraw-Hill, New York, 18-69

Hanhart J., Kramers H., Westerterp K.R., 1963, The residence time distribution of the gas in an agitated gas liquid contactor. *Chem. Eng. Sci.*, **18**, 503-509

Harvey W.W., 1980, Process for removing hydrogen sulfide and ammonia from gaseous streams, *US Patent 4,191,854*.

Higbie R., 1935, The rate of absorption of a pure gas into a still liquid during short periods of exposure, *Trans. Am. Inst. Chem. Eng.* **35**, 36-60.

Horvath A.L., 1985, Handbook of aqueous electrolytes solution physical properties, estimation and correlation methods, John Wiley & Sons, New York.

Joshi J.B., Pandit A.B., Sharma M.M., 1982, Mechanically agitated gas-liquid reactors; *Chem. Eng. Sci.*, **37**, 813-844

Kohl, A.L., Nielsen, R.B., 1997, Gas Purification 5th ed., Gulf Publishing Co. Houston.

Kroschwitz J.I., Howe-Grant M., 1991, Encyclopedia of chemical technology Kirk-Othmer 4th ed., Wiley & Sons. New York.

Manning W.P., 1979, Chemsweet, a new process for sweetening low value sour gas, *Oil and Gas Journal*, **77**, 42-p122-4.

Maat H. ter, Hogendoorn J.A., Versteeg G.F., 2005, The removal of hydrogen sulfide from gas streams using an aqueous metal sulfate absorbent: Part I. The absorption of H_2S in metal sulfate solutions, *Sep. Pur. Tech.*, **43**, 183-97.

Mishra K.K., Kapoor M.L., 1978, Kinetics of liquid-gas reactions through bubbles, *Hydrometallugy*, **3**, 75-83.

Newman J.S., 1973, Electrochemical systems, *Prentice Hall Inc. Englewood Cliffs N.Y.*

Nielsen, A.E., 1964, Kinetics of nucleation*, Pergamon Press Ltd*

Oktaybas C., Acma E., Arslan C., Addemir O., 1994, Kinetics of copper precipitation by H_2S from sulfate solutions, *Hydrometallurgy*, **35**, 129-37.

Randolph A.D., Larson M.A., 1988, Theory of Particulate Processes 2nd edition, Academic Press, New York.

Reith T., 1968, Physical aspects of bubble dispersion in liquids, *Delfse uitgevers maatschappij NV, Delft, PhD thesis.*

Söhnel O, Garside J., 1992, Precipitation, basic principles and Industrial Applications, Butterwoth Heinemann Ltd., Oxford.

Spevack J.S., 1980, Process for controlling environmental pollution from steam containing H_2S, *US Patent 4,202,864*.

Trambouze P, Van Landeghem H., Wauquier, 1988, Chemical reactors - design engineering operation , *Edition technip, Paris*

Westerterp, K.R., van Swaaij, W.P.M., Beenackers, A.A.C.M., 1984. Chemical Reactor Design and Operation, *John Wiley & Sons Ltd.*

Westerterp K.R., Van Dierendonck L.L., De Kraa J.A., 1963. *Chem. Eng. Sc.* **18**, 495

Yagi H., Yoshida F., 1975*, Ind. Eng. Chem. Proc. Des. Dev*. **14** (4), 488

Appendix A : Interpretation of the results and determination of mass transfer characteristics

The physical absorption of a gas A in a liquid involves several steps (Fig. A.1):

- The diffusion of the gas from the bulk of the gas to the gas liquid interface;
- The dissolution of the gaseous component into the liquid at the G/L interface;
- The diffusion of the gas from the gas liquid interface to the bulk of the liquid.

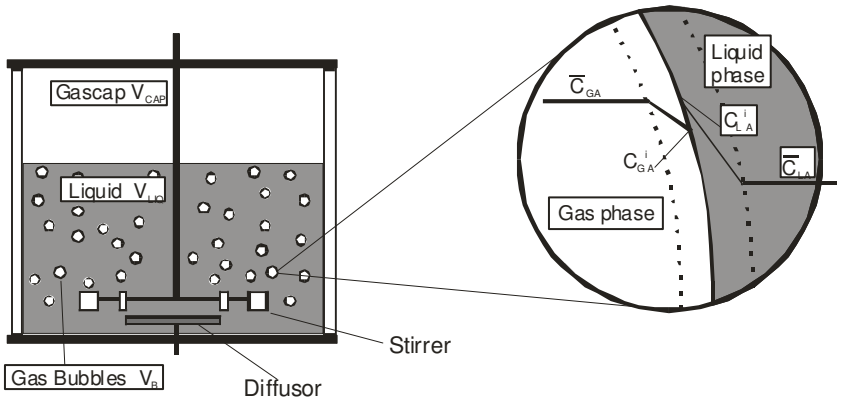

Figure A.1: Schematic representation of the mechanically agitated gas-liquid reactor

Generally, the absorption rate J of component A dissolving in a liquid without reaction can be described by:

$$J_A = k_{OV}\left(\overline{C_{G,A}} - \overline{C_{L,A}}/m\right) \quad \text{with} \quad \frac{1}{k_{OV}} = \frac{1}{k_G} + \frac{1}{mk_L} \qquad \text{(A.1)}$$

When the physical parameters, the local gas- and liquid phase bulk concentrations, and the local flux are known, the mass transfer coefficient k_{OV} can be determined. Unfortunately, the local gas and liquid phase concentrations and the local absorption flux cannot be determined, as the experimental setup used in this work only allows for integral measurements. Therefore, the following assumptions were made:

- The pressure drop in the reactor is negligible
- There is no bubble break[6]-up or coalescence[7]

[6] This is the case if $N < N_{RM}$ (Westerterp, 1963), thus for all experiments where N<900 rpm

- All bubbles have an identical diameter
- Absorption from the gas cap into the liquid is negligible
- The liquid phase is well mixed.
- The gas phase residence time distribution may be described by the CISTR's in series model.

A gas phase mass balance over a gas bubble can now be set up:

$$V_{Bubble}\frac{d\overline{C_{GA}}}{dt} = A_{Bubble}k_{ov}\left(\overline{C_{G,A}} - \overline{C_{L,A}}/m\right) \qquad (A.2)$$

Since $A_{Bubble}/V_{Bubble} = a/\varepsilon_G$, this can be expressed as:

$$\frac{d\overline{C_{GA}}}{dt} = \frac{k_{ov}a}{\varepsilon_G}\left(\overline{C_{G,A}} - \overline{C_{L,A}}/m\right) \qquad (A.3)$$

Since a pseudo-steady state may be assumed (residence time gas bubble is short compared to the time needed for significant change in liquid concentration), Eq A.3 can be solved by integrating between the boundaries t = 0 (the moment the gas enters the reactor) and t = t. The concentration of A in a bubble as a function of the time passed since the bubble has entered the reactor at t=0 can now be expressed as:

$$\ln\left[\frac{\overline{C_{GA}}(t) - \overline{C_{LA}}/m}{\overline{C_{GA}}(t=0) - \overline{C_{LA}}/m}\right] = -\frac{k_{OV}at}{\varepsilon_G} \qquad (A.4)$$

The time passed since the bubble has entered the reactor at t=0 can be replaced by the dimensionless time θ', where $\theta' = t / \tau = t/(\varepsilon_G \tau_{supG})$. The concentration of A in a bubble leaving reactor can be expressed as:

[7] This is the case for electrolytic solutions at low ε_{gas} (Fair , 1984), thus for the experiments carried out using a $CuSO_4$ or NaOH solution.

$$\ln\left[\frac{\overline{C_{GA}}(\theta') - \overline{C_{LA}}/m}{\overline{C_{GA,in}} - \overline{C_{LA}}/m}\right] = -k_{OV} a \theta' \tau_{supG} \qquad \text{(A.5)}$$

Due to stirring, not all bubbles have the same residence time. For the residence time distribution in the gas, the expression for n CISTR's in series may be used (Westerterp, 1984, p183):

$$E(\theta') = \frac{(n)^n}{(n-1)!}(\theta')^{n-1} e^{-n\theta'} \qquad \text{(A.6)}$$

The residence time distribution must be taken into account to obtain the average concentration of the gas entering the gas cap of the reactor (Fig. A.1). Expression A.7. gives the average concentration of the gas entering the gas cap:

$$\overline{C}_{G,out} = \int_0^\infty E(\theta') \overline{C_{AG}}(\theta') \, d\theta' \qquad \text{(A.7)}$$

The rate at which the concentration of A in the bulk of the liquid, C_{LA}, changes can now be described with :

$$\frac{dC_{LA}}{dt} = \frac{\Phi_{G,in} C_{GA,in} - \Phi_{G,out} C_{GA,out}}{V_L} \qquad \text{(A.8)}$$

This above set of equations cannot be solved analytically and must be integrated numerically to obtain the average concentration of A in the gas entering the gas cap (C_{LA}) and the average concentration of A in the liquid phase of the reactor ($C_{GA,out}$) as a function of time. The rate at which the concentration of A in the gas cap of the reactor $C_{Cap,A}$, changes can be described by:

$$\frac{dC_{Cap,A}}{dt} = \frac{\Phi_{G,out}}{V_{GasCap}}\left(C_{GA,cap,in} - C_{GA,cap,out}\right) \qquad \text{(A.9)}$$

Again, this expression must be integrated numerically to obtain $C_{GA,cap,out}$ as a function of time.

Summarizing: Eq.'s A.1. to A.9 can be used to describe the concentration of A in the reactor effluent $C_{GA,cap,out}$ as a function of time. The following parameters are used:

- the volumetric mass transfer coefficient $k_{OV}a$,
- the solubility coefficient m,
- the residence time distribution of the gas bubbles in the liquid,
- the gas flow rate Φ_G,
- the volume of the liquid in the reactor V_L,
- the volume of the gas cap V_{GasCap}

The gas flow rate Φ_G, the volume of the liquid in the reactor V_L and the volume of the gas cap V_{GasCap} are known. The solubility coefficient m is either known from literature or independent measurements and the residence time distribution can be found in literature. Therefore, if $C_{GA,cap,out}$ in time is known, the only unknown parameter, the volumetric mass transfer coefficient $k_{OV}a$, can be determined.

Chapter 4: The oxidation of copper sulfide – an experimental study.

Summary

The oxidation of copper sulfide is studied experimentally using a Thermo Gravimetric Analyzer (TGA) at temperatures ranging from 450ºC to 750 ºC and oxygen concentrations of 5 and 10 V%. Aim of this study was to investigate the possibilities for a selective and efficient method to convert copper(II)sulfide (CuS) into copper(II)oxide (CuO). It appeared that the products formed upon the oxidation of copper sulfide depend on the reaction temperature. However, in all cases the conversion time using the powdered samples was much shorter than expected based on literature results (typically 3 minutes versus 1-3 hours as mentioned in literature). The first reaction step in the oxidation of copper sulfide always was the fast decomposition of CuS into Cu_2S and gaseous sulfur, which immediately is oxidized further to SO_2. Subsequently, Cu_2S is then oxidized, the route depending on the reaction conditions. Oxidation experiments carried out at various temperatures showed that Cu_2S is oxidized selectively to CuO at temperatures above 650 ºC, while at temperatures below 650 ºC (basic) copper sulfate was also formed. The oxidation from Cu_2S to CuO appeared to be the result of two consecutive reactions. Cu_2S is first converted into Cu_2O, which is subsequently oxidized to CuO. The experimental results allowed for the determination of the following rate expression and (Arrhenius) relation for the reaction rate constant of the conversion of Cu_2S to Cu_2O between 650 and 750 ºC and oxygen concentrations between 5 and 10 V%.

$$R = k_{app} * m * C_{O2}^{0} \qquad [\text{mol } Cu_2S\ s^{-1}]$$

With

$$k_{app} = k_0 * e^{\frac{-E_A}{RT}} \qquad [\text{mol kg}^{-1}\ s^{-1}]$$

Where $k_0 = 1.28 * 10^3$ mole kg^{-1} s^{-1} and $E_A = 71 * 10^3$ Joule $mole^{-1}$. Although the kinetics of the reaction of Cu_2O to CuO could not be determined, it is shown that the conversion rate is of the same order of magnitude as for the reaction of Cu_2S to Cu_2O.

1 Introduction

Hydrogen sulfide (H_2S) is a component often present in industrial gases. The removal of H_2S from these gases is necessary because of its poisonousness (the MAC value is 10 ppm), and the corrosive and catalyst poisoning properties. Furthermore, the oxidation products of H_2S, SO_2 and SO_3 are considered to be among the main contributants to the so-called acid rain. To purify a gas stream containing H_2S a host of methods has been developed. Kohl and Nielsen (1997) give an extensive review of the hydrogen sulfide removal methods employed nowadays and in the past. In regenerative desulfurization processes the chemicals used for

the removal of H_2S are regenerated and can be re-used. During the regeneration process hydrogen sulfide is recovered and can be converted into marketable products. Other processes, the chemical consuming processes, use the H_2S removing chemical only once or a limited number of times. After use, the reagent must be processed or disposed of (landfill).

The gas stream that has to be desulfurized usually contains other acid components besides H_2S; carbon dioxide (CO_2) being the most common. Co-absorption of these acid components can take place when a basic agent is used in the desulfurization process. Examples of gas-liquid processes using basic washing liquors are the amine based processes and the caustic soda processes. Co-absorption of CO_2 is usually not desired, since it leads to an increase in both the amount of absorbent needed, and in the dimensions of the process equipment respectively. Therefore both the capital and operational costs of the desulfurization process are substantially higher. Furthermore, when the desulfurization process is regenerative the co-absorption causes increased energy consumption during regeneration and may even cause problems during the conversion of the recovered H_2S to end products. Since these phenomena do not occur when co-absorption of components other than hydrogen sulfide is avoided, a selective desulfurization of acidic gas streams is an attractive alternative to non-selective desulfurization.

A selective desulfurization process can be obtained by using an agent that does not utilize an acid-base reaction to remove hydrogen sulfide. An industrially applied example of such a selective desulfurization process uses iron chelates. Iron(III)chelates oxidize hydrogen sulfide directly to elemental sulfur according to:

$$H_2S + 2\,Fe^{3+}L^{n-} + H_2O \Rightarrow S^0 + 2Fe^{2+}L^{n-} + 2\,H_3O^+ \qquad (1)$$

In this step iron is reduced from Fe^{3+} to Fe^{2+}. In a separate unit, the oxidizer, iron chelate is then reoxidized to Fe^{3+} using oxygen from air.

$$O_2 + 4Fe^{2+}L^{n-} + 2H_2O \Rightarrow 4Fe^{3+}L^{n-} + 4OH^- \qquad (2)$$

The overall net process is the conversion of hydrogen sulfide and oxygen (from air) to elemental sulfur and water.

Another reaction of hydrogen sulfide that is not based on the basic properties of the reagent is a precipitation reaction that occurs when hydrogen sulfide reacts with metal ions present in an aqueous solution. Especially bivalent metal ions are suitable for this application since the solubility of the sulfides of these metals is usually very low. When a bivalent metal ion and

hydrogen sulfide are brought in contact with each other the following overall precipitation reaction can take place if the solubility product of the metal sulfide is exceeded.

$$Me^{2+} + H_2S + 2H_2O \leftrightarrow MeS\downarrow + 2H_3O^+ \qquad (3)$$

A selective absorbent, i.e. an absorbent that does not react with carbon dioxide, can be obtained when the metal ion and process conditions are chosen such that the precipitation of the corresponding metal carbonate does not occur. Investigations on the reaction of H_2S and CO_2 with aqueous metal sulfate solutions (Broekhuis, 1992, Ter Maat, 2002) have shown that a copper sulfate solution is a suitable choice for such a selective desulfurization process. Procede Twente has patented a new regenerative gas desulfurization process based on this precipitation reaction (Ter Maat and Versteeg, 1997). A simplified scheme of the process under development is shown in Figure 1.

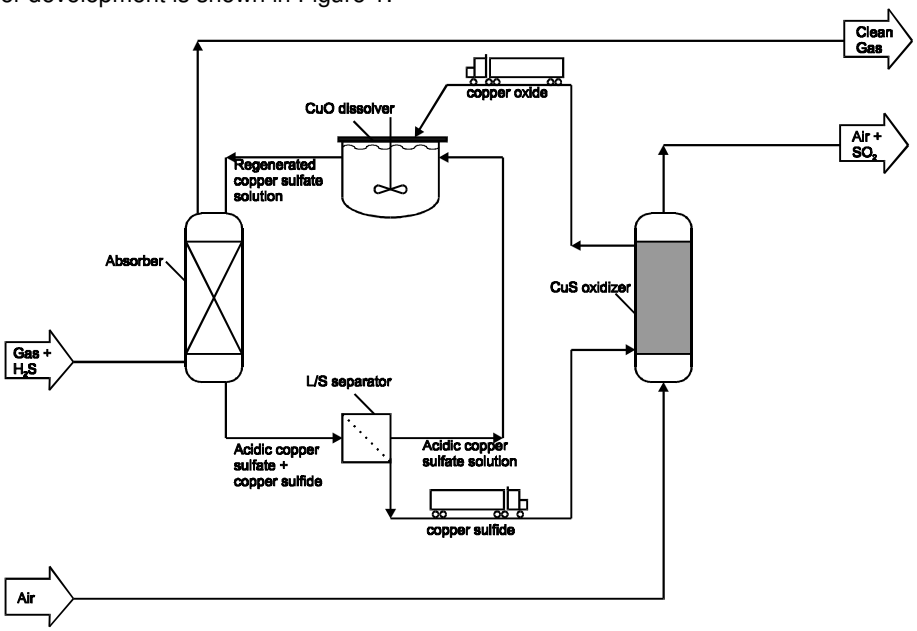

Figure 1: Process scheme of the Procede gas desulfurization process

In this process the gas stream contaminated with hydrogen sulfide is brought in contact with the washing liquor in a gas liquid contactor, the absorber. In the absorber H_2S reacts with the aqueous $CuSO_4$ solution under the formation of solid CuS and an aqueous solution of sulfuric acid. The now desulfurized gas stream is available for further processing. The precipitates in the acidic copper sulfate solution that leaves the absorber are removed from the absorbent stream in a liquid-solid separator. The now solids-free solution is brought to a dissolver. In the

dissolver a make up stream of solid CuO is added to the acidic $CuSO_4$ solution. In the dissolver CuO reacts according to :

$$CuO + 2H_3O^+ + SO_4^{2-} \leftrightarrow Cu^{2+} + 3H_2O + SO_4^{2-} \qquad (4)$$

By dissolving CuO in the acidic $CuSO_4$ solution both the acidity generated in the scrubbing step is neutralized and the scrubbing solution (Cu^{2+}) is replenished. Also a relatively small amount of water will be formed. Thus by adding solid CuO instead of e.g. solid $CuSO_4$ the need for adding an additional neutralizing agent is omitted. Summarizing it can be concluded that the absorption section of the desulfurization process consumes CuO and produces CuS and a treated, clean gas stream. This process step can function as a stand alone unit, but for economic reasons it is preferred to avoid the external purchase of CuO but to regenerate the produced solid CuS in the desulfurization process itself. A regeneration step complementary to the absorption step can be created by the oxidation of CuS to CuO. During this process step the sulfur bound by the copper will be released as SO_2, which can easily be oxidized to SO_3, which in turn can be used for the production of concentrated sulfuric acid.

For application of this desulfurization process on a small scale it might not be economically feasible to give each absorption unit its own oxidizer. This problem can be overcome if a regenerative process is composed of one single, centralized large regeneration unit that is supplied by several small scale desulfurization units. By re-using the absorbent a competitive edge may be gained on the current generation of small scale, non regenerable desulfurization units.

The object of the current investigation is to illuminate the reactions that can occur during the oxidation of copper sulfide, the products formed and the rate at which these reactions occur. The results can then be used to enable an optimal design of an oxidizing process for the regeneration of copper sulfide.

2 Literature

The oxidation reactions of copper sulfide are of importance in the refining of ore containing natural occurring copper sulfides, or copper-iron sulfide. Therefore the subject has been studied frequently. Peretti (1948) developed a method to study the reactions that occur during the roasting of CuS. A cylindrical pellet of CuS (with a diameter and a length of 28.6 mm) was placed in a furnace and oxidized in a stream of air. The temperature of the furnace used in the experiments was varied between 430 and 965 ºC. The course of the reaction was followed by removing a pellet from the furnace, allowing the pellet to cool down and cut the reacted pellet transversely, and measure the visible phase boundaries. Peretti found that CuS

is first converted into Cu_2S under the release of (gaseous) sulfur. The formed Cu_2S is then oxidized into Cu_2O, which is subsequently converted into CuO. At temperatures above 663 ºC CuO was the only observed final product; at temperatures below 663 ºC copper sulfate was also found. At temperatures below 500 ºC the reaction nearly ceased after a certain period of time. An analysis of the observed reaction rate as a function of temperature learned that a diffusion process was the rate determining step. The total reaction time needed to convert all CuS into CuO was reported to vary between 80 and 180 minutes.

Lewis *et al.* (1949) have studied the oxidation of powdered Cu_2S (with a particle size between 0.149 mm and 0.074 mm) in both air and in pure oxygen at temperatures between 250 and 700 ºC. The main interest was to determine the amount of water soluble and acid soluble copper components formed. These amounts were determined by leeching the obtained samples first with water and then with sulfuric acid. The water soluble copper component that may be formed during the experiments is $CuSO_4$. Acid soluble copper components that are likely to be formed during the experiments are CuO, $CuO.CuSO_4$ and possibly Cu_2O. Lewis *et al.* found the optimum temperature for the formation of water soluble copper components to be 450 ºC, when using air or oxygen as reaction gas. At a temperature of 700 ºC a complete conversion to acid soluble copper substances was found to be possible in 60 minutes when using air as oxidizing agent. When using pure oxygen as oxidizing agent only 8% of the Cu_2S was converted into water soluble copper components. The remainder of the copper was present as acid soluble copper components.

Ganguly and Mukherjee (1967) have studied the oxidation of CuS in a fixed bed in a nitrogen/oxygen atmosphere at temperatures varying between 340 º C and 410 ºC. The course of the reaction was followed by stopping the reaction after a certain 'time of reaction'. Then the solid products were analyzed using a method adapted from Hurd (1936). The reaction was stopped by switching off the oxygen feed to the reactor and cooling down the reactor. The amount of SO_2 evolved during the 'time of reaction' was determined titrimetrically by the determination of the amount of SO_2 that had been absorbed in the alkali absorbers through which the outlet gases were led. Ganguly and Mukherjee found that the main solid product formed during the oxidation reaction was cuprous oxide (Cu_2O). Besides cuprous oxide small amounts of cupric oxide (CuO) and $CuSO_4$ were formed. Ganguly and Mukherjee also found indications that the first step in the overall reaction was the decomposition of CuS to Cu_2S and elemental sulfur according to :

$$4\,CuS \leftrightarrow 2\,Cu_2S + S_x \qquad (5)$$

The formed elemental sulfur is, in the presence of oxygen, immediately oxidized to sulfur dioxide. No reaction was observed when the temperature was below 340ºC. At temperatures above 400 ºC the reaction in the fixed bed proceeded so vigorously that an uncontrollable temperature rise in the reactor could not be avoided. The main product was Cu_2O, while only a minor amount of $CuSO_4$ was formed. The amount of $CuSO_4$ formed increased with increasing temperature. Only a negligible amount of CuO was found at the temperatures used. Ganguly and Mukherjee also tried to establish a reaction mechanism, and to estimate the kinetic constants for that mechanism. The determined kinetic constants however are most likely influenced by the fact that the reactor did not operate isothermally during the experiments. An indication for this non-isothermality is the fact that the reaction was going to completion in a relatively short time (approximately 7-15 minutes) after an induction period up to 20 minutes.

Ramakrishna and Abraham (1971) have studied the rate of the reactions that occur during the roasting of Cu_2S. They performed experiments in which a spherical pellet of CuS (with a diameter of 12.2 mm) was placed in a reactor and oxidized in a stream of air. The temperature in the reaction was varied between 750 and 950 ºC. The course of the reaction was followed by measuring the temperature of the pellet and the amount of sulfur that left the reactor as SO_2. They found that, after an initial period, the diffusion of oxygen through the formed CuO was likely to be the rate determining step. During the initial period the temperature of the pellet differed from the temperature of the reactor. They found that the time needed for a complete conversion of a pellet of Cu_2S to CuO was approximately 280 minutes.

Açma *et al.* (1995) studied the roasting of iron ore concentrates containing small amounts of Cu_2S, CuS and $CuFeS_2$ and other metal sulfides in a rotary furnace. The object of that study was to determine the experimental conditions for the conversion of the non–ferro metal sulfides to compounds soluble in water or acidic aqueous solutions. It was found that the copper sulfides were converted mainly to basic copper sulfate ($CuO.CuSO_4$) in an atmosphere containing approximately 13 V% SO_2, and 4 V% oxygen (a typical roast gas composition found in the process used to process the ore concentrates). The optimal roasting temperature for conversion towards soluble copper components was found to be 690 ºC. The optimal time of reaction needed was found to be 3.5 hr. This optimal time was mainly determined by the need to prevent overoxidation of the iron oxide present in the sample. The overoxidation of iron oxide causes a decrease in the amount of valuable substances that can be extracted from the roasted concentrates. Their experimental results show that the formation of $CuSO_4$ and $CuO.CuSO_4$ is possible if the experimental conditions and the

reaction times allow the formation of these components even at temperatures as high as 690 ºC.

The oxidation of a pellet of Cu_2S at atmospheric pressure and various temperatures and oxygen concentrations has been studied by Asaki *et al.* (1986). The reaction temperature was varied between 750 and 850 ºC. The oxygen concentration was varied between 5 and 20 V%. The diameter of the pellets used was approximately 6 mm. The mass of the sample, determined using a microbalance, and the concentration of SO_2 in the gas leaving the reactor, measured using an infrared gas analyzer, were used to determine the course of the reaction. The oxidation of Cu_2S appeared to be a 2 stage process. First Cu_2S was oxidized to Cu_2O, which was then oxidized further to CuO. This hypothesis was supported by the intersection of a partly oxidized pellet. This pellet showed a layered structure; the core was found to be unconverted Cu_2S, the inner layer was Cu_2O, and the outer layer consisted of CuO. Under the experimental conditions the gas phase mass transfer resistance initially determined the rate of the reaction. As the reaction proceeded, diffusion through the product layer was assumed to become rate determining. Except for one experiment carried out at 750 ºC copper sulfate was not formed. At a temperature of 850 ºC the pellets melted partly due to the exothermic reaction. The time needed to completely convert a single pellet of Cu_2S to CuO was approximately 3 hours.

3 Thermodynamics

In Figure 2 a phase diagram of the Cu-S-O system is shown as a function of the partial pressure of SO_2 and O_2 at a temperature of 727 ºC. This diagram is composed using the thermodynamic data given by Barin (1993). This diagram indicates that at a temperature of 727 ºC CuO is the most stable component when a Cu-sulfur component is brought in contact with a gas mixture with a partial pressure of SO_2 less than 10^{-2} bar and a partial pressure of O_2 more than 10^{-4} bar.

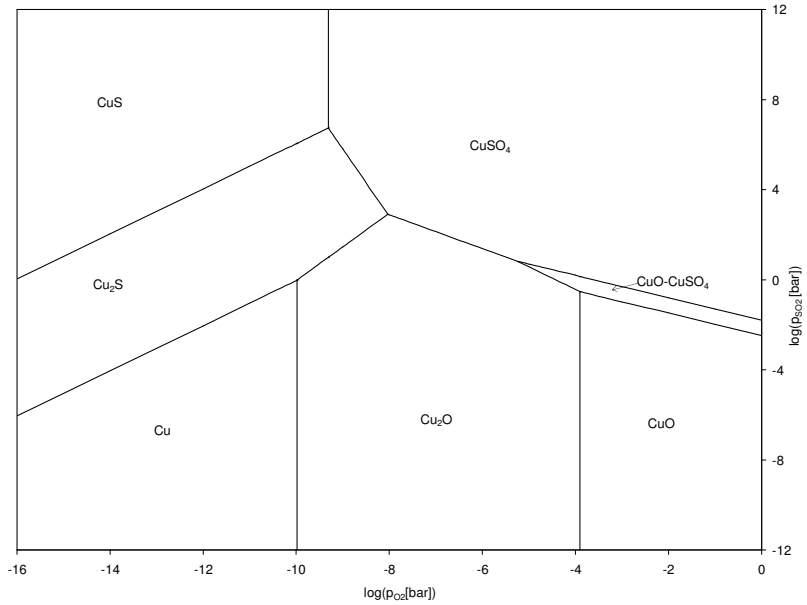

Figure 2 : Phase diagram of the Cu-S-O system at a temperature of 727 ºC

In order to establish the possible gas solid reactions during the oxidation of copper sulfide the changes in Gibbs free energy accompanying these reactions where calculated at temperatures ranging from 227 ºC to 727 ºC using the data compiled by Barin (1993). The partial pressure of O_2 and SO_2 used in these calculations was 10^{-1} bar and 10^{-6} bar respectively. The temperature range and the partial pressure of O_2 for which these calculations were performed are corresponding with the temperature range and partial pressure of O_2 at which the current copper sulfide oxidation experiments were carried out. During the experiments (tabulated in appendix A, Table A.1 and A.2) the temperature was varied between 300 ºC (near the temperature at which CuS starts to react with air) and 750 ºC, the temperature above which copper sulfate decomposes rapidly into copper oxide and SO_2, and the partial pressure of O_2 varied between $2.5*10^{-2}$ and $2*10^{-1}$ bar (being the partial

pressure of oxygen in air at atmospheric pressure). The partial pressure of SO_2 used in the calculations was set to a value of 10^{-6} bar (1ppm at atmospheric pressure) to represent the conditions at the end of an experiment, when virtually all sulfur present in the sample is converted to sulfur dioxide, and the sulfur dioxide vapor pressure in the reaction gases is very low. An overview of the gas solid reactions that can possibly occur and the Gibbs free energy that accompanies these reactions is given in Table 1.

Table 1: Possible reactions and Gibbs free energy accompanying these reactions at various temperatures and at $P_{SO2} = 10^{-6}$ bar, $P_{S2} = 10^{-3}$ bar and $P_{O2} = 10^{-1}$ bar (Barin, 1993)

	Reaction	ΔG [kJ/mol product] $P_{SO2} = 10^{-6}$ bar, $p_{O2} = 10^{-1}$ bar			
No	Stoichiometry	227 ºC	427 ºC	627 ºC	727 ºC
5	$2\,CuS \longrightarrow Cu_2S + \frac{1}{2}\,S_2$	10	-24	-59	-75
6	$S_2 + 2\,O_2 \longrightarrow 2\,SO_2$	-344	-337	-330	-326
7	$2\,CuS + O_2 \longrightarrow Cu_2S + SO_2$	-334	-361	-390	-402
8	$CuS + 2\,O_2 \longrightarrow CuSO_4$	-515	-435	-356	-318
9	$Cu_2S + 3\,O_2 + SO_2 \longrightarrow 2\,CuSO_4$	-697	-509	-323	-233
10	$Cu_2S + 1\frac{1}{2}\,O_2 \longrightarrow Cu_2O + SO_2$	-385	-381	-374	-372
11	$Cu_2S + O_2 \longrightarrow 2\,Cu + SO_2$	-258	-270	-280	-286
12	$Cu_2O + 1\frac{1}{2}\,O_2 + 2\,SO_2 \longrightarrow 2\,CuSO_4$	-311	-129	51	139
13	$Cu_2O + \frac{1}{2}\,O_2 \longrightarrow 2\,CuO$	-82	-60	-38	-28
14	$2\,Cu + \frac{1}{2}\,O_2 \longrightarrow Cu_2O$	-128	-111	-94	-86
15	$2\,CuSO_4 \longrightarrow CuO \cdot CuSO_4 + \frac{1}{2}\,O_2 + SO_2$	111	30	-50	-90
16	$CuO \cdot CuSO_4 \longrightarrow 2\,CuO + \frac{1}{2}\,O_2 + SO_2$	118	39	-39	-77
17	$Cu_2O + \frac{1}{2}\,O_2 + SO_2 \longrightarrow CuO \cdot CuSO_4$	-200	-99	1	49

From Table 1 it can be seen that it is possible to convert copper sulfide (CuS or Cu_2S) directly or indirectly into copper oxide (CuO or Cu_2O), $CuSO_4$ or basic copper sulfate ($CuO.CuSO_4$). At temperatures below 527 ºC the conversion of $CuSO_4$ into $CuO.CuSO_4$ is possible, but $CuO.CuSO_4$ itself is a stable component, even at SO_2 vapor pressures as low as 10^{-6} bar. At temperatures above 527 ºC the conversion of $CuO.CuSO_4$ into the desired end product CuO becomes possible if the SO_2 vapor pressure is lower than the equilibrium pressure. The phase diagram given in Figure 3 illustrates the relation between the temperature, the partial pressures O_2 and SO_2 and the stable component in the Cu-S-O system.

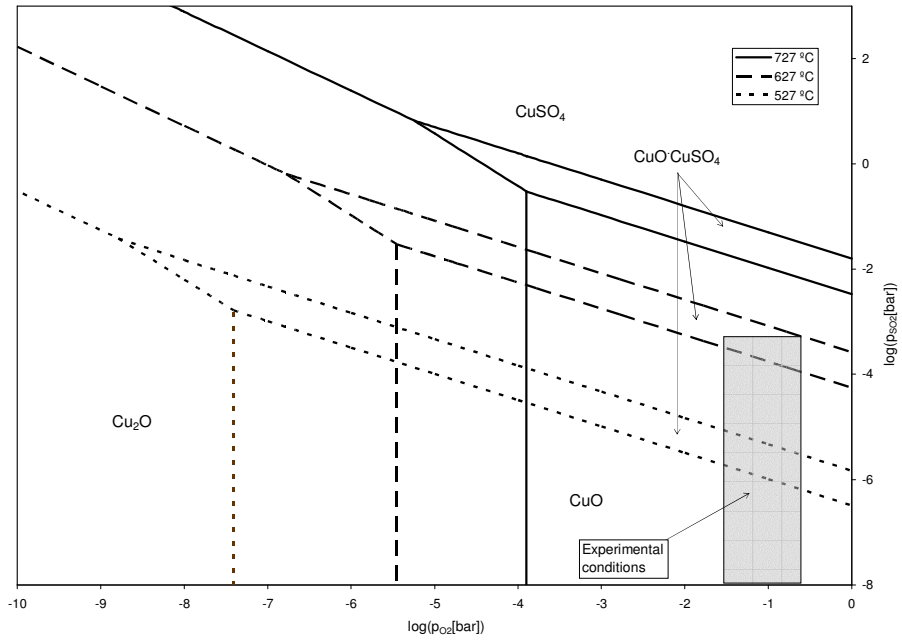

Figure 3 : Detail of the phase diagram of the Cu-S-O system at temperatures, oxygen and sulfur dioxide vapor pressures relevant to the experiments.

The experimental conditions, also shown in Figure 3, indicate that during the experiments, depending on the gas phase composition, $CuO.CuSO_4$ may be formed from CuO at temperatures well above the aforementioned 527 ºC. The occurrence of $CuSO_4$ and $CuO.CuSO_4$ in the end product is undesired since these components do not, or to a lesser extent as CuO, act as a base in the dissolving/neutralizing section of the proposed desulfurization process, shown in Figure 1. Therefore, when $CuSO_4$ or $CuO.CuSO_4$ is present in the end product of the regeneration section the addition of additional base in the dissolver is needed in order to realize a closed loop operation of the desulfurization process. To avoid the extra costs associated with the addition of base, it desirable to convert the copper sulfide selectively and completely into CuO. Therefore this experimental study will be focused not only on the determination of the overall reaction rate of the oxidation of copper sulfide, but will also try to establish the influence of the reaction conditions (e.g. temperature and oxygen concentration) on the reaction path of the oxidation of copper sulfide. This will allow the determination of the optimal reaction conditions in an industrial oxidizer.

4 Experimental set-up and procedure

The experiments have been performed in a Thermo Gravimetric Analyser (TGA). The experimental set-up is schematically shown in Figure 4. The experimental set-up can be subdivided in three sections; a gas mixing section to prepare the desired gas mixture, a reactor section (the TGA), and a gas analysis section.

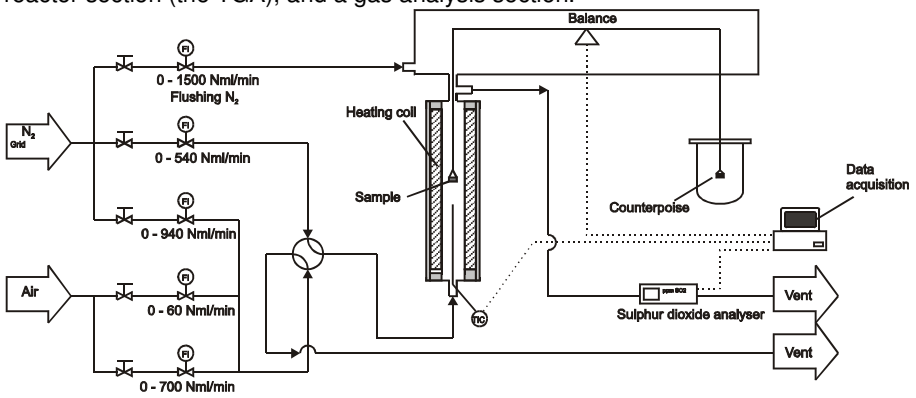

Figure 4 Schematical representation of the Thermo Gravimetric Analyzer

The reactor section of the TGA consists of two concentrically placed quartz glass tubes. In the annular space between the tubes a heating coil is present. The reactor module is thoroughly insulated. A stainless steel casing provides additional mechanical strength to the reactor assembly. The temperature in the reactor is measured using 2 K-type thermocouples and controlled by a Eurotherm 91^e type controller. This type of temperature controller makes it also possible to apply a temperature ramp to the reactor. A small sample is brought in the reactor on a small quartz cup that is attached to one end of the lever of a Sartorius 4406 microbalance by means of a small platinum hook. The dimensions of the quartz cups are given in Figure 5 and Table 2. A counterpoise is attached to the other end of the lever. The mass of counterpoise can be altered to match the weight of the sample plus the quartz cup. To avoid corrosion of the microbalance by the sulfur dioxide released during the course of the oxidation reaction, the upper section of the microbalance is continuously flushed with a stream of nitrogen. A Brooks R-2-15-A flowmeter is used to control this flow. The reaction gas enters the reactor via the bottom. A four-way valve is used to select if a stream of pure nitrogen or a mixture of nitrogen and air enters the reactor. Brooks E 5850 TR mass flow controllers are used to control the flow of the pure nitrogen stream and the flowrate and composition of the mixture of nitrogen and air. The sulfur dioxide content of the gas that leaves the reactor is continuously monitored using a MAIHAK UNOR 610 infrared sulfur dioxide analyzer.

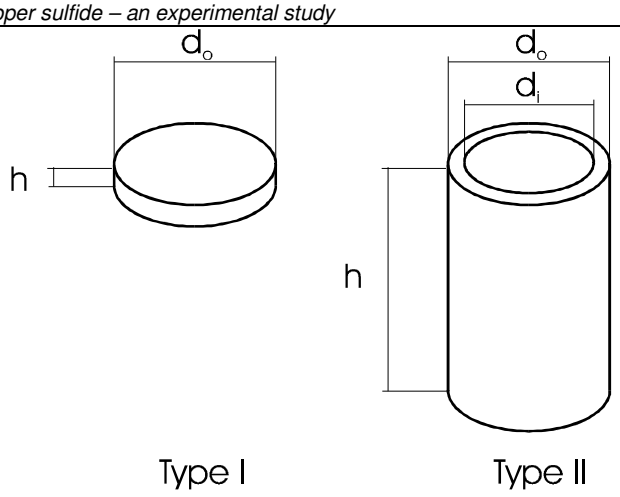

Figure 5: Quartz cups used

Table 2: Dimensions of the cups used

	Cup type I	Cup type II
h [m]	$2 \cdot 10^{-3}$	$8.5 \cdot 10^{-3}$
d_o [m]	$4.5 \cdot 10^{-3}$	$7 \cdot 10^{-3}$
d_i [m]		$4.0 \cdot 10^{-3}$

Unless stated otherwise, the following experimental procedure was applied. The selected quartz glass cup was filled with a sample of copper sulfide of a precisely known weight varying between 1 and 32 mg. The cup was then attached to the platinum hook in the TGA oven. The oven was then flushed continuously with pure nitrogen and was heated to a preset temperature at a rate of 15 ºC/min. When the desired temperature was reached the four-way valve was switched and the air/nitrogen mixture was allowed to enter the reactor, starting the reaction. During the experiment the weight of the sample, the sulfur dioxide concentration in the gas leaving the reactor and the temperature of the reactor were recorded. During a number of experiments the air/nitrogen mixture was fed to the reactor during the temperature ramp.

Sieve fractions of reagent grade copper sulfide (Cu_2S) and reagent grade copper sulfide (CuS) (-100 mesh) were used during the experiments. The Cu_2S (originally -325 mesh) was sieved using 32, 38, and 45 µm sieves.

Copper(I)sulfide (Cu_2S) and copper(II)sulfide (CuS) of 98% resp. 99+% purity were obtained from Aldrich. Nitrogen and air were obtained from Hoek Loos. The nitrogen was of 99.9% purity and the composition of the air was 21% oxygen and 79% nitrogen. The calibration gas for the IR analyzer was prepared by Praxair and had a calibrated composition of 424 ppm $SO_2 \pm 9$ ppm.

The gross composition of the sample can be determined from the mass balances. The remaining sulfur content of the sample can be determined using the data gathered by the IR and the effluent gas flow rate. The oxygen content of the sample can then subsequently be determined from the total mass of the sample as measured by the microbalance and the mass of sulfur in it as determined from the integrated results of the IR. The gross composition of the sample can then be used to determine the (relative) amounts of the components present in the sample during the experiment. As a check of the sulfur mass balance the total amount of sulfur dioxide emitted by the sample is used. On average the total amount of sulfur brought into the reactor as Cu_2S matched the amount leaving the reactor as determined by the sulfur dioxide analyzer within 10 %. As a check on the total mass balance the mass of the completely reacted sample was compared with the original mass of the unreacted sample. Since the molar masses of the reagent (Cu_2S) and the desired end product (CuO) are known the mass that the sample should have at the end of an experiment can be calculated.

5 Results

5.1 Reaction path and stoichiometry

An exploratory study into the reaction path of the oxidation of copper sulfide was carried out by performing experiments using the TGA. A copper sulfide sample of a known weight was brought in the TGA and was gradually heated to a temperature of 725 ºC in an oxygen containing atmosphere. The intermediate products formed during the oxidation of copper sulfide were analyzed using the method described by Ganguly *et al.* (Ganguly, 1967). Figure 6 represents the mass of the sample and the temperature in the TGA during the experiment.

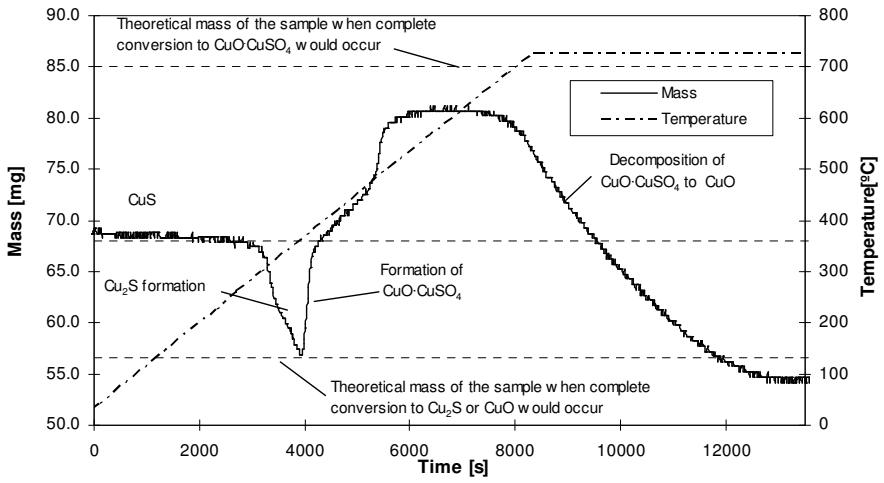

Figure 6: Exploratory TGA experiment, using 68 mg CuS as starting material, the sample heating rate was 5 ºC/min, the gas flow rate through the reactor was 1.1 Nml/s and the gas entering the reactor contained 20 V% oxygen. The horizontal dotted lines show the weight that the sample would have if all copper in the sample would be converted into CuO.CuSO4 (top line), CuS (middle dotted line) or Cu2S or CuO (Bottom line).

From Figure 6 it can be seen that the conversion of CuS into Cu_2S starts to take place at a relatively low temperature of approximately 300 ºC. CuS decomposes into Cu_2S and elemental sulfur according to Equation 5. The gaseous elemental sulfur (S_x) that is liberated during this step is oxidized into sulfur dioxide *(Eq. 6)* when it comes into contact with the oxygen from the gas surrounding the sample. Only when the conversion of CuS towards Cu_2S is completed, Cu_2S is oxidized further to $CuO{\cdot}CuSO_4$. As can be seen in Figure 3 $CuO{\cdot}CuSO_4$ is an unstable component at temperatures above 527 ºC, but only at temperatures above approximately 650 ºC the decomposition of $CuO{\cdot}CuSO_4$ takes place at a rate that is measurable with the experimental set-up used in the present study.

The object of this study is to establish a method for the conversion of CuS towards CuO on an industrial scale. To avoid excessive costs associated with the further processing of the produced SO_2 to H_2SO_4 a concentration of SO_2 in the oxidizer off gas of at least 3 V% should be maintained (Sander *et al.* 1984). Furthermore, the presence of (basic) copper sulfate in the product of the oxidizer is not desired since it does not (or to a lesser extent) act as a base in the make up section of the process scheme depicted in Figure 1, and should therefore be avoided. Given the relatively low equilibrium partial pressure of SO_2, the decomposition of basic copper sulfide $CuO{\cdot}CuSO_4$ will not take place below 727 ºC if the reaction gas contains a significant amount of SO_2. At a temperature of 727 ºC the decomposition of $CuO{\cdot}CuSO_4$

into CuO may take place if the amount of SO_2 does not exceed 1 V% at atmospheric pressure (See also Figure 3). Thus starting from $CuO{\cdot}CuSO_4$ a (basic) copper sulfate free product can only be obtained at a temperature well above 727 ºC. However, operating an oxidizer at very high temperatures is not desired since it is known, from the experiments performed by Açma *et al.* (1995), that the copper oxide produced at high temperatures (i.e. above 700ºC) does not completely dissolve in an acidic solution. Açma also found that the amount of copper oxide that does not dissolve increases with the reaction temperature. An explanation for this behaviour may be found in the sintering or even the partial melting of the copper sulfide at very high temperatures, an effect also noted by Asaki *et al.* (1986) at temperatures of 850 ºC. To avoid both the presence of (basic) copper sulfate and insoluble compounds in the end product a method is needed to convert CuS selectively in CuO at the lowest possible temperature without the production of $CuSO_4$ or $CuO.CuSO_4$ as intermediate products.

5.2 Oxidation of Cu_2S

In order to find such a possible reaction route the oxidation of copper sulfide at temperatures up to 750 ºC has been studied in detail experimentally. CuS very rapidly decomposes into Cu_2S and gaseous sulfur at temperatures above 300 ºC, both in the presence and absence of O_2. Therefore the current oxidation experiments were performed with Cu_2S (always being the first product of the decomposition reaction of CuS) as reactant. During the experiments performed to study the oxidation of Cu_2S a number of parameters was varied systematically; the diameter of the sample particles, the reactor temperature, the amount of sample in the reactor and the gas flow rate. The experimental conditions applied during the experiments are summarized in Appendix A

5.2.1 Reaction route as a function of temperature

In order to establish the reaction route of the oxidation of Cu_2S a number of experiments was carried out using cups of type I filled with approximately 1 mg of Cu_2S sample to minimize the influence of possible mass transfer limitations. The results of these experiments are given in Figure 7 through 10. The experiments carried out using a reaction gas containing 10 V% oxygen are shown in Figure 7 and 8, for 5 V% oxygen the results can be found in Figures 9 and 10. The mass increase found during runs 15 (450 ºC) and 16 (550 ºC), shown in Figure 7 confirms the formation of copper sulfate or basic copper sulfate. At a temperature of 550 ºC it appeared that the (basic) copper sulfate is converted into copper oxide since the final Δmass of the sample used during experiment 16 did not differ significantly from the final Δmass observed in the other experiments shown in Figure 7 (It should be noted that the plot given in Figure 7 is truncated after just 300 seconds.). These experimental results indicate that at a temperature of 550 ºC or higher, CuO is the final product. However, at a temperature of 450 ºC the formed copper sulfate does not react further. This is in line with the predominance

diagram given in Figures 2 and 3. When a reaction gas containing 5 V% oxygen is applied, the formation of copper sulfate or basic copper sulfate is not found during the experiments performed at temperatures of 550 ºC and above.

At temperatures above 650 ºC the powdered samples were completely converted in less than approximately 180 seconds. This is a relatively very short period when compared to the 1 -3 hours as mentioned in literature for the conversion of Cu_2S in a pelletized shape (Asaki, 1986; Ramakrishna and Abraham, 1971 and Perreti, 1948). The decreasing reaction time with increasing temperature (Figure 7 and Figure 9) and the increase in the maximum sulfur dioxide concentration in the effluent gas with increasing temperature (Figures 8 and 10) are indications that an increase in reaction rate is observed when the temperature is increased. However, since the influence of the external mass transfer was not determined during this initial set of experiments the accuracy of the experimental results is insufficient to allow the derivation of kinetic constants. A series of additional experiments using the dedicated type II cups has been carried out to determine the exact influence of mass transfer on the overall reaction rate.

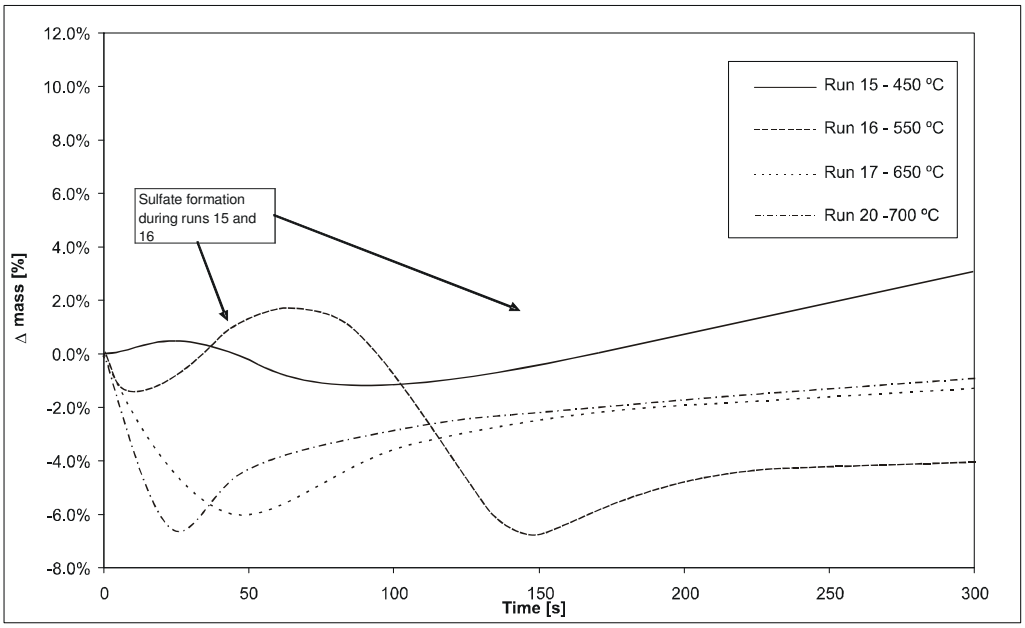

Figure 7: Mass of the sample as a function of time for various temperatures (runs 15 through 21).The temperature was varied between 450 and 725 ºC. The concentration of oxygen in the feed gas was 10 V%. The initial sample mass was approximately 1 mg.

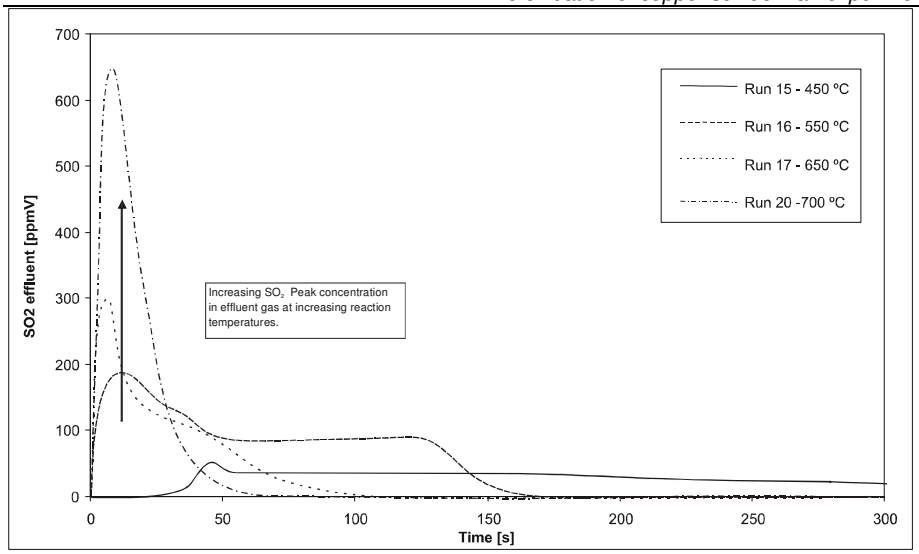

Figure 8: The sulfur dioxide concentration in the effluent gas as a function of time for various temperatures (runs 15 through 21).The temperature was varied between 450 and 725 ºC. The concentration of oxygen in the feed gas was 10 V%. The initial sample mass was approximately 1 mg.

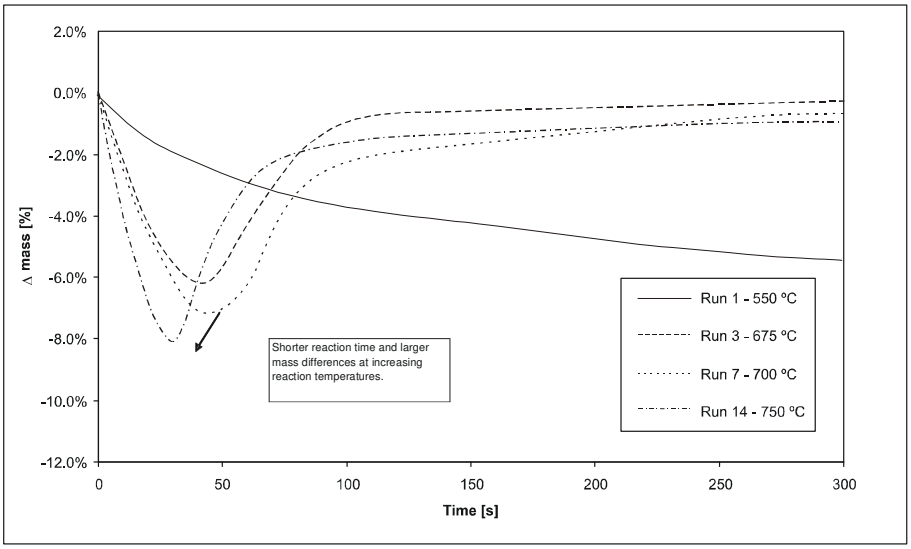

Figure 9: Mass of the sample as a function of time for various temperatures (runs 1 through 14).The temperature was varied between 550 and 725 ºC. The concentration of oxygen in the feed gas was 5 V%. The initial sample mass was approximately 1 mg.

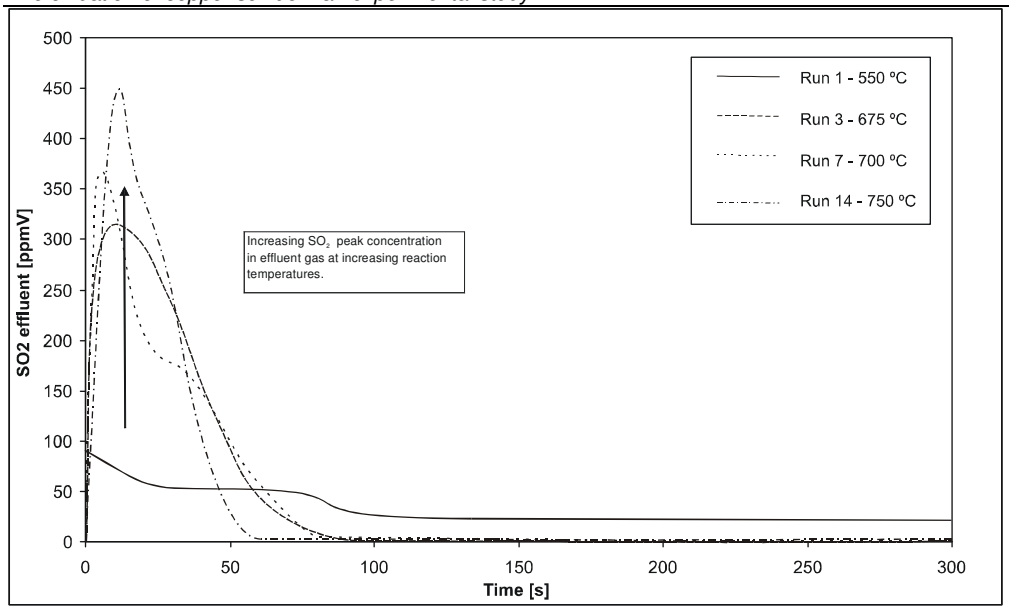

Figure 10: The sulfur dioxide concentration in the effluent gas as a function of time for various temperatures (runs 1 through 14).The temperature was varied between 550 and 725 ºC. The concentration of oxygen in the feed gas was 5 V%. The initial sample mass was approximately 1 mg.

Except for the experiments 15 and 16 (during which (basic) copper sulfate was also formed) the only components present in the sample during the experiments mentioned in Table A.1 are Cu_2S, Cu_2O and CuO. As a representative example the relative amounts of Cu_2S, Cu_2O and CuO as a function of time present during run 3 are shown in Figure 11. From Figure 11 it can be seen that the oxidation of Cu_2S to CuO does not take place in a single reaction step, but that Cu_2S is first converted into Cu_2O, which is then further oxidized to CuO. This reaction path has also been observed by Perreti (Perreti, 1948) and Asaki (Asaki, 1986).

In Figure 11 it is also shown that the time during which the reaction takes place can be divided in three separate stages. During stage I Cu_2S is almost solely converted into Cu_2O and SO_2. Only a small fraction of the Cu_2O formed reacts further to CuO. This means that during this stage of the experiment the rate of the oxygen consumption is almost completely determined by the oxidation of Cu_2S to Cu_2O. During the final stage of the experiment (stage III) virtually all of the Cu_2S has already been converted into Cu_2O. During this stage the reaction responsible for the oxygen consumption is the conversion of Cu_2O into CuO. During stage II both reactions contribute to the rate of oxygen consumption.

Since the rate of oxygen consumption during stage I is completely determined by the oxidation of Cu_2S to Cu_2O, this rate, which can be derived from the experimental results, may be used to derive the reaction rate from the experimental data. Unfortunately, the reaction rate of the oxidation of Cu_2O to CuO could not be determined accurately from the experimental results, since the observed change in mass due to the oxygen consumption during stage III was too small.

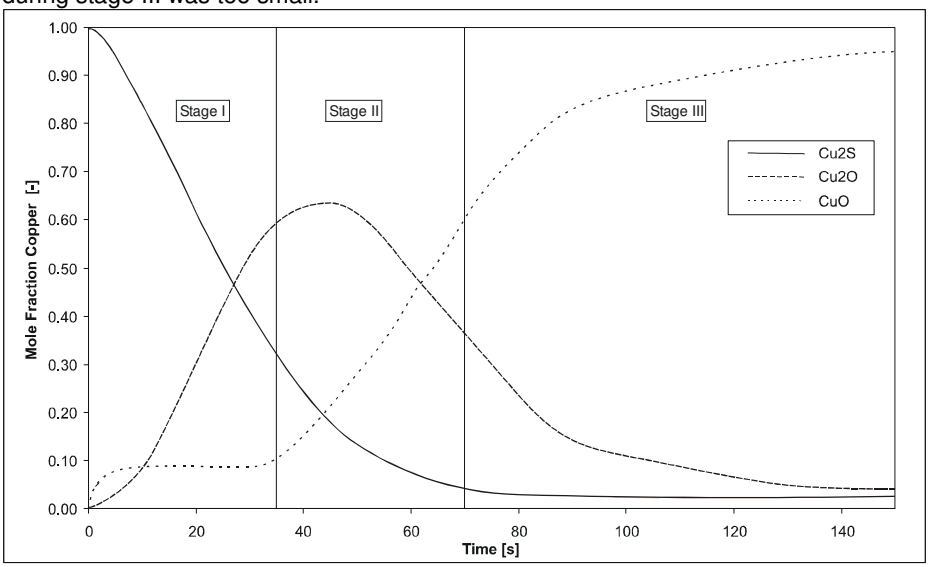

Figure 11: Various components formed as a function of time during run 3. These results represent the typical behavior for Cu_2S samples for temperatures above 550 ºC.

5.2.2 Reaction rate constant measurement

In order to determine some parameters which influence the reaction rate of the oxidation of Cu_2S to CuO a number of experiments was carried out. In order to allow the mass of the sample to be varied from 1 to 32 mg the type II cups had to be used. (See Figure 5). The experimental conditions are given in Table A.2. During these experiments the reaction temperature, the sample mass and the oxygen concentration in the reaction gas were varied.

The first step in the oxidation of Cu_2S to CuO is given by the following reaction equation.

$$Cu_2S + 1\tfrac{1}{2}O_2 \longrightarrow Cu_2O + SO_2 \qquad (10)$$

From Figure 11 it can be seen that this step is distinguishable as a separate reaction step in stage I. Therefore the rate at which this reaction proceeds initially can be determined using the current experimental set-up. The following steps are involved in the oxidation of Cu_2S.

1. The diffusion of oxygen towards the sample cup.
2. The diffusion of oxygen within the sample bed
3. The diffusion of oxygen within the sample particles
4. The chemical reaction
5. The diffusion of the formed sulfur dioxide within the sample particles
6. The diffusion of the formed sulfur dioxide through the sample bed
7. The diffusion of sulfur dioxide from the sample cup.

Since the oxidation of Cu_2S to Cu_2O may be considered to be irreversible (see Table 1), only step 1,2 3 and 4 can be rate controlling.

When the reaction between oxygen and Cu_2S is described using a simple power law rate equation and is considered to be nth order in oxygen, the rate at which this reaction proceeds can be calculated using equation 18.

$$R = k_{app} * C_{O2}^{n} * m \qquad [\text{mole } Cu_2S \text{ s}^{-1}] \qquad (18)$$

The corresponding oxygen demand of the reaction can be determined from the reaction stiochiometry. Taking diffusion resistances into account the overall oxygen consumption can now be expressed as

$$N_{O_2} = \frac{1}{\frac{1}{k_{diff} * A * C_{O2}} + \frac{1}{\nu * k_{app} * C_{O2}^{n} * m}} \qquad (19)$$

In equation 19 k_{diff} is a mass transfer coefficient in which all diffusion mass transfer resistances not directly related to the amount of sample are lumped.

5.2.3 Experimental results

A number of experiments in which the reaction temperature and the sample size have been varied were performed using Type II cups. In stage I, the oxidation of Cu_2S to CuO is predominant, and this reaction has been used for the determination of the oxygen consumption rate. By varying the amount of the sample and plotting the oxygen consumption rate N as a function of the sample mass m both the parameters k_{diff} and k_{app} can be obtained from the experimental data. A representative example of such a plot is given in Figure 12.

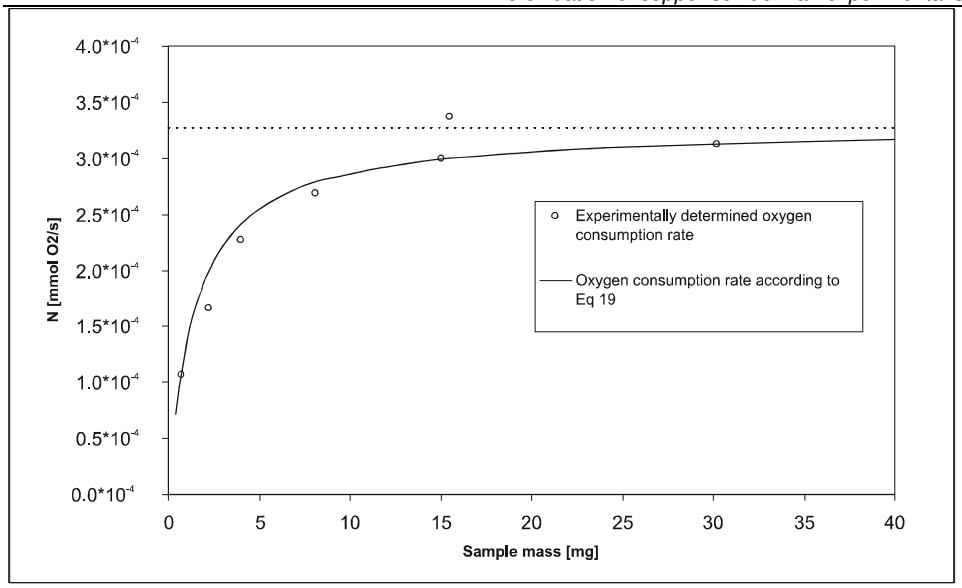

*Figure 12: The experimentally determined oxygen consumption rate as a function of the sample mass at a T= 650 ºC and C_{O2} = V% and the oxygen consumption rate according to Eq 19, with a k_{Diff} of 5.03*10-7 m3 s-1 and a k_{app} of 2.27*10-1 mole kg-1 s-1. The dashed line shows the reaction rate for a completely mass transfer limited process.*

It can be seen that at high sample masses the mass transfer rate at which oxygen can be transported towards the reaction zone, either externally or internally, becomes rate determining. At low sample masses the overall rate becomes dependent on the mass of the sample also, so both the mass transfer process and the chemical reaction rate determine the oxygen consumption rate. E.g. for experiment 24, shown in Figure 12, the resistance to mass transfer contributes still 32 % to the overall resistance. The fraction of the overall resistance that can be ascribed to mass transfer resistance increases with increasing sample mass; at sample masses of 4 and 32 mg mass transfer contributes 73 and 95 % to the overall resistance respectively. The experiments carried out were split in several series, each carried out at the same temperature and oxygen concentration. The value of k_{diff} has been determined for all experimental series by determining the height of the dashed plateau as shown in Figure 12. With the overall mass transfer resistance known, the apparent reaction rate constant can be estimated for each experiment that is not completely determined by mass transfer. The reaction appeared to be of zeroth order in oxygen. The obtained apparent reaction rate constants are plotted in the Arrhenius plot given in Figure 13. The obtained relationship can be expressed by equation 20 given in Table 3. The activation energy found for this oxidation reaction is 71 kJ/mole. The order of magnitude of the activation energy

confirms that the conversion is not limited by a diffusion process, which generally displays a substantially lower activation energy than a chemical reaction.

Table 3: The oxidation of Cu_2S to Cu_2O

	Equation	Eq no.	Units
Oxidation reaction	$Cu_2S + 1\frac{1}{2} O_2 \longrightarrow Cu_2O + SO_2$	*(10)*	
Rate expression	$R = k_{app} * m * C_{O2}^{0}$	*(18)*	[mol Cu_2S s^{-1}]
Reaction rate constant	$k_{app} = 1.28 \cdot 10^{3} * e^{\frac{-71 \cdot 10^{3}}{RT}}$	*(20)*	[mol kg^{-1} s^{-1}]

In Figure 14 a parity plot is given in which the oxygen consumption rate as obtained from the experimental results is plotted vs. the oxygen consumption rate derived from Eq 19 and Eq. 20 for all experiments carried out using Type II cups.

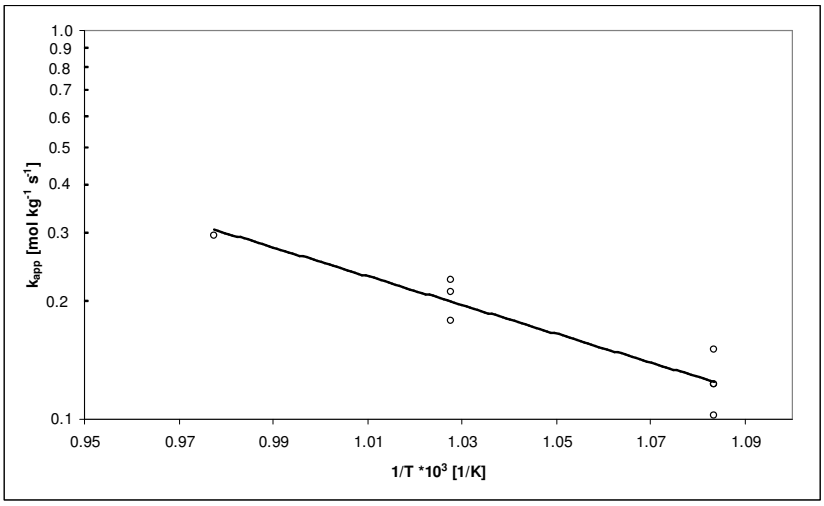

Figure 13: Arrhenius plot for reaction 10.

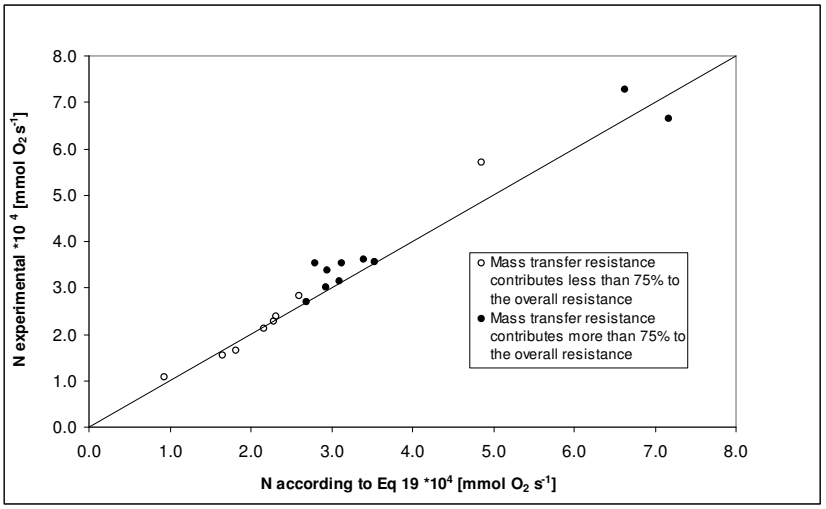

Figure 14: Experimental oxygen consumption rate vs. oxygen consumption rate according to Eq 19, for all experiments mentioned in Table A.2.

Diffusion processes

A comparison of the experimentally determined values of the mass transfer coefficients and the values of the mass transfer coefficients according to the relations mentioned in literature is given in Appendix B. It is shown that not internal mass transfer (sample bed diffusion), but external mass transfer is (partially) rate limiting at the experimental conditions applied. Furthermore it appeared that the experimentally determined values for the external mass transfer coefficient agrees reasonably well with the values obtained using the well-known Ranz-Marshall relation (*Eq. 21)* as given by Ranz and Marshall (1952).

$$\mathrm{Sh} = 2 + 0.6\mathrm{Re}^{1/2}\mathrm{Sc}^{1/3} \qquad (21)$$

A comparison on the experimental values and the values obtained using the Ranz-Marshall relation is given in Figure 15. The discrepancy between the experimental and the theoretical values amounts approximately 15 to 30%, but can e.g. be ascribed to variances in mass transfer coefficients between the front and back-end of the sample cup (Lee and Barrow, 1968) caused by turbulence in the wake of the sample cup.

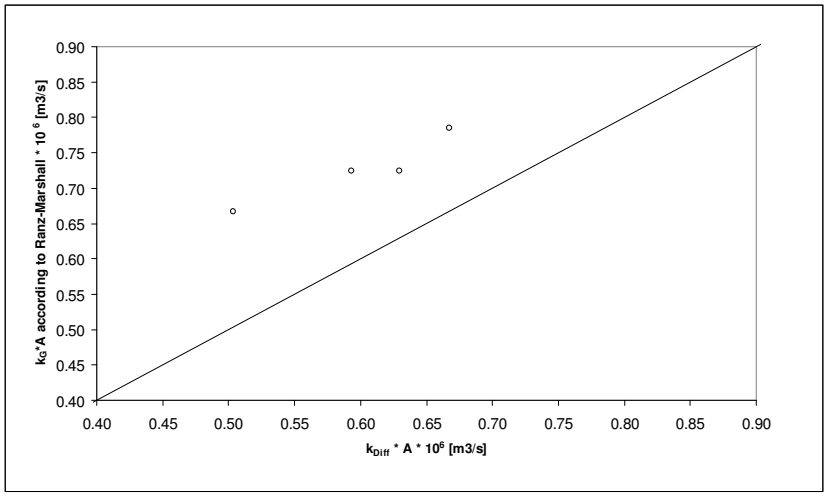

Figure 15: Experimentally determined k_{diff} vs. k_{diff} according to B.1.

Heat effects

The influence of the reaction heat generated during the oxidation of Cu_2S to Cu_2O on the temperature of the sample is estimated in Appendix C. A conservative estimate learns that the temperature of the sample was never more than 15 ºC higher than the temperature of its surroundings. And therefore it is concluded that the influence of the heat effects on the experimental results is limited.

5.3 Decomposition of CuS in the presence of O_2

Perreti (1948) and Ganguly and Mukherjee (1967) have reported that the first reaction step in the oxidation of CuS is the decomposition of CuS to Cu_2S. According to Ganguly and Mukherjee (1967) the decomposition of CuS takes place at a notable rate at temperatures above 340 ºC. The rate at which this reaction takes place depends on the presence of oxygen in the reaction gas. The presence of oxygen greatly enhances the decomposition rate. A number of experiments has been performed to verify their findings. The temperature during these experiments was varied between 275 and 375 ºC. Experiments were carried out using a nitrogen/air mixture containing 5V% oxygen as reactor feed gas. An overview of the experiments carried out is given in Appendix A, in Table A.3

It appeared that the conversion of CuS in the presence of oxygen at a constant temperature is a two stage process that proceeds similarly to the oxidation of CuS heated at a constant temperature rate. First, CuS decomposes into Cu_2S and elemental sulfur which is subsequently oxidized to SO_2 (shown as *Eq. 5* and *Eq. 6*). Only after all CuS is converted to Cu_2S, the formed Cu_2S is oxidized further to, in this case, (basic) copper sulfate (*Eq. 22*).

$$2x\,CuS \longrightarrow Cu_2S + S_x \qquad (5)$$

$$S_x + x\,O_2 \longrightarrow x\,SO_2 \qquad (6)$$

$$Cu_2S + 2\,{}^1\!/\!_2\,O_2 \longrightarrow CuO \cdot CuSO_4 \qquad (22)$$

The formation of (basic) copper sulfate was due to the low temperatures (see also Figures 6 and 7). The rate at which the conversion of CuS to Cu_2S takes place (expressed in moles S converted per second) is shown as a function of temperature in Figure 16.

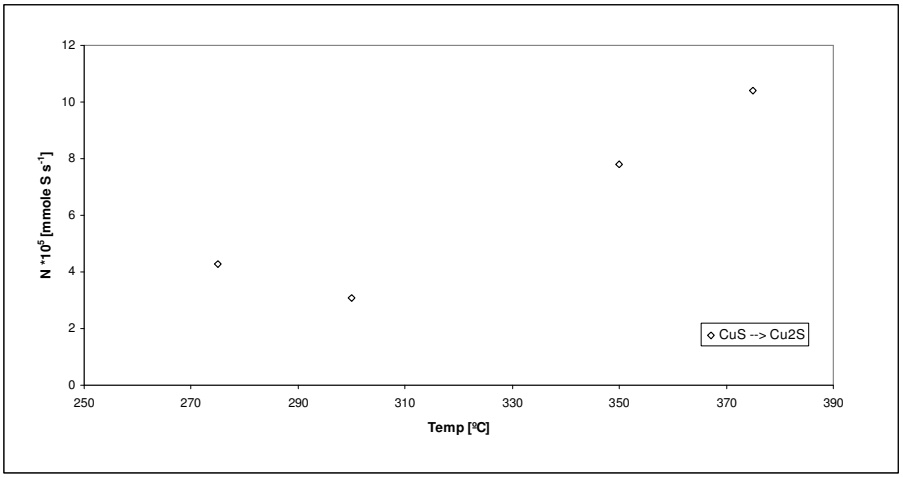

Figure 16: The experimentally determined rate of reaction of CuS to Cu_2S as a function of temperature. The sample mass was 32 mg and the oxygen concentration of 5 V%.

It appeared that the observed reaction rate of the conversion of CuS to Cu_2S increased with temperature. The only result deviating from this trend, (an experiment carried out at T = 275 ºC), came from an experiment that also showed a different behavior regarding the consecutive reaction. The final solid product of the consecutive reaction of the experiment carried out at 275 ºC contained significantly less oxygen than the final product of the experiments carried out at the higher temperatures. Using the data available and the same procedure as used in the section 5.2.2, an estimate of the apparent reaction rate constant of reaction 7 was made neglecting the experiment at 275 ºC. Since the concentration of oxygen was not varied during these experiments the reaction order in oxygen could not be determined and the reaction between oxygen and CuS is described using a simple rate equation (*Eq 23)* in which the oxygen effect is implemented in k_{app}.

$$R = k_{app} * m \qquad [\text{mole CuS s}^{-1}] \qquad (23)$$

By lack of experimental data the external mass transfer coefficient was estimated using the previously mentioned Ranz-Marshall equation (Ranz, 1952). This seems allowed as Figure 15 shows that the Ranz-Marshall equation gives reasonably accurate results in the present case. It appeared that the external mass transfer resistance contributed less than 30% to the overall mass transfer resistance as estimated by Eq 21.

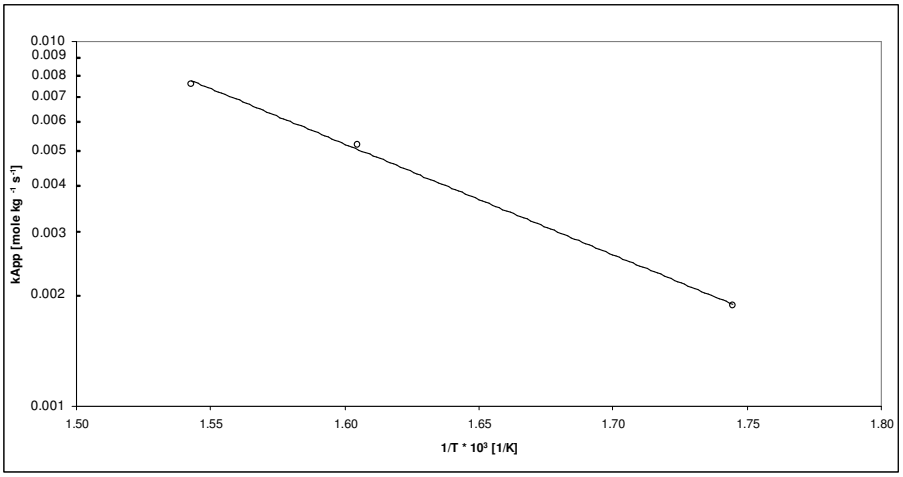

Figure 17:k_{app} for reaction 7 as a function of temperature.

The obtained apparent reaction rate constants are shown in Figure 17. The obtained Arrhenius relationship can be expressed by equation 24, Shown in Table 4. The activation energy found for this oxidation reaction was 58 kJ/mole. The order of magnitude of the activation energy indicates that the reaction rate is again most probably not limited by a diffusion process, which generally displays a substantially lower activation energy than chemical kinetics.

Table 4: The conversion of CuS to Cu_2S

	Equation	Eq no.	Units
Reactions	$2x\,CuS \longrightarrow Cu_2S + S_x$	*(5)*	
	$S_x + x\,O_2 \longrightarrow x\,SO_2$	*(6)*	
Rate expression	$R = k_{app} * m$	*(23)*	[mol CuS s^{-1}]
Reaction rate constant at a oxygen concentration of 5 V%	$k_{app} = 3.76 \cdot 10^3 * e^{\frac{-58 \cdot 10^3}{RT}}$	*(24)*	[mol kg^{-1} s^{-1}]

The obtained value of the reaction rate constant and the increase of the reaction rate as a function of temperature indicates that the conversion of CuS to Cu_2S, at higher temperatures, is not a rate determining step in the overall oxidation of CuS to CuO.

6 Conclusions

In the current study the oxidation of CuS to CuO at temperatures in the range of 450 to 750 ºC and oxygen concentration as encountered during roasting (5 - 10 V%) has been studied experimentally using a thermo gravimetric analyzer. Thermodynamics show that the formation of CuO from CuS is possible if the SO_2 partial pressure is sufficiently low. Besides CuO some by- or intermediate products like (basic) copper sulfate or Cu_2O may be formed during the oxidation of CuS. The stability of these byproducts depends on the process conditions like temperature, sulfur dioxide and oxygen concentration. At temperatures up to 527 ºC (basic) copper sulfate is a stable component. At temperatures above 527 and below 727 ºC, depending on sulfur dioxide and oxygen concentration, the conversion of the (basic) copper sulfate to copper oxide becomes thermodynamically possible. At the temperature range (275 to 750 ºC) and oxygen concentrations (varied from 2.5 V% to 20 V%) investigated the conversion of Cu_2O to CuO was always possible.

Experiments have shown that the oxidation of CuS to CuO consists of several reaction steps, the conversion of CuS to Cu_2S being always the first step. Since this reaction appeared to be a fast reaction compared to the other reactions that may occur, Cu_2S was chosen as starting material for the oxidation experiments carried out at temperatures above 400 ºC. (above this temperature CuS spontaneously reacts to Cu_2S both in the presence and absence of oxygen).

The first series of experiments already indicated that the time needed for a complete conversion of the copper sulfide to copper oxide was very short when compared to the reaction times mentioned in literature. At temperatures above 650 ºC the powdered Cu_2S samples were completely converted to CuO in less than approximately 3 minutes as compared to the 1 to 3 hours reaction time typically mentioned in literature for the conversion of Cu_2S in a pelletized shape

The experimental results showed that at temperatures up to 550 ºC CuS and Cu_2S may be converted (partially) into (basic) copper sulfate. Above this temperature it is possible to convert Cu_2S selectively and completely to CuO. The oxidation of Cu_2S to CuO appeared to be a two step process. The first reaction step is the oxidation of Cu_2S to Cu_2O. The second step is the subsequent oxidation of Cu_2O to CuO. The rate at which Cu_2S is converted into Cu_2O increased with temperature. Both chemical reaction and mass transfer influenced the conversion rate. To derive the intrinsic kinetics from the experimental results a number of experiments was performed in which the temperature and amount of sample used were varied. The kinetics of the oxidation reaction of Cu_2S to Cu_2O have thus been determined as a function of temperature and are summarized in the subsequent Table.

The oxidation of Cu_2S to Cu_2O

	Equation	Eq no.	Units
Oxidation reaction	$Cu_2S + 1\frac{1}{2} O_2 \longrightarrow Cu_2O + SO_2$	*(10)*	
Rate expression	$R = k_{app} * m * C_{O2}^{0}$	*(18)*	[mol Cu_2S s^{-1}]
Reaction rate constant	$k_{app} = 1.28 \cdot 10^{3} * e^{\frac{-71 \cdot 10^{3}}{RT}}$	*(20)*	[mol kg^{-1} s^{-1}]

It was not possible to determine the kinetics for the subsequent oxidation of Cu_2O to CuO because of the limited weight change during this reaction step, but the reaction rate is in the same order of magnitude as for the reaction of Cu_2S to Cu_2O.

It can be concluded that the current experimental results demonstrate that a conversion of copper sulfide to copper oxide, preventing the formation of by-products is possible at temperatures in the range of 550-750 ºC and oxygen concentrations of 5-10%.

7 Nomenclature

Symbols

d	characteristic diameter of the sample cup	[m]
g	acceleration by gravity	[m^2 s^{-1}]
h	height of sample cup	[m]
k	Mass transfer coefficient	[m s^{-1}]
k	Reaction constant	[mol kg^{-1} s^{-1}]
m	Sample mass	[kg]
v	Velocity	[m s^{-1}]
A	Cross sectional area of the sample cup	[m^2]
C	Concentration	[mole m^{-3}]
C_p	Specific heat	[J kg^{-1} K^{-1}]
D	Diffusion coefficient	[m^2 s^{-1}]
H	Enthalpy	[J $mole^{-1}$]
P	Pressure	[Pa]
N	Oxygen consumption rate	[mole s^{-1}]
R	Reaction rate	[mole s^{-1}]
T	Temperature	[K]
U	Heat transfer coefficient	[W m^{-2} K^{-1}]

Dimensionless groups

Gr	Grashof number $g*d^3*\beta_H*\Delta T*\rho_G/\eta$	[-]
Nu	Nusselt number $U*d/\lambda$	[-]
Re	Reynolds number $\rho*v*d/\eta$	[-]
Pr	Prandtl number $C_p*\eta/\lambda$	[-]
Sh	Sherwood number $k_G/(d*D_{O2})$	[-]
Sc	Schmidt number $\eta/(D_{O2}*\rho)$	[-]

Greek

β_H	coefficient of thermal expansion	[K^{-1}]
ε	Porosity of the sample bed	[-]
ε	Emmisivity coefficient	[-]
η	viscosity	[Pa s]
λ	thermal conductivity	[W m^{-1} K^{-1}]
ν	stoichiometric coefficient	[-]
ρ	density	[kg m^{-3}]
s	Bolzmann constant	[W m^{-2} K^{-4}]

Superscripts

n reaction order

Subscripts

app apparent
diff diffusion
e effective
i inner
o outer
sup Superficial
G Referring to the gas phase
R Denoting reaction
Δ Denoting a difference

8 References.

Açma, E., Oktaybas, C., Sesigür, H., Addemir, O., 1995, Benification of Divrigi tailings by flotation, sulfatizing roasting, leaching and H2S precipitation., *Erzmetall*, **58**, 572-7

Asaki, Z., Ueguchi, A., Tanabe, T., Kondo, Y., 1986, Oxidation of Cu_2S Pellet, *Transactions of the Japan Institute of Metals*, **27**, 361-71

Barin, I., 1993, Thermochemcial data of pure substances, *VCH Weinheim*

Johnson, D.W. Gallagher 1971, Kinetics of the Decomposition of Freeze-Dried Aluminum Sulfate and Ammonium Aluminum Sulfate, *J. Am. Cer. Soc.* **54**, 461-5

Broekhuis, R.R., Koch, D.J., Lynn, S., 1992, A medium temperature process for removal of hydrogen sulfide from sour gas streams with aqueous metal sulfate solutions, *Ind. Eng. CHem. Res.*, **31**, 2635-42

Fuller, E.N., Schetter, P.D., Gidding, J.C., 1966, *Ind. Eng. Chem.*, **58**, 18-

Ganguly, N.D., Mukherjee, S.K., 1967, Studies on the mechanism and kinetic of the oxidation of copper sulphide, *Chem. Eng. Sci.*, **22**, 1091-1105.

Hurd, L.C., Clark, A.R., 1936, Determination of Metallic Copper in Cuprous Oxide - Cupric Oxide mixtures, *Ind. Engng. Chem.*,**8**, 380-2

Kohl, A.L., Nielsen, R.B., 1997, Gas Purification, *Gulf Publishing Co. Houston*

Lee, K., Barrow, H., 1968, *Int J. Heat Mass Trans.*, **11**, 1013

Lewis, J.R., Hamilton, J.H., Nixon, J.C., Graversen, C.L., 1949, The Oxidation of Chalcocite in Air Compared with Its Oxidation in Pure Oxygen, *TMS-AIME*, **182**, 177-85

Lide, D.R., 1995, Handbook of Chemistry and Physics, *CRC Press Inc.*

Maat, H. ter., Versteeg, G.F., 1997, Werkwijze en systeem voor het selectief verwijderen van verontreinigingen uit gasstromen. Dutch Patent No,.1006200.

Maat, H. ter., Hogendoorn, J.A., Versteeg, G.F., 2002, The absorption of hydrogen sulfide in metal sulfate solutions. Chapter 2 of this thesis.

Sander, U.H.F., Fischer, H., Rother, U., More, A.I., 1984, Sulphur, sulphur dioxide and sulphuric acid : an introduction to their industrial chemistry and technology, *British Sulphur Corporation*

Peretti, E.A., 1948, A New Method for Studying the Mechanism of Roasting Reactions*, Disc. Faraday. Soc.*, **4**, 174-9

Ramakrishna Rao V.V.V.N.S., Abraham. K.P., 1971, Kinetics of Oxidation of Copper Sulfide, *Met. Trans.* **2**, 2463-70

Ranz, W.E,. Marshall, W.R. Jr., 1952, Evaporation from Drops, Part II, *Chem. Eng. Progr.*, **48**, 173-80

Szekely, S., Evans, J.W., Sohn, H.Y., 1976, Gas-Solid Reactions, *Academic Press.*

Wakao, N., Smith, J.M., 1962, Diffusion in Catalyst Pellet, *Chem. Eng. Sci*, **17**, 825-34

Younglove, B.A., 1982, Thermophysical Properties of Fluids Part I, *J. Phys. Chem. Ref. Data*, **11**, suppl 1; erratum, **14**., 619

Younglove, B.A., Ely, J.F., 1987, Thermophysical Properties of Fluids Part II, *J. Phys. Chem. Ref. Data*, **16**, 577

Appendix A Experimental conditions.

Table A.1: Experimental conditions applied during runs 1 through 22, during these runs cups of type I were used, the starting material was Cu_2S, the samples were heated at a rate of 15 ºC per minute to the reaction temperature in a nitrogen atmosphere .

Run	Sample mass	Reaction temperature	Reaction gas		Sieve fraction
			Flowrate	Oxygen content	
[No.]	[mg]	[ºC]	[Nml/s]	[V%]	[µm]
1	0.90	550	9	5	$45< d_p <38$
2	0.50	650	11.4	5	$d_p <32$
3	1.10	675	11.4	5	$d_p <32$
4	0.50	700	11.4	5	$45<d_p<38$
5	1.10	700	11.4	5	$d_p <32$
6	1.10	700	11.4	5	$38< d_p <32$
7	1.00	700	11.4	5	$45< d_p <38$
8	1.10	700	4	5	$45< d_p <38$
9	1.10	700	9	5	$45< d_p <38$
10	1.30	700	11.4	5	$45< d_p <38$
11	1.90	700	11.4	5	$45< d_p <38$
12	1.10	725	11.4	5	$38< d_p <32$
13	0.50	750	11.4	5	$45< d_p <38$
14	0.90	750	11.4	5	$45< d_p <38$
15	1.00	450	9	10	$45< d_p <38$
16	1.00	550	9	10	$45< d_p <38$
17	0.90	650	11.6	10	$45< d_p <38$
18	1.10	675	11.6	10	$45< d_p <38$
19	1.00	675	9	10	$45< d_p <38$
20	1.10	700	11.6	10	$45< d_p <38$
21	1.10	725	9	10	$45< d_p <38$
22	0.60	750	9	10	$45< d_p <38$

Table A.2: Experimental conditions applied during runs 24 through 44, during these runs cups of type II were used, the starting material was Cu_2S, the samples were heated at a rate of 15 ºC per minute to the reaction temperature in a nitrogen atmosphere .

Run	Sample mass	Reaction temperature	Reaction gas		Sieve fraction
			Flowrate	Oxygen content	
[No.]	[mg]	[ºC]	[Nml/s]	[V%]	[µm]
24	0.70	650	9	5	$45< d_p <38$
25	2.20	650	9	5	$45< d_p <38$
26	4.00	650	9	5	$45< d_p <38$
27	8.10	650	9	5	$45< d_p <38$
28	15.50	650	9	5	$45< d_p <38$
29	15.50	650	9	5	$45< d_p <38$
30	32.00	650	9	5	$45< d_p <38$
31	1.00	700	9	5	$45< d_p <38$
32	2.10	700	9	5	$45< d_p <38$
33	3.90	700	9	5	$45< d_p <38$
34	7.20	700	9	5	$45< d_p <38$
35	15.20	700	9	5	$45< d_p <38$
36	31.10	700	9	5	$45< d_p <38$
37	1.05	750	9	5	$45< d_p <38$
38	4.20	750	9	5	$45< d_p <38$
39	15.20	750	9	5	$45< d_p <38$
40	30.50	750	9	5	$45< d_p <38$
41	1.30	700	9	10	$45< d_p <38$
42	4.30	700	9	10	$45< d_p <38$
43	15.00	700	9	10	$45< d_p <38$
44	30.00	700	9	10	$45< d_p <38$

Table A.3: Experimental conditions applied during runs 53 through 60, during these runs cups of type II were used, the starting material was CuS, the samples were heated at a rate of 15 ºC per minute to the reaction temperature in an inert atmosphere. The particle size was: 32<d_P<100µm

Run	Sample mass		Reaction	Reaction gas	
	Initial	Final	temperature	Flowrate	Oxygen content
[No.]	[mg]	[mg]	[ºC]	[Nml/s]	[V%]
53	31.9	34.3	275	9	5
54	31.8	36.3	300	9	5
55	32.2	38.9	350	9	5
56	31.3	38.3	375	9	5
57	31.8	30.5	275	9	0
58	32.0	30.4	300	9	0
59	31.9	28.6	350	9	0
60	32.1	26.6	370	9	0

Table A.4: Experimental conditions applied during runs 46 through 52, during these runs cups of type II were used, the starting material was Cu_2S.

Run	Sample	Reaction	Reaction gas		Sieve fraction
	mass	temperature	Flowrate	Oxygen content	
[No.]	[mg]	[ºC]	[Nml/s]	[V%]	[µm]
46	7.0	700	9	5	45< d_p <38
47	15.1	700	9	5	45< d_p <38
48	7.4	725	9	5	45< d_p <38
49	14.8	725	9	5	45< d_p <38
50	7.9	750	9	5	45< d_p <38
51	15.5	750	9	5	45< d_p <38
52	29.9	750	9	5	45< d_p <38

Appendix B: The diffusional resistance.

The observed mass transfer resistance can originate from both external mass transfer limitation (i.e. the rate at which oxygen can be transferred from the reaction gas surrounding the cup to the cup), and internal mass transfer limitation (i.e. the rate at which oxygen can diffuse through the sample in the cup towards the reaction zone) respectively. To determine which process is rate limiting the experimentally obtained values for k_{diff} will be compared with the estimates known from literature.

External mass transfer

The external gas film mass transfer coefficient k_G of the sample cup can be estimated by e.g. the Ranz-Marshall equation (Ranz, 1952).

$$\mathrm{Sh} = 2 + 0.6\mathrm{Re}^{1/2}\mathrm{Sc}^{1/3} \qquad \text{(B 1)}$$

The physical properties, the numerical values, and the mass transfer coefficients are given as a function of temperature in Table B.1 for a reaction tube diameter of 12 mm, and a gas composition of 5 V% oxygen, balance nitrogen.

Table B.1: Estimation of physical properties and mass transfer coefficient for diffusion of oxygen toward a type II cup as a function of temperature.

Gas characteristics.						
Temperature	[ºC]	650	675	700	725	750
C_{O2}	[mole m^{-3}]	0.65	0.63	0.62	0.60	0.59
$D_{O2} * 10^4$ (Fuller, 1966)	[$m^2 s^{-1}$]	1.53	1.60	1.67	1.75	1.83
ρ	[kg m^{-3}]	0.37	0.36	0.35	0.34	0.33
$\eta * 10^5$ Lide (1995)	[Pa s]	3.08	3.18	3.27	3.36	3.44
Superficial gas velocity * 10^2	[m s^{-1}]	6.17	6.34	6.51	6.67	6.84
Dimensionless Groups						
Re		6.25	6.07	5.90	5.74	5.60
Sc		0.55	0.55	0.56	0.56	0.57
Sh (Ranz-Marshall)		3.23	3.21	3.20	3.19	3.18
$k_G * 10^2$	[m s^{-1}]	5.80	6.05	6.31	6.57	6.83

The density of the reaction gas has been calculated using the ideal gas law. The viscosity of the reaction gas was taken to be the viscosity of nitrogen at the reaction temperature. With the dimensions of the equipment and the cups known, the mass transfer coefficient k_G can be determined from equation B.1. The effective mass exchanging area can be calculated from

the cup dimensions. In Figure B.1 a comparison of the obtained values of k_GA according to the Ranz-Marshall equation is plotted vs. the experimentally obtained values for k_{diff}. From Figure B.1 it can be seen that the mass transfer coefficient as determined during the experiments agrees reasonably well (within 30%) with the mass transfer coefficient as determined using the Ranz-Marshall equation.

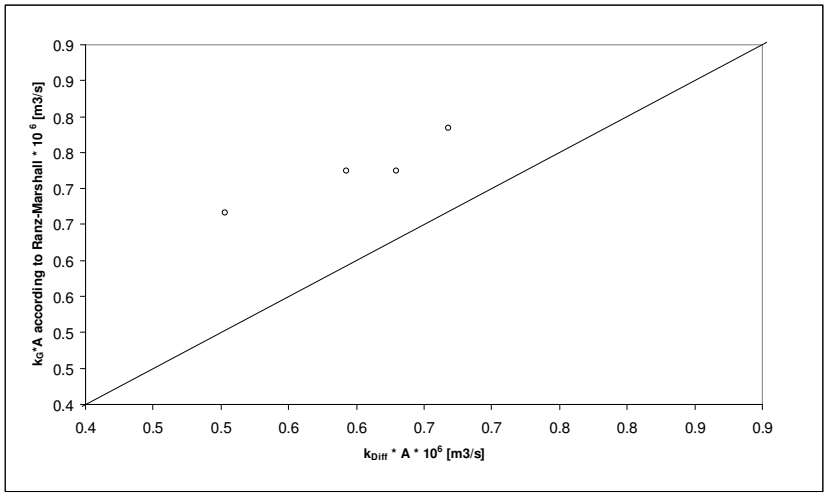

Figure B.1: Experimentally determined k_{diff} vs. k_{diff} according to B.1.

Internal mass transfer

Internal mass transfer can become rate limiting when both the oxidation reaction rate and the external mass transfer are sufficiently fast. When internal mass transfer completely determines the oxidation rate, a reaction plane will arise. As the reaction proceeds, the reaction plane will move gradually downward. The situation in the sample cup in this case is schematically given in Figure B.2

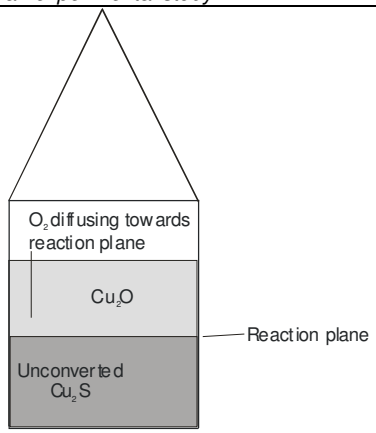

Figure B.2: Experimentally determined k_{diff} vs. k_{diff} according to B.1.

The rate at which the oxygen diffuses through the product layer can be described by e.g. the Fick equation (Eq. B.2).

$$J = D_e \frac{dC_{O_2}}{dx} \ [\text{mole m}^{-2} \text{ s}^{-1}] \qquad \text{(B.2)}$$

The oxygen concentration gradient follows from the (time dependent) thickness of the Cu_2O layer and the oxygen concentration in the bulk of the reaction gas. The thickness of the Cu_2O layer is in turn a function of the amount of Cu_2O formed. When the effective diffusion coefficient in the sample bed, D_e is estimated using Equation B.3, as given by Wakao and Smith, (1962) the degree to which internal mass transfer determines the overall reaction rate can be estimated using equation B.2.

$$D_e = \varepsilon^2 D \qquad \text{(B.3)}$$

It appeared that the influence of sample bed diffusion was negligible for the type II cups under the experimental conditions, as it appeared that sample bed diffusion was very fast with respect to the external mass transfer when the amount of Cu_2O formed was smaller than 60 mg.

Appendix C: Thermal behaviour of the reacting components.

The oxidation of copper sulfide to copper oxide could be sufficiently exothermic to cause a temperature change of the reacting solid large enough to influence the course of reaction. In order to determine the magnitude of the thermal effects an analysis has been carried out. The method of analysis followed is described by Szekely *et al.* (1976).

To ensure that the temperature difference between the solid reactants and surroundings is not underestimated a worst-case analysis has been carried out. In this analysis a sphere-shaped geometry of the sample has been chosen since this geometry offers the lowest possible surface area to volume ratio. During the experiments the sample actually has a disc shaped geometry with a h/d_i ratio below 1, and the larger experimental heat exchanging area therefore will generally allow the generated heat to be transported from the sample to its surroundings at a lower driving force in comparison with the driving force (temperature difference) needed for a sphere shaped geometry.

The energy generated during the course of the reaction will be transferred from the sample to its surroundings. Energy can be transported by a number of transport mechanisms. These mechanisms are conduction, convection and radiation. Of these three mechanisms conduction is usually negligible for the transfer of heat from a sample to its surroundings. Energy transport by convection can be subdivided in energy transport by forced convection and energy transport by free convection.

Energy transport by forced convection

To estimate the heat transport caused by forced convection the Ranz-Marshall (1952) correlation has been adapted by replacing the Sherwood and Schmidt dimensionless numbers with the Nusselt and Prandtl groups. The resulting correlation is given as Eq C-1.

$$\mathrm{Nu} = 2 + 0.6\mathrm{Re}^{1/2}\mathrm{Pr}^{1/3} \qquad [C\text{-}1]$$

Energy transport by free convection

For free convection the Nusselt number is a function of the Grashof and Prandtl numbers. One of relations used to estimate the heat transfer coefficient due to free convection is the relation given by Ranz and Marshall (1952).

$$\mathrm{Nu} = 2 + 0.6\mathrm{Gr}^{1/4}\mathrm{Pr}^{1/3} \qquad [C\text{-}2]$$

Energy transport by radiation

At high temperatures thermal radiation is an important heat transfer mechanism. The amount of heat transported from the sample to its surroundings can be expressed using Eq C-3, provided that the surface area of the sample is negligible with respect to the surface area of its surroundings, as is the case when a small spherical pellet is placed in a pipe with a much larger diameter.

$$Q = \varepsilon\sigma(T_{Sample}^4 - T_{Surroundings}^4) \qquad [C\text{-}3]$$

The physical properties, the numerical values, and the heat transfer parameters are given as a function of temperature in Table C-1 for a reaction tube diameter of 12 mm, and a gas composition of 5 V% oxygen, balance nitrogen. The calculations have been made for a spherical sample consisting of 30 mg Cu_2S, which is converted into Cu_2O. The conversion rate that has been used in the calculation is 3.5 * 10^{-7} mol O_2 per second, which was approximately the value of the external gas phase mass transfer determined oxidation rate during experiments 24 through 36.

The density of the reaction gas and the thermal expansion coefficient were calculated using the ideal gas law. The viscosity, the thermal conductivity and the specific heat capacity of the reaction gas were taken to be the viscosity, thermal conductivity and the specific heat capacity of nitrogen at the reaction temperature respectively.

The dimensions of the sample bed were estimated using a porosity ε of 0.35, and a density of 4000 kg/m^3. The heat of reaction for the oxidation of Cu_2S to Cu_2O is expressed as Joules per mole of reacted oxygen. The emissivity coefficient of copper oxide is taken to be 0.88, a value tabulated by Lide (1995).

With the dimensions of the equipment and the sample bed known, the heat transport due to forced convection, free convection and radiation, and the sample temperature were estimated using an iterative procedure. It appeared that the temperature of the sample was never more than 15 ºC higher than the temperature of its surroundings. It may therefore be concluded that the influence of the temperature difference on the experimental results is limited.

Table C-1: Estimation of physical properties and heat transfer parameters as a function of temperature.

Gas characteristics.						
Temperature	[ºC]	650	675	700	725	750
ρ	[kg m^{-3}]	0.37	0.36	0.35	0.34	0.33
$\eta * 10^5$ (Lide, 1995)	[Pa s]	3.08	3.18	3.27	3.36	3.44
$\lambda * 10^2$ (Lide, 1995)	[W m^{-1} K^{-1}]	6.09	6.21	6.33	6.45	6.57
C_P (Lide, 1995)	[J kg^{-1} K^{-1}]	1148	1153	1159	1164	1169
$\beta * 10^3$	[K^{-1}]	1.08	1.05	1.03	1.00	0.98
Superficial gas velocity $* 10^2$	[m s^{-1}]	6.17	6.34	6.51	6.67	6.84
Sample characteristics						
Sample Mass $* 10^6$	[kg]	30	30	30	30	30
Diameter sample $* 10^3$	[m]	2.8	2.8	2.8	2.8	2.8
Area sample $* 10^6$	[m^2]	25	25	25	25	25
Temperature Sample	[ºC]	664	688	713	737	762
Heat production						
Reaction rate $* 10^6$	[mol O_2 s^{-1}]	0.35	0.35	0.35	0.35	0.35
$\Delta H_R * 10^{-3}$ (Barin, 1993)	[J mole^{-1} O_2]	266	266	266	266	266
$Q * 10^3$	[W]	93.1	93.1	93.1	93.1	93.1
Forced Convection						
Re	[-]	2.06	2.00	1.95	1.89	1.85
Pr	[-]	0.58	0.59	0.60	0.61	0.61
Nu	[-]	2.72	2.71	2.71	2.70	2.69
$U_{Forced\ convection}$	[W m^{-2} K^{-1}]	59	60	61	62	63
$Q_{Forced\ convection} * 10^3$	[W]	21	20	19	19	18
Free Convection						
Gr	[-]	0.47	0.39	0.32	0.27	0.23
Nu	[-]	2.41	2.39	2.38	2.36	2.35
$U_{Free\ convection}$	[W m^{-2} K^{-1}]	52	53	54	54	55
$Q_{Free\ convection} * 10^3$	[W]	18	18	17	16	16
Radiation						
$T_{sample}^4 * 10^{-12}$	[K^4]	0.77	0.85	0.94	1.04	1.15
$T^4 * 10^{-12}$	[K^4]	0.73	0.81	0.90	0.99	1.10
$Q_{Radiation} * 10^3$	[W]	54	56	57	58	60

Chapter 5: Selective desulfurization of natural gas using copper sulfate solutions – Process design and economic evaluation.

Summary

The process design and economic potential of a novel selective desulfurization process that is based on the use of a copper sulfate solution were studied. The high selectivity towards H_2S of this process, along with the relatively high value of the obtained final products are key advantages. The economic performance of this process was studied using a Discounted Cash Flow analysis (DCF). Aim of this study was to establish the economic performance of the novel type of desulfurization process in comparison to its main, large scale, competitor: the amine based gas sweetening process.

The process design has been made using the following design basis.

Capacity:	200000 Nm^3 gas /hr (natural gas production) at 50 bar
Composition:	85 V% CH_4, 10 V% CO_2, 5 V% H_2S
Specification product:	Natural gas with 4 ppmV H_2S

Although both processes (logically) cost money when the product revenues were neglected, the economic performance of the novel process was substantially better than the economic performance of a conventional, amine based desulfurization unit for this design basis. Owing to the relatively low operating costs, retrofitting an existing amine based desulfurization unit can be a very attractive option. A sensitivity analysis, in which the feed gas composition was varied, showed that the competitive edge of the novel process improved at higher CO_2 or lower H_2S concentrations in the feed gas, but decreases when copper losses during regeneration occur.

Furthermore as the copper sulfate based process produced considerably more sulfuric acid (56 € per ton acid) than the conventional amine based process produced elemental sulfur (78 € per ton sulfur), the economic advantage of the copper sulfate based process over the amine based process increased further when the product revenues were taken into account.

1 Introduction.

1.1 Desulfurization of gas streams

An important aspect in both the production of natural gases and the treatment of industrial gases are the costs associated with the removal of hydrogen sulfide. In general hydrogen

sulfide must be removed before the gas can be used since it can give rise to corrosion in process equipment, poisoning of catalysts and because of its toxic nature. A large number of desulfurization processes, both of the absorbent consuming and of the absorbent re-using type, have been developed. Some processes remove hydrogen sulfide selectively, while others also remove other components (e.g. carbon dioxide) from the gas phase.

Large-scale desulfurization of gas streams is typically performed using a process that regenerates the absorbent. Of course, in these processes equipment is required to regenerate the absorbent. This usually results in a complex layout of these processes and consequently it makes these processes capital intensive. On the other hand the re-use of the absorbent keeps the operating costs low in comparison to its more simple (non absorbent regenerating) competitors. Examples of regenerative large-scale desulfurization processes are the amine-Claus processes and the iron chelate processes (for example the SulFerox process). The reagent consuming processes usually have a very simple process layout. This results in low capital costs for these processes. The main cost driver for the reagent consuming processes is associated with the consumed chemicals. The origin of the costs of the different process types dictates that each type has its own market (Nagl, 1997). The reagent consuming processes are competitive when a small desulfurization capacity (approximately 10-50 kg sulfur per day) is required. The large-scale amine based desulfurization processes cover the other end of the market. They are the best alternative when a desulfurization capacity in excess of 50 ton sulfur per day is needed, but may be viable, under specific conditions, for capacities as small as 5 ton sulfur per day. For the capacities between 50 kg per day and approximately 30 tons per day other process alternatives (e.g. the iron chelate based processes) are better suited.

A drawback of the desulfurization processes that make use of a basic absorbent (e.g. the amine or caustic soda based processes), is that they are not selective when carbon dioxide (or another acidic gas) is also present in the gas. For amine based processes this non-selectivity has the effect that carbon dioxide that is present in the gas stream to be desulfurized will, along with the hydrogen sulfide, also be absorbed in the amine solution. This has a pronounced negative effect on the economy of the process. A direct operational consequence of a decrease in selectivity is that the flow of the amine solution that has to be circulated increases. This causes an increase in the dimensions of the absorber column, the stripper column, circulation pumps and piping and therefore an increase in capital costs. Also, since CO_2 has to be stripped from the amine solution in the regeneration section, the energy consumption of this section will increase. The stripped CO_2 will also decrease the H_2S concentration of the H_2S rich gas that leaves the stripper. The lower H_2S concentration makes

the subsequent process step (the conversion of H_2S to elemental sulfur in a Claus reactor) normally less efficient, and may even cause operational problems in the Claus reactor.
For the sodium hydroxide based process (an example of a small scale non-regenerative process based on the use of a basic absorbent) the absorption of acidic components other than H_2S results in an increase in the consumption of the amount of reagent used. Since the reagent consumption is the main cost driver in this type of desulfurization process, the effects of the non-selectivity can be detrimental to the economy of the overall process.

A further aspect that is of importance for the economics of selective H_2S removal processes is the fact that a non-selective process suffers from the fact that a more stringent H_2S specification will usually lead to a much higher co-absorption of CO_2 (increasingly lower selectivity), and therefore to much higher desulfurization costs. Since the H_2S specification of the treated gas becomes ever more stringent due to new (environmental) legislation, selective desulfurization processes will become more competitive with respect to non-selective processes.

Taking the above into account, it will be clear that a regenerative desulfurization process that can treat a gas stream selectively will, in principle, have a competitive advantage over (non)-regenerative non-selective gas desulfurization processes. One such selective desulfurization process that is being developed is a desulfurization process based on the precipitation reaction (*Eq. 1*) that occurs when hydrogen sulfide is brought in contact with copper ions present in an aqueous solution (Ter Maat, 1997). [15]

$$Cu^{2+} + H_2S + 2H_2O \rightarrow CuS\downarrow + 2H_3O^+ \qquad (1)$$

Several key aspects of this selective process, e.g. the process conditions required for selective removal of H_2S from a gas stream and the regeneration of the formed copper sulfide to copper oxide have been described elsewhere (Ter Maat *et al*, 2004a, Ter Maat *et al*, 2004b). In the present contribution the economic feasibility of this process for the desulfurization of carbon dioxide containing gas streams on a large scale is investigated. In order to evaluate the proposed process technically and economically a process design is made. The economic performance of the process is compared with the updated economic performance of an amine based process described in literature (Blauwhoff *et al*., 1985).

Another possible market niche for this selective process can be created by making use of the fact that solid metal sulfides are relative compact and safe storage media for sulfur and

[15] Other (bivalent) metal ions can also be used, but are less suitable.

therefore (economically) transportable. By having a number of small scale absorption units in combination with a central, larger regeneration unit an attractive overall process may result. The absorption units will generate metal sulfide locally, which will be collected and converted into a reusable form in the regeneration unit. The relative low operating costs for the absorption units may also give a competitive edge over the current single use processes. However, the possibilities for decentralized desulfurization, combined with centralized regeneration are not investigated in this study.

2 Process description and design considerations

The design basis for the process, as presented in this paragraph, has been chosen such that it enables a good comparison with existing (large scale) process alternatives. The process design section comprises not only selection and sizing of the equipment, but also some general considerations concerning the lay-out of the process.

2.1 Design basis

A continuously operated plant was designed to desulfurize a gas stream of 200000 $Nm^3\ hr^{-1}$ containing 5 V% H_2S. Further details of the design basis are given in Table 1. Both with respect to the amount of treated gas and removed sulfur this capacity amounts to approximately 10% of the total German sour gas treating capacity. The concentration of H_2S in the desulfurized gas stream was specified at 4 ppmV (pipeline specification for natural gas). The desulfurization capacity of the plant to be designed and evaluated in this study is chosen such that the main competitors are the amine based processes. For the design basis stated in Table 1. Blauwhoff *et al.* (1985) made an economic evaluation for an amine based desulfurization plant that, after updating, also gives a good indication of the current capital and operating cost of such a desulfurization plant (See Appendix C). Furthermore, the design given by Blauwhoff *et al.* is detailed enough to allow for a parameter sensitivity study in which e.g. the H_2S and CO_2 content of the sour gas stream are varied. The aim of the study performed by Blauwhoff *et al.* was to demonstrate how the economic efficiency of the amine based process can be improved by increasing the selectivity of the H_2S absorption (over that of CO_2). The selection of the same design basis in the current study enables a good economic comparison of the two regenerative processes.

Table 1: Design basis

Gas stream to be treated & specification	
Flow	200000 Nm^3/hr[16]
Pressure	50 bara
Composition	85 V% CH_4
	10 V% CO_2
	5 V% H_2S
Specification	4 ppmV H_2S
Desulfurization Unit	
Capacity	103000 tons S/annum
% SO_2 in feed gas	8.7 %
On-stream	8000 hr/yr

2.2 Design procedure

The aim of the process design is to size all the equipment to enable an economic evaluation with an "order of magnitude" accuracy (accuracy not better than 40%-50%). Therefore only the main dimensions of the required equipment need to be determined. In some cases a more detailed design of the apparatus was made, however in other cases (e.g. pumps, and compressors) knowing the duty and type of the apparatus suffices for a cost estimate. A description of the unit operations shown in the flow sheet of Figure 1 is given in Appendix A.

The following design procedure has been used. First the overall process has been subdivided in unit operations and the mass and energy balances of the process have been solved by setting up a model description for each unit operation, linking these models and solving the obtained relations. In Table 3 the obtained numerical values for the mass flows and composition of the process streams necessary for the sizing of the equipment are tabulated. With the size, composition, temperature and pressure of all relevant process flows known, the utilities usage and the duty of each unit operation could be calculated. Then the appropriate type of equipment used could be selected and the main dimensions of the equipment could be calculated. From these data the capital and operating expenditure for each unit operation were estimated.

[16] Unlike STP conditions which are internationally defined, normal conditions are not internationally defined. In this study T = 25 ºC and P = 10^5 Pa are taken as normal conditions.

The mass balance of the process designed to desulfurize a gas stream of 200000 Nm^3 hr^{-1} containing 5V% H_2S is shown in Table 3. The flow sheet of the process is given in Figure 1. The choice and sizing of equipment can be found in Appendix A, equipment sizes are summarized in Table 4.

2.3 Flow scheme

A simplified flow scheme of a regenerative desulfurization unit using a copper sulfate solution as absorbent is shown in Fig 1. The flowsheet can be subdivided in 3 functional sections.

- the absorber unit and particle separator
- the copper reclamation unit
- the absorbent make up section.

In the absorber the hydrogen sulfide containing gas will be brought in contact with the aqueous copper sulfate solution. The removal of H_2S from this gas stream takes place according to the overall absorption reaction shown in Eq. 2 (Table 2). The sweetened gas stream and the absorbent stream containing copper sulfide particles leave the absorber. The formed CuS particles are separated from the spent washing liquor in a subsequent processing step. The CuS is brought into a fluid bed reactor and is oxidized (using air) at a temperature of 1000 K. The overall oxidation reaction is given in Eq. 4 (Table 2). The formed copper oxide is then brought in a contact with the spent (acidic) washing liquor in a regeneration unit. In this unit CuO reacts with the hydronium ions under the formation of water and Cu^{2+} ions (Eq. 3 in Table 2). To assure a swift and complete dissolution of copper oxide, an excess of hydronium ions is needed. Note that this does imply that the absorbent stream that leaves the make-up section, and is subsequently used as fresh absorbent in the absorber, is acidic. The reaction equations of the 3 process steps are summarized in Table 2. Note that the dissolution reaction of CuO consumes the hydronium ions formed during the absorption step, so that the overall process does not require addition or removal of H^+ ions.

Table 2: Overall reactions of the 3 processing steps and the net reaction of the process

Processing step	*Reaction*
Absorption of H_2S in CuSO4 solution (Eq. 2)	$Cu^{2+} + H_2S + 2\,H_2O + SO_4^{2-} \rightarrow CuS\downarrow + 2\,H_3O^+ + SO_4^{2-}$
Dissolution reaction (Eq. 3)	$CuO + 2\,H_3O^+ + SO_4^{2-} \rightarrow Cu^{2+} + 3\,H_2O + SO_4^{2-}$
Oxidation of CuS (Eq. 4)	$CuS + 1\,1/2\,O_2 \rightarrow CuO + SO_2$
Overall reaction (Eq. 5)	$H_2S + 1\,1/2\,O_2 \rightarrow H_2O + SO_2$

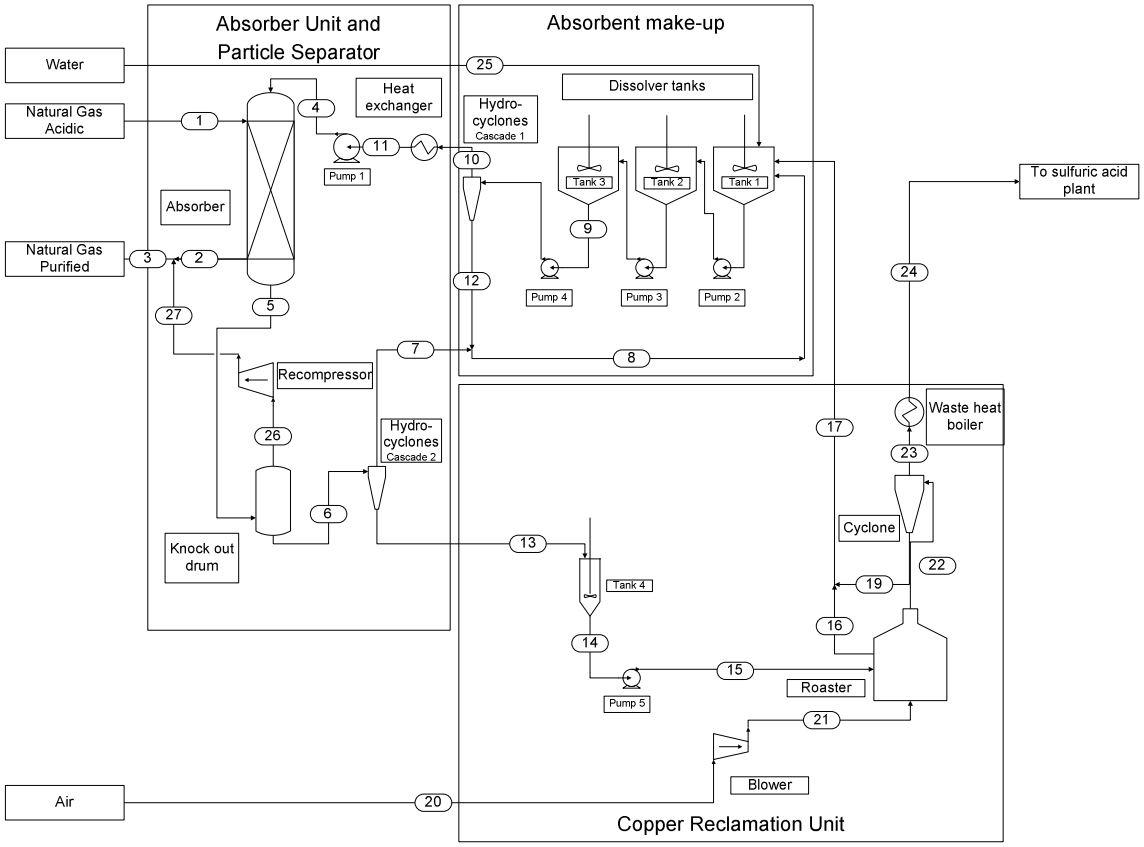

Figure 1: Simplified flowsheet of the copper sulfate based desulfurization process

2.3.1 Absorber unit and particle separation

The hydrogen sulfide containing gas is brought in contact with the acidic copper sulfate solution in a packed bed absorber. Since the reaction between $CuSO_4$ and H_2S may be considered fast and irreversible under the conditions applied (Ter Maat *et al*., 2004a), the local driving force of absorption will not depend on the fact whether the column is operated in counter- or co-current flow mode (Zarzycki and Chacuk, 1993 p432). Since the co-current flow mode allows a flow rate over the column (no risk of column flooding, and less problems with plugging) in comparison to counter-current flow, and the co-current flow mode offers the further advantage of higher gas- and liquid phase mass transfer coefficients (at the same pressure drop over the column) the absorption column will be operated co-currently. In the absorber hydrogen sulfide is removed from the gas stream, and is precipitated as copper sulfide according to Eq. 2.

$$Cu^{2+} + H_2S + 2\,H_2O + SO_4^{2-} \rightarrow CuS\downarrow + 2\,H_3O^+ + SO_4^{2-} \qquad (2)$$

The purified gas stream leaves the absorber, and is available for further processing. The acidic metal sulfate solution, now containing precipitated copper sulfide, is depressurized in a flash vessel fitted with an entrainment separator. Gases physically dissolved in the absorbent slurry are desorbed in the flash vessel. This gas, a mixture of mainly carbon dioxide and methane, is recompressed and added to the purified gas stream (the most cost effective method in this overall exothermic process). The solid copper sulfide is then separated from the degassed absorbent using hydrocyclones. The underflow from these hydrocyclones, a concentrated slurry of solid copper sulfide, is converted to copper oxide in the copper reclamation section. The spent (virtually solids free) absorbent is fed to the high pressure absorbent make up unit.

2.3.2 Absorbent make-up unit

In the absorbent make up unit the copper concentration in the absorbent is brought back to its original value by dissolving the copper oxide produced in the copper reclamation unit. Copper oxide dissolves as it reacts with the hydronium ions present in the metal sulfate solution (See Eq. 3).

$$CuO + 2\,H_3O^+ + SO_4^{2-} \rightarrow Cu^{2+} + 3\,H_2O + SO_4^{2-} \qquad (3)$$

This reaction takes place in a cascade of 3 stirred tanks. Unreacted (solid) copper oxide that leaves the cascade is separated from the absorbent stream by means of hydrocyclones and recycled to the dissolvers. The temperature rise caused by the heat of the dissolution reaction is compensated with cooling water using a heat exchanger. The absorbent stream is fed back to the absorption column by means of a multistage centrifugal pump.

2.3.3 Copper reclamation unit.

In the copper reclamation unit copper sulfide is converted into copper oxide that can subsequently be converted back into copper sulfate in the absorbent make-up unit. The copper sulfide slurry transported to the reclamation unit section is first brought in a small vessel and from there fed to the roaster. In the roaster the copper sulfide is oxidized to copper oxide and sulfur dioxide using air (Eq. 4).

$$CuS + 1\,{}^1\!/\!_2\,O_2 \rightarrow CuO + SO_2 \qquad (4)$$

Copper sulfate, dissolved in adhering mother liquor, that is also brought into the roaster will dissociate into copper oxide and sulfur dioxide (Ter Maat, 2004b). Sulfuric acid, also present in the adhering mother liquor will dissociate into water and sulfur dioxide. The formed copper oxide is then transported pneumatically to the absorbent make up unit. The air needed for the

oxidation of copper sulfide is provided by a roots blower. The gas stream leaving the roaster contains the sulfur dioxide released during the oxidation. That gas stream is cooled by water, and the sulfur dioxide present in that gas stream is then available for further processing, e.g. in a sulfuric acid plant. The excess heat generated during the oxidation may be used for e.g. the production of steam. A mass balance for the copper based desulfurization plant given in Figure 1, for the design basis given in Table 1 is given in Table 3 parts 1 and 2. An overview of the process equipment, its duty, and the dimensions needed for a cost estimate is given in Table 4. The utilities usage as determined in Appendix A, and the labor demand (Ulrich (1984)), of the equipment are shown in Table 5. The utillities usage and labor demand of the roast gas conversion plant are not stated here, but the costs associated with them will be taken into account in the economic evaluation.

Table - part 1: Mass balance for the copper based desulfurization plant given in Figure 1, for the design basis given in Table 1.

Mass balance																
Stream		**1**	**2**	**3**	**4**	**5**	**6**	**7**	**8**	**9**	**10**	**11**	**12**	**13**	**14**	**15**
P	[bara]	50	49	49	50	49	4	1.0	1.0	2.0	1.0	1.0	1.0	1.0	1.0	1.6
T	[K]	300	311	311	300	311	311	311	311	322	322	300	322	322	300	300
Total	[kmol hr^{-1}] * 10^{-3}	8.0	7.5	7.7												
Gas	[Nm3 hr^{-1}] * 10^{-3}	200	188	190												
Total	[kmol hr^{-1}]*10^{-3}				40.0	40.0	40.0	39.1	39.1	40.0	40.0	40.0	0.04	0.9	0.9	0.9
H_2O	[ton hr^{-1}]				720	720	720	703	704	721	720	720	0.7	16.5	16.5	16.5
	[m^3 hr^{-1}]				600	600	600	586	587	601	600	600	1	14	14	14
Gas																
H_2S	[V %]	5.0														
CO_2	[V %]	10.0	9.9	10.5												
CH_4	[V %]	85.0	90.0	89.4												
O_2	[V %]															
N_2	[V %]															
SO_2	[V %]															
H_2O (G)	[V %]		0.1	0.1												
Solid																
CuS	[ton hr^{-1}]					38.5	38.5		0	0			0	38.5	38.5	38.5
$CuSO_4$	[ton hr^{-1}]															
CuO	[ton hr^{-1}]								1.6	1.6			1.6			
Solution																
CO_2(L)	[kmol m^{-3}]				0.07	0.16	0.08	0.08	0.08	0.07	0.07	0.07	0.07	0.08	0.08	0.08
CH_4(L)	[kmol m^{-3}]				0.00	0.06	0.00	0.00	0.00	0.00	0.00	0.00	0.00	0.00	0.00	0.00
Cu^{2+}	[kmol m^{-3}]				0.80	0.13	0.13	0.13	0.13	0.80	0.80	0.80	0.80	0.13	0.13	0.13
H_3O^+ (total acid)	[kmol m^{-3}]				1.29	2.64	2.64	2.64	2.64	1.29	1.29	1.29	1.29	2.64	2.64	2.64
SO_4^{2-} (total sulfate)	[kmol m^{-3}]				1.45	1.45	1.45	1.45	1.45	1.45	1.45	1.45	1.45	1.45	1.45	1.45
pH	[-]				0.6	0.02	0.02	0.02	0.02	0.6	0.6	0.6	0.6	0.02	0.02	0.02

Table 3 - part 2: Mass balance for the copper based desulfurization plant given in Figure 1, for the design basis given in Table 1.

Mass balance									
Stream		**17**	**20**	**21**	**23**	**24**	**25**	**26**	**27**
P	[bara]	1.0	1.0	1.6	1.0	1.0	1.0	4.0	49
T	[K]	1000	300	300	1000	700	300	311	311
Total	[kmol hr^{-1}] * 10^{-3}		4.0	4.0	4.7	4.7		0.1	0.1
Gas	[Nm3 hr^{-1}] * 10^{-3}		99	99	117	117		2.2	2.2
Total	[kmol hr^{-1}]*10^{-3}						0.6		
H_2O	[ton hr^{-1}]						10.3		
	[m^3 hr^{-1}]						9		
Gas									
H_2S	[V %]								
CO_2	[V %]				0.0	0.0		58.4	58.4
CH_4	[V %]							40.8	40.8
O_2	[V %]		21.0	21.0	4.4	4.4			
N_2	[V %]		79.0	79.0	67.0	67.0			
SO_2	[V %]				8.7	8.7			
H_2O (G)	[V %]				19.9	19.9		0.9	0.9
Solid									
CuS	[ton hr^{-1}]								
$CuSO_4$	[ton hr^{-1}]	2.6							
CuO	[ton hr^{-1}]	30.9							
Solution									
CO_2(L)	[kmol m^{-3}]								
CH_4(L)	[kmol m^{-3}]								
Cu^{2+}	[kmol m^{-3}]								
H_3O^+ (total acid)	[kmol m^{-3}]								
SO_4^{2-} (total sulfate)	[kmol m^{-3}]								
pH	[-]								

Note: Streams that are irrelevant for the sizing of the equipment (e.g. the internal recycles in the roaster, streams 16, 18, 19 and 22) are omitted in this Table.

Table 4: Main dimensions of the process equipment, of the copper based desulfurization plant, 200000 $Nm^3\ hr^{-1}$, p= 50 bar, H_2S_{in} = 5 V%, $CO_{2,in}$ = 5V%, H_2S_{spec} = 4 ppmV.

Dimensions of the process equipment used								
Apparatus	operating pressure	operating temperature	volume flow	Construction material	motor power	height	Diameter	area
	P [bara]	T [K]	Φ [$m^3\ hr^{-1}$]		Q [kW]	h [m]	D [m]	A [m^2]
Absorber Unit and Particle Separator								
Absorber (dual, parallel))	60	311		SS		10	1.5	
Packing (2x)		311		SS 316		6.5	1.5	
Flash vessel	10	311		SS		7	2..8	
Pump (1)	1-50	311		SS	1000			
Recompressor, (rotary + el. motor)	4-49	311		CS	400			
Hydrocyclones (1)		311	600	SS				
Absorbent make-up								
Pump (2)	1-2	322		SS	20			
Pump (3)	1-2	322		SS	20			
Pump (4)	1-3	322		SS	40			
Dissolver (Tank 1) + agitator, 8kW	1	322		SS		9.5	3.8	
Dissolver (Tank 2) + agitator, 8kW	1	322		SS		9.5	3.8	
Dissolver (Tank 3) + agitator, 8kW	1	322		SS		9.5	3.8	
Hydrocyclones (2)		322	600	SS				
Heat exchanger		322		CS/SS				1150
Copper reclamation unit								
Stirred Tank (Tank4)	1	322		SS		2	1.5	
Pump (5)	1-2	322		SS	5			
Fluid bed roaster, brick-lined	1	1000		SS		4	5	
Blower + el. motor (Compressor, rotary)		300	97000	CS	1000			
Cyclone		1000		SS				
Pneumatic conveyor		1000	350000	SS	200			
Waste heat boiler				CS/SS				412

Table 5: Utilities usage and labor demand of the process equipment, of the copper based desulfurization plant, for 200000 $Nm^3\ hr^{-1}$, p= 50 bar, H_2S_{in} = 5 V%, $CO_{2,in}$ = 5V%, H_2S_{spec} = 4 ppmV.

Apparatus	Dimensions of the process equipment used				
	Electrical power Q [MW]	Cooling water Φ [$m^3\ hr^{-1}$]	Boiler feed water [Ton hr^{-1}]	Steam HP [Ton hr^{-1}]	Operating labor [operator $shift^{-1}$]
Absorber Unit and Particle Separator					
Absorber (dual)					0.5
Flash vessel					0.3
Pump (1)	1.0				
Recompressor, (rotary + el. motor)	0.4				0.2
Hydrocyclones (1)					0.3
Absorbent make-up					
Pump (2)	0.01				
Pump (3)	0.01				
Pump (4)	0.01				
Dissolver (Tank 1) + agitator, 8kW	0.01				0.3
Dissolver (Tank 2) + agitator, 8kW	0.01				0.3
Dissolver (Tank 3) + agitator, 8kW	0.01				0.3
Hydrocyclones (2)					0.3
Heat exchanger		1637			0.1
Copper reclamation unit					
Stirred Tank (Tank4)					0.3
Pump (5)	0.01				
Roaster, brick-lined			5.0	-5.0	0.5
Blower + el. motor (Compressor, rotary)	0.8				0.15
Cyclone					
Pneumatic conveyor	0.2				0.2
Waste heat boiler			17.3	-17.3	0.1
Total	2.4	1637	-22.3	0.0	4

3 Economic evaluation

In order to determine the economic feasibility of the proposed copper sulfate based desulfurization process a cost estimate for such a desulfurization unit located in the Netherlands has been made using a discounted cash flow analysis. This estimate of the costs has been based upon an estimate for both capital investment and operating costs and will be compared with the costs of desulfurization using conventional technology, i.e. desulfurization using Amine/Claus-based technology (Blauwhoff *et al,* 1985). A brief introduction to the amine based process type is given in Appendix C.

3.1 Total capital investment

The total capital investment consists of the fixed capital investment, the working capital and the start-up costs. The fixed capital has been calculated from the costs of the equipment using an adapted version of Guthrie's factorial estimate method (Ulrich, 1984, p274-284). The inside battery limits (ISBL) costs are the sum of the process module costs. The total outside battery limits capital investment (OSBL), working capital and start-up costs were estimated using the guidelines given by Peters and Timmerhaus (2003).

3.1.1 Equipment costs

The equipment costs have been estimated from the equipment sizes given in Table 4, using the data presented by Ulrich (1984, p285-317). If the equipment size was not available a quick estimate of the main dimensions was made using the guidelines given in Walas (1988). Bare equipment costs given by Ulrich have been verified using a more recent source of equipment prices (Dace Prijzenboekje, 2000), and were, after adjusting for escalation, found to be within a range of 20%.

3.1.2 ISBL-costs

The ISBL costs were estimated from the equipment costs using the adapted Guthrie's factorial estimate method. To obtain the chemical process module costs, the bare equipment costs (C_p[17]) were multiplied by a factor (C_{BM}) to account for materials used for installation (e.g. piping, insulation, electrical wiring, instrumentation, insulation), direct labor and indirect costs (e.g. freight, insurance, taxes, construction overhead and engineering costs). The C_{BM} also takes the effects of the material of construction and operating pressure on the module cost into account. The factor (C_{BM}) differs for each piece of equipment and depends on the construction material, working pressure and type of equipment. The factor (C_{BM}) has been estimated using the graphs given by Ulrich (1984, p 285-317). The inside battery limits costs

[17] Bare equipment costs are determined for a piece of equipment operating at atmospheric pressure and made from the standard material of construction (usually carbon steel).

can now be calculated from the sum of all chemical process module costs and adding indirect costs (contractor fee and contingency).

3.1.3 OSBL-costs

The outside battery limits costs account for e.g. site preparation (land and its improvements), auxiliary buildings, and offsite and storage facilities (e.g. electrical power generators, cooling towers, final product storage, fire protection utilities, yard lighting, unloading docks etc.). The OSBL costs have been estimated from the ISBL costs (Ulrich, 1984). The figure proposed by Ulrich for a large plant constructed in a well developed area (30% of total module costs) was used. This number corresponds well with more recent data given by Peters and Timmerhaus (2003) (11-38% of total fixed capital) and Perry (1997) (20-40% of total installed plant cost). An overview of the equipment used, the bare equipment costs C_P, the C_{BM} factors, the chemical process module costs and the total ISBL and OSBL costs is given in Table 7, where the C_{BM} factor is a function of the material factor F_M and a pressure factor F_P. These factors have also been listed.

The costs for the sulfuric acid plant used to convert the roast gas into sulfuric acid has been estimated from data given by Perry (1997), Brennan (1998), Peters and Timmerhaus (2003) and Garret (1989, p338 & p359). Data for a sulfuric acid plant using elemental sulfur as feedstock have been adapted for the use of a different feedstock (i.e. gas containing a lower SO_2 percentage) using the data given by Luedtke and Kreuser. An overview of the various sources is given in Table 6. In the base case of the current study a value of 13.5 MEur, 2003 has been chosen. In a sensitivity analysis the fixed capital investment associated with the roast gas conversion has been varied between 9 and 19 MEur, 2003.

Table 6: Estimating the fixed capital of the sulfuric acid unit for the roast gas conversion from literature data .

Literature data		*Feedstock*	*Fixed capital estimate at a capacity of 317 kt H_2SO_4 yr^{-1} [MEur, 2003]*
Literature source	Capacity range [kt H_2SO_4 yr^{-1}]		
Perry (1997)	30-300	S	9.0
Brennan (1998)	350	S	10.0
Peters & Timmerhaus (2003)	30-300	S	11.0
Garret (1989)	100-1300	S	19.1
Brennan (1998)	370	SO_2 rich gas	13.3

From Table 7 it can be concluded that a very important fraction of the total costs (approximately 60%) is accounted for by the unit used for the roast gas conversion. This unit converts the sulfur dioxide present in the roast gas into a saleable product (sulfuric acid). Furthermore, Table 7 shows that the remainder of the (ISBL) capital investment is divided (approximately) equally over the three processing units (Absorption unit and particle separation, copper reclamation unit and the absorbent make-up unit).

3.1.5 Location and inflation

The location factor for chemical plants given by Perry (Perry, 1984) was used to account for the differences in costs caused by the location of the plant. The value used was 1.00. To convert to the local currency a conversion factor of 1.1 k€/kUS$ (mid 2003) was used. To adjust for inflation the Chemical Engineering cost index, published biweekly in "Chemical Engineering" was used. Therefore the fixed (ISBL+OSBL) capital investment in the Netherlands in the year 2003 will be 25.7 M€.

3.1.6 Working Capital and Start-up expenses.

The working capital was estimated using the method given by Peters and Timmerhaus (2003) and comprises the costs for 1 month worth of inventories (e.g. raw materials, and finished products), monthly paid operating expenses (e.g. wages, spare parts and operating supplies), accounts receivable minus accounts payables and cash.

The start-up expenses were estimated to be 8 % of the ISBL+OSBL capital investment (Perry, 1997). The total capital investment could now be calculated from Fixed (ISBL+OSBL) capital investment, the working capital and the start-up costs and did amount to M€ 30.9. A break down of the total fixed capital investment is given in Table 8.

Table 8 : Break down of the total capital investment

Total Capital Investments			
			k€ 2003
Fixed (ISBL+OSBL) capital investment			25753
Working capital	(Peters and Timmerhaus, 2003)		3105
Start-Up Expenses	in % ISBL + OSBL	8	2030
Total fixed capital investment	k€ 2003		30920

Table 7 : Fixed ISBL + OSBL capital investment for the copper based desulfurization plant 200000 $Nm^3 hr^{-1}$, p= 50 bar, H_2S_{in} = 5 V%, $CO_{2,in}$ = 5V%, H_2S_{spec} = 4 ppmV.

Process Equipment Description	Bare equipment cost C_p 2003 k€	Factors needed to estimate module cost F_M	 F_P	 C_{BM} =f(F_MxF_P)	module costs 2003 K€
Absorber Unit and Particle Separator					
Absorber (dual)	56.4	4	4	30	1693
Packing (2x)	13.5			4.2	57
Flash vessel	45.1	4	1.5	13	587
Pump	60.9	1.9	2.2	8.2	500
Compressor, rotary + electric motor	28.2			3.5	99
Hydrocyclones (50)	56.4			4	226
Absorbent make-up					
Pump (after dissolver tank 1)	7.9			4.5	36
Pump (after dissolver tank 2)	7.9			4.5	36
Pump (after dissolver tank 3)	7.9			4.5	36
Dissolver tank 1 + agitator 8 kW	67.7	4	1	9	609
Dissolver tank 2 + agitator, 8kW	67.7			9	609
Dissolver tank 3 + agitator, 8kW	67.7			9	609
Hydrocyclones	56.4			4	226
Heat exchanger	62.1	2.8		4.5	279
Copper reclamation unit					
Stirred Vessel	6.8			9	75
Pump	5.6	1.9		4.5	25
Roaster, brick-lined	180.6			6	1083
Compressor, rotary+ electric motor	20.3			2.2 1.5	45
Pneumatic conveyor	141.0				310
Cyclone	152.3			5	762
Waste heat boiler	48.1			2.1	101
Total module Investment					7987
Contingency and Fee	in % Total module Investment			18	1438
Fixed ISBL Capital investment	k€ 2003				9426
Fixed OSBL Capital investment	in % ISBL			30	2828
Roast gas conversion (incl. OSBL)	Sulfuric acid plant				13500
Fixed (ISBL+OSBL) capital investment	k€ 2003				25753

3.2 Production costs

In order to carry out a cash flow analysis it is necessary to determine the operating expenses of the desulfurization unit and roast gas conversion unit. Table 9 gives a rough breakdown of the operating expenses.

Table 9 : Break down of the operating expenses [Peters and Timmerhaus (2003)]

Operating expenses			
production costs			*General Expenses*
Direct operating costs	*Indirect operating costs*	*Overhead*	*(fixed and variable)*
Raw materials	Local taxes	Purchasing, warehousing	Sales and Marketing
Utilities	Insurance	Site overhead	Distribution
Maintenance and repairs	Rent	Medical services	Quality management
Operating labor		Safety and protection	Engineering services
Supervision		Cafeteria and recreation	Research and Development
Laboratory charges		Laboratories	Finance and Administration
Operating supplies		Logistic services	Personnel
Patents and royalties		Fringe benefits personnel	Management services

3.2.1 Direct operating costs and overhead

The amount of raw materials and utilities needed was taken from the mass- and heat balances. The local (dutch) prices for these raw materials and utilities were used (Dace Prijzenboekje, 2000). Given the ever increasing reliability of the equipment, the annual costs for maintenance were set at 2% of the total fixed capital investment (the lower end of the range given by Peters and Timmerhaus, 2003). The operating labor is the labor needed to actually run the plant. This excludes supervision, maintenance, laboratory and support personnel. Data given by Ulrich (1984, p 328-330) state the number of operators needed for various types of process equipment (See also Table 5). These data were used in the current analysis. 5 shifts of 4 operators each are needed for a continuous operation. The costs for supervisory labor and laboratory costs were both set at 15 % of the operating labor (Ulrich, 1984, Peters and Timmerhaus, 2003), while the costs for operating supplies have been set at 15% of the maintenance costs (Ulrich, 1984, p330, Peters and Timmerhaus, 2003). Finally the charges for patents and royalties amount to 3% of the total operating expenses (Ulrich, 1984, p335, Peters and Timmerhaus, 2003). The numbers for the operating expenses are tabulated in Table 10.

3.2.2 Indirect operating costs and overhead

Indirect production costs consist of the costs for local taxes and insurance. A value of 1 % of the total fixed capital per year (Peters and Timmerhaus, 2003) was chosen. Overhead costs have been based on the sum of operating labor, supervision and maintenance. A range of 50 - 70 % of this sum was found to represent overhead and miscellaneous expenses adequately (Ulrich, 1984, p335 - p337, Peters and Timmerhaus, 2003). In the current analysis 60 % has been chosen. The indirect production costs and overhead are given in Table 10. A capital charge was not included because a DCF analysis has been performed.

3.3 General Expenses

In addition to direct and indirect operating expenses, a certain portion of corporate management costs, sales expense and research effort must be financed from plant revenues. The administrative costs (finance and administration) are proportional to the plant staff and can be scaled as a fraction (approximately 25%) of overhead (Ulrich, 1984, p337 - p338), or as a fraction (approximately 20%) of operating labor (Peters and Timmerhaus, 2003). In this case both approaches yielded approximately the same result. For the costs of research and development 3-5 percent of the total operating expenses costs is a good estimate for most chemical products (Ulrich, 1984, p337 - p338, Peters and Timmerhaus, 2003). The budget for sales and marketing is usually based on the product value. Ten percent of the total operating expenses costs is a realistic estimate for most chemical products (Ulrich, 1984, p337 - p338, Peters and Timmerhaus, 2003). Considering the large size of the desulfurization plant and the marketability of sulfuric acid 3 % (near the lower end of the range mentioned by Peters and Timmerhaus) of the total operating expenses costs seems a more realistic number and has been used in this study. The operating costs for the sulfuric acid plant used to convert the roast gas into sulfuric acid has been estimated from the graph given by Garret, (1989, p359). The estimated production costs in 1989 amount to 32 US$ per ton of sulfuric acid, however a large fraction (approximately 70%) thereof is accounted for by the raw materials (elemental sulfur). Since raw materials are available at no charge for the plant under investigation these costs were omitted. The operating costs of the sulfuric acid unit were updated to 2003 using the CE-index. The operating expenses have been summarized in Table 10 and amount to 6.5 M€/yr. This is € 65 per ton of Sulfur removed, or € 21 per ton of sulfuric acid produced

Table 10: Operating expenses for the copper based desulfurization plant, 200000 $Nm^3\ hr^{-1}$, p= 50 bar, H_2S_{in} = 5 V%, $CO_{2,in}$ = 5V%, H_2S_{spec} = 4 ppmV. Byproduct credits (steam) not taken into account.

Operating expenses					
Direct operating costs					
				k€/yr	k€/yr
Raw materials	k€/unit	units used	basis		
H_2S (ton)	0	13,7	Hr^{-1}	0	0
Utilities (See also Table 5)					
electric power (MWh)	0.065	2.25	hr^{-1}	1148	
cooling water (m^3)	0.000050	1637	hr^{-1}	654	
natural gas (GJ)	0.003	0.00	hr^{-1}	0	
steam HP (ton)	0.016	-22.3	hr^{-1}	0	
Boiler feed water (ton)	0.00070	22.3	hr^{-1}	0	
Maintenance and repairs	2	% total fixed capital		515	
operating labor	20	operator a k€ 40	yr^{-1}	800	
Supervision	15	% operating labor		120	
laboratory charges	15	% operating labor		120	
Operating supplies	15	% Maintenance and repairs		77	
Patents and royalties	3	% total expenses		195	
Sulfuric acid plant (Garret, 1989)				1155	
Total direct operating costs				4785	4785
Indirect operating costs and overhead					
Local taxes and insurance	2	% total fixed capital		258	
overhead	60	% operating labor, super-vision and maintenance		861	
Total indirect operating costs				1119	1119
General expenses					
Administrative costs	25	% overhead		215	
Research & Development	3	% total expenses		195	
Sales and Marketing	3	% total expenses		195	
Total general expenses				606	606
Total operating expenses					6509

3.4 DCF analysis

With the operating expenses and total fixed capital determined a discounted cash flow analysis (DCF) has been made. A similar DCF analysis was prepared for the competing amine based desulfurization process. The discounted cash flow has been made using the following assumptions.

- The cost of capital is 12 % annual (rate of return or discount rate *i*);
- The project lifetime is 10 year;
- The plant will be built in two years (year -1 and year 0) The fixed (ISBL+OSBL) capital investments will be split equally over these two years;
- The start-up costs will be made in year 0;
- The investment for the working capital will be made in year 0 and will be completely recovered in year 10;
- The plant will be depreciated linearly in 10 years;
- The salvage value is 10 % of the initial total fixed investment;
- The tax rate is 35 %.

The cash flow in a certain year was calculated from the cash inflows (sales revenues), operating expenses, depreciation, (dis)investments and the tax rate using Eq. 6 (Peters and Timmerhaus, 2003).

$$\text{Cashflow} = (1-\text{tax}) * (\text{Sales Revenue} - \text{Operating Expenses}) + \text{tax} * \text{Depreciation} + (\text{Dis})\text{investment} \qquad \textit{(Eq. 6)}$$

The cash flow in year n was then used to calculate the present value from that year (PV_n) using Eq. 7 (Peters and Timmerhaus, 2003).

$$\text{PV}_\text{n} = \frac{Cashflow_n}{(1+i)^n} \qquad \textit{(Eq. 7)} \qquad\qquad \text{NPV} = \sum_{n=-1}^{n=10} \text{PV}_\text{n} \qquad \textit{(Eq. 8)}$$

The sum of all present values is the Net Present value of the project (Eq 8). An example of a cash flow table (base case + product revenues for copper sulfate based desulfurization, see also Fig 6) is given in Table 11. In the example a sales price of € 56 per ton of sulfuric acid [Rotterdam, 2003 technical grade, truckload] was used.

Table 11: Cash flow table "base case + product revenues for copper sulfate based desulfurization" for a sulfuric acid price of € 56 per ton

Yr		*Cash flow components*					*Present value*	
Yr	$\frac{1}{(1+i)^n}$	(Dis)invest-ment	Sales revenue	Operating expenses	Depre-ciation	Cash flow	Year n	Accumulated to year n
		[kEur]	[kEur]	[kEur]	[kEur]	[kEur]	[kEur]	[kEur]
-1	1.12	-12876				-12877	-14422	-14422
0	1.00	-18030				-18030	-18031	-32453
1	0.89		17741	6509	2318	8112	7243	-25210
2	0.80		17741	6509	2318	8112	6467	-18743
3	0.71		17741	6509	2318	8112	5774	-12969
4	0.64		17741	6509	2318	8112	5155	-7814
5	0.57		17741	6509	2318	8112	4603	-3211
6	0.51		17741	6509	2318	8112	4110	898
7	0.45		17741	6509	2318	8112	3669	4568
8	0.40		17741	6509	2318	8112	3276	7844
9	0.40		17741	6509	2318	8112	2925	10769
10	0.32	5669	17741	6509	2318	13781	4437	15206

3.4.1 Base case: costs of desulfurization, no revenues taken into account

The results of the discounted cash flow analysis are shown in Figure 2. The present value and the accumulated present value are plotted versus time. The revenues from the sulfuric acid and steam produced have not been taken into account. Especially the earnings for the steam produced will depend heavily on the presence of consumers in the immediate vicinity of the desulfurization unit. Also the earnings for the sulfuric acid will, to a great extent, depend on the location of the desulfurization unit, and may vary significantly in time since the price for sulfuric acid is determined by the free market mechanism. For these reasons the product revenues have been omitted in the base case scenario.

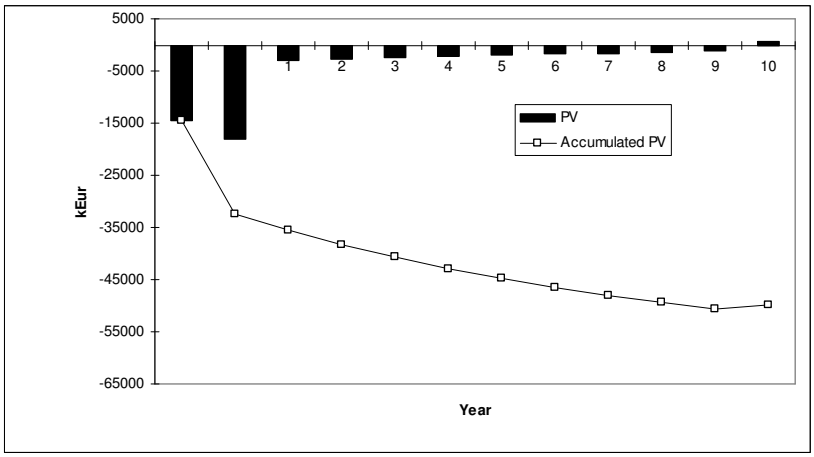

Figure 2: Discounted cash flow "Base case Copper based desulfurization process"; 200000 $Nm^3\ hr^{-1}$, p= 50 bar, H_2S_{in} = 5 V%, $CO_{2,in}$ = 10V%, H_2S_{spec} = 4 ppmV, 103 kt S yr^{-1}, no product revenues

Over 10 years the total accumulated discounted cash flow amount to -50 M€. The total costs of desulfurization amounts to € 0.0083 per m^3 of gas treated or € 129 per ton of sulfur removed[18].

As a comparison the costs of desulfurization was calculated in the same manner for a commonly used competitive process (amine-based desulfurization). The ISBL investment and operating expenses for the amine-based desulfurization have been taken from Blauwhoff *et al.* (1985) and were verified using more recent cost estimates, and adjusted for location and inflation. Furthermore the underlying additional assumptions (for both calculations were taken to be identical (See also appendix C).

The results of the discounted cash flow analysis for the amine based desulfurization process are shown in Figure 3 in which the present value and the accumulated present value are plotted versus time. Also in this case the revenues for the sulfur and steam produced were not taken into account.

[18] In the DCF method the value of the costs made and revenues received is time dependent (See Eq. 7). In case of applying the DCF method to a non-profitable process, future losses are also valued lower than the current losses. A "price" per ton of sulfur removed can be calculated by assigning a constant value per ton of sulfur removed as "sales revenue" (The NPV is set to zero in this manner). However, in the remainder of this study the (negative value of the) NPV will be used as a measure for evaluating process alternatives and cost scenarios at identical discount rates unless stated otherwise.

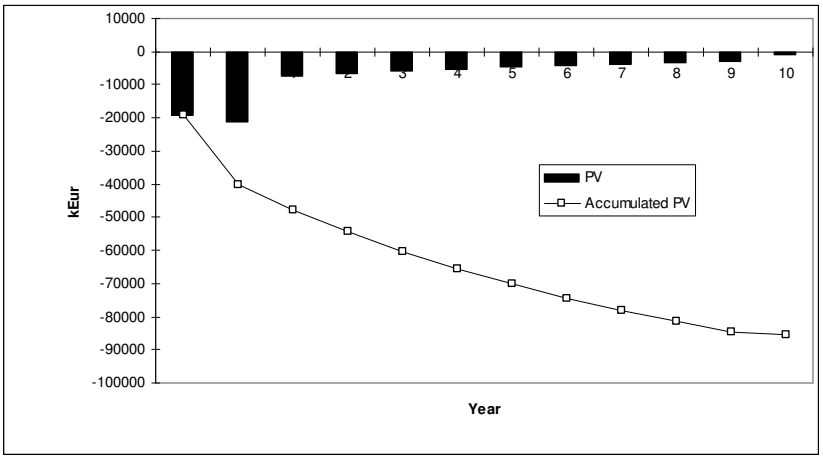

Figure 3: Discounted cash flow "Base case Amine based desulfurization process"; 200000 Nm^3 hr^{-1}, p = 50 bar, H_2S_{in} = 5 V%, $CO_{2,in}$ = 10V%, H_2S_{spec} = 4 ppmV, 103 kt S yr^{-}1,no product revenues.

Over 10 years the total accumulated discounted cash flow amounts to -86 M€. The costs of desulfurization can then be calculated to be € 0.016 per m^3 of gas treated or € 253 per ton of sulfur removed.

From Figures 2 and 3 it can be concluded that the costs of desulfurization for the proposed, new process are substantially considerably lower than the costs associated with a conventional amine process.

3.4.2 Sensitivity analysis

To study the impact of important parameters on the costs of desulfurization for the copper sulfate based process a sensitivity analysis has been performed. The influence of the H_2S and CO_2 content of the gas stream, the potential sales revenues of the products and the total capital expenditures on the economics of the process were investigated.

Carbon dioxide and hydrogen sulfide content of the gas stream

The selective copper sulfate base process, of course, is hardly influenced by the amount of CO_2 but only by the amount of H_2S present in the gas stream. The selectivity, and therefore the economics, of the amine based desulfurization process, on the other hand are significantly influenced by both the concentration of CO_2 and the concentration of H_2S.

An estimation of the costs of desulfurization for both the copper sulfate based process and the amine based process has been made as a function of the carbon dioxide content and the

hydrogen sulfide content of the natural gas stream. Subsequently the costs for both processes are compared.

The influence of the concentration of carbon dioxide in the natural gas on the costs of desulfurization for the copper sulfate based desulfurization process is very small, therefore it has been neglected in the current study. The extrapolation made for a copper sulfate based desulfurization plant has been made using the following assumptions :

- Usage of utilities/raw materials directly linked to sulfur processing is proportional to the hydrogen sulfide content of the natural gas stream (i.e. proportional to the amount of sulfur processed);
- Equipment costs directly linked to sulfur processing is proportional to the hydrogen sulfide content of the natural gas stream raised to the power six tenth.

The extrapolation made for an amine based desulfurization plant has been made using the following assumptions

- Usage of utilities/raw materials directly linked to sulfur processing is proportional to the hydrogen sulfide content of the natural gas stream;
- Usage of utilities/raw materials directly linked to carbon dioxide processing is proportional to the carbon dioxide content of the natural gas stream;
- Usage of utilities/raw materials directly linked to both sulfur and carbon dioxide processing is proportional to the hydrogen sulfide content plus the carbon dioxide content of the natural gas stream;
- Equipment costs directly linked to sulfur processing is proportional to the hydrogen sulfide content of the natural gas stream raised to the power six tenth;
- Equipment costs directly linked to carbon dioxide processing is proportional to the carbon dioxide content of the natural gas stream raised to the power six tenth;
- The equipment costs of the absorber/regenerator unit are constant.

Figure 4 shows the NPV for an amine based desulfurization plant in comparison to the NPV for the copper sulfate based process as a function of the carbon dioxide content in the natural gas. It can be seen that the copper sulfate based process has a higher (less negative) NPV if the carbon dioxide content exceeds 3.3 V%.

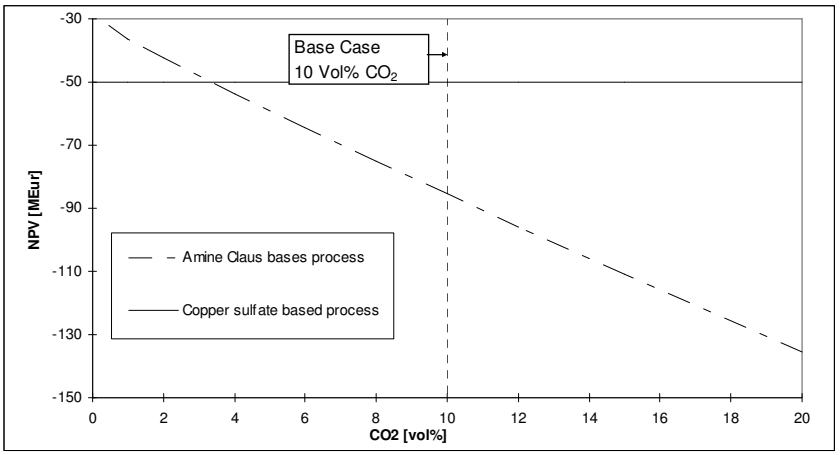

Figure 4: Costs comparison of amine based and copper sulfate based desulfurization process, 200000 $Nm^3\ hr^{-1}$, p = 50 bar, H_2S_{in} = 5 V%, $CO_{2,in}$ = varied, H_2S_{spec} = 4 ppmV, no product revenues.

Figure 5 shows the NPV for an amine based desulfurization plant in comparison to the NPV for the copper sulfate based desulfurization plant as a function of the hydrogen sulfide content in the natural gas for two levels of carbon dioxide in the natural gas. It can be seen that the high selectivity of the copper sulfate based process causes a further improvement of the NPV of the copper sulfate based process over the NPV of the amine based process if the hydrogen sulfide content decreases or the carbon dioxide content increases. Figure 5 also shows that the CO_2 content of the gas stream will not influence the economics of the copper based desulfurization plant, but strongly influences the economic viability of the amine based process.

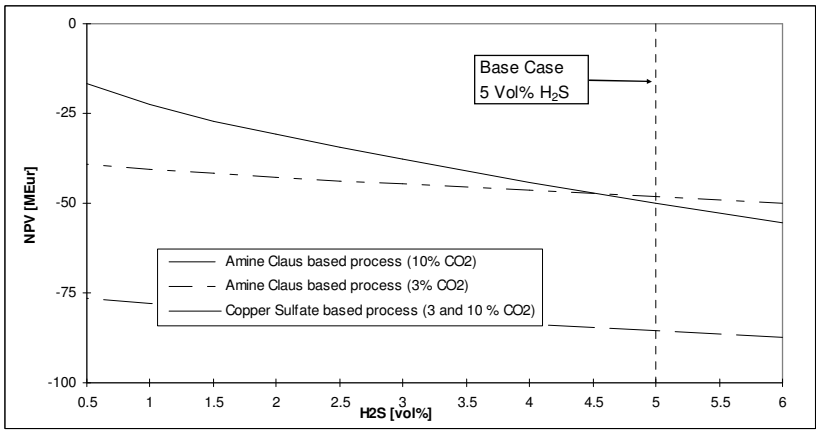

Figure 5: Costs comparison of amine based and copper sulfate based desulfurization process, 200000 $Nm^3\ hr^{-1}$, p = 50 bar, H_2S_{in} = varied, $CO_{2,in}$ = 3V% and 10V%, H_2S_{spec} = 4 ppmV, no product revenues.

Product revenues

The price for sulfuric acid may vary substantially in time. The current price for sulfuric acid [Rotterdam, 2003 technical grade, truckload] is € 56 per ton (this implies a revenue of 172 € per ton of sulfur removed as 1 ton of sulfur is converted into 3.1 tons of sulfuric acid). When the revenues for the sulfuric acid produced are taken into account the NPV for the copper sulfate based desulfurization unit amounts 15 M€, as compared to a NPV of -50 M€ when the product revenues are not taken into account. The present value and the accumulated present value for the base case are plotted versus time in Figure 6. This Figure shows that the copper sulfate based desulfurization process is profitable. However, note that the NPV is a function of the discount rate i, and that the NPV becomes smaller (or even negative) at higher discount rates. The cost of capital has been set at 12% in this analysis.

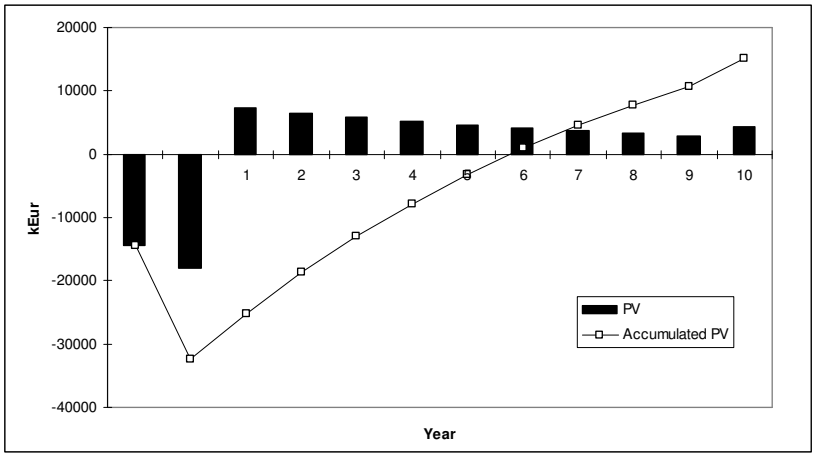

Figure 6 : Discounted cash flow "Copper sulfate based desulfurization process" Base Case + product revenues (revenues 56 € per ton H_2SO_4, or 172 € per ton of sulfur removed)

As a comparison the costs of desulfurization is calculated in the same manner for the amine-based desulfurization unit. When the revenues for the elemental sulfur produced [€ 78 per ton, Rotterdam 2003] are taken into account the NPV for the desulfurization unit amounts to -57 M€ as compared to a NPV of -86 M€ when the product revenues are not taken into account. The present value and the accumulated present value are plotted versus time in Figure 7. Note that in this case also the NPV is a function of the discount rate i and becomes more negative at higher discount rates.

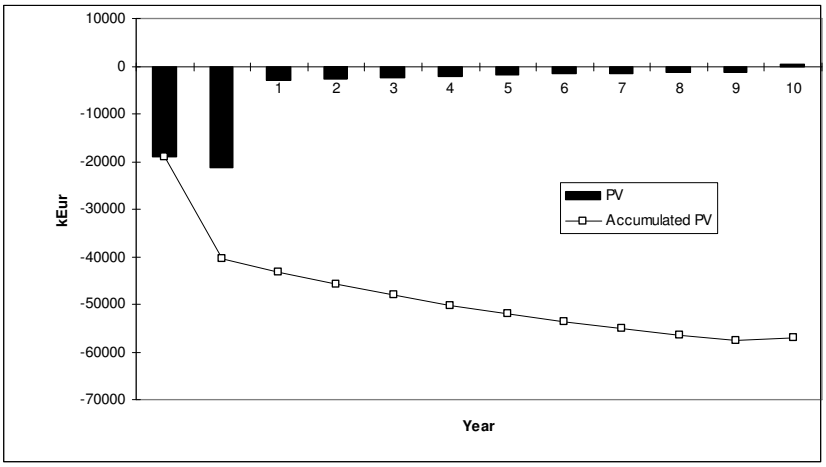

Figure 7: Discounted cash flow "Amine based desulfurization process" Base Case + product revenues (revenues 78 € per ton S)

It was already concluded that the costs of desulfurization for the proposed, new process are substantially lower than the costs associated with conventional processes. But if the products of the respective processes can be sold at current market prices the advantage for the copper sulfate based process will be significantly larger. This is caused by the overall higher revenues for the copper sulfate based process. It even makes the desulfurization profitable, which is extremely exceptional for these type of processes.

Capital expenditures

Given the fact that the total capital investment needed for the desulfurization unit has a large impact on the cost of desulfurization, and that this investment has a large uncertainty, the influence of this investment on the process economics has been investigated. The total ISBL + OSBL capital investment has been varied from 19 to 37 M € (thus varied from minus 20% to plus 45% from the base case scenario of 25.7 m€). Again the proceeds for the steam produced have not been taken into account. The results are shown in Figure 8.

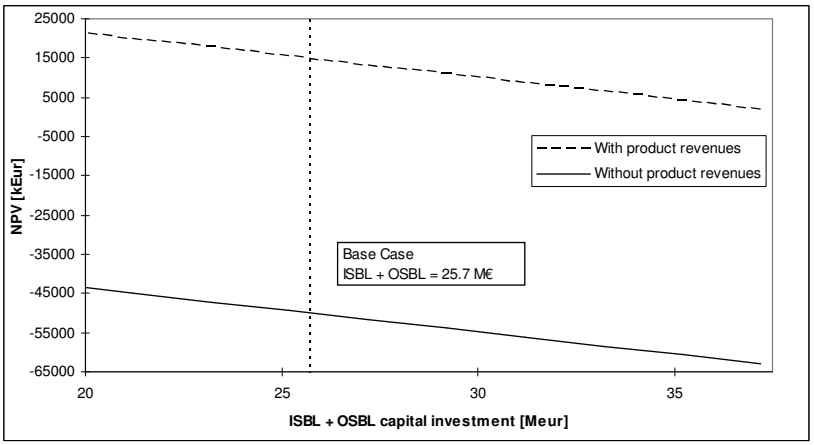

Figure 8: Influence of the capital expenditures on process economics of the copper sulfate based desulfurization process

It appears that the NPV varies between M€ -62 and € -42 when the product revenues are not taken into account, and between M€ 2 and M€ 22 when the product revenues are taken into account. From these results it can be concluded that the uncertainty in the total capital investment has a large impact on the process economics, however it does not alter the conclusions already drawn.

Copper Regeneration efficiency

In the current analysis it is assumed that copper loss does not occur, and that all copper sulfide is converted into reusable copper components. Of course some copper loss will always occur. The oxidation of copper sulfide to copper oxide for example is a high temperature process, and some degree of sintering of copper oxide or the formation of unwanted copper components may occur. Given the relatively high copper price this will have an influence on the overall economy of the process. In Table 12 the impact of these losses (expressed as a percentage loss per oxidation cycle) on the costs of desulfurization is shown. The copper loss must be compensated by adding e.g. copper sulfate (€ 755 per ton of $CuSO_4.5H_2O$) to the circulating liquid. The oxidizer by products that are formed may be sold as secondary raw material to copper smelters (for approximately € 1250 per ton of Cu it contains)

Table 12 : The influence of the regeneration losses on desulfurization costs

Copper loss		*Copper replenishment*	*Costs of desulfurization (product revenues not taken into account)*		
[%] *per regeneration cycle*	[ton yr^{-1} Cu]	[ton yr^{-1} $CuSO_4$ 5 H_2O]	[k€ yr^{-1}] copper losses	[€ per ton of sulfur removed]	[€ per m^3 of gas treated]
10.0 %	20523	80638	35215	493	0.0318
3.0 %	6156	24191	10564	238	0.0154
1.0 %	2052	8063	3521	165	0.0107
0.3 %	615	2419	1056	139	0.0090
0.1 %	205	806	352	132	0.0086
0.0 %	0	0	0	129	0.0083

From Table 12 it can be seen that copper loss does have a significant influence on the costs of desulfurization, and that high copper losses (i.e. 3% per cycle or higher) are detrimental for the attractiveness of the process. However if the copper losses can be kept below 3% per regeneration cycle, the copper sulfate based desulfurization process is a cost effective desulfurization process in comparison to conventional amine based desulfurization.

Absorbent flow rate.

The absorbent flow rate is determined by the amount of copper sulfate converted in the absorber, by the maximum solubility of copper sulfate in the absorption liquid and by the safety margins applied e.g. to prevent scaling and to cope with small fluctuations in the H_2S concentration in the gas stream that has to be desulfurized. If a lower copper sulfate concentration or a larger flow rate is desirable e.g. because of a lower operating temperature (scaling) or a larger safety margin (fluctuations in the H_2S concentration of the sour gas stream) this will influence the overall process. Not only will the process equipment, that handles the absorbent flow, have larger dimensions (absorbers, flash vessel, recompressor, hydrocyclones, dissolver units and liquid pumps), also the energy consumption associated with these process units will increase. In Table 13 the influence of the absorbent flow rate on the economy of the process is shown. It is assumed that the energy consumption of the recompressor and high pressure circulation pump is linear with the absorbent flow rate, and that the capital costs of the process modules is a function of its size raised to the power 0.6.

Table 13 : The influence of the absorbent flow rate on desulfurization costs

Costs of desulfurization		
Absorbent flow rate [m^3 hr^{-1}]	[€ per ton of sulfur removed]	[€ per m^3 of gas treated]
450	123	0.0081
600	129	0.0083
750	134	0.0087
900	139	0.0090
1050	144	0.0093
1200	149	0.0096

Table 13 shows that the influence of the absorbent flow rate can be significant, but it does not effect the overall attractiveness of the process.

Retrofitting existing desulfurization units.

An attractive option could be the adaptation of existing amine desulfurization units to make them suitable for copper sulfate based desulfurization. Retrofitting an existing desulfurization amine plant has the advantage that the amount of new equipment that has to be purchased can be reduced significantly. In the current study the amine based desulfurization unit as described by Blauwhoff (1985) will be retrofitted. Note that the absorbent circulation flow for the amine based desulfurization unit is larger than the copper sulfate absorbent flow (900 vs. 600 m3 hr^{-1}), therefore the possibilities for the re-use of equipment are significant.

Table 14: Equipment that can possibly be re-used

Apparatus	Former use	possibilities for re-use	Notes
Absorber Unit and Particle Separator			
Absorber	High pressure absorber	Good	
High pressure Pump	High pressure booster pump	Fair/good	Re-use depends on construction material
Flash vessel	Flash vessel	Good	
Recompressor, (rotary + el. motor)	Recompressor	Good	
Absorbent make-up			
Dissolver tanks (3 x) + agitator, 8kW	Claus reaction vessel	Fair	Oversized / needs agitator
Heat exchanger	Lean/rich heat exchanger	Fair/Good	Re-use depends on construction material

Items that are not present in the amine-claus unit, like hydrocyclones, slurry pumps, and the items needed in the high temperature section of the copper reclamation unit will have to be bought. Also the blower used for sulfur oxidation is too small to serve as blower for the roasting air.

Depending on the amount of equipment that can be re-used (Table 14) the total capital investment (including working capital and start-up costs) for the retrofit can vary between 24 and 28.4 M€. When this is compared to the total capital investment needed for a new copper sulfate based desulfurization unit (30.9 M€), the difference varies between 2.5 and 6.9 M€. However, since the capital investment associated with the conversion of the sulfur dioxide from the roast gasses into sulfuric acid determines a large fraction of the total remaining capital investment it is hardly possible to achieve a larger reduction.

The main advantages of the copper sulfate based desulfurization process are the low operating costs (in comparison to the conventional amine based desulfurization), and the higher product revenues. A discounted cash flow analysis of the retrofit has been performed, and the results (of the best case scenario) are shown in Figure 9. In this analysis only the total capital investment needed for the retrofit has been taken as upfront investment and the savings on the operating expenses are taken as income. The increased sales revenues are (in this case) not taken into account. To keep the results comparable with the other results in this study the discount rate i has been set at 12%.

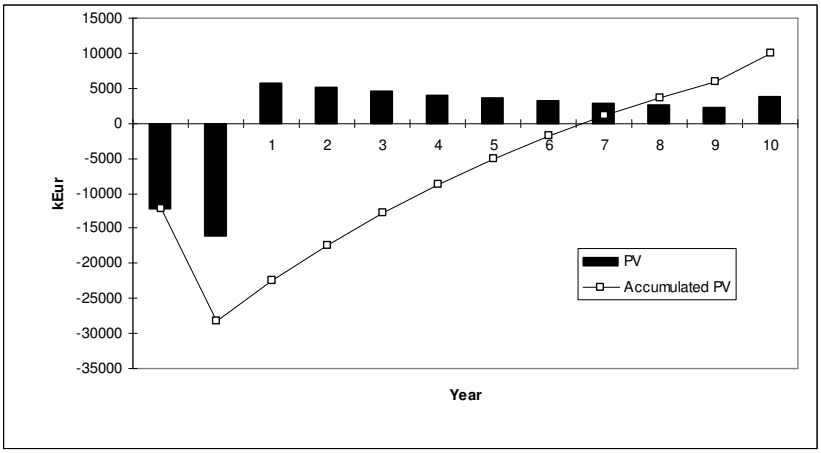

Figure 9: Discounted cash flow "Retrofit Copper based desulfurization process"; 200000 $Nm^3\ hr^{-1}$, p= 50 bar, H_2S_{in} = 5 V%, $CO_{2,in}$ = 10V%, H_2S_{spec} = 4 ppmV, 103 kt S yr^{-1}, no product revenues, savings on operating expenses are taken as income

From Figure 9 it can be seen that retrofitting does have a positive NPV and thus is a viable option. The internal rate of return (IRR)[19] of the project is 18.9% (15.5% in the worst case scenario). Because such a retrofit is a voluntary investment (and not an obliged one as is the case when desulfurization must be carried out due to environmental legislation or downstream requirements) the IRR has to be higher than the hurdle rate imposed by the operating company. Usually this figure is approximately 16% (lower for cost reducing projects, and higher (up to 20%) for new products). However, when the product revenues are taken into account retrofitting becomes an very attractive option. The IRR of the project in this case is 42.4% in the best case scenario, and still 36.5% in the worst case scenario.

4 Conclusions

A process design for a novel type of desulfurization process, based on the use of a copper sulfate solution as absorbent, is presented and evaluated technically and economically. The design capacity of the desulfurization unit was 200000 $Nm^3 hr^{-1}$ natural gas, containing 10 V% CO_2 and 5V% H_2S.

The economic performance of the copper sulfate based desulfurization unit has been compared to the economic performance of an amine based desulfurization unit (its main competitor on this large scale) for the same design basis. Also the economic viability of a retrofit of an existing amine based desulfurization unit has been investigated. A discounted cash flow analysis has been used to compare both processes. It was concluded that the Net Present Value for the proposed desulfurization process is better (less negative) than the Net Present Value (NPV) for a conventional desulfurization process when the product revenues are not taken into account. When the product revenues of both processes (sulfuric acid and elemental sulfur, respectively) can be sold at current market prices the advantage of the copper sulfate based process will increase substantially, and it will even become profitable. Due to the lower operating expenses, retrofitting an existing desulfurization plant appeared to be a viable option, even when the higher product revenues are not taken into account. When the product revenues are taken into account, retrofitting becomes a very attractive possibility. Furthermore a sensitivity analysis has shown that the economic advantage of the copper sulfate based process further improves if the hydrogen sulfide content decreases or the carbon dioxide content increases, since the performance of the copper sulfate based process in not influenced by an unselective removal of H_2S. The possible copper losses that may occur during the regeneration have a significant negative effect of the economy of the new desulfurization process. However when the copper losses are below a certain level

[19] The internal rate of return (IRR) of a project is the rate of return (or cost of capital) that would make the net present value of future cash flows plus the final market value of the project equal the current market price of the investment.

(approximately 3 % per regeneration cycle when product revenues are not taken into account) the new desulfurization process is still viable.

5 Nomenclature

Symbols

a	Interfacial area	[m^2 m^{-3}]
h	Height	[m]
I	discount rate	[%]
k	Mass transfer coefficient	[m s^{-1}]
n	year number	[-]
pH	Degree of acidity	[-]
r	Radius	[m]
t	Time	[s]
A	Area	[m^2]
C	Concentration	[mole m^{-3}]
D	Diameter	[m]
H	Enthalpy	[J $mole^{-1}$]
ISBL	Inside battery limits	
K	equilibrium constant	[$mole^2$ m^{-6}]
NPV	Net present Value	[€]
OSBL	Outside battery limits	
P	Pressure	[Pa]
PV	Present Value	[€]
Q	Power	[W]
T	Temperature	[ºC]
U	Heat transfer coefficient	[W m^{-2} K^{-1}]
V	Volume	[m^3]
W	Dissolution rate	[µm min^{-1}]

Greek

α	Degree of conversion	[-]
ε	Packing porosity	[-]
η	Efficiency	[-]
ρ	Density	[kg m^3]
Δ	Denoting a difference	
Φ	Volume flow	[m^3 s^{-1}]

Subscripts

i Initial

w Wetted

G Referring to Gas

L Referring to liquid

6 References

Barin, I., 1993, Thermochemcial data of pure substances, *VCH Weinheim*

Blauwhoff, P. M. M., Kamphuis, B., Swaaij, W.P.M. van. Westerterp, K.R., 1985, Absorber Design in Sour Natural Gas Treatment Plants: Impact of Process Variables on Operation and Economics, *Chem. Eng. Process*, **19**, 1-25

Bradley, D., 1965, The Hydrocyclone, *Pergamon Press, Oxford*

Brennan, D., 1998, Process Industry Economics, an international perspective, *IchemE*

Cakici, A.; Colak, S.; Ekinci, Z.; 1994, Dissolution kinetics of Copper(II) Oxide in water saturated by sulfur dioxide, *International Journal of Chemical Kinetics*, **26**, 737-742

Charpentier, J.C., 1976, Recent Progress in Two Phase Gas-Liquid Mass Transfer in Packed Beds, *Chem. Engng J.*, **11**, 161-181

Coulson, J.M., Richardson, J.F., 1983, Chemical Engineering Volume 1, Pergamon Press, Oxford

DACE, 2000, DACE prijzenboekje 21e editie december 2000, *H.J.M. Klein Gunnewiek, Doetinchem*

Fogg, P. et al, 1987, The Solubility of Gases in Liquids, *Wiley, Chichester*,

Gorichev, I.G.; Batrakov, V.V.; Dorofeev, M.V.; 1995, Kinetics of copper(II)oxide dissolution, *Russian Journal of Electrochemistry*, **31**, 292-301

Gorichev, I.G.; Dorofeev, M.V.; Shaplygin, I.S.; et al., 1994, Modeling of the dissolution of oxide phases, *Russian Journal of Electrochemistry*, **30**, 1491-1497

Kohl, A.L., Nielsen, R.B., 1997, Gas Purification 5th ed.,. Gulf Publishing Co. Houston

Linke, W. F., Seidell, A. 1958, Solubilities, Inorganic and Metal-organic Compounds, *Van Nostrand, Princeton*

Maat, H. ter. Versteeg, G.F. 1997, , Method and system for selective removal of contamination for gas flows.. European Patent EP19980925979

Maat, H. ter., Hogendoorn, J.A., Versteeg, G.F., 2004, The removal of hydrogen sulfide from gas streams using an aqueous metal sulfate absorbent - part I: The absorption of hydrogen sulfide in metal sulfate solutions, *Separation and Purification Technology*, accepted for publication.

Maat, H. ter., Hogendoorn, J.A., Versteeg, G.F., 2004, The removal of hydrogen sulfide from gas streams using an aqueous metal sulfate absorbent - Part II: the regeneration of copper

sulfide to copper oxide - an experimental study, *Separation and Purification Technology*, accepted for publication.

Maples, R.E., 2000, Petroleum Refinery Process Economics, 2nd edition, *PennWell Corporation, Tulsa,*

Nagl, G., 1997, Controlling H2S Emisions, *Chem. Engng.* **3**, 125-131.

Oldshue, J.Y.;1983, Fluid mixing Technology, *McGraw-Hill Publications Co., New York*

Perry, R.H., Green, D., 1997, Perry's Chemical Engineers' Handbook 7th edition ,*McGraw Hill*

Peters, M.S., Timmerhaus, K.D., 2003, Plant design and Economics for Chemical Engineers, *McGraw Hill*

Ratnam, G.S.V.; Ananth, M.S.; Varma, Y,B,G.; 1993, A Model for the Pressure Drop in Gas-Liquid Cocurent Downflow through Packed Beds. *Chem. Eng. J.*, **51**, 19-25

Reiss, L.P., 1967, Cocurrent Gas-Liquid Contacting in packed Columns, *Ind. Eng. Chem. Proc. Des. Dev.*, **6**, 486-98

Scheiman, A.D.; 1963. Size Vapor-Liquid Separators Quicker by Nomograph, **42** (**10),** *Hydrocarbon Processing & Petroleum refiner*

Stepanoff A.J., 1965, Pumps and Blowers: Selected advanced topics, Two-Phase Flow: flow and pumping of solids in suspension and fluid mixtures, *John Wiley & Sons, New York***.**

Trambouze P., Landegem H., Wauquire J.P., Marshall N., 1988, Chemical Reactors: design, engineering operation, p 251, *Paris : Editions Technip*

Ulrich G.D., 1984, A Guide to Chemical Engineering Process Design and Economics, *John Wiley & Sons*

Versteeg, G.F., van Swaaij, W.P.M., 1988, On the kinetic between CO2 and alkanolamines both in aqueous and non-aqueous solutions. *J. Chem. Engng. Data*, **34**, 29-34

Walas S.M., 1988, Chemical Process Equipment: Selection and design, *Butterworths-Heinemann*

Zarzycki R., Chacuk A., 1993, Absorption, fundamentals & applications, *Pergamon Press*

Appendix A : Equipment design.

A.1 General design procedure

To estimate the (operational and capital) costs associated with the equipment used in the desulfurization plant it is necessary to know the main dimensions and the utilities usage of the main equipment. These parameters have been determined using the following procedure.

First the absorbent flow was determined and the mass and energy balance of the overall process were solved. With the size, composition, temperature and pressure of all process flows that relate to each unit operation known, the duty of the equipment used for each unit operation was calculated. Then the required equipment type was selected and sized. Finally, the capital expenses and operating costs for each unit operation (needed for the economic evaluation) were estimated. In this appendix a brief description, and when appropriate the design procedure, of the equipment used for each unit operation is given.

A.1.1 Absorbent flow

One of the most important parameters to be fixed was the absorbent flow. From an economical point of view it is desirable to choose the absorbent circulation flow as small as possible. Therefore a high concentration of copper ions in the acidic copper sulfate solution entering the absorber is preferred. A copper ion concentration of the liquid entering the absorber of 0.8 kmol m^{-3} was chosen. Even at the worst case conditions (a degree of acidity of 0.6 kmol m^{-3} sulfuric acid and a temperature of 293 K) this concentration assures that scaling of copper sulfate in the equipment will not occur since the amount of copper ions is only 75% of the maximum solubility (Data provided by Linke et al. (1958) were used in this determination, see Appendix B). Choosing the volume flow of the absorbent so that the amount of copper ions converted in the absorber is 85%, an absorbent volume flow of 600 m^3/hr was obtained. The resulting composition of the absorbent flow is given in Table 3 in the main text.

A.2 Main Equipment

A.2.1 The absorption column

The gas stream that has to be desulfurized will be brought in contact with the absorbent in a gas-liquid contactor. In order to be able to determine the costs associated with the main absorber it is required to determine not only the duty of the column, but also its main dimensions.

The gas stream and the absorbent flow entering the absorber have already been fixed (See Table 1 of the main text). The hydrogen sulfide in the gas stream is absorbed in the copper sulfate solution and reacts with copper sulfate to insoluble copper sulfide and sulfuric acid. The hydrogen sulfide concentration of the gas leaving the absorber has to meet the required specification. The slurry that leaves the absorber for further treatment (for its composition and other process flows see Table 3 in the main text). Some of the carbon dioxide and methane present in the feed stream are physically absorbed in the solution, while some of the water is evaporated from the solution. The amounts absorbed and desorbed for components other than H_2S are estimated by assuming that physical equilibrium exists between the gas and the liquid stream leaving the absorber. The solubility of CO_2 and methane in the slurry is taken to be equal to the solubility of the components in pure water. The solubility of methane and carbon dioxide in water can be found in the work of Fogg (1987). The vapor pressure of water is taken from Perry (1997). In determining the main dimensions of the absorber it is assumed that the mass transfer parameters calculated by using relations presented in open literature (generally valid at low pressure only) can be converted to the high operating pressure of the column. This conversion is done by assuming a penetration theory dependency of k_G on the diffusivity (A.1).

$$k_{G,P} = k_{G,P} * \sqrt{\frac{D_P}{D_{SP}}} \qquad (A.1)$$

The diffusivity itself is assumed to be inversely proportional to the pressure, an assumption that holds at the operating temperature if the reduced density of the main component in the gas mixture (methane) is smaller than 1. In the studied case the value of the reduced density is approximately 0.25. Other alternatives are not available since high pressure mass transfer correlations are not given in the open literature

Column type

Most common gas liquid contactor types are, in decreasing order of liquid holdup, thus increasingly suitable for fast absorption reactions (Trambouze, 1988): the bubble column, mechanically stirred columns or tanks, plate columns, packed columns (co- and countercurrent), and the scrubber (spray or venturi) type respectively. Desired properties for the current G/L contactor are: suitable for a fast or instantaneous reaction (since the reaction between H_2S and an aqueous $CuSO_4$ solution is a fast reaction (Ter Maat *et al*., 2004a), high capacity, high reactant conversion in the gas phase (since the H_2S specification is very low) and a low pressure drop for the gas. Based on the guidelines for G/L contactor selection given by Trambouze (1988) it was concluded that good contactor types are the counter- or co-current packed columns. Main drawback of the packed column contactor type is the poor

solids handling. Given the fact that the solids hold up in the spent absorbent is up to 1.5 V% the selected contactor type is the co-current packed column because of its lower pressure drop and better solids handling properties in comparison to the counter current packed bed contactor[20]. (The co-current flow mode does, in this case, not have its usual drawback of a lower average driving force for absorption since the reaction between $CuSO_4$ and H_2S may be considered fast and irreversible under the conditions applied) However, to avoid downtime associated with plugging problems a second packed column is installed. With the column type known, parameters to be determined are the operating regime, packing type and the column diameter and height. For a given gas and liquid volume flow, the column diameter and the packing type determine the operating regime and the mass transfer parameters. The obtained mass transfer parameters were incorporated in a model and the packing length needed to meet the specifications was calculated. The local flux of H_2S absorbing into the copper sulfate solution was calculated using the film model for both the gas and the liquid phase, assuming an instantaneous, irreversible reaction between H_2S and the copper sulfate solution. (Ter Maat et *al*., 2004a, Ter Maat *et al*., 2004b).

To avoid plugging caused by the solids a relatively high specific pressure drop is desired. The pulse flow regime gives a high specific pressure drop combined with high values for the mass transfer parameters. Therefore the chosen operating regime was the pulse flow regime. The flow pattern diagram given by Charpentier (1976) was used to verify if the column is operated in the pulse flow regime. In the main absorption column Glitsch Mini Cascade Rings will be used because of their ability to handle solids present in the absorbent. Some characteristics of the rings are given in Table A.1.

[20] Plugging problems due to the formation of solids are also encountered in another type of desulfurization process, the iron chelate based processes. The absorbers used in the iron chelate based processes ranges from liquid filled sparged vessels (Kohl & Nielsen, 1997), in which the liquid is the continuous phase, via venturi scrubbers and spray chambers (in which the gas phase is continuous), to packed bed absorbers and moving bed absorbers. The plugging problems in LO-CAT- type processes are worsened by the "sticky" nature of the produced sulfur. Given the similarities of the $CuSO_4$ based process and the iron chelate based processes and the fact that CuS does not show a sticky behavior, as was shown during pilot plant tests (Ter Maat 2004a), it is believed by the authors that the proposed design (a packed bed contactor) can cope with the CuS slurry without excessive plugging problems. Furthermore note that altering the packed bed design to e.g. a spray tower or a venturi contactor will only have a minor impact on the economical viability of the overall process owing to the fact that the costs directly associated with the absorber make up for only a small fraction of the costs for the overall process.

Table A.1. Characteristics Glitsch Mini Cascade Rings No. 5

Design parameter	*Value*
Interfacial area a (dry)	83.7 m^2/m^3
Void fraction	65.2 %
Density, ρ_p	837 kg/m^3

Using the relations given by Ratnam (1993) the pressure drop over the column was calculated. The equations given by Reiss (Reiss, 1967) were then used to determine the mass transfer parameters k_La and k_Ga.

The obtained mass transfer parameters have been implemented in a local flux model (Eq A.1) in order to determine the column height (ter Maat *et al.*, 2004b) In the overall absorber model plug flow of both phases has been assumed respectively.

$$J = \frac{\overline{C}_{G,H_2S} - \overline{C}_{L,H_2S} / m_{H_2S}}{\frac{1}{k_G} + \frac{1}{m_{H_2S} k_L E_{H_2S,\infty}}} \quad With \quad E_{H_2S,\infty} = 1 + \frac{D_{Cu^{2+},eff} * \overline{C}_{L,Cu^{2+}}}{D_{H_2S,eff} * m_{H_2S} * C^i_{G,H_2S}} \qquad (A.2)$$

Table A.2 shows the resulting main dimensions of the absorption column. To avoid an excessively high pressure drop a column diameter of 1.5 m was chosen.

Table A.2: Sizing main absorption column

	unit	
Diameter	m	1.5
Height packing	m	6.5
Temperature	°C	20
Pressure	Pa	50 10^5
$(Cu^{2+})_0$	mole m^3	800
mass flow liquid	Kg h^{-1}	720000
mole flow H_2S	Mole h^{-1}	410000
Liquid loading	Kg m^{-2} s^{-1}	113
Gas loading	Kg m^{-2} s^{-1}	25
Hydrodynamic regime		Pulse flow
ΔP_{LG}	Pa m^{-1}	14800
k_La	m s^{-1}	0.56
a_w	m^2 m^{-3}	450
k_Ga	s^{-1}	44

A.2.2 The copper sulfide oxidizer

The conversion of copper sulfide to copper oxide is called roasting. The roaster that will be designed must be capable of converting 38.5 tons of CuS per hr into CuO (See Table 3 in the main text). Important parameters for the design and cost estimate are the roaster volume, the pressure drop over the roaster, the operating temperature and the volume flow of air needed to convert the copper sulfide to copper oxide.

Different types of roasters are currently used on an industrial scale. For a fluidized bed roaster (kiln) Capital and Operating & Maintenance costs are substantially lower than for a comparable rotary kiln or multiple hearth furnace. Furthermore, the fluidized bed roaster seems a suitable choice since fluidized bed kilns are already applied for the roasting of sulfuric copper ores and for the roasting of other naturally occurring sulfuric ores (e.g. FeS) to provide SO_2 for sulfuric acid manufacture (Perry, 1997, p20-72). Therefore that type of roaster was chosen to convert copper sulfide produced in the absorption column into copper oxide. Other components that are dissolved into the slurry can possibly also undergo reactions. Side reactions that are assumed to take place are the oxidation of methane to carbon dioxide and water and the dissociation reaction of entrained sulfuric acid to sulfur dioxide, water and oxygen. Since some H_2SO_4 will be withdrawn from the circulating washing liquid with the slurry, a way had to be found to avoid a decrease of the H_2SO_4 concentration in the circulating washing liquid. To maintain a constant degree of acidity in the circulating liquid two possible solutions exist. Either pure H_2SO_4 can be added to the absorbent stream, or a small fraction of the CuS fed to the roaster can be converted into non basic or less basic $CuSO_4$ or $CuO.CuSO_4$. Since the SO_2 that is released in the roasting process will ultimately be converted into H_2SO_4 this decision will only have minor economic consequences. In the current process design the second option was chosen. That ment that approximately 4% of the CuS fed to the roaster had to be converted into $CuSO_4$ (the remaining 96% was converted into CuO) in order to maintain a constant degree of acidity of the washing liquor.

Operation

A concentrated slurry of copper sulfide enters the fluidized bed roaster (stream 15 in Fig 1 in the main text). Air is used as fluidizing medium. In the fluidized bed copper sulfide is oxidized to copper oxide and copper sulfate. The temperature of the bed can be used to control the selectivity to CuO (Ter Maat *et al*., 2004c). Product streams of the roaster are a flow of solids and roast gases. The selectivity of the conversion of copper sulfide to copper oxide must be controlled within a certain range to keep the acidity of the washing liquor in the desired range. The mass balance shows that with a selectivity of 96 % towards copper oxide this can be achieved, however slight deviations with respect to the desired selectivity will only have a minor impact on the degree of acidity in the washing liquor. Another parameter to be fixed

was the sulfur dioxide content in the roast gases. A sulfur dioxide content in the roast gases of 10 V% is usually chosen to ensure easy and economic operation of the commercial sulfuric acid plant. The amount of air entering the roaster is adjusted to set the sulfur dioxide content of the roast gas to 10 V%. The products of the roaster, copper oxide particles (stream 15 in Fig. 1 in the main text) and a sulfur dioxide containing gas (stream 24 in Fig 1 in the main text) are led to the dissolution section and sulfuric acid plant respectively.

The roasting takes place at a temperature of approximately 1000 K and low pressure (1.0-1.2 bara). The roaster volume is determined by the mass flow of CuS and the required residence time of copper sulfide in the roaster. The residence time is conservatively estimated at 2200 seconds (Ter Maat *et al*., 2004c). At a bed porosity of ε =0.5, and a freeboard having twice the volume of the fluid bed, the volume of the roaster then becomes 60 m^3. This volume will also allow installing sufficient heat exchanging area in the roaster to take up the energy released during the oxidation of CuS to CuO. With a roaster diameter of 4 m, the pressure drop over the bed was calculated to be 19000 Pa. When the pressure drop over the gas distributor was taken at 50% of the pressure drop over the fluidized bed (this is needed for a good gas distribution) the overall pressure drop for the roaster (including gas distributor) is approximately 0.3 bar. Since the concentration of SO_2 in the roaster off gas is 10% (on a dry basis), the flow of air through the bed becomes 26.5 Nm^3/s.

A.2.3 Dissolver section

The dissolver is used to regenerate the spent absorbent so that it can be re-used in the absorber. In order to accomplish this, copperions that have been converted in the absorber and are taken away from the absorption liquid as solid CuS must be replenished. This is done by dissolving the product of the roaster (mainly CuO) (stream 17 in Fig 1 in the main text) in the spent absorbent (stream 7 in Fig 1 in the main text). Copper oxide dissolves as it reacts with the hydronium ions present in the metal sulfate solution (See Eq. A.3).

$$CuO + 2\,H_3O^+ + SO_4^{2-} \leftrightarrow Cu^{2+} + 3\,H_2O + SO_4^{2-} \qquad (A.3)$$

Note that the consumption of hydronium ions in the reaction A.3 will also compensate for the hydronium ions formed during the absorption of H_2S in the copper sulfate solution in the absorber, making a closed loop operation process basically possible

The dissolver must be able to dissolve 33.5 tons of roaster products per hour in the spent absorbent (614 m^3/hr acidic copper sulfate solution (See Table 3, main text)). The contact between the solid and the liquid can be accomplished in e.g. a (series of) stirred tank(s), a packed bed or even through heap leaching. A (series of) stirred tank reactor(s) will be used

because of its good slurry handling capabilities, the fact that it can operate in a continuous manner and relatively intense L/S contact (especially with respect to heap leaching).

A good compromise between a plug flow character (smallest possible reactor size) and good slurry handling capacity is a cascade of stirred tank reactors. A preliminary economic analysis showed that a cascade of three equally sized stirred tank reactors yields the most economic configuration.

In the dissolver the spent absorbent is replenished (Eq. A.3). Solid roaster product and spent solids free absorbent enter the dissolver. The copper oxide dissolves in the acidic spent absorbent. The dissolver is also the place where make-up water is added to the solvent stream. The stream leaving the dissolver is a liquid stream also containing some remaining undissolved copper oxide. The undissolved copper oxide particles are separated from the dissolver section outflow and recycled. The solids free solution (stream 11 in Fig 1 in the main text) is now cooled to absorber temperature and transported to the absorber. The pressure of the dissolver is atmospheric.

The main dimensions (diameter and height) of the dissolver depend on the rate of dissolution of copper(II)oxide, the type of reactor chosen as dissolver, the copper(II)oxide characteristics (a.o. the particle diameter), the temperature inside the dissolver and the desired conversion. Gorichev *et al*. (1994, 1995) have measured the dissolution rate of copper(II)oxide in acidic media. They give the following equation to describe the dissolution rate :

$$\frac{d\alpha}{dt} = \frac{W_i}{r_0}\alpha(1-\alpha)^{2/3} \qquad (A.4)$$

in which α is the fraction of the copper oxide that has been dissolved, r_0 is the original radius of the dissolving particle (μm) and W_i is the dissolution rate of the particle (μm/min). For the dissolution of copper oxide in sulfuric acid (pH=0.43, T = 20 °C) a dissolution rate of 5.20 μm/min has been reported.
The rate of dissolution at temperatures other than 20 °C has been estimated using a conservative estimation for the activation energy. While Gorichev reports an activation energy of ± 80 kJ/mole, a relatively low value of 66.5 kJ/mole as determined by Cakici (1994) was chosen as a conservative estimate. Note that the (high) value of the activation energy as determined by both authors seems to indicate that the chemical kinetics, rather than mass transfer (typically exhibiting a much lower activation energy), determine the overall dissolution rate.

The particle diameter of the copper oxide solids coming from the roaster is estimated to be 100 μm (Jayaveera, 1989). The temperature inside the dissolver is approximately 40 °C. The desired degree of dissolution is set at 95 % of the amount of copper oxide entering the dissolver. A higher desired conversion leads to a much larger reactor size; a lower desired conversion gives only a slightly smaller reactor size. Combining the dissolution kinetics, the residence time distribution in a cascade of 3 stirred tanks in series, and the desired conversion this leads to a required tank of 87.3 m^3. The height and the diameter of each tank are 9.5 m and 3.8 m respectively. The slurry height inside the tank will be 7.6 m. Designing the stirrer according to the guidelines given by Oldshue (1983, p94 - p124) gives a vessel with dual mounted impellers. The diameter of the impellers should be 1.9 m. The motor power required is approximately 8 kW.

A.3 Auxiliary Equipment

The auxiliary equipment has not been designed in great detail, because for a cost estimate the duty and type of equipment needed generally suffice.

A.3.1 Flash vessel

When the spent absorbent leaves the high pressure absorber (stream 5 in Fig 1 in the main text), it is depressurized before further treatment can take place. During depressurizing some of the gases that are physically dissolved in the solution, will desorb. A flash vessel is needed to separate the desorbed gas from the slurry leaving the absorber.

Streams leaving the flash vessel are a gas stream (stream 26 in Fig 1 in the main text) and a slurry stream (stream 6 in Fig 1 in the main text). In the flash vessel the pressure is chosen to be 4 bar. This pressure is high enough to attain the flow of the slurry through the separation section and low enough to allow most of the absorbed gas to desorb. For the mass balance it is assumed that equilibrium between the gas and the liquid phase exists in the flash vessel. The data needed for the determination of the costs of a flash vessel are the height and the diameter of the vessel. The pressure influence has been taken into account via a pressure costs factor (Ulrich, 1984, p285-337). Therefore, a determination of the wall thickness is not needed. For the design of the flash vessel the method of Scheiman (1963) was used. A vessel diameter and height of 2.8 respectively 4 m were obtained; the disengaging height was calculated to be 3 m.

A.3.2 S/L-separator

The particles formed in the absorber need to be separated from the liquid to convert the CuS particles to CuO in a roaster. The high density of the particles enables a separation by sedimentation in spite of the small particle size. For separating particles with a diameter

between 3-600 μm in a concentration between 3 and 30 V% from a liquid, a hydrocyclone seems to be the best suited S/L-separator (Coulson and Richardson, 1983). Main advantage of the hydrocyclone is that the hydrocyclone is simple, inexpensive and robust. A cascade of hydrocyclones is also used to separate the unconverted CuO particles leaving the dissolver section with the replenished absorbent stream.

Hydrocyclones for separation of CuS particles from the spent absorbent.

The slurry stream from the flash vessel (stream 6 in Fig 1 in the main text) enters the hydrocyclones. In the hydrocyclones the slurry stream is concentrated. Streams leaving the hydrocyclones are a liquid stream (the overflow, stream 7 in Fig 1 in the main text) and a concentrated slurry stream, (the underflow, stream 13 in Fig 1 in the main text). The parameter to be fixed is the solids content of the concentrated slurry stream. The water content of the concentrated slurry strongly influences the heat balance of the roaster. The underflow concentration can reach 70-80 wt% solids (Bradley, 1965), while the upper limit for the transport of a slurry in a pump is 70-89 wt% solids as well (Stepanoff, 1965, p 161). The hydrocyclones have been sized to attain an underflow containing 70 wt% solids. This high concentration of solids minimizes the energy losses in the roaster. The concentrated underflow is stored in a stirred tank and then fed to the roaster. The overflow of the hydrocyclones is fed to the dissolver section for regeneration.

Hydrocyclones for separation of unconverted CuO particles from the stream leaving the dissolver section.

The stream leaving the dissolver section (stream 9 Fig 1 in the main text), still containing some unreacted CuO particles, is cleared using hydrocyclones. The cleared liquid stream (stream 10 in Fig 1 in the main text) is fed to the absorber as regenerated absorbent. The underflow of the hydrocyclones (stream 12 in Fig 1 in the main text) is recycled to the dissolver and added to the first tank together with the initial roaster product. Again the concentration of solids in the underflow has been set at 70 wt% solids.

Sizing the Hydrocyclones

Design parameters of importance are the diameter of the cyclone (the smaller the diameter, the more effective the cyclone becomes); the maximum allowable pressure drop over the cyclone (a function of feed flow rate (to the power 2) and diameter (to the power minus 4) of the cyclone), the size of the particles that have to be removed and the feed flow rate. The method described by Bradley (Bradley, 1965, Coulson and Richardson 1983, Vol6, p 329) has been used to estimate the dimensions of the hydrocyclones. The size of the particles to be removed, the pressure drop over the cyclone and the flow per hydrocyclone have been fixed. The ratio underflow/overflow determines the number of hydrocyclones that have to be

used in series to attain a certain holdup of solids in the slurry stream. Finally it was possible to calculate the pressure drop over the cascade of hydrocyclone.

Summarizing, the cyclones were sized to remove 99% of the particles of 15 μm or larger (approximately the diameter of CuS particle conglomerates), maintaining a maximum allowable pressure drop over a cyclone of 1.26 bars. Following the design procedures, this resulted in a hydrocyclone with a diameter of 20 cm. The feed flow rate through one hydrocyclone was only 0.004 m^3 s^{-1}. Since the total feed flow rate for both cascades of hydrocyclones is 0.16 m^3 s^{-1} a circuit with 40 parallel hydrocyclones was needed. A cascade of two (batteries of) cyclones has been applied for a thickening from 1 V % to over 35 V % solids. The pressure drop over a cyclone has been estimated using the equation given by Bradley (1965).

A.3.3 Compressors, Pumps and conveyors.

Recompressor

The desorbed gas leaving the flash vessel (stream 26 in Fig 1 in the main text) has to be compressed to 50 bar and is then added to the gas stream leaving the absorber to give the purified natural gas stream. Ulrich (1984, p285-317) gives the purchase costs of rotary compressors as a function of the motor power. For the compressor that brings the gaseous outflow of the flash vessel back to 50 bar a motor power of about 0.4 MW is required. A preliminary economic analysis showed that recompressing is to be preferred above flaring the gas. Using the gas at low pressure, for e.g. heating purposes, thereby avoiding the costs associated with the recompression would be the most preferred option, however, in this overall, exothermic process no good use can be found for this gas.

Air blower to supply fluidizing air to the roaster

The air needed for roasting of the copper sulfide ((stream 21 in Fig 1 in the main text) is supplied by means of an air blower. The duty and type of blower suffice for a cost estimate of the blower. The method described by Coulson and Richardson (1983, Vol. 6, p377) has been used to estimate the type of the air blower used. For a volume flow of 27 m^3/s and a pressure ratio P_{out}/P_{in} of 1.3 a roots blower is a good choice. The power required is approximately 1 MW.

Pumps

The design of pumps comprises the determination of pump type and pump shaft power. The pump type determines the pump efficiency at a given flow rate. The pump shaft power can then be directly related to the purchase costs. The pump used to feed the liquid absorbent to the high pressure (50 bars) packed column is a multistage centrifugal pump, the other required pumps in the process are single staged centrifugal pumps. The efficiency of

centrifugal pumps depends on their size (Coulson, 1983, p380). For a flow of 600 m^3/hr the efficiency is around 83% (±5%). The characteristics of the various required pumps are given in Table A.3.

Table A.3: Pump Characteristics.

	ΔP [bar]	η_P [%]	Q [MW]
Absorber feed pump	50	83	1.00
Pump after dissolver tanks 1 and 2	1	83	0.02
Pump after dissolver tanks 3	2	83	0.04

Pneumatic conveyor to transport CuO from the roaster to the dissolver

The copper oxide resulting from the roasting of the copper sulfide ((stream 18 in Fig 1 in the main text) is transported to the dissolver by means of a pneumatic transporter. The method described by Perry (1997) has been used to estimate the size of the conveyor used. For a mass flow of 9 kg/s and a solids ratio of 3, a pressure drop of 30 kPa results. This indeed enables the use of a pneumatic conveyor. The power required is approximately 200 kW. The power needed suffices for a cost estimate of the pneumatic conveyor.

A.4 Energy Balance

A.4.1 Energy Balance

If the flow size, temperature and composition are known the internal energy of a flow can be calculated. If this is done for all streams a heat balance can be set up and the energy duty for each processing unit can be calculated. The following simplifications have been made.

- Pumping and compression energy added to the circulation streams due to pressure drops are small in comparison to the chemical energy released in the course of the reaction.
- The temperature of the gas stream leaving the absorber is equal to the temperature of the leaving absorbent stream.

Processing units with non-negligible duties are: the absorber, the dissolving units, the roaster and the heat exchangers. The amount of heat generated during the chemical reactions that occur in these processing units has been estimated using the data summarized in Table A.4 (Barin, 1993).

Table A.4: Reaction enthalpy of the main chemical reactions at various temperatures

Reaction	ΔH [kJ/mol product]			
Overall reaction	25 ºC	127 ºC	527 ºC	727 ºC
$H_2S\,(g) + 2\,O_2\,(g) \longrightarrow H_2SO_4(l)$	-793	-788		
Main reactions				
$CuSO_4\,(s) + H_2S\,(g) \longrightarrow H_2SO_4\,(l) + CuS\,(s)$	-75	-69		
$CuS\,(s) + 1\,{}^1\!/_2\,O_2\,\,(g) \longrightarrow CuO\,(s) + SO_2(g)$	-400	-400	-400	-400
$CuO\,(s) + H_2SO_4\,(l) \longrightarrow CuSO_4\,(s) + H_2O\,(l)$	-87	-91		
Side reaction				
$CuS\,\,(s) + 2\,O_2\,(g) \longrightarrow CuSO_4(g)$	-718	-719	-710	
Roast gas conversion				
$SO_2\,(g) + H_2O\,(l) + {}^1\!/_2\,O_2\,\,(g) \longrightarrow H_2SO_4(l)$	226	228		

Using these numbers it cal be calculated that, in the absorber 8.3 MW is generated and in the dissolver units 7.2 MW. A large amount of heat is released during the copper sulfide oxidation reaction in the roaster (42.4 MW). However the vast majority of the released reaction heat is absorbed by the temperature increase of the reactants to the reaction temperature (a temperature increase from 300 K to 1000 K). The remainder of the reaction heat (approximately 3.9 MW) has to be removed from the roaster.

2.4.2 Heat Exchangers

Heat exchanger used for absorbent stream

The purpose of this heat exchanger is to remove the energy generated in the absorber (8.3 MW) and dissolver (heat added with the hot CuO particles: 3.6 MW; dissolution energy: 7.2 MW). In this shell and tube heat exchanger, the process stream has to be cooled down from 54 ºC to 27°C. Cooling water has been chosen as cooling agent. The estimated heat transfer coefficient has been taken from Ulrich (1984, p162). The main dimensions of the heat exchanger are given in Table A.5.

Table A.5 : Summary of heat exchanger characteristics

Parameter	Absorbent stream	Roast gas
Duty	19.1 MW	13.5 MW
$T_{hot,in}$	54 °C	723 °C
$T_{hot,out}$	27 °C	423 °C
$T_{cold,in}$	30 °C	233 °C
$T_{cold,out}$	20 °C	233 °C
Average (logarithmic) temperature difference	13.8 °C	327 °C
Heat transfer coefficient U	1200 W/m^2K	100 W/m^2K
Heat exchanging area A	1150 m^2	412 m^2
Heat exchanger type	shell and tube	shell and tube

Heat exchanger used for roast gas

The purpose of this heat exchanger is to cool roast gases from the roaster (1000K) to a temperature suitable for further processing in the sulfuric acid plant (700 K). This liberates 13.5 MW. This heat will be used for the generation of high pressure steam (510 K). Boiling water (at 32 bar) has been chosen as cooling agent. The estimated heat transfer coefficient has been taken from a Table given by Ulrich (Ulrich 1984, p 162). The main dimensions are given in Table A.5.

Appendix B Solubility of Copper Sulfate in an acidified aqueous solution

The solubility of copper sulfide in a mixture of water and sulfuric acid as a function of the temperature and sulfuric acid concentration was determined experimentally by Linke (1958) (See Figure B.1).

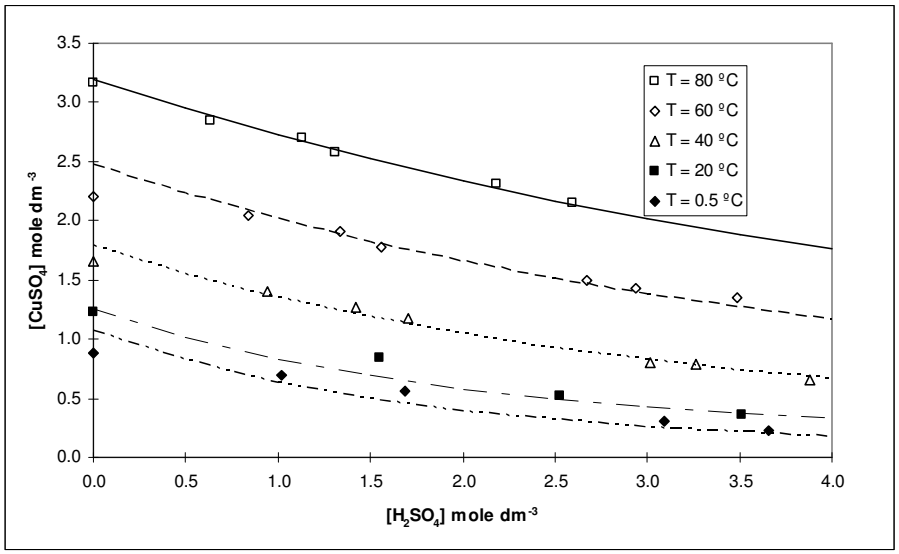

Figure B.1: Solubility of copper sulfate in a mixture of water and sulfuric acid

The solubility data have been fitted (Eq. B.1) using a least square method. The fitted copper sulfate solubility is shown as drawn lines in Figure B.1

$$K_{pseudoSP,CuSO4} = 1.14 - 9.5*10^{-3}*T + 1.5*10^{-3}*T^2 - \frac{1.09*[H_2SO_4]}{T - 10.3} \qquad (B.1)$$

The temperature in Equation B.1 is given in degrees Celsius and the (pseudo) solubility product constant is defined as given in Eq. B.2. When determining if scaling of copper sulfate is likely to occur, this expression for the (pseudo) solubility product constant is convenient to use.

$$K_{pseudoSP,CuSO4} = [H_2SO_4]*([H_2SO_4] + [CuSO_4]) \qquad (B.2)$$

The concentrations of sulfuric acid and copper sulfate have been defined as the total amount of sulfuric acid or copper sulfate present in to the solution respectively, and are expressed as mole per dm^3 solution.

Appendix C: The amine based gas treating process

One of the industrially applied large scale processes for the removal of hydrogen sulfide from a gas stream is the scrubbing of H_2S containing gases with aqueous solutions of alkanolamine. The alkanolamine technology has been in use since the 1930's. An excellent overview of the various amine based gas treating processes is given in the book "Gas Purification" of Kohl and Nielsen (Kohl, 1997).

A layout of the amine based process is shown in Figure C.1. The desulfurization unit can be subdivided in 3 process steps; a H_2S absorber combined with a stripper, a Claus unit and a Claus off-gas treating unit. In the absorber the acid hydrogen sulfide reacts with the basic alkanolamine, preferably at low temperature (313-373 K) and high pressure (7-70 bar). The loaded alkanolamine solution is then brought into the stripper, where the alkanolamine solution releases the hydrogen sulfide at high temperature and low pressure. The regenerated alkanolamine solution is led back into the scrubber and the concentrated hydrogen sulfide stream is processed further. The concentrated hydrogen sulfide stream can, in a Claus plant, be converted into elemental sulfur. The off-gases of the Claus-unit are treated in a Tail Gas Unit (TGU).

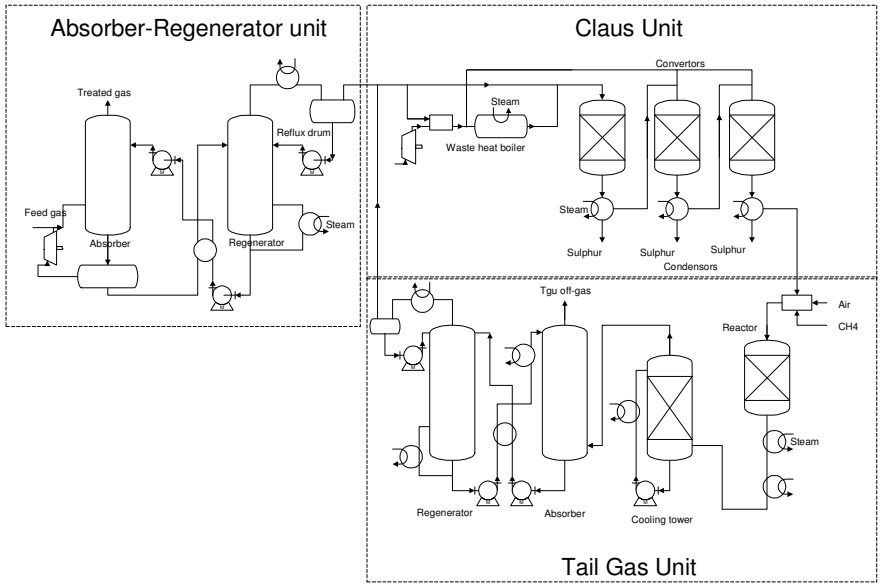

Figure C.1 : Schematic drawing of a amine based desulfurization unit.

Chemistry

In the absorber the acid-base reaction between hydrogen sulfide and the amine (a tertiary amine in this case) takes place according to the following reaction equation.

$$H_2S + R_1R_2R_3N \leftrightarrow HS^- + R_1R_2R_3NH^+ \qquad (C.1)$$

This reaction is instantaneous. Carbon dioxide, which also absorbs in the liquid, reacts, at a finite rate, with the amine according to :

$$CO_2 + H_2O + R_1R_2R_3N \leftrightarrow HCO_3^- + R_1R_2R_3NH^+ \qquad (C.2)$$

The rate at which this reaction takes place has been reported by, among others, Versteeg and van Swaaij (1988).

In the stripper the loaded amine is stripped of the H_2S and CO_2. Reactions C.1 and C.2 take place in the reverse direction. The concentrated hydrogen sulfide, liberated in the stripper is converted in elemental sulfur in the Claus unit. In the Claus unit a part of the hydrogen sulfide is first converted in sulfur dioxide (Eq. C.3).

$$H_2S + \tfrac{3}{2} O_2 \longleftrightarrow H_2O + SO_2 \qquad (C.3)$$

The remainder of the hydrogen sulfide is then, together with the sulfur dioxide converted into elemental sulfur according to Eq C.4.

$$2\,H_2S + SO_2 \longleftrightarrow 2\,H_2O + \tfrac{3}{x} S_x \qquad (C.4)$$

Economics

Blauwhoff *et al.* (1985) have investigated the economics of the amine based desulfurization process as a function of various process parameters, using the same design basis as used in the current study. In this study that economic analysis has been updated and used as comparison basis to determine the economic viability of the copper sulfate based desulfurization process on a large scale.

In the analysis of Blauwhoff *et al.* the amine based desulfurization plant is subdivided in 3 processing units; the absorber-regenerator unit, the Claus unit and the Tail Gas Unit (a SCOT unit). Blauwhoff *et al.* estimated the ISBL capital investment of each processing unit using a factored estimate. The numbers determined by Blauwhoff *et al.* have been updated to the current costs using the CE-plant cost index. To ensure a good comparability, the OSBL

capital investment, the working capital and the start-up costs have been estimated using the same procedure as applied in the economic analysis of the copper based desulfurization process. The obtained fixed capital investment needed for the amine based desulfurization unit is shown in Table C.1. More recent information (Maples, 2000) about the investments needed for an amine based gas sweetening process shows that the date given by Blauwhoff are still accurate within 30%, and may thus be used in the current economical analysis. Since the information given by Maples is very concise, it cannot be used for e.g. a sensitivity analysis. Therefore the more detailed information given by Blauwhoff has been used.

Table C.1 : Fixed capital investment

Process Equipment Unit Description			module costs 2003 K€
Absorber-Regenerator unit			11125
Sulfur Recovery Unit			4980
Tail Gas unit			10065
Total module Investment	k€ 2003	ΣC_{BM}	26169
Contingency and Fee	in % ΣC_{BM}	0	0
Fixed ISBL Capital investment	k€ 2003		26169
Fixed OSBL Capital investment	in % ISBL	30	7851
Fixed (ISBL+OSBL) capital investment	k€ 2003		34020

Table C.2 : Break down of the total capital investment

Total Capital Investments			
			k€ 2003
Fixed (ISBL+OSBL) capital investment			34020
Working capital	(Peters and Timmerhaus, 2003)		1543
Start-Up Expenses	in % ISBL + OSBL	8	2722
Total capital investment	k€ 2003		382847

Blauwhoff *et al.* also gave an estimate of the raw materials and utilities usages of an amine based desulfurization unit. The current costs associated with raw materials and utilities usage are estimated using the results of Blauwhoff *et al.* using current prices. Also the number of operating staff needed to run the desulfurization plant is taken from his work. To ensure a reliable economic comparison with the copper based desulfurization process, the remainder of the direct and indirect operating costs and the general expenses are estimated using the same method as is used in the estimation of the operating expenses for the copper based desulfurization method. The breakdown of the operating costs of an amine based desulfurization process is given in Table C.3.

Table C.3: Operating expenses

Operating expenses					
Direct operating costs					
				k€ per ton S	k€/yr
Raw materials	k€/unit	units used	basis		
Replacement amine etc	xxx	xxx	hr	818	
Utilities					
electric power (MWh)	0.065	2.78	hr	1447	
cooling water (m3)	0.000050	2756	hr	1101	
natural gas (GJ)	0.003	0.00	hr	0	
steam HP (ton)	0.016	44.4	hr	5768	
steam LP (ton)	0.012	0.00	hr	0	
Maintenance and repairs	2	% total fixed capital		680	
operating labor (yr)	27	operator a k€	40	1080	
Supervision	15	% operating labor		162	
laboratory charges	15	% operating labor		162	
Operating supplies	15	% Maintenance and repairs		102	
Patents and royalties	3	% total expenses		432	
Total direct operating costs				11752	11752
Indirect operating costs and overhead					
Local taxes and insurance	1	% total fixed capital		340	
overhead	60	% operating labor, supervision and maintenance		1153	
Total indirect operating costs				1494	1494
General expenses					
Administrative costs	25	% overhead		288	
Research & Development	3	% total expenses		432	
Sales and Marketing	3	% total expenses		432	
Total general expenses				1152	1152
Total operating expenses					14398

Chapter 6: Patent for the novel desulfurization process

METHOD AND SYSTEM FOR SELECTIVE REMOVAL OF CONTAMINATION FROM GAS FLOWS

The present invention relates to a method for removal of contaminants from gas flows, in particular the selective removal of sulphur and sulphur-containing compounds from gas flows. The invention further relates to a system of equipment for performing this process and to a process and system comprising this process, whereby sulphuric acid and/or sulphur dioxide is provided.

Many industrial gases are contaminated with hydrogen sulphide (H_2S). The presence of H_2S makes the direct application and/or use of these gases (for instance) natural gas, coal gas or biogas (impossible or at the very least) very hazardous. H_2S must be removed because it is extremely toxic, causes environmental pollution after combustion and produces problems, for instance catalyst poisoning, in subsequent industrial processes. This means that a gas cleaning step is necessary to remove H_2S in advance, before the resulting gases can be used.

DE-A-33 00 402 discloses a process for the removal of H_2S using an aqueous acidic culture medium which micro-organisms grow. These micro-organisms are used for the conversion of the metal sulphide into sulphate. The excess of formed sulphate may be removed by precipitation. Due to the use of micro-organisms, the aqueous absorption medium has a particular composition dictated buy the growth conditions of the micro-organism. The composition of the absorption medium is indicated in page 10 of D2

US-A-4 192 854 relates to a process for removing H_2S and ammonia from gas stream using a solution comprising copper sulphate an ammonium sulphate. Recycled is copper sulphate and from this process is removed ammonium sulphate and elemental sulphur. Furthermore, this process requires the addition of ammonium sulphate for maintaining the pH in a desired range.

DE-A-23 04 497 relates to a process for removing H_2S from gas streams in which is required the use of a copper sulphate solution which comprises in addition chlorine or bromine ions required for the oxidation of the formed copper sulphide into elemental sulphur.

US-A-5 147 620 relates to a process for the purification of a gas stream in which H_2S in absorbed in an aqueous solution of acidic copper nitrate. In the regeneration of the absorption solution, nitrogen dioxide and elemental sulphur are formed, nitrogen dioxide subsequently converted into nitric acid.

The object of the present invention is to provide an improved process for the removal of contaminants from gas flows. According to a first aspect of the present invention there is provided a method is provided for selective removal of undesired contamination, in the form of sulphur and/or sulphur-containing compounds from gas flows, according to claim 1

In the method according to the present invention the hazardous and undesired contaminants can thus be selectively precipitated, wherein substantially no other gas components react together with the metal ion, whereby a very efficient system is provided.

The inventors have demonstrated that the concentrations of S^{2-} and CO_3^{2-} in the liquid phase are dependent on the pH, wherein a good selective removal of S^{2-} relative to CO_3^{2-}, in particular occurs with a pH of less than 7, i.e. wherein the method selectivity is enhanced.

Furthermore, the inventors have shown that by carrying out the process at a pH above about -0.05 preferably 0.0, other metal salts are substantially not precipitated out of the gas flow at the expense of the metal sulphide, i.e. wherein the method performance is enhanced.

The inventors have accordingly demonstrated that via the method according to the present invention sulphur-containing compounds can be removed in a selective manner in relation to substantially non-hazardous gas components.

The metal ion is chosen such that the corresponding metal sulphide thereof is substantially non-soluble, wherein the metal is chosen from the group substantially consisting of Zn, Fe, Cu,

wherein the metal ion is placed in contact with the gas flow in the form of an aqueous metal sulphate solution.

When an aqueous solution containing $CuSO_4$ is placed in contact with for instance an H_2S-containing gas, the following reactions occur:

$$H_2S(G) \Leftrightarrow H_2S(L)$$
$$H_2S(L) + H_2O \Leftrightarrow HS^- + H_3O^+$$
$$HS^- + H_2O \Leftrightarrow S^{2-} + H_3O^+$$
$$S^{2-} + Cu^{2+} \Leftrightarrow CuS\downarrow$$

When the metal sulphide is very poorly soluble, these reactions can be considered practically irreversible, whereby a very effective H_2S removal process is realized. Since the metal sulphide is chosen because it is very poorly soluble, a process efficiency decrease in the pH will substantially not occur because in solution the metal ions are virtually wholly consumed.

A very good removal of sulphur-containing compounds from gas flows is obtained with copper sulphate. In the case of copper sulphate, the pH is preferably maintained in a range of between 0.25 and 7.0, since below 0.25 solid copper sulphate may be precipitated at the expense of the metal sulphide. Furthermore, when using copper sulphate, the pH on initially placing the gas flow in contact with the aqueous copper sulphate is preferably about 4.0 or above in order to provide a good efficiency.

When the gas flow contains COS, it may be subjected to an initial or simultaneous step of hydrolysing ($COS + H_2O \Rightarrow H_2S + CO_2$), whereafter the H_2S can be removed as above. In this way, COS can be very effectively removed from the gas stream.

When for instance the metal ion is zinc, a pH of 6 or less, preferably 5 or less and most preferably in the range between 0.23 and 4.37 pH can be used in order to remove H_2S from the gas flow in very selective manner relative to CO_2.

When the metal ion is for instance iron, a pH of about 6.7 or less can be chosen in order to provide a very good removal of H_2S, and can lie between about 2.5 to 4.5 if a very good removal of H_2S relative to CO_2 is desired.

In addition, unused metal salt solution is also fed back into the process wherein, before feedback of this unused metal salt solution, it can be supplied with an additional metal ion. The acid formed during the precipitation of the metal sulphide is preferably neutralized in order to cause the process to run well. The metal sulphate solution is preferably supplied by means of one or more of the following steps of:

i) dissolving the metal by means of an electric current. Situated in the make-up unit, for instance, are a metal electrode and an inert electrode. These are connected to a circuit.
ii) adding metal sulphate and neutralizing the acid separately.
iii) dissolving a metal oxide or hydroxide, for instance dissolving $Me(OH)_2$.

During these steps sulphuric acid produced during the process is consumed while metal is solubilized. According to a second aspect, the present invention relates to a system of equipment for performing the above stated method as defined in claim 13.

This system of equipment may be provided for providing sulphuric acid. The present invention will now be described with reference to the description and figures hereinbelow.

Theoretical background of the chemistry of the method according to the present invention

It is known that the sulphides of the metals zinc, iron, copper, silver, lead, cadmium, cobalt, magnesium, manganese, nickel and tin

are very poorly soluble. Use can be made hereof for the removal of H_2S from gas flows. A sample reaction is:

$$S^{2-} + Zn^{2+} \Leftrightarrow ZnS\downarrow \qquad (1)$$

The overall reaction, including the dissociation of H_2S is:

$$S^{2-} + Zn^{2+} \Leftrightarrow ZnS\downarrow \qquad (2)$$

A reaction wherein H_2S reacts with Zn^{2+} with the formation of zinc sulphide and acid.

Liquid equilibriums

When H_2S or CO_2 is dissolved in water, it behaves as a divalent acid. H_2S, HS^-, S^{2-}, CO_2, HCO_3^- and CO_3^{2-} will be present in the solution. The following equilibrium reactions will occur. The equilibrium constants of these reactions are given at 25°C (K_w, K_3, K_4) or 18°C (K_1 and K_2)

$$2H_2O \Leftrightarrow H_3O^+ + OH^- \qquad K_w = [H_3O^+][OH^-] = 10^{-14} \qquad (3)$$

$$H_2S + H_2O \Leftrightarrow H_3O^+ + HS^- \qquad K_1 = \frac{[H_3O^+][HS^-]}{[H_2S]} = 9.1*10^{-8} \qquad (4)$$

$$HS^- + H_2O \Leftrightarrow H_3O^+ + S^{2-} \qquad K_2 = \frac{[H_3O^+][S^{2-}]}{[HS^-]} = 1.1*10^{-12} \qquad (5)$$

$$CO_2 + 2H_2O \Leftrightarrow H_3O^+ + HCO_3^- \qquad K_3 = \frac{[H_3O^+][HCO_3^-]}{[CO_2]} = 4.3*10^{-7} \qquad (6)$$

$$HCO_3^- + H_2O \Leftrightarrow H_3O^+ + CO_3^{2-} \qquad K_4 = \frac{[H_3O^+][CO_3^{2-}]}{[HCO_3^-]} = 5.6*10^{-11} \qquad (7)$$

Precipitation equilibriums

When a metal is now present in ion form in the solution, the following precipitation reaction can occur if the solubility product K_{SP} is exceeded.

$$m\,M^{n+} + nX^{m-} \Leftrightarrow p\,M_{m/p}N_{n/p} \qquad K_{SP} = \sqrt[p]{\left[M^{n+}\right]^m \left[X^{m-}\right]^n} \qquad (8)$$

The driving force for this reaction ΔG_r (The difference in Gibbs energy between starting substance and products) can be calculated with:

$$\Delta G_r = RT \ln\left[\frac{K_{SP}}{\sqrt[p]{\left[M^{n+}\right]^m \left[X^{m-}\right]^n}}\right] \qquad (9)$$

Table 1 shows the solubility product K_{SP} at 25°C for a number of combinations of anions and metals on which the research will be further concentrated.

Table 1: Solubility products

	X^{m-}		
M^{n+}	S^{2-}	CO_3^{2-}	OH^-
Fe^{2+}	$1.6*10^{-19}$ (FeS)	$3.1*10^{-11}$ ($FeCO_3$)	$4.9*10^{-17}$ $Fe(OH)_2$
Zn^{2+}	$2.9*10^{-25}$ (ZnS)	$1.2*10^{-10}$ ($ZnCO_3$)	$4.1*10^{-17}$ $Zn(OH)_2$
Cu^{2+}	$1.3*10^{-36}$ (CuS)		

For $CuCO_3$ and $Cu(OH)_2$ solubilities are known of 0.03 wt% respectively 0.0059 g/l at 20°C. Using the foregoing, it is possible to calculate whether the precipitation reaction represented in reaction equation (8) can take place

Using as an example a gas composition of 10 volume ppm H_2S and 30 volume % CO_2,and assuming that, gas and liquid phase are in mutual equilibrium the concentration of S^{2-} and CO_3^{2-} can be calculated using equation (3) to (7).

Surprisingly, the inventors have found that these concentrations are shown to be greatly dependent on the pH. When the concentration

$[M^{n+}]$ is set at 1 mol/l, it is possible to calculate using (9) whether the precipitation reaction (8) can take place ($\Delta G_r<0$).

Precipitation reactions of copper and zinc

In Figure 1 the ΔG_r is shown as a function of the pH of the reactions which result in the formation of copper(II)sulphide, zinc(II)sulphide zinc(II)carbonate and zinc(II)hydroxide.

Conclusions: On the basis of the above stated starting points, it is found that

- copper sulphide can always be formed
- zinc sulphide can be formed if the pH is higher than 0.23
- zinc carbonate can be formed if the pH is higher than 4.37
- zinc hydroxide can be formed if the pH is higher than 5.80
- If 0.23<pH<4.37 it is found that zinc sulphide can result, but not zinc carbonate.

Precipitation reactions of iron

In Figure 2 the ΔG_r is shown as a function of the pH of the reactions which result in the formation of iron(II)sulphide, iron(II)carbonate and iron(II)hydroxide.

Conclusions: On the basis of the above stated starting points, it is found that

- iron sulphide can be formed if the pH is higher than 3.10
- iron carbonate can be formed if the pH is higher than 4.03
- iron hydroxide can be formed if the pH is higher than 5.85
- If 3.10<pH<4.03 it is found that iron sulphide can result, but not iron carbonate.

Experimental

A number of experiments were performed with metal sulphates, with copper sulphate, iron sulphate and zinc sulphate. Experiments were performed in order to study the precipitation reactions with H_2S (sulphide) and CO_2(carbonate). A reference experiment with caustic soda was also performed.

Experiment 1

300 ml aqueous solution of 74.9 gram of $CuSO_4.5H_2O$ was brought into the stirred cell. The temperature of the cell was kept constant at 20 °C. A gas stream of 3.5 ml/s containing 5 vol% H_2S, 10 vol% CO_2, balance nitrogen was applied to the reactor. Both gas and liquid phase in the reactor were continuously stirred. Measurements of the H_2S and CO_2 concentrations and the total gas volume flow at the exit of the reactor showed that (See also Figure 5):

- More than 99% of all hydrogen sulfide applied to this specific reactor is absorbed by the cupric sulfate solution
- In steady state condition no absorption of carbon dioxide occurred.

An overview of calculated pH values assuming ideal behavior of the solution and a dissociation constant (pKa) of 1.9 for the second dissociation step of sulfuric acid yields the following table of pH's as a function of time during the experiment.

Time (min)	pH
2	4.18
16	3.25
26	3.03

Experiment 1 demonstrated that hydrogen sulfide can be selectively and to a substantial degree be removed from a gas stream containing carbon dioxide using a washing liquor containing metal ions.

Experiment 2

300 ml aqueous solution of 7.5 gram of $CuSO_4.5H_2O$ was brought into the stirred cell. The temperature of the cell was kept constant at 20 °C. A gas stream of 3.5 ml/s, 10 vol% CO_2, balance nitrogen was applied to the reactor. When steady state condition was reached the experiment was started:

A gas stream of 3.5 ml/s containing 5 vol% H_2S, 10 vol% CO_2, balance nitrogen was applied to the reactor. Both gas and liquid phase in the reactor were continuously stirred. Measuring the H_2S and CO_2 concentrations and the total gas volume flow at the exit of the reactor showed that (see also Figure 6):

- More than 97% of all hydrogen sulfide applied to this specific reactor is absorbed by the acidified cupric sulfate solution. When the cupric sulfate solution is depleted the hydrogen sulfide conversion in the reactor drops dramatically
- During the entire experiment no absorption of carbon dioxide was observed.

An overview of calculated pH values assuming ideal behavior of the solution and a dissociation constant (pKa) of 1.9 for the second dissociation step of sulfuric acid yields the following table of pH's as a function of time during the experiment.

Time (min)	pH
2	3.19
6	2.68
10	2.41
20	1.99
40	1.43
66	1.02
70	0.97

This demonstrated that hydrogen sulfide can be selectively and to a substantial degree be removed from a gas stream containing carbon dioxide using a washing liquor containing metal ions, even at very low metal ion concentrations

Experiment 3

300 ml aqueous solution of 7.5 gram of $CuSO_4.5H_2O$ and 30 grams of H_2SO_4 were brought into the stirred cell. The temperature of the cell was kept at 20 °C.

A gas stream of 3.5 ml/s, 10 vol% CO_2, balance nitrogen was applied to the reactor. When steady state condition was reached the experiment was started:

A gas stream of 3.5 ml/s containing 5 vol% H_2S, 10 vol% CO_2, balance nitrogen was applied to the reactor. Both gas and liquid phase in the reactor were continuously stirred. Measuring the H_2S and CO_2 concentrations and the total gas volume flow at the exit of the reactor shows that (see also Figure 7):

- More than 96% of all hydrogen sulfide applied to this specific reactor was absorbed by the acidified cupric sulfate solution. When the cupric sulfate solution was depleted the hydrogen sulfide conversion in the reactor drops dramatically
- During the entire experiment no absorption of carbon dioxide occurred.

An overview of calculated pH values assuming ideal behavior of the solution and a dissociation constant (pK_a) of 1.9 for the second dissociation step of sulfuric acid yields the following table of pH's as a function of time during the experiment.

Time (min)	pH
0	0.04
20	0.01
40	-0.01
70	-0.04

This demonstrated that hydrogen sulfide can be selectively and to a substantial degree be removed from a gas stream containing carbon dioxide using an acidified washing liquor containing metal ions, even at very low metal ion concentrations.

Experiment 4

300 ml aqueous solution of 7.5 gram of $CuSO_4.5H_2O$ and 30 grams of H_2SO_4 were brought into the stirred cell. The temperature of the cell was kept at 20 °C. A gas stream of 3.5 ml/s, 10 vol% CO_2, balance nitrogen was applied to the reactor. When steady state condition ($CO_{2out} = CO_{2in}$) was reached the experiment was started.

A gas stream of 3.5 ml/s containing 0.05 vol% H_2S, 10 vol% CO_2, balance nitrogen was applied to the reactor. Both gas and liquid phase in the reactor were continuously stirred. Measuring the H_2S and CO_2 concentrations and the total gas volume flow at the exit of the reactor shows that (see also Figure 8):

- More than 95% of all hydrogen sulfide applied to this specific reactor was absorbed by the acidified cupric sulfate solution.

An overview of calculated pH values assuming ideal behavior of the solution and a dissociation constant (pK_a) of 1.9 for the second dissociation step of sulfuric acid yields the following table of pH's as a function of time during the experiment.

Time (min)	pH
0	0.04
100	0.04

This demonstrated that hydrogen sulfide can be selectively and to a substantial degree be removed from a gas stream containing carbon dioxide using an acidified washing liquor containing metal ions, even at very low hydrogen sulfide concentrations

Experiment 5

A control experiment with sodium hydroxide as washing liquor.

300 ml aqueous solution of 12 gram of NaOH was brought into the stirred cell. The temperature of the cell was kept at 20 °C. A gas stream of 3.5 ml/s, 10 vol% CO_2, balance nitrogen was applied to the reactor. After 50 minutes the composition of the gas stream was changed to 5 vol% H_2S, 10 vol% CO_2, balance nitrogen. The total gas volume flow was not changed. Both gas and liquid phase in the reactor were continuously stirred. Measuring the H_2S and CO_2 concentrations and the total gas volume flow at the exit of the reactor showed that (see also Figure 9):

- More than 99% of all hydrogen sulfide applied to this specific type of reactor was absorbed by the sodium hydroxide solution.

- Approximately 90% of all carbon dioxide applied to this specific type of reactor was absorbed by the sodium hydroxide solution.

The pH value was, throughout the entire experiment between 14 and 13.95.

Experiment 6

Control experiment with metal sulfate solution as washing liquor.

300 ml aqueous solution of 74.9 gram of $CuSO_4.5H_2O$ was brought into the stirred cell. The temperature of the cell is kept at 20 °C. A gas stream of 3.5 ml/s, 10 vol% CO_2, balance nitrogen was applied to the reactor. After 50 minutes the composition of the gas stream was changed to 5 vol% H_2S, 10 vol% CO_2, balance nitrogen. The total gas volume flow was not changed. Both gas and liquid phase in the reactor were continuously stirred. Measuring the H_2S and CO_2 concentrations and the total gas volume flow at the exit of the reactor showed that (see also figure 10):

- More than 96.5% of all hydrogen sulfide applied to the reactor was absorbed by the cupric sulfate solution.

An overview of calculated pH values assuming ideal behavior of the solution and a dissociation constant (pKa) of 1.9 for the second dissociation step of sulfuric acid yields the following table of pH's as a function of time during the experiment.

Time (min)	pH
2	4.17
16	3.25
26	3.03
46	2.72
64	2.59
80	2.45
100	2.35

Experiment 7

300 ml aqueous solution of 3.0 grams of $ZnAc.2H_2O$ and 6.0 grams of ZnO were brought into the stirred cell. The temperature of the cell was kept at 20 °C. After this al gasses were removed from the cell using a vacuum pump. Then a predetermined amount of gaseous carbonyl sulfide was brought into the cell. The gas and the liquid phase of the cell were continuously stirred. The gas phase and the liquid phase of the cell are operated batchwise. Monitoring the degree of carbonyl sulfide conversion in time of showed that (see alo Figure 11):

- The hydrolysis reaction of COS to H_2S and CO_2 in aqueous solutions of zinc acetate takes place at a 4 to 5 times higher rate than the hydrolysis reaction of COS in pure water in an identical reactor keeping all other parameters constant.

This demonstrated that the hydrolysis of carbonyl sulfide to hydrogen sulfide and carbon dioxide in aqueous solutions can be substantially enhanced by the presence of zinc acetate in this solution.

Experiment 8

300 ml aqueous solution of 2.5 grams of $CuAc.2H_2O$ and 6.0 grams of CuO were brought into the stirred cell. The temperature of the cell was kept at 20 °C. After this al gasses were removed from the cell using a vacuum pump. Then a predetermined amount of gaseous carbonyl sulfide was brought into the cell. The gas and the liquid phase of the cell were continuously stirred. The gas phase and the liquid phase of the cell were operated batchwise. Monitoring the degree of carbonyl sulfide conversion in time of showed that (see also Figure 12):

- The hydrolysis reaction of COS in aqueous solutions of copper acetate takes place at a 3 to 4 times greater rate than the hydrolysis reaction of COS in pure water in an identical reactor keeping all other parameters constant.

This demonstrated that the hydrolysis of carbonyl sulfide to hydrogen sulfide and carbon dioxide in aqueous solutions can be substantially enhanced by the presence of copper acetate in this solution.

The inventors have furthermore investigated the solubility of copper sulphate in aqueous sulphuric acid at various temperatures and as a function of pH, the results of which are shown in Figure 13.

A graphical representation of the capacity of an cupric sulfate solution acidified with sulfuric acid vs acidity (pH) clearly shows a substantial reduction of the capacity of the solvent at two pH values.

1. at a pH of approximately 4
2. at a pH of approximately 0.25

An embodiment (figure 3) of the system according to the present invention consists of a scrubber 10, a filter unit 12 and a make-up unit 14, wherein metal sulphate/sulphuric acid solution is processed to enable it to be fed back to scrubber 10. In use the gas flow for cleaning (A) is guided into scrubber 10, wherein it encounters for instance a copper sulphate counterflow (B). The copper sulphate/sulphuric acid solution (C) which leaves scrubber 10 is subsequently separated from copper sulphide in filter unit 12. This copper sulphate/sulphuric acid solution (flow D) is subsequently fed back to make-up unit 14. Here copper oxide (G) can be dissolved in the acid formed during the absorption step. The copper sulphide (flow E) leaving filter unit 12 can be converted into either copper oxide. The cleaned gas flow F is guided out of the scrubber.

CLAIMS

1. Method for selectively removing sulphur and/or sulphur containing contaminant compounds from a gas flow, which may also comprise CO_2, said method comprising the steps of:

- placing the gas flow into contact with a metal sulphate solution wherein the metal is selected from copper, zinc and iron, at a pH lying in the range of between about -0.05 and about 7.0, wherein the metal sulphate solution and the contaminants react together in order to form solid metal sulphide which precipitates and aqueous sulphuric acid.
- Removing the solid metal sulphide from the gas flow contacted metal sulphate solution,
- Converting the solid metal sulphide into metal oxide,
- Dissolving the thus formed metal oxide in the metal sulphate/sulphuric acid solution obtained in the above removing step in order to regenerate metal sulphate, and then feeding the resulting solution to the gas flow contacting step.

2. Method according to claim 1 wherein the gas flow contains H_2S and/or COS.

3. Method according to claim 1 or 2, wherein the metal sulphate is copper sulphate.

4. Method according to claim 4, wherein the pH range lies between about 0.0 and 7.0, preferably 0.25 and 7.0.

5. Method according to claim 4, wherein the pH range lies between about 0.25 and about 6.0.

6. Method according to claims 1-5 , wherein the start pH on initially placing the gas flow in contact with the aqueous copper sulphate is about 4.0 or above.

7. Method according to any of the claims 1 or2, wherein, when the metal comprises zinc, a pH of about 6 or less, preferably 5 or less is maintained.

8. Method as claimed in claim 7, wherein the pH lies in the range between 0.23 and about 4.37.

9. Method as claimed in any of the claims 1 or 2, wherein, when the metal comprises iron, a pH of about 6.7 or less is maintained, wherein the pH preferably lies in the range between about 2.5 and about 4.5.

10. Method as claimed in any of the foregoing claims, wherein a buffer is added.

11. Method according to any of the preceding claims further comprising an initial or simultaneous step of transforming COS in the gas flow to H_2S, by means of exposing the gas flow to a metal acetate solution, in particular being selected from the group consisting of zinc acetate and copper acetate.

12. Method as claimed in any of the foregoing claims, wherein sulphuric acid is provided.

13. System of equipment for performing the method as claimed in any of the foregoing claims, comprising:

- a scrubber column in which the gas flow for cleaning can be brought into contact with a metal sulphate solution,
- a filter unit for separating precipitated metal sulphide, and
- a regeneration unit in which the metal sulphide can be regenerated into metal oxide.

14. System as claimed in claim 13 for providing sulphuric acid and/or sulphur dioxide.

Figures

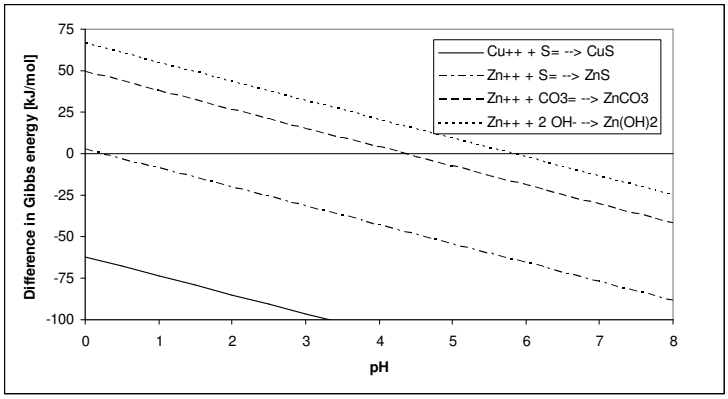

Fig 1: ΔG_r vs. pH precipitation reaction of zinc and copper

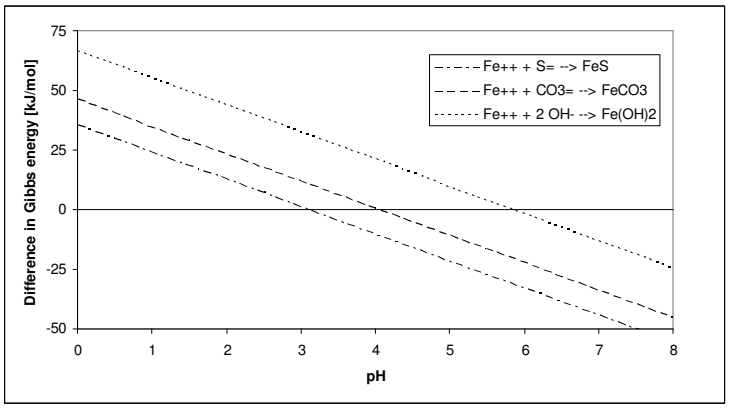

Fig 2: ΔG_r vs. pH precipitation reaction of iron

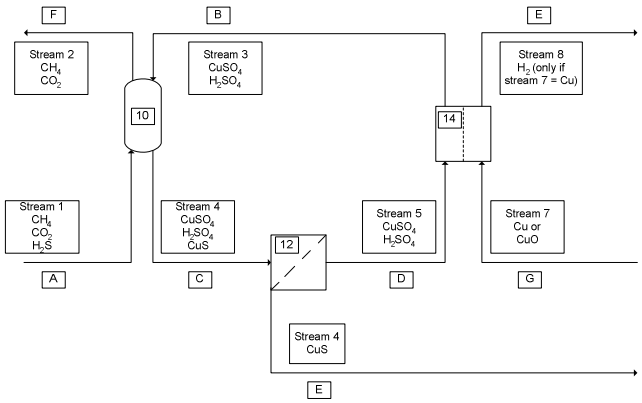

Fig 3

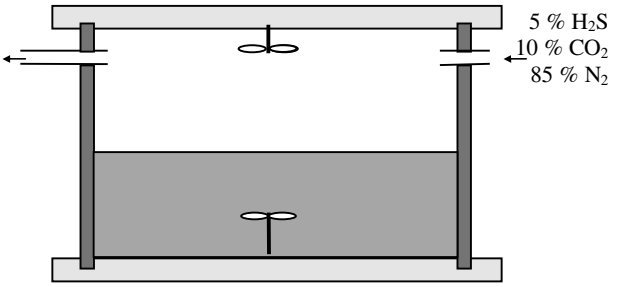

Fig 4

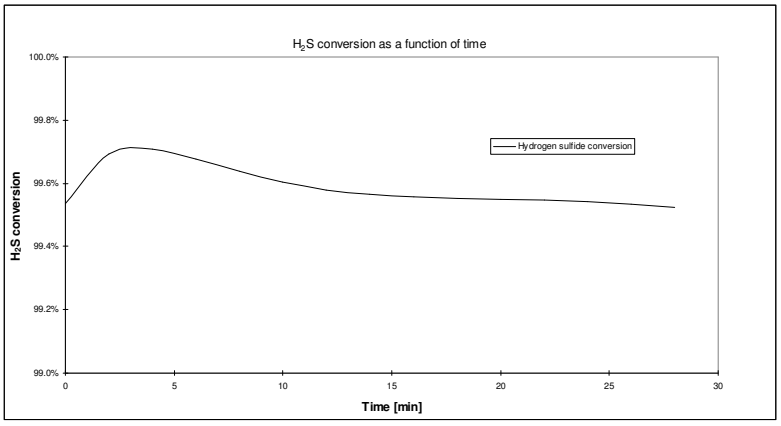

Fig 5

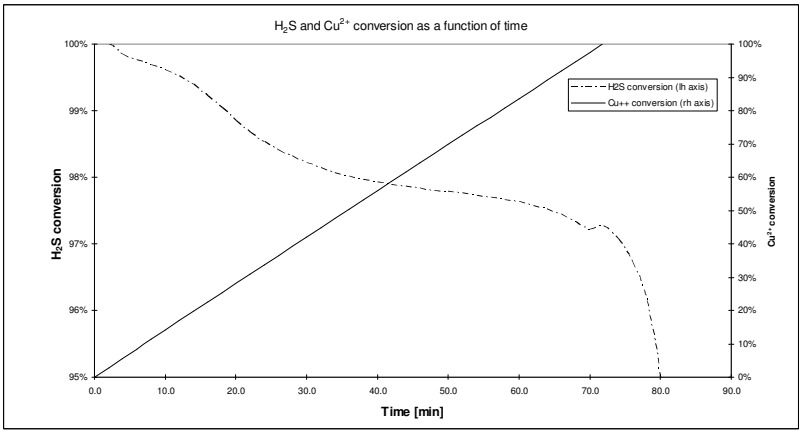

Fig 6

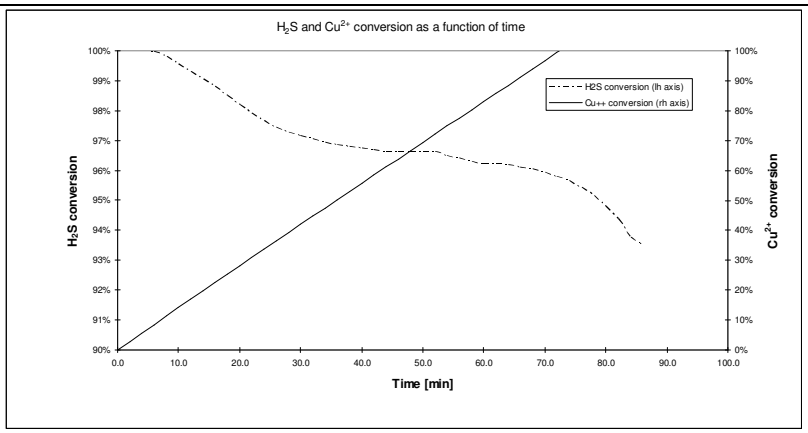

Fig 7

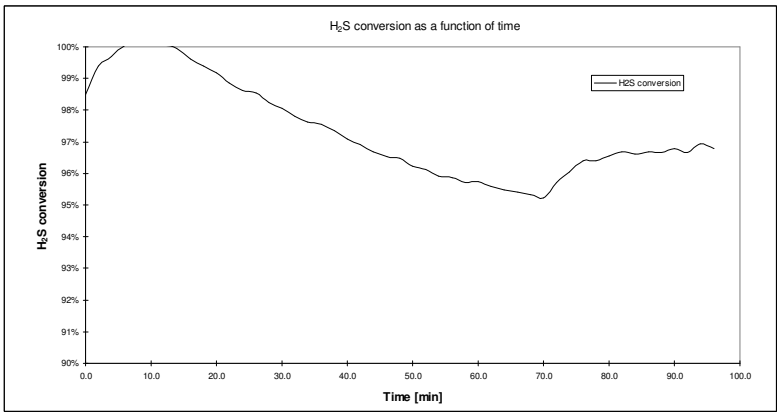

Fig 8

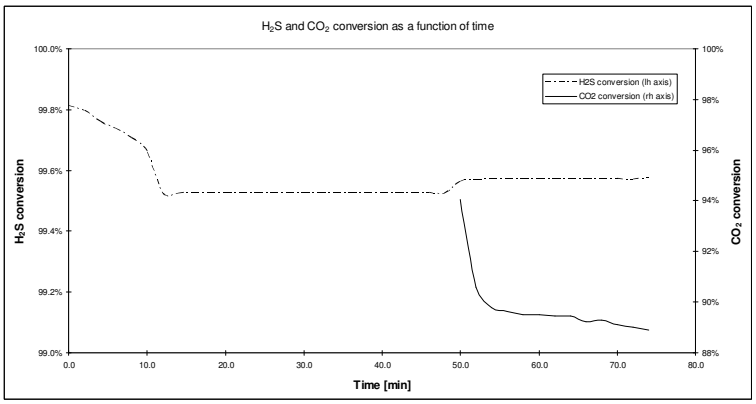

Fig 9

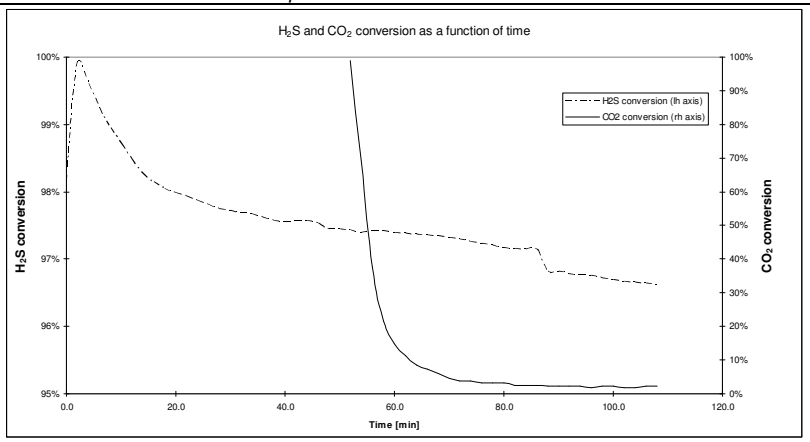
H2S and CO2 conversion as a function of time
H2S conversion (lh axis)
CO2 conversion (rh axis)
H2S conversion
CO2 conversion
Time [min]
100%
99%
98%
97%
96%
95%
90%
80%
70%
60%
50%
40%
30%
20%
10%
0%
0.0
20.0
40.0
60.0
80.0
100.0
120.0

Fig 10

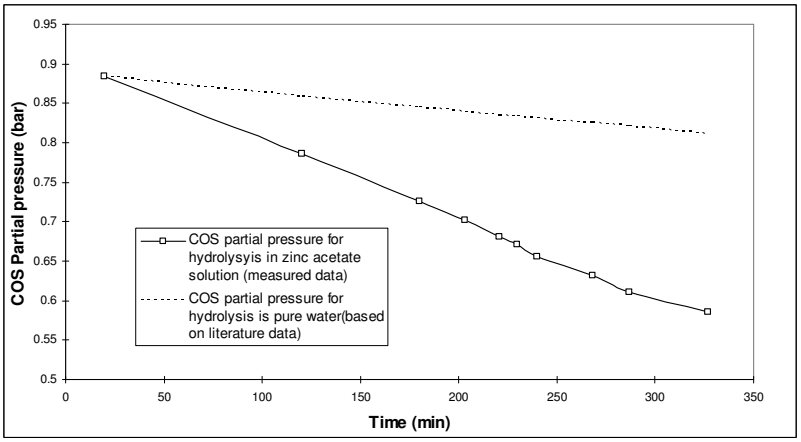
COS Partial pressure (bar)
Time (min)
COS partial pressure for hydrolysyis in zinc acetate solution (measured data)
COS partial pressure for hydrolysis is pure water(based on literature data)
0.95
0.9
0.85
0.8
0.75
0.7
0.65
0.6
0.55
0.5
0
50
100
150
200
250
300
350

Fig 11

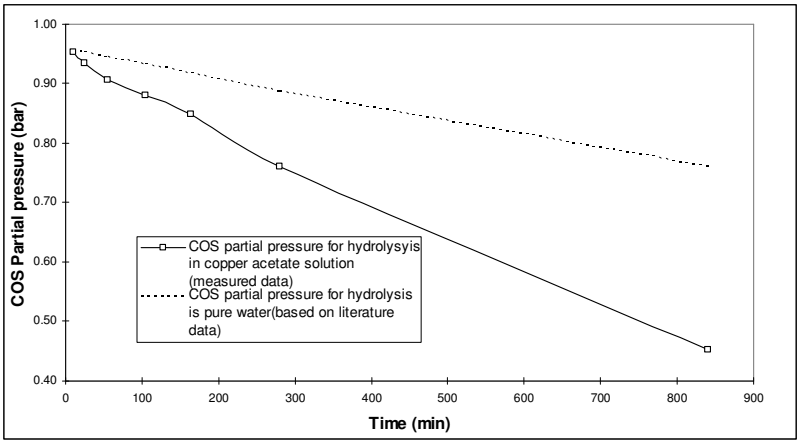
COS Partial pressure (bar)
1.00
0.90
0.80
0.70
0.60
0.50
0.40
0
100
200
300
400
500
600
700
800
900
Time (min)
COS partial pressure for hydrolysyis in copper acetate solution (measured data)
COS partial pressure for hydrolysis is pure water(based on literature data)

Fig 12

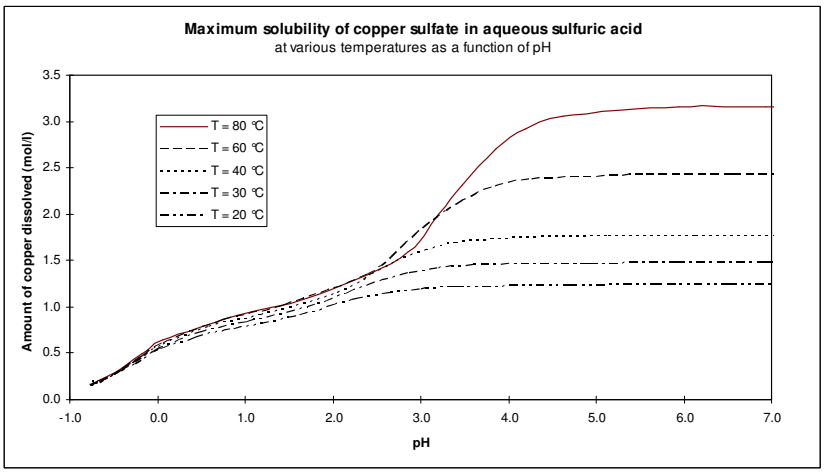
Maximum solubility of copper sulfate in aqueous sulfuric acid
at various temperatures as a function of pH
Amount of copper dissolved (mol/l)
3.5
3.0
2.5
2.0
1.5
1.0
0.5
0.0
-1.0
0.0
1.0
2.0
3.0
4.0
5.0
6.0
7.0
pH
T = 80 °C
T = 60 °C
T = 40 °C
T = 30 °C
T = 20 °C

Fig 13

Dankwoord

Bij dezen zou ik mijn promotor (Geert Versteeg) en, co-promotor (Kees Hogendoorn) willen bedanken voor de kansen die mij geboden zijn en het geduld dat ze met mij hebben gehad.
Verder zou ik iedereen die op een of andere wijze heeft bijgedragen aan het welslagen van dit project willen danken voor zijn inzet.

Résume

Henk ter Maat (1968) has completed various technical educations before entering the labor market. His was given his introduction to process technology at the Dr. Groen College of Almelo. In 1988 he finished that education with a diploma, and subsequently wandered off into the world of materials engineering. In 1992 he completed his study at the Enschede Polytechnic in that field and was entitled to the degree of Bachelor. In 1993 he started working for Procede Twente. Procede Twente offered him the opportunity to continue his education by allowing him to follow both parts of the Process Technology course given at the Twente University of Technology. After completion of the Process Technology course in 1996 and fulfilling the additional requirements he graduated at the faculty of Chemical Technology from Twente University of Technology. In 1997 he started (supported by Procede Twente) a post graduate course at the Process Development School of the Twente University of Technology, and in 1999 he completed that course and has been officially registered as a Technical Designer by the KIVI (the Dutch Royal Institute of Engineers). The main subject of study during that course was the development of a novel selective gas desulfurization process. In 2006 he completed a PhD thesis on the same subject.

List of publications

H. ter Maat, G.F. Versteeg, 1998, Method and System for Selective Removal of Contamination from Gas Flows., European Patent Application no. 98.925979.1

H. ter Maat, J.A. Hogendoorn, G.F. Versteeg, 2005, The removal of hydrogen sulfide from gas streams using an aqueous metal sulfate absorbent - Part I: The absorption of hydrogen sulfide in metal sulfate solutions, Separation and Purification Technology Vol 43, p 199-213

H. ter Maat, J.A. Hogendoorn, G.F. Versteeg, 2005. The removal of hydrogen sulfide from gas streams using an aqueous metal sulfate absorbent - Part II: The regeneration of copper sulfide to copper oxide – an experimental study, Separation and Purification Technology Vol. 43, p 183-197

H. ter Maat, J.A. Hogendoorn, C.J. Asselbergs, G.F. Versteeg, 2005. Selective desulfurization of natural gas using copper sulfate solutions – Process design and economic evaluation. Presented at the 7th World Conference of Chemical Engineering.

H. ter Maat, M. Al-Tarazi, J.A. Hogendoorn, J.P.M. Niederer, G.F. Versteeg, 2006, Theoretical and experimental study of the absorption rate of H2S in CuSO4 solutions: The effect of enhancement of mass transfer by a precipitation reaction. Presented at the Distillation and Absorption 2006 conference and submitted for publication in Chemical Engineering Research and Design.

.